Molecular profiling $CD8^+$ T-cell memory inflation

Thesis submitted in partial fulfilment of the requirements for the degree of Doctor of Philosophy in Clinical Medicine



Stuart Sims

Klenerman Group
Nuffield Department of Medicine
and
Brasenose College
University of Oxford
2012

Abstract

Infection with murine cytomegalovirus (MCMV) induces a large population of virus-specific $CD8^+$ T-cells that is maintained at a high frequency in the peripheral organs for the lifetime of the host. This striking response to MCMV is termed “memory inflation”. It has also been shown that a similar response occurs after immunization with a non-replicating adenovirus expressing a transgene. The key features which distinguish “inflating” $CD8^+$ T-cell memory responses from classical “non-inflating” $CD8^+$ T-cell memory responses have not been fully defined. To determine the molecular signature of memory inflation I sorted antigen-specific cells ex vivo and compared the gene expression profiles of inflationary $CD8^+$ T-cells to those of central memory and effector $CD8^+$ T-cells. This data showed that memory inflation has a distinct expression profile, with high expression of KLR receptors, specific chemokine receptors such as CX3CR1, transcription factors such as T-bet and Foxk1, and survival factors, such as Bcl-X_L and down regulation of inhibitory molecules such as BTLA. These inflationary cells are functional - expressing an array of cytokines, granzymes, IFNγ, and TNFα, and lack transcriptional features of T-cell exhaustion. Similar features were identified in $CD8^+$ T-cells undergoing memory inflation using both the MCMV and adenovirus models. To address the turnover of these “inflationary” CD8+ T cells and their role in vivo, I created tetramers bound to the toxin saporin to specifically knock out inflationary cells. I found that they contribute to the control of viral replication, since depletion was followed by a rise in viral load and a subsequent rebound increase in the $tetramer^+$ population. In the final chapter I addressed the role of one specific cell surface molecule, CD73, during $CD8^+$ T-cell memory. I found that although CD73 is thought to play a role in immune regulation, $CD73^{-/-}$ mice showed normal memory inflation and classical non-inflationary memory development.

Overall the data in this thesis define for the first time the transcriptional profile associated with $CD8^+$ T-cell memory and show the distinct nature of this T-cell programme in vivo. Future work using further genetically modified mouse strains should allow definition of the critical molecules and pathways involved in the development of these important memory pools.

Acknowledgments

Over the years there have been numerous people that have helped me to finally reach this point.

I would first and foremost like to thank my supervisor, Professor Paul Klenerman. Paul has always been supportive, considerate and understanding, I am truly grateful for this opportunity that he has given me.

Two past members of the Klenerman Lab, deserve special thanks, Jenny Smith and Geraldine O'hara, these two ladies have encouraged me through the bad times and cheered me up no end, with out them work just wouldn't have ever been the same. Another member of the Klenerman lab, Beatrice Bolinger, who joined the lab half way through my DPhil I an indebted to; with out her knowledge and guidance I would have never got his far.

Life is just not about work, over the years Brasenose College has provided a pleasant distraction away from the lab. Chris Tudor, Samir Bhatt and Robert Cashmore have made my time in Oxford a wonderful experience, knowingly or not they have provided a constant source of entertainment and I hope we will stay friends forever.

Lastly I would like to thank my fiancée Sara Burkhard, we met at a conference during my DPhil, and so if nothing else this piece of work is responsible for introducing me to the most caring and beautiful person I could have ever dreamt of meeting. Thank you for you patience with me over the time it has taken me to write this.

Table of Contents

Acknowledgments 3

1 Introduction 9

1.1 Antigen processing and presentation by major histocompatibility (MHC) class I molecules 9

1.2 CD8+ T-cell response to infection 12

1.3 Primary memory CD8+ T cell development and differentiation 14

1.4 Secondary CD8+ T-cell response and secondary memory 19

1.5 Requirement for a 3rd signal for CD8+ T-cell differentiation 20

1.6 CD8+ T-cell transcriptional programming 22

1.7 Memory inflation 31

1.8 Transcriptional studies of CD8+ T cell development 39

1.9 Aims of this thesis 41

2 Materials and Methods 42

2.1 Mice 42

2.2 Viruses 42

2.3 Production of MHC class tetrameric complexes 43

2.3.1 Production and purification of proteins 43

2.3.2 Refolding, concentration, biotinylation and purification of MHC class I complexes 44

2.3.3 Peptides 45

2.3.4 Tetramerization 45

2.4 Cell preparation and cell Separation in vitro 45

2.4.1 Isolations of lymphocytes 45

2.4.2 Sorting cells by MACS 46

2.4.3 Cell sorting by MoFLO 47

2.4.4 Peptide restimulation 47

2.5 Flow Cytometry **48**

2.5.1 Tetramer staining 48

2.5.2 Extracellular antibody staining 48

2.5.3 Intracellular antibody staining 50

2.6 *In vivo* assays **50**

2.6.1 *In vivo* cytotoxicitiy assay (In vivo killing assay) 50

2.6.2 Adoptive transfer 51

2.7 Transcriptional analysis **51**

2.7.1 RNA extraction amplification and hybridization 51

2.7.2 DNA extraction 52

2.7.3 Microarray data analysis 52

2.7.4 Further methods for gene transcriptional analysis 53

2.7.5 Quantitative real-time PCR for selected genes 53

3 CD8+ T-cell memory inflation induced by MCMV **55**

3.1 Introduction **55**

3.1.1 Key questions in this chapter 57

3.2 Results **58**

3.2.1 MCMV-specific $CD8^+$ T-cells are maintained at a high frequency and remain functional 58

3.2.2 Tetramer sorting of MCMV-specific $CD8^+$ T-cells and gene expression array analysis 62

3.2.3 Gene ontology analysis of unique gene sets 66

3.2.4 K-means clustering and gene ontology analysis 69

3.2.5 Cytokine and chemokine expression profile of MCMV-specific $CD8^+$ T-cells 74

3.2.6 Expression of NK-cell receptors on inflationary $CD8^+$ T-cells 82

3.2.7 Cell cycle analysis 87

3.2.8 Receptors of the SLAM family are up-regulated on MCMV-specific $CD8^+$ T-cells 90

3.2.9 Expression of other cellular receptors 92

3.2.10 Exhaustion-associated surface inhibitory receptors 97

3.2.11 Profiling apoptotic proteins in MCMV-specific CD8+ T-cells 99

3.2.12 Differential expression of co-stimulatory molecules 102

3.2.13 Production of effector molecules in M38- and M45-specific CD8+ T-cells 105

3.2.14 Transcription factor expression profile of M38-inflationary CD8+ cells 109

3.2.15 Suppression of the Jak-Stat pathway in inflationary cells 113

3.3 Discussion 115

3.3.1 Chapter summary 118

4 CD8+ T-cell memory inflation induced by adenovirus 119

4.1 Introduction 119

4.1.1 Key questions in this chapter 120

4.2 Results 122

4.2.1 Epitope specific CD8+ T-cell memory inflation induced by adenovirus vector 122

4.2.2 Tetramer sorting of Ad-LacZ-specific CD8+ T-cells and gene expression analysis 124

4.2.3 Gene ontology analysis of unique gene sets 127

4.2.4 Expression of NK-cell receptors on inflationary CD8+ T-cells 130

4.2.5 Induction of effector molecules in βgal_{96}- and βgal_{497}-specific CD8+ T-cells 130

4.2.6 Transcription factor profile of βgal_{96}-specific CD8+ T-cells 131

4.2.7 Cell cycle analysis 134

4.2.8 Cytokine and chemokine receptor profile of Ad-LacZ-specific CD8+ T-cells 139

4.2.9 Receptors of the SLAM family up-regulated on Ad-LacZ-specific CD8+ T-cells 142

4.2.10 Expression of exhaustion markers on Ad-LacZ specific CD8+ T-cells 144

4.2.11 Differential expression of co-stimulatory receptors on Ad-LacZ-specific CD8+ T-cells 146

4.2.12 Expression of adhesion molecules on Ad-LacZ- specific CD8+ T-cells 148

4.2.13 K-means clustering and gene ontology analysis of MCMV- and Ad-LacZ-specific CD8+ T-cells 151

4.2.14 Comparison between M38- and βgal$_{96}$-specific CD8+ T-cells 155

4.2.15 Gene network of inflationary CD8+ T-cells 157

4.3 Discussion 159

4.3.1 Chapter summary 160

5 Function and stability of inflationary CD8+ T-cells 161

5.1 Introduction 161

5.1.1 Key questions in this chapter 164

5.2 Results 166

5.2.1 In vivo killer assay 166

5.2.2 Adoptive transfer 169

5.2.3 Tetramer Saporin experiments 175

5.3 Discussion 191

5.3.1 Chapter summary 194

6 CD73 - a potent suppressor of immune response - has no effect on generation of inflationary CD8+ T-cells 195

6.1 Introduction 195

6.2 Results 198

6.2.1 Frequency of MCMV-specific CD8+ T-cells. 198

6.2.2 Proliferation 201

6.2.3 Cytotoxicity and cytokine secretion 203

6.2.4 Phenotype 205

6.2.5 Viral loads 208

6.3 Discussion 210

6.3.1 Chapter summary 211

7 Conclusion **212**

7.1 Future work **220**

8 Papers during my DPhil period. **221**

9 References **224**

1 Introduction

This thesis is about memory inflation in MCMV and adenovirus infection; in the introduction I am going to first discuss T-cell memory, its regulation and then memory inflation. Finally I am going to briefly discuss the use of transcriptional approaches to define $CD8^+$ T-cell responses to viruses.

1.1 Antigen processing and presentation by major histocompatibility (MHC) class I molecules

Naïve $CD8^+$ T-cells migrate between the lymph nodes, blood and spleen. This recirculation throughout the secondary lymphoid compartment means that many naïve $CD8^+$ T-cells fail to directly encounter pathogens. For naïve $CD8^+$ T-cells to encounter antigen, they require engagement with mature professional antigen-presenting cells (APCs) such as dendritic cells (DCs). DCs encompass a heterogeneous population of cells that survey the surroundings, capture and process foreign antigens into peptide fragments and presenting antigenic peptides on MHC class I molecules to $CD8^+$ T-cells. This allows naïve $CD8^+$ T-cells to survey the entire body for the presence of pathogens by scanning DCs for presentation of antigen that have migrated to the secondary lymphoid compartment. Once naïve $CD8^+$ T-cells encounter a DC, the $CD8^+$ T-cells are activated, proliferate and differentiate and then enter the peripheral tissue to engage the pathogen.

The two routes by which antigens gain access to the MHC class I pathway are endogenously synthesized or exogenously acquired. In the classical MHC class I pathway, endogenously produced proteins are cleaved in the cytoplasm by the proteasome to generate peptides. Most MHC class I associated peptides are 8-11

amino acids long(1), and are transported from the cytoplasm to the endoplasmic reticulum (ER) by the ER resident protein transporter for antigen processing (TAP). Here the peptides are loaded onto MHC class I molecules by a multi-component complex(2,3). Once loaded onto the binding groove, the peptide stabilizes the membrane-bound heavy chain and the soluble β2-microglobulin chain, waiting in the ER membrane, forming a peptide-bound MHC class I molecule which is subsequently released from the ER and transported to the plasma membrane(4). This classical pathway plays the dominant role in activating, $CD8^+$ T-cells, to most infections. Viruses hijack the hosts translation machinery to make their own proteins; therefore viral derived antigens efficiently gain access to the hosts classical MHC class I assembly pathway. However not all pathogens infect DCs and pathogen infected DCs are often functionally impaired(5,6).

The alternative method of $CD8^+$ T-cell priming is cross-presentation. This involves exogenously acquired antigen to be taken up and presented on the MHC class I molecules by DCs(7). Controversy exists as to the molecular process of exogenously acquired antigen uptake, processing and loading on MHC class I. However, it has been shown that $CD8^+$ DCs, are efficient at cross-presentation(1,4,8).

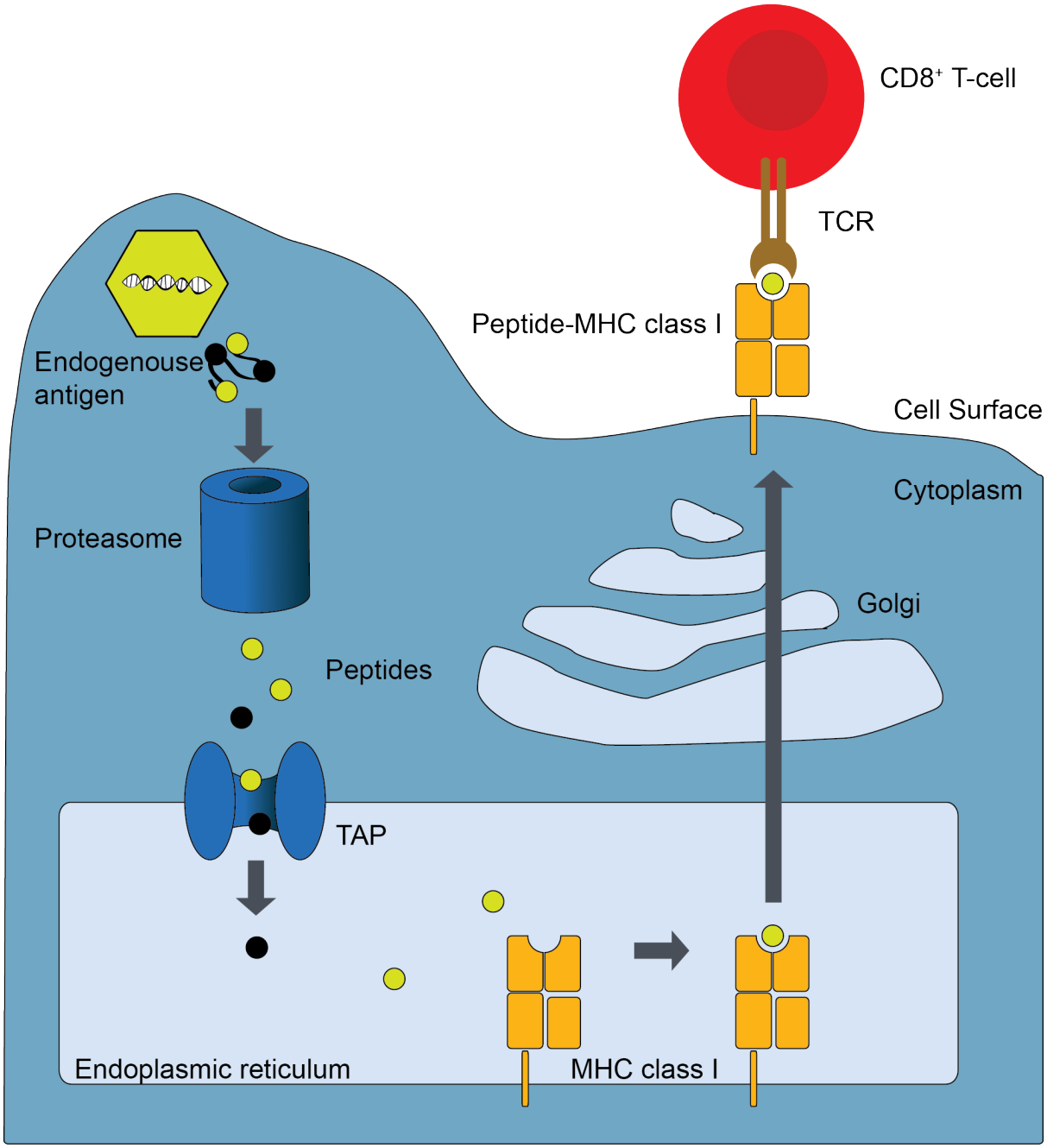


Figure 1-1 Cytosolic and nuclear proteins are degraded by the proteasome into peptides. The transporter for antigen processing (TAP) then translocates peptides into the lumen of the endoplasmic reticulum (ER). MHC class I heterodimers wait in the ER for peptide. Peptide binding is required for correct folding of MHC class I molecules and release from the ER and transport to the plasma membrane, through the golgi, where the peptide is presented to the immune system. The $CD8^+$ T-cell recognises the peptide-MHC class I by the T-cell receptor (TCR).

1.2 $CD8^+$ T-cell response to infection

$CD8^+$ T-cells play an essential role in defending the host against intracellular pathogens, such as bacteria and viruses. In naïve mice $CD8^+$ T-cells cells with TCRs for any given specificity are present at a low number, ranging from tens to thousands of cells per mouse(9-11). This rarity of any single specificity is thought to maximize the diversity of the naïve $CD8^+$ T-cell repertoire to protect the host against a vast array of potential pathogens.

In order to combat infection, $CD8^+$ T-cells with specificity against the pathogen must multiply in number and acquire effector functions such as cytotoxic activity and cytokine production. Naïve $CD8^+$ T-cells circulate between the blood and secondary lymphoid organs by virtue of a defined set of homing markers (CD62L and CCR7), where they scan mature DCs displaying pathogen-derived peptide on MHC class I molecules. Following infection, DCs acquire and process foreign antigens as a consequence of either direct infection of the DC or phagocytosis of infected cells. In addition to antigen acquisition, immature DCs also receive activating signals, from inflammatory cytokines or CD40-dependent interaction with $CD4^+$ T-cells, to differentiate into mature DCs, up-regulate co-stimulatory molecules, and migrate to secondary lymphoid organs where they encounter naïve $CD8^+$ T-cells. Presentation by immature DCs results in tolerance induction, whereas presentation by activated mature DCs stimulates the generation of CTLs and memory(12). Studies of $CD8^+$ T-cell and DC encounters have shown that the initial transitory interactions eventually result in the establishment of a conjugation that last for hours(13).

After receiving signal 1 (TCR/MHC), signal 2 (co-stimulation) and signal 3 (pro-inflammatory cytokines) naïve $CD8^+$ T-cells embark on a differentiation program

leading to the formation of memory $CD8^+$ T-cells(14). This process is characterized in 3 distinct phases: expansion, contraction, memory generation and maintenance. During the expansion phase, antigen-specific $CD8^+$ T-cells clonally proliferate, with one precursor giving rise to more than 10,000 daughter cells over 5-8 days(15,16), differentiate into effector cells, down-regulating lymph-node homing molecules (CD62L and CCR7) and leave the secondary lymphoid organs. They enter the blood and migrate to sites of infection. Such cells acquire effector functions, kill cells (through perforin and granzyme production) and secrete cytokines (such as IFNγ and TNFα) to combat the infection.

Following expansion, whether the $CD8^+$ T-cell response has eliminated infection or not, comes the contraction phase where the effector $CD8^+$ T-cells decline in number, with the majority dying by apoptosis. In general, 5-10% of $CD8^+$ T-cells survive the contraction phase, and mature into memory $CD8^+$ T-cells, to respond against future reinfection. Memory cell potential is not inherited equivalently by all effector $CD8^+$ T-cells, as some are intrinsically better than others to persist and populate the memory $CD8^+$ T-cell population. In models such as lymphocyte choriomenigitis virus (LCMV), a subset of effector $CD8^+$ T-cells expressing high levels of IL-7Rα, CD27 and Bcl-2 and low levels of KLRG1, are enriched for memory precursor cells(17-19). However, these markers do not exclusively distinguish memory $CD8^+$ T-cells: this may be more dependent on the type of infection, as apoptosis is observed in the IL-$7R^{Hi}$ effector $CD8^+$ T-cells and the frequency of IL-$7R^{Lo}$, $KLRG^{Hi}$ can vary across types of infection(20,21). Furthermore, long lived IL-$7R^{Lo}$, $KLRG^{Hi}$ memory $CD8^+$ T-cells are observed in secondary infections(22,23).

After acute infection, memory $CD8^+$ T-cell number can be stably maintained in the absence of antigen(24), through the actions of IL-7 and IL-15, which promote survival of memory $CD8^+$ T-cells and homeostatic proliferation, to maintain cell numbers(25). In contrast to effector $CD8^+$ T-cells, memory $CD8^+$ T-cells are characterised by their rapid ability to generate effector functions, proliferate in response to antigen and produce secondary CTLs to contain secondary infection. However, memory $CD8^+$ T-cell effector functions and proliferation potential differ according to their phenotype(26).

Many factors can affect the frequency and function of memory $CD8^+$ T-cells, such as antigen, cytokines, co-stimulatory molecules and environmental cues, altering the transcriptional profile, metabolism and differentiation.

1.3 Primary memory $CD8^+$ T cell development and differentiation

Studying memory $CD8^+$ T-cells *in vivo* at the population level has proved challenging since substantial phenotypic and functional heterogeneity is observed in populations of antigen-specific memory $CD8^+$ T-cells that are examined following infection. There is no single marker that indisputably identifies and defines memory $CD8^+$ T-cells. Thus, the expression of multiple cell surface molecules together with various functional attributes is used to distinguish between naïve, effector and memory $CD8^+$ T-cells. Furthermore, the memory $CD8^+$ T-cell pool is comprised of multiple subpopulations. Subsets within the memory population are defined and studied by differential expression of cell surface markers. One central question in the field of memory $CD8^+$ T-cell biology is how these cells develop following infection?

The three major subsets of $CD8^+$ T-cell memory are central memory T-cell (T_{CM}), effector memory T-cells (T_{EM}) and tissue resident T-cells (T_{RM}). These have been defined on their differential expression of lymphoid homing receptors, CCR7 and CD62L. The T_{EM} cells are mainly $CCR7^{Lo}$ $CD62L^{Lo}$ and most commonly found in non-lymphoid tissue, while T_{CM} are $CCR7^{Hi}$ $CD62L^{Hi}$, homing to secondary lymphoid organs and bone marrow. In addition, there are functional differences; T_{CM} make less IFNγ and more IL-2 and mount a more robust recall response compared to T_{EM} (26,27). Since T_{CM} and T_{EM} subsets have different migratory potential and effector function, research has focused on the developmental relationship between these two subsets.

Recently a new subset of memory cells has been described, these T_{RM} are long lived in the brain and mucosal tissue and show limited levels of egress and recirculation. They are characterised by a $CD103^{Hi}$, $CD69^{Hi}$, $CD27^{Hi}$ phenotype and high levels of granzyme B expression(17-19,28-30). There are at least four different models proposed for memory $CD8^+$ T-cell developmental pathway.

Separate-precursor model. This model suggests that naïve T-cells are pre-programmed during thymic development to adopt a certain differentiation state following activation (Figure 1-2.A). This is probably not the case, since using adoptive transfer of single $CD8^+$ T-cells or by "barcoding" $CD8^+$ T-cells it has been demonstrated that a single naïve $CD8^+$ T-cells is multipotent and can give rise to both effector $CD8^+$ T-cells, T_{CM} and T_{EM} cells(20,21,31,32). These experiments were however carried out using TCR transgenic $CD8^+$ T-cells - therefore, there is potential for different TCR signalling strengths to affect $CD8^+$ T-cell differentiation in wild type (WT) mice.

Decreasing-potential model. This model proposes that repetitive stimulation of $CD8^+$ T-cells by antigen and pro-inflammatory cytokines drives greater proliferation and terminal effector cell differentiation (Figure 1-2.B)(33). With increased stimulation, $CD8^+$ T-cells acquire a terminally differentiated state; they retain effector functions and cytolytic capacity but lose memory cell properties such as enhanced longevity and proliferation potential. This model provides a spectrum of effector $CD8^+$ T-cells at various differentiation states depending on the history of signals received. Experiments have shown that truncating the duration of antigen exposure and decreasing inflammation through antibiotic treatment memory $CD8^+$ T-cells formation can be accelerated and $CD8^+$ T-cells that are subject to inflammatory signals late in infection preferentially acquire T_{CM} cell phenotypes(34-36).

Signal Strength model. The formation of heterogeneous effector populations is altered by the overall strength of the signals delivered by antigen (signal 1) co-stimulation (signal 2) and pro-inflammatory cytokines (signal 3) early during T-cell priming (Figure 1-2.C) (37,38). Receiving a strong signal will drive greater clonal expansion and select $CD8^+$ T-cells capable of forming memory cells. However after a threshold has been reached a strong signal will cause the $CD8^+$ T-cells to become terminally differentiated(39). This is different to the decreasing potential model in that different cell fates are determined early in response according to the intensity of the signals received in a divergent manner rather than linear, by multiple rounds of stimulation.

Asymmetric model. In this model, the division of naïve $CD8^+$ T-cells following antigenic stimulation into two daughter cells with unequal inheritance of cellular proteins determines their fate (Figure 1-2.D). The daughter cell that inherits the immunological synapses receives stronger TCR signalling, and due to its proximity to

the APC will receive pro-inflammatory signals, becomes the T_{EM}. In contrast, the daughter cell distal to TCR signalling becomes an early T_{CM} precursor. Based on the asymmetric division model, the number of memory precursors should equal the number of effector daughter cells(40-42). However, the majority of cells found at the peak of expansion exhibit an effector phenotype.

The four different models provide a useful conceptual framework for investigating how memory $CD8^+$ T-cells develop from naïve precursors following antigenic stimulation. These models are not mutually exclusive and in the end lead to the development of effector T-cells with greater memory potential and others that are terminally differentiated. In between these two memory $CD8^+$ T-cell types are a variety of effector $CD8^+$ T-cells with intermediate properties. While these models propose different $CD8^+$ T-cells developmental pathways, they do not address the rate of memory $CD8^+$ T-cells generation.

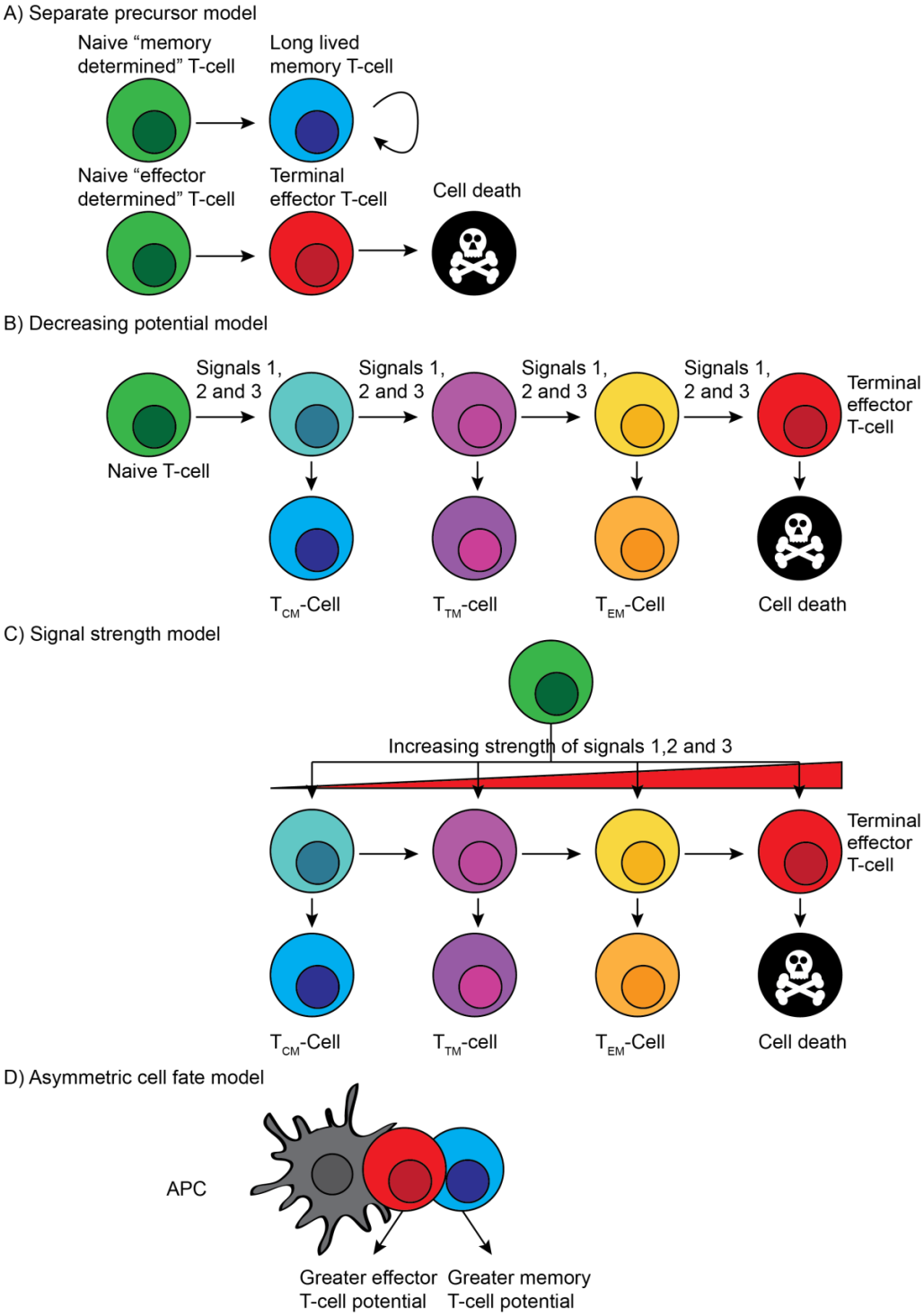


Figure 1-2 **Models of effector and memory T-cell generation**. A) Separate precursor model; naïve T-cells are pre-programmed to adopt certain differentiation states following activation. B) Decreasing potential model; effector T-cells adopt numerous differentiation states according to the cumulative history of signals they have received. Repetitive stimulation drives effector T-cells to become terminally differentiated. C) Signal strength model; Heterogeneous effector T-cell populations is dependent on the overall strength of signals encountered early during T-cell priming. Strong signals drive clonal expansion and development of memory but excess signal may cause terminal differentiation. D) Asymmetric cell fate model; effector and memory T-cells arise from a single precursor, the cell that is closer to the APC adopts an effector cell fate and the distal cell adopts a memory fate.

1.4 Secondary $CD8^+$ T-cell response and secondary memory

Our understanding of memory $CD8^+$ T-cell development primarily comes from analysis during primary acute infection and primary vaccination. Much less is known about the generation and maintenance of secondary or tertiary memory $CD8^+$ T-cells. During an individuals lifetime $CD8^+$ T-cells will be repeatedly – or, in the case of chronic infections, persistently - stimulated. The effects caused by repeated stimulation vary depending on the type of infection. The secondary $CD8^+$ T-cell response to infection by the same pathogen is characterized by robust proliferation of antigen-specific $CD8^+$ T-cells. Memory $CD8^+$ T-cells persist in a extended T_{EM} cell state, with increased cytotoxicity and high levels of granzyme B and KLRG1, and low levels of CD62L, CCR7 and CD27(43,44). Secondary and tertiary memory cells express IL-7Rα and can persist long term despite their reduced ability to undergo homeostatic proliferation.

Compared to primary memory $CD8^+$ T-cells, secondary memory $CD8^+$ T-cells are slow to acquire central memory phenotype and exhibit less basal proliferation(43). In addition, the kinetics of a secondary response exhibit a faster expansion peak, sustained effector functions and a protracted contraction phase compared to primary responses. As with primary $CD8^+$ T-cells, the phenotype of secondary memory $CD8^+$ T-cells is affected by the pre-existing memory cell precursor frequency, the amount and type of inflammation and the level of T-bet expression(45,46). These secondary memory $CD8^+$ T-cells look more like effector $CD8^+$ T-cells, with increased expression of CCR5, IL-2Rα, T-bet, ID2 and Blimp1 and decreased levels of CCR7, CD62L, TCF1 and ID3 compared to primary memory $CD8^+$ T-cells(44). Repetitive stimulation does not induce $CD8^+$ T-cell exhaustion such as up-regulation of PD1 and LAG3.

With the loss of T_{CM} cells in secondary infection there is the possibility that over repeated stimulations the pool of memory $CD8^+$ T-cells may become senescent: this has been documented in adoptive transfer experiments (47). In contrast, multiple infections of immune mice shows that the $CD8^+$ T-cells can be repeatedly stimulated, increasing the numbers of antigen specific memory $CD8^+$ T-cells(48). This increase in frequency may form a "herd immunity" by reducing re-exposure of memory $CD8^+$ T-cells to signals that drive terminal differentiation, maintaining the fitness of the $CD8^+$ T-cell pool.

1.5 Requirement for a 3rd signal for $CD8^+$ T-cell differentiation

Naïve $CD8^+$ T-cells can be stimulated by antigen and CD28–dependent co-stimulation to undergo several rounds of cell division, but programming for survival, effector function and memory requires a third signal. Four pro-inflammatory cytokines, IL-12, type I interferon (IFNα), type II interferon (IFNγ) and IL-21 have been identified as capable in providing signal 3 for optimal $CD8^+$ T-cell expansion and development of effector function.

Using artificial APCs (aAPCs) cells to determine the minimal requirements for activating naïve and memory $CD8^+$ T-cell from transgenic-TCR mice it was found that aAPCs containing MHC/peptide and B7 ligands were ineffective in stimulating $CD8^+$ T-cells responses (49). The addition of IL-12, type I IFNs or IL-21 promoted clonal expansion and acquisition of effector functions by the responding naïve CD8 T cells(50)

Signal 3 cytokines play a role in the development in programming memory. By stimulating purified $CD8^+$ T-cells under defined conditions, followed by transfer into

naive mice to monitor the transition to memory it has been shown that $CD8^+$ T-cells stimulated for 3 days in vitro, under conditions with signal 3, could rapidly differentiate into memory $CD8^+$ T-cells and persist long term upon transfer(51,52) but without signal 3 cells die within a few days of transfer(53). In contrast, the addition of IL-12, stimulated $CD8^+$ T-cells continued to expand for several days following transfer, then contracted and surviving cells included both a T_{CM} and T_{EM} cells.

Experiments using adoptive transfer of transgenic $CD8^+$ T-cells lacking the receptor for either type I IFNs or type II IFNs in a viral infection model provided evidence that direct signalling by these cytokines to responding $CD8^+$ T-cells is essential for an optimal response(54,55). Analysis revealed that clonal expansion was almost completely abrogated, and $CD8^+$ T-cells failed to accumulate due to decreased survival during proliferation when compared to the receptor-sufficient cells. However, memory $CD8^+$ T-cell generation and maintenance is still detectable in the absence of type I IFN signalling or IL-12 signalling following viral or bacterial infection(56). Interestingly, the requirement of specific cytokine signalling for optimal $CD8^+$ T-cell responses is dependent on the pathogen. For example, type I IFN signalling in $CD8^+$ T-cells appeared critical for expansion in LCMV infection model while the absence of IL-12 or IFNα signalling resulted in a much less severe defect in this model(57). IL-21 can also provide a signal 3 activity(58); during chronic infection it can provide a signal to $CD8^+$ T-cells to prevent deletion(59-61).

During $CD8^+$ T-cell differentiation, IL-12 can promote the expansion of terminally differentiated $CD8^+$ T-cells in a T-bet dependent manner(62,63). However, IL-12 can provide a crucial signal needed for memory development under conditions where the promotion of terminally differentiated $CD8^+$ T-cells does not occur(53). Neither IL-12

nor IFNα signalling are required for the formation of terminally differentiated $CD8^+$ T-cells - however it has been shown that continuing Ag signalling can lead generation of such cells (18).Together these results suggest that IL-12 can provide a signal necessary for the development of central and effector memory $CD8^+$ T-cells.

Strong evidence has accumulated over the past decade demonstrating the role of inflammatory cytokines in regulating multiple aspects of the $CD8^+$ T-cell response following infection. However, much less is known about the impact of inflammatory cytokines on memory $CD8^+$ T-cells differentiation and generation.

1.6 $CD8^+$ T-cell transcriptional programming

When a $CD8^+$ T-cell is activated it is exposed to an array of stimulatory signals, such as chemokines, cytokines, growth factors, nutrients and co-stimulatory molecules. These signals are transmitted and translated into gene expression patterns that promote differentiation through transcription factors. Over the past decade several transcription factors that regulate different differentiation pathways have started to be elucidated, some of which function in pairs that form counter-regulatory axes to control effector and memory potential. Further increasing our understanding of the transcriptional profile that regulates differentiation could allow us to produce more effective vaccines by inducing the correct response required for controlling infection.

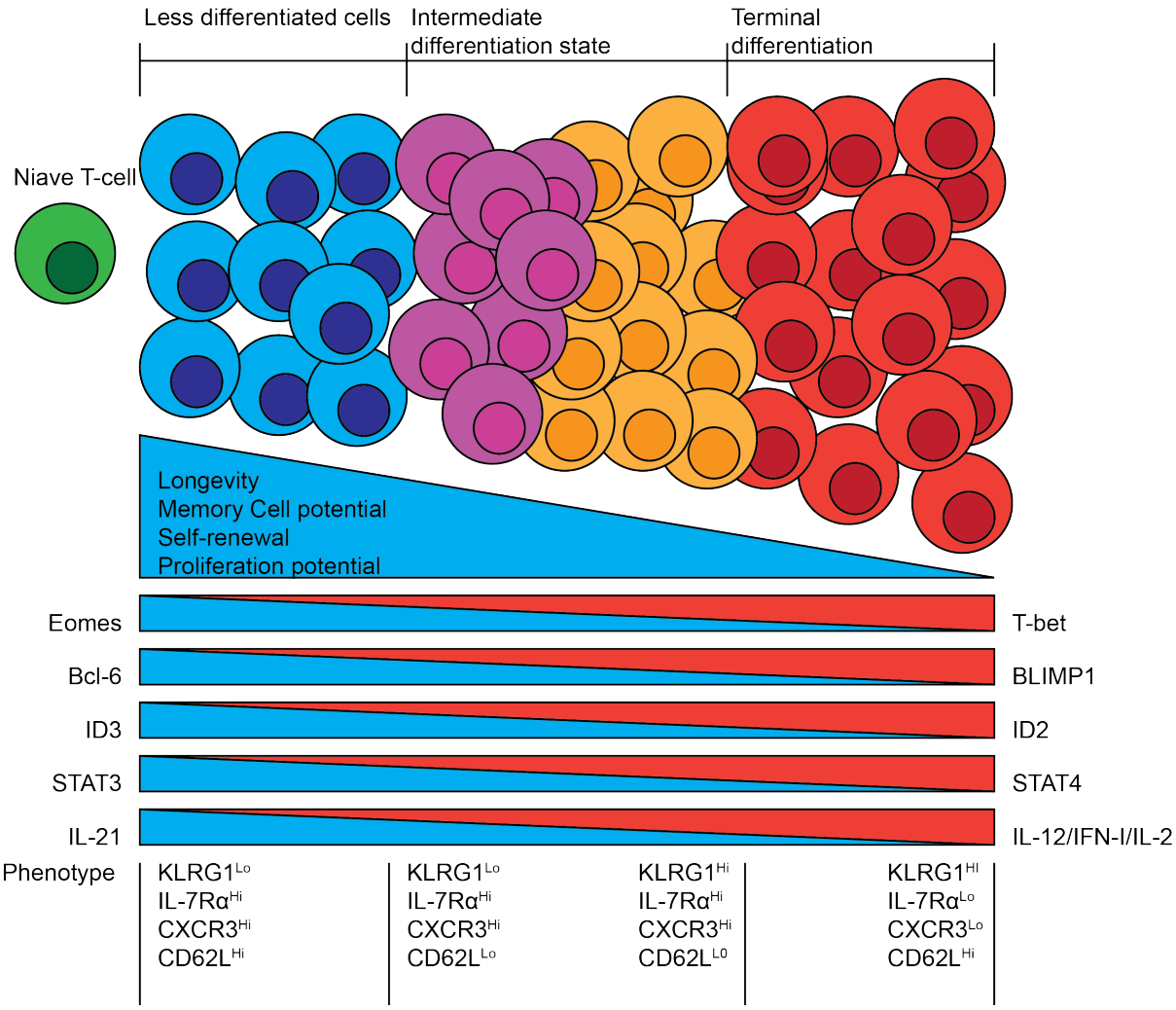


Figure 1-3 **Graded activity of transcriptional programmes that control memory CD8$^+$ T-cell generation**. Inflammatory cytokines type I IFN, IL-2 and IL-21 dictate the balance between short-lived effector and memory generation. In this model cells with a greater longevity and proliferation potential are at one end and terminally differentiated effector CD8$^+$ T-cell are at the other. In between these two extremes are effector and intermediate differentiation states. The transcriptional programmes that control terminal effector and memory CD8$^+$ T-cell differentiation are based on graded expression of certain competing sets of transcription factors. The heterogeneous differentiation states of effector CD8$^+$ T-cells can be distinguished by their expression of several markers such as KLRG1, IL-7Rα, CXCR3 and CD62L.

T-bet and Eomes. These T-box transcription factors have crucial roles in the formation and function of effector and memory $CD8^+$ T-cells. They co-operate through partially redundant mechanisms, creating CTLs by inducing expression of IFNγ, Granzyme B, perforin and CXCR3(64-66). T-bet expression is induced by TCR signalling and amplified by IL-12 mediated signals and mTOR activity in $CD8^+$ T-cells(67,68). Eomes expression is induced in a RUNX3 dependent manner and is amplified by IL-2, while IL-12 represses expression and mTOR partially, through inhibition in of FOXO1 transcription(68-70).

Memory $CD8^+$ T-cells are sustained by co-operation between T-bet and Eomes through the expression of IL-2Rβ (CD122), enabling IL-15 mediated signalling and homeostatic proliferation(64,65). $CD8^+$ T-cells devoid of T-bet are impaired in forming terminally differentiated effector cells ($KLRG1^{Hi}$, IL-$7R\alpha^{Lo}$), also over-expression of T-bet drives $CD8^+$ T-cells into terminal differentiation; thus, achieving a balance in expression level of T-bet is important in inducing a long lasting functional memory response(62). In comparison $CD8^+$ T-cells lacking Eomes are capable of forming terminally differentiated effector cells, but are unable to form memory cells with normal expression of CD122, CD62L and CXCR3, which are involved in lymph node homing and homeostatic proliferation. Therefore deficiency in Eomes leads to a lack of T_{CM} cells and impaired homeostatic proliferation(65).

While T-bet and Eomes have overlapping functions, their expression pattern in CD8+ T-cells is divergent. T-bet expression is up-regulated in early effector $CD8^+$ T-cells, then declines as memory $CD8^+$ T-cells form(45). In contrast Eomes expression is up-regulated in early effector $CD8^+$ T-cells, by IL-2, but further increases expression as $CD8^+$ T-cells progress from effector to memory cells, due to its role in

homeostasis(71). The balance in expression levels of Eomes and T-bet determines the function and memory potential of effector $CD8^+$ T-cells. However, there is little known about how the ratio of these transcription factors is determined, although the balance of pro-inflammatory cytokines (IL-12 and IL-2) and other factors during infection are able to regulate expression, so the cytokines that $CD8^+$ T-cells are exposed to will determine the cells' fate.

Blimp1 and Bcl-6. These transcription factors are antagonistic and function as genetic switches for cell fate decisions in B- and T-cells(72). Blimp1 is a transcriptional repressor, highly expressed by effector $CD8^+$ T-cells, induced by IL-2, IL-12 and IL-21(73,74). Expression declines in memory $CD8^+$ T-cells and it is expressed at low levels in T_{CM} cells. Blimp1 is one of the transcription factors involved in the formation of terminally differentiated effector $CD8^+$ T-cells and enhancing CTL functions such as IFNγ and Granzyme B(75,76). Knockout studies have shown that mice form a greater number of central memory $CD8^+$ T-cells(77), although these animals have impaired ability to clear influenza virus due to their inability to recruit $CD8^+$ T-cells to the lung(78). However, longitudinal studies showed that differences between wild type and Blimp1 deficient memory $CD8^+$ T-cells over time are very small due to homeostatic pressure and that Blimp1 expression declines in the memory phase.

Bcl-6 is an antagonist of Blimp1: its expression inversely correlates with that of Blimp1 in effector and memory $CD8^+$ T-cells(79). Central memory $CD8^+$ T-cells express higher levels of Bcl-6 than effector $CD8^+$ T-cells, gradually increasing expression as $CD8^+$ T-cells mature. Expression is induced by IL-10 and IL-21 signalling through STAT3. Bcl-6 is critical for the formation of central memory $CD8^+$

T-cells(80) and over-expression leads to increased numbers of central memory $CD8^+$ T-cells(81). Recent studies show that Bcl-6 and T-bet directly interact. One mechanism T-bet uses is to directly repress transcription is by recruiting Bcl-6 to a subset of target genes(82). Furthermore, T-bet can block the DNA binding domain of Bcl-6, thus repressing its ability to repress target genes(83,84). Thus low levels of Bcl-6 are required for T-bet to effectively modulate T-cell gene programs, and the levels of expression of both T-bet and Bcl-6 will determine effector and memory $CD8^+$ T-cell formation.

ID2 and ID3. These gene products are key transcriptional regulators that control many aspects of lymphocyte development. ID proteins heterodimerize with E proteins (such as E2A and HEB) preventing their binding to target sites(85,86). ID2 supports the survival of effector $CD8^+$ T-cells in the early stages of naïve to effector maturation. However, ID3 supports the survival of $CD8^+$ T-cells in the memory phase(87-89). In addition, ID2 is important in the formation of terminal effector $CD8^+$ T-cells, knockout studies showed that ID2 deficient cells generated a robust response, reaching their peak of expansion sooner than wild type. However, as the response proceeded far fewer cells were generated and the few cells that survived rapidly declined, due to greater apoptosis(87). In contrast, ID3 is important in the generation of central memory $CD8^+$ T-cells, being high in memory precursor $CD8^+$ T-cells, and its expression increases the survival of effector $CD8^+$ T-cells that would normally die in the contraction phase(87). The regulation and expression levels of ID2 and ID3 differ in effector $CD8^+$ T-cells. ID3 is a direct target of Blimp1 mediated repression. While ID2 mediates expression of pro and anti-apoptotic genes including Bcl-2 and BIM, ID3 induces expression of FOXM1, a transcription factor involved in

DNA replication, both functioning in a non-redundant manner to modulate differentiation and survival of $CD8^+$ T-cells.

STATs. The JAK-STAT signalling pathway controls many downstream pathways in the differentiation of $CD8^+$ T-cells, their survival and homeostasis. The binding of a cytokine to its surface receptor results in receptor dimerization and subsequent activation of JAK tyrosine kinases. Following this, specific tyrosine residues on the receptor are phosphorylated by activated JAKs and serve as docking sites for the family of cytoplasmic transcription factors, STATs. STATs are phosphorylated by JAKs, then dimerize and subsequently leave the receptor and translocate to the nucleus, where they activate gene transcription(90). Multiple STATs can activate downstream of a single receptor, complicating the process of elucidating the function of individual STATs. STAT1 and STAT4 are activated by type I IFNs. In effector $CD8^+$ T-cells STAT1 levels decline as they proliferate during viral infection(91); STAT4 is activated by IL-12, enhances T-bet expression and terminal differentiation of effector $CD8^+$ T-cells (53). This shows that type I mediated signalling quantitatively changes a STAT1 dominated response to STAT4 response. STAT5a and STAT5b can enhance responses by regulating T-bet and IL-12R(92) They are essential for the survival of viral-specific $CD8^+$ T-cells and expression of Bcl-2(93). STAT3 is also important, mediating signals by IL-10 and IL-21. Expression of such molecules as Eomes, Bcl-6 and Blimp1 are all reduced in Stat3 deficient $CD8^+$ T-cells(79).

While activation of STATs drives transcription of genes involved in cell proliferation, function and survival, they also induce the transcription of Suppressor of cytokine signalling (SOCS) genes. SOCS proteins are important inhibitors that refine the quality and quantity of JAK-STAT signalling in $CD8^+$ T-cells. SOCS members act as negative feedback inhibitors, induced by cytokines and subsequently inhibiting their

function. There are four major ways SOCS proteins inhibit cytokine signalling: (1) blocking STAT recruitment to the cytokine receptor; (2) targeting the receptor for degradation by the proteasome; (3) binding JAKs and directly inhibiting their kinase activity; (4) targeting JAKs for degradation by the proteasome. There are eight members of the SOCS family (SOCS1-7, and CIS) that all contain a conserved SOCS box.

SOCS proteins are regulated at the transcriptional, translational and post-translational levels. Transcription is initiated by many cytokines and IFN families(94,95). It has become clear that they play critical roles in regulating $CD8^+$ T-cell development, differentiation and function. SOCS1 knockout mice gradually accumulate $CD8^+$ T-cells(96). Up-regulation of SOCS3 by IL-6 in the bone marrow promotes the generation of $CD8^+$ T-cells, in part by the up-regulation of Notch1 on $CD8^+$ T-cells(97). SOCS members play a non-redundant role in $CD8^+$ T-cell maturation. Cytokines in the γc family, such as IL-2, IL-7, IL-15 and Il-21, play are role in maturation and function of $CD8^+$ T-cells. These cytokine signals, transmitted by STAT molecules, (98) are regulated by SOCS family members. SOCS1 blocks IL-7 signalling in naïve $CD8^+$ T-cells and SOCS1 depletion results in a skewing towards the $CD8^+$ T-cell lineage (99,100).

Naïve cells fail to proliferate in response to IL-7 and IL-15, but do so when combined with IL-21(101). Priming of naïve $CD8^+$ T-cells by IL-21 can arrest differentiation(102) resulting in the generation of a subset of T-cells designated “T memory stem cells”(103). IL-21 induces SOCS1 expression in $CD8^+$ T-cells(104), and in SOCS1 deficient mice, IL-21 potentiates IL-7 and IL-15 induced proliferation in $CD8^+$ T-cells. These mice have increased numbers of central memory $CD8^+$ T-cells(96,105), and

the generation of memory $CD8^+$ T-cells could be due to unobstructed IL-15 signalling pathway(106).

Other SOCS members may be involved in the regulation of effector memory $CD8^+$ T-cells. Two such members are SOCS3 and CIS as both are implicated in blocking IL-2 signalling (107,108). Additionally, however, SOCS2 might be involved in the degradation of SOCS3 which may enhance IL-2 signalling and thus generation of effector memory $CD8^+$ T-cell(109). The function of $CD8^+$ T-cells can be altered by the SOCS family - specifically SOCS1 is up-regulated in T_{EM} and its removal results in enhanced T_{EM} cell proliferation and IFNγ production(110). Deletion of SOCS3, which regulates IL-2, IL-6 and IL-27, can enhance $CD8^+$ T-cell proliferation(111), although over-expression does not impair $CD8^+$ T-cell function.

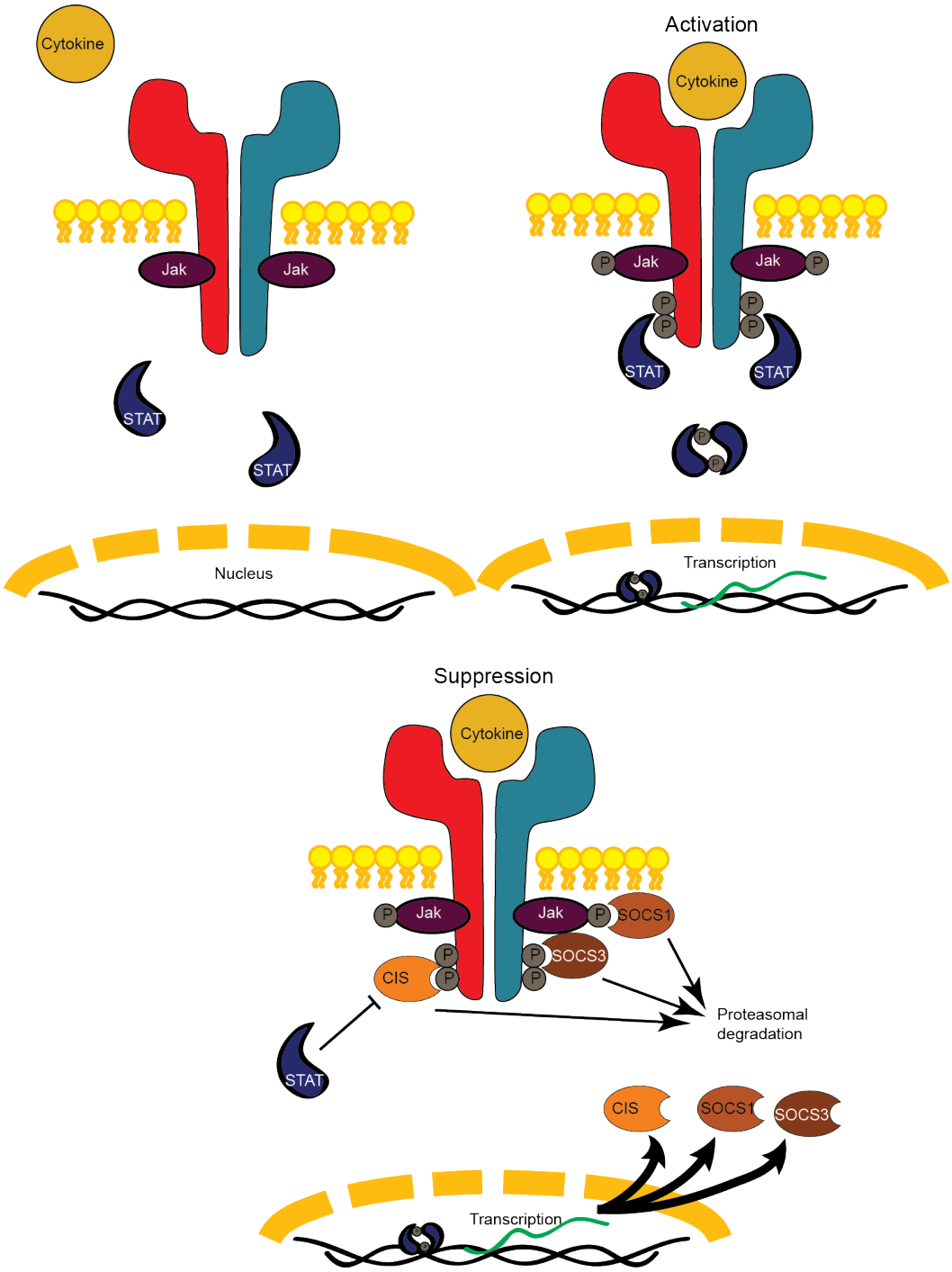


Figure 1-4 **SOCS proteins are negative-feedback inhibitors of cytokine signal transduction**. In unstimulated cells, signalling molecules - Jaks and STATs - are inactive. After receptors bind cytokines, aggregation occurs, and receptor associated Jaks are brought together allowing phosphorylation and activation. STATs are recruited through specific interactions with phosphorylated tyrosine residues on receptors. The STATs become phosphorylated, dimerize and translocate to the nucleus, activating transcription of cytokine responsive genes such as SOCS proteins. The SOCS proteins act in a negative feedback loop to terminate signal transduction. SOCS1 interacts with Jaks directly inhibiting their catalytic activity. CIS binds to receptor sites and blocks the recruitment and activation of STATs. SOCS3 inhibits Jaks after gaining access to receptor binding. SOCS proteins also interact with cellular ubiquitination machinery and directly associated proteins such as Jaks or receptors for ubiquitin mediated proteasomal degradation.

Summary: Overall, the transcriptional programmes that control effector $CD8^+$ T-cells differentiation and memory cell potential are based on graded expression of competing transcription factors. A increased in expression of T-bet. BLIMP1, ID2 and STAT4 leads to an increase in effector $CD8^+$ T-cell terminal differentiation, this is associated with reduction in proliferation and longevity of $CD8^+$ T-cells. In contrast, an increase in Eomes, Bcl-6, ID3, TCF1, and STAT3 prevents terminal differentiation and leads to a T_{CM} response, enhancing survival and proliferation potential of $CD8^+$ T-cells.

1.7 Memory inflation

Cytomegalovirus (CMV) is a herpesvirus that establishes persistent infection. It is well controlled by the immune system; however, controlling reactivation requires consistent T-cell immune surveillance. Virus-specific $CD8^+$ T-cells do not uniformly contract after the virus enters latency and are maintained at a high frequency, are functional and have an effector memory phenotype(112,113). Recent studies have shown that CMV is an effective vaccine vector candidate due to its ability to induce high numbers of functional effector $CD8^+$ T-cells that traffic to peripheral tissue(114,115).

Herpesviruses are large DNA viruses that have evolved an estimated 180-220 million years ago and have co-speciated with their hosts ever since(116). Herpesviruses establish persistence or latent infection and induce little pathology in healthy hosts. Human cytomegalovirus (CMV) is a ubiquitous member of the β-subfamily of herpesviruses with 60-80% of people in the developed world being infected by 80 years of age(117). Primary infection typically occurs in childhood and

is usually asymptomatic. After an acute phase during which infectious virions are shed, CMV is controlled to levels that are just below the detectable limit. Persistent CMV infection is characterised by periods of viral reactivation and shedding, and consistent immune surveillance to keep the virus under control(117).

During viral infections, $CD8^+$ T-cells encounter antigen and proliferate, forming large populations in the acute phase, contracting as they enter the memory phase. In comparison, a few HCMV-specific $CD8^+$ T-cells responses do not contract in the memory phase and are maintained at a high frequency, one epitope specific $CD8^+$ T-cell making up to 10% of the $CD8^+$ T-cell compartment(112). This specific $CD8^+$ T-cell response has been termed “memory inflation”.

Using murine CMV (MCMV) as a model it has been possible to study memory inflation to try and elucidate the specific requirements that allow $CD8^+$ T-cells to be maintained a high frequency. Inflation was first described in BALB/c mice(118) and further analysed in longitudinal studies(112). During acute infection of C57BL/6 mice there are $CD8^+$ T-cells specific for at least 24 epitopes derived from 18 viral proteins. However, in latency, all but five epitope specific $CD8^+$ T-cells contract(119). These inflationary responses are derived from both immediate early and late genes; the general assumption is that these populations are the direct result of ongoing viral activation.

MCMV-specific $CD8^+$ T-cells produce perforin, granzymes, can kill target cells, and they secrete IFNγ and TNFα but produce limited IL-2. Many of the MCMV-specific $CD8^+$ T-cells that were immunodominant during the acute phase, contract in the memory phase, persisting at low levels, and have a central memory phenotype ($CD62L^{Hi}$, $CD127^{Hi}$, $CD27^{Hi}$, $KLRG1^{Lo}$). However, inflationary $CD8^+$ T-cells have a

phenotype of repeated antigen stimulation, and display an effector memory phenotype ($CD62L^{Lo}$, $CD127^{Lo}$, $CD27^{Lo}$, $KLRG1^{Hi}$)(113). These inflationary cells are low in expression of CD62L and the chemokine receptor CCR7 that allow access to the lymph nodes, and they are found patrolling the peripheral organs(113,120) although, they are also found at low numbers in hematopoietic organs. They have low expression of IL-7 and IL-15 receptors, cytokines important in homeostatic maintenance of memory T-cells. In humans they have short telomeres, indicating extensive proliferation(121). The frequency of these cells correlates with the amount of virus at the peak of infection(122). Importantly they remain functional and do not show features of exhaustion(113,123). The specific combinations of stimuli that produce these effector cells and induce proliferation are poorly understood, although they are now being addressed.

Beyond the phenotype described above, inflationary $CD8^+$ T-cells up-regulate a number of NK-cell receptors including the activating receptor NKG2D and inhibitory receptors NKG2A and KLRG1(113,124,125). KLRG1 expression is associated with repeated antigen stimulation(23); however, it is also up-regulated during acute viral infections. It has been postulated that these cells are senescent due to the up-regulation of KLRG1, although in adoptive transfer experiments inflationary $CD8^+$ T-cells divide after MCMV challenge(113).

Antigen persistence: Inflationary $CD8^+$ T-cells' requirement for antigen in order to be maintained was analysed by adoptive transfer experiments. If these inflationary $CD8^+$ T-cells are transferred into naïve recipients they failed to divide and survive, whereas the same cells were maintained when transferred into chronically infected mice(113). These cells seem to be repeatedly stimulated, while non-inflationary

$CD8^+$ T-cells retain co-stimulatory molecules, suggesting they are not repeatedly stimulated and are maintained when adoptively transferred into naïve hosts.

Expression of the epitope is key to inducing inflation. Epitopes capable of inducing inflation in the context of MCMV, were not capable of inducing inflation any longer expressed in a recombinant vaccinia virus (112). Taken with a recent study, showing that a MCMV mutant unable to spread between cells by deletion of the essential glycoprotein L did not impair memory inflation(126), these data suggest that consistent expression is required in latency to induce inflation.

Epitopes for non-inflationary and inflationary $CD8^+$ T-cells can be found in the same genes(119), so merely the level of gene expression is not enough to dictate if an inflationary response will occur. Recent data showed that non-inflationary and inflationary epitopes have different processing requirements. Non-inflationary epitopes depend on the immunoproteasome for production(127). The immunoproteasome is constitutively expressed by professional antigen presenting cells, while non-professional antigen presenting cells do not constitutively express the immunoproteasome. Thus these peptides may rarely be produced during chronic infection. There is evidence that non-hematopoietic cells - particularly endothelial cells - are a major site of MCMV latency(128-130), and using bone marrow chimeras, it has been shown that inflation is depended on antigen presentation by non-hematopoietic cells. This has led to an interesting hypothesis, that these non-haematopoietic antigen presenting cells would only be able to process and present antigens whose processing is independent of the immunoproteasome. It has still not been defined by which process such cells present inflationary antigens during latency, whether by direct or cross–presentation. Recent work showed that in $BATF^{-/-}$

mice, which are impaired in cross-priming due to the lack of $CD8\alpha^+$ and $CD103^+$ DCs, inflation still occurred but at a lower frequency(131).

In acute infection MCMV replicates in diverse tissue such as the spleen, liver and lung, whereas the salivary glands are the primary site for the persistent phase(132). However, removal of the salivary glands does not influence inflation(117,133). The tissue where latent virus reactivates is important; this includes the lung, where sporadic reactivation produces intermittent or transcripts(117,133) and $CD8^+$ T-cells control viral reactivation by epitope-specific sensing of transcriptional reactivation.

Co-stimulation and help: While locating the cell type expressing the inflationary epitopes are key to further out understanding, further work has assessed the importance in co-stimulation. Co-stimulatory molecules providing the "second signal" and cytokines ("third signal") have been shown to be important in affecting the size and duration of $CD8^+$ T-cells responses. Knockout studies show that CD28, one of the key co-stimulatory molecules which binds to CD80 on APCs, is dispensable for inflation(134). While it affects the levels of $CD8^+$ T-cells in the acute phase, inflationary $CD8^+$ T-cells reach the same levels as WT in the memory phase.

In comparison, the stimulatory molecule OX40, in knockout (KO) studies had no effect in the acute phase, but in the memory phase inflationary $CD8^+$ T-cells were diminished in number(135). This is potentially due to OX40L expression on $CD4^+$ T-cells rather that on $CD8^+$ T-cells. OX40 has no effect on the proliferation abilities of $CD4^+$ T-cells in the first three days of infection, however after this $CD4^+$ T-cells have and increased rate of apoptosis due to low levels of anti-apoptosis proteins (Bcl-2, $Bcl\text{-}X_L$ and SURVIVIN) (136,137). In the acute phase of MCMV infection, there was

no difference in IL-2 production by $CD4^+$ T-cells in wild-type (WT) and OX40 Kos - however in the memory phase, cells from WT mice produced substantially more IL-2.

Another co-stimulatory molecule, 4-1BB, is up-regulated by activated T-cells and participates in regulation of T-cell functions. In mice lacking 4-1BB, an increase in MCMV-specific $CD8^+$ T-cells was seen in the acute phase, but memory inflationary $CD8^+$ T-cells were decreased in comparison to WT mice(138). 4-1BB co-stimulates responses of both $CD4^+$ and $CD8^+$ T-cells, and signalling via this molecule also results in the activation of T-regs(139). This would explain the increase in MCMV-specific $CD8^+$ T-cells in the acute phase, but not the decrease in inflationary $CD8^+$ T-cells, since it has been shown that IL-10 helps to control the level of inflation(139). 4-1BB/L has not been show to be up-regulated on inflationary $CD8^+$ T-cells, so while knockout studies showed it to be important in inflation, whether it has a direct or indirect effect on inflationary $CD8^+$ T-cells has not been addressed.

CD8 T-cells require cytokines for proliferation, differentiation and survival. In the case of inflationary $CD8^+$ T-cells, that cannot produce IL-2(119), it has been shown that IL-2 is essential for the maintenance of inflationary $CD8^+$ T-cells but not for non-inflationary $CD8^+$ T-cells. This was shown using a bone marrow chimeric mouse model with wild type and IL-$2RA^{-/-}$ cells(140). As well as stimulating proliferation, cytokines such as IL-10 can limit proliferation, IL-10 has been shown to limit the expansion of inflationary $CD8^+$ T-cells(139). Other cytokines such as IL-7 and IL-15, which are important in homeostatic proliferation and IL-12 for providing a “third signal”, will play important role in MCMV-specific $CD8^+$ T-cell responses but their roles in inflationary $CD8^+$ T-cells have yet to be elucidated.

While $CD4^+$ T-cells are required for control of MCMV infection(141), during chronic infection, they are important in the development and maintenance of inflationary $CD8^+$ T-cells(142,143). This could be through providing cytokines such as IL-2 and as mentioned previously or providing co-stimulatory signals (OX40 and 4-1BB).

Mechanisms that drive a T-cell to become inflationary or central memory $CD8^+$ T-cells are still unclear. In HCMV infection, studies of specific $CD8^+$ T-cells indicate that individual T-cell clones can be found within both the inflationary and memory populations(144); this shows that the population does not arise from a specific T-cell receptor. Following the lineage of specific $CD8^+$ T-cells by barcoding may provide more clues to the differences in the differentiation of specific $CD8^+$ T-cells(32,145), being able to follow them through the acute phase and into memory.

Turnover and longevity: Questions remain as to the longevity of inflationary $CD8^+$ T-cells. There is little proliferation of inflationary $CD8^+$ T-cells in the memory phase(112,120). One hypothesis is that these inflationary $CD8^+$ T-cells are long lived, resting effector cells that circulate for long periods and suppress reactivation or replication of the virus. The inflationary $CD8^+$ T-cells may not undergo much cell division after each stimulation due to down regulation of co-stimulatory receptors, unless the appropriate conditions are met, and it has been shown that CMV-specific clones can persist for years(144,146). To support this hypothesis in humans, CD45RA+ CMV specific $CD8^+$ T-cells only emerge after resolution of acute infection(147), and restimulation in vitro promotes re-expression of CD45RO(148), this suggests that this subset is resting and have not recently been stimulated. Accumulation of inflationary $CD8^+$ T-cells occurs due to their long half-life and sporadic cell division.

Alternatively the inflationary $CD8^+$ T-cell population could be made-up of a mixed population of effector and memory $CD8^+$ T-cells. The effector $CD8^+$ T-cells will make up the majority of the inflationary $CD8^+$ T-cell population, being short lived and continually replaced as they die. This hypothesis is supported by the fact that adoptive transfer of inflationary $CD8^+$ T-cells into naive or chronically infected animals failed to be maintained(113). As these short-lived effector $CD8^+$ T-cells die, they are continuously being replaced, by new short lived effector $CD8^+$ T-cells to maintain the size of the inflationary population that are arising from the lymph node after stimulation(129). However, adoptive transfer experiments showed that an insufficient number of $CD8^+$ T-cells were recruited from the naïve pool to maintain inflation(113), therefore a population of memory $CD8^+$ T-cells generated during the acute phase must be repeatedly stimulated to produce new short-lived effector $CD8^+$ T-cells

Other settings for memory inflation: Inflation has subsequently been discovered in responses to other persistent infections. Herpes simplex virus 1 is a ubiquitous α-herpes virus that establishes latency within sensory neurons. Lifelong infection is associated with spontaneous virus reactivation with persistent viral gene expression(149,150). $CD8^+$ T-cells are important in controlling virus and establishment of latency(151). In the sensory ganglia $CD8^+$ T-cells specific for glycoprotein B-derived epitope gradually accumulate(152). These gB-specific $CD8^+$ T-cells block HSV-1 reactivation from latently infected ganglia(153), remain functional and are maintained at a high frequency for the lifetime of the host. Memory inflation also occurs in murine polyomavirus (PyV) persistent infection model. $CD8^+$ T-cells recognising a peptide presented by Q9, an MHC class Ib molecule, increase in frequency over 3 months before being stability maintained(154). Data from human

studies include, in addition to HCMV, similar data from human parvoviruses B19(155) and PARV4(156) As more epitopes are screened the number of viruses inducing inflationary $CD8^+$ T-cells is likely to expand.

1.8 Transcriptional studies of CD8+ T cell development

Using flow cytometry has allowed longitudinal studies to be performed and has led to a wealth of information on the development of different $CD8^+$ T-cell subtypes, but it is limited by the use of specific antibodies and on our current understanding of immunology. Combining flow cytometry with gene arrays to analyse large-scale gene expression of $CD8^+$ T-cells has brought about an unprecedented wealth of data about the complexity of $CD8^+$ T-cells and will help lead to a more complete understanding into $CD8^+$ T-cell development. Also with groups continuously adding new makers to the cell types they are studying and describing them as novel, by analysing the complete transcriptome it will avoid such confusion in the description of specific cell types and the supposed specific markers. A gene expression signature could be used to define a cell state or phenotype rather than a few markers for biological interest.

Networks of genes control the $CD8^+$ T-cell, sometimes acting as negative feedback loops, so analysing the full transcriptome is probably the most reliable method of deciphering the networks that control the development of a $CD8^+$ T-cell. It has been possible to define groups of genes whose expression is co-ordinated by shared regulatory networks. With the addition of computational methods for reverse engineering it is possible to apply a model of the cells' control system(157).

The first studies on $CD8^+$ T-cells using gene arrays confirmed what was all already known about the activation state, cell cycle control and changes after stimulation of T-cell(158,159). Subsequently the molecular profile of $CD8^+$ T-cell differentiation was measured by sorting tetramer specific $CD8^+$ T-cells after LCMV infection(160). From this study it suggested that memory cells were not just at a resting state but were actually in a distinct state of differentiation, and that these changes are slow in occurring, with differentiation still occurring after viral clearance. It has been suggested that expression profiles of memory $CD8^+$ T-cells are intermediate between those of naïve and effector $CD8^+$ T-cells(161).

It has now become relatively common to use gene arrays to analyse $CD8^+$ T-cells following the differentiation(162) and distinguishing between naïve, effector T_{EM} and T_{CM} subsets(163) and using improved RNA extraction methods arrays can even be used to analyse small number of cells from cord blood(164). Using new and ever more complex analyse methods it has been possible to elucidate networks of enriched pathways in $CD8^+$ T-cells associated with specific diseases such as HIV(165). Recently gene arrays were applied to memory exhaustion after LCMV infection and discovered a connection to inhibitory receptors PD1, TIM3, CD160 and Lag3(166) which has then be used to elucidate the underlying transcription factors that control the inhibitory function of these cells(167) and the gene network that is linked to exhaustion(168).

Following this, studies on $CD8^+$ T-cell development after HCMV infection have been carried out revealing that infection induces a up-regulation of NK-cell receptors(169) and looking in further depth at the transcription factors up-regulated such as T-Bet and their effector function(123). The mouse model of MCMV provides a highly controlled setting to address these profiles in more detail, with a focus on memory

inflation in contrast to conventional memory, in the same animal in response to the same defined pathogen challenge

1.9 Aims of this thesis

1: Analyse the transcriptional profile of $CD8^+$ T-cell memory inflation induced by MCMV and compare this to conventional “non-inflating” memory.

2: Analyse the transcriptional profile of $CD8^+$ T-cell memory inflation induced by a recombinant non-replicating adenovirus vector and find a specific transcriptional signature for memory inflation.

3: Define the turnover rate and stability $CD8^+$ T-cell memory inflation.

4: Address whether expression of the surface molecule CD73 has an impact on $CD8^+$ T-cell memory inflation

2 Materials and Methods

2.1 Mice

C57BL/6 mice we bred in a specific pathogen free animal facility at University of Oxford, Biomedical Sciences (BMS), UK, or obtained from Harlan UK. C57BL/6 CD45.1 and C57BL/6 $CD73^{-/-}$ mice were bred in a specific pathogen free animal facility at University of Oxford, BMS, UK. Experiments were performed using age matched control mice with the permission of the Home office according to the Animals Procedures Act of 1986.

2.2 Viruses

MCMV strain (Strain Smith, ATCC: VR194) was used and kindly provided by Professor U,H, Koszinoswki, Department of Virology, Max von Pettenkofer Institute, Munich Germany. MCMV was propagated and titrated on NIH 3T3 cells (ECACC, UK), stored at -80°C and injected intravenously at a dose of $2x10^6$ pfu.

Recombinant adenovirus expressing the βgal protein under the control of the human CMV promoter (Ad-LacZ) and lacking E1 and E3 genes was used. Ad-LacZ was propagated on permissive HER-911 cells and was purified with the Vivapure AdenoPack 20 (Sartorius, Stedim biotech, 13781 Aubagne Cedex, France) according to the manufacturer's specifications. Ad-LacZ was stored at -80°C in PBS and injected intravenously at a dose of $2x10^9$ pfu.

2.3 Production of MHC class tetrameric complexes

2.3.1 Production and purification of proteins

The MHC class I heavy chain was modified: the leader sequence, trans-membrane region and the cytoplasmic tail were removed and a biotinylation signal sequence for the BirA enzyme was added to the C-terminus. The vector used for the expression of the H-2Kb and H-2Db was the pET24a. And isopropyl-ß-D-thiogalactopyranoside (IPTG) inducted T7 polymerase system was used. This vector was transformed into BL21(DE3)pLYsS *E.coli* strain by heat shock. 1ul of plasmid was added to the 20ul competent bacteria and incubated on ice for 2 minutes. 100ul lysogeny broth (LB) medium was added to the bacteria and incubated at 37°C for an hour before being plated out onto an agar plate containing ampicillin and chloramphenicol. The plates were incubated overnight at 37°C and the next day a single colony was picked to inoculate a 5ml of LB medium containing ampicilin and chloramphenicol, this was incubated overnight at 37°C on a shaking platform. The next day this was used to inoculate 3 litres LB medium. The bacterial growth was monitored by optical density (OD) at 600nm and when it reached an OD 0f 0.6, 1ml of 1M IPTG was added to each litre to induce the protein production. The bacteria were then grown for a further 6 hours. The bacteria were then spun down at 3000g for 30 minutes at 4°C. The bacterial pellet was resuspended in 40ml resuspension buffer (50mM Tris, 100mM NaCl, 1mM EDTA, 5mM DTT, 0.1% azide, pH 8.0). The solution was sonicated (5-10 bursts or 30 seconds) on cell disruption complete. The solution was then centrifuged at 2700g for 10 minutes at 4°C. The supernatent was discarded and the inclusion bodies were subjected to three triton washes (0.5% Triton, 50mM Tris, 100mM NaCl,

1mM EDTA, 5mM DTT, 0.1% azide, pH 8.0). Each wash was performed by resuspending the pellet, homogenisation, then pelleting at 2700g for 10 minutes at 4°C. The protein was finally resuspended in 10ml of urea buffer (8M Urea, 50mM MES, 0.1M EDTA, 1mM DTT) and left overnight on a rolling platform at 4°C. Then the protein concentration was measured and stored at -80°C in 15mg aliquots.

2.3.2 Refolding, concentration, biotinylation and purification of MHC class I complexes

1mg of the appropriate peptide dissolved in 100ul DMSO was added to 500ml of pre-cooled refolding buffer (100mM Tris pH 8. 400mM L-arginine, 2mM EDTA, 5mM reducing Glutathione, 0.5mM oxidising Glutathione). 15mg of MHC class I heavy chain was then added drop-wise to the solution followed by 15mg of $ß_2$-microglobulin. The solution was left with a constant stirring at 4°C for 12 hours. To eliminate precipitate the solution was filtered through a 70µm filter and using a 10kDa hollow fiber (MiniKros Sampler, JM seperations) concentrated down to 20ml. The solution was then added to a 10kDa Centricon Plus (Milipore) for further concentration and spun at 2000g until there was 2.5ml of solution left. Using disposable PD10 columns (Amersham), a buffer exchange into BirA buffer (10mM Tris pH 8) was performed. First the columns were equilibrated with 25ml of BirA buffer, then 2.5ml of concentrated refold was added onto the column followed by 3.5ml of BirA and the eluent collected. 3.5ml of BirA buffer was added to the eluent along with 4µg/ml leupeptin (Sigma), 1µg/ml pepstatin (Sigma) and 2.4µg/ml AEBSF (Sigma). For the biotinylation reaction 1ml of Biomix A (0.5M bicine, pH 8.3), 1ml of Biomix B (100mM ATP, 100mM MgOAc, 200µM biotin, pH 8), d-biotin (500µM) and 5ug of BirA (Avidity) was added and incubated overnight at room temperature.

The refolded, biotinylated complexes were then purified by size exclusion get filtration chromatography, using Superdex-75 HiLoad 26/70 column (GE healthcare). The column was equilibrated with 400ml FPLC buffer (20mM Tris pH8, 50mM NaCl, filtered through a 0.22µm filter). The appropriate fractions were collected and concentrated using 10kDa Centricon Plus (Milipore). The protein was concentration was determined using nanodrop (Thermo Scientific) and diluted to a concentration of 0.5ug/ul. 4µg/ml leupeptin (Sigma), 1µg/ml pepstatin (Sigma) and 2.4µg/ml AEBSF (Sigma) was added and the monomers were stored at -80°C.

2.3.3 Peptides

Peptides derived from MCMV, M38316-323 (SSPPMFRV) and M45985-993 (HGIRNASFI) were purchased from Proimmune, Oxford, UK. The βgal96-103 (DAPIYTNV) and the βgal497-504 (ICPMYARV) peptides were purchased from Mimotopes (Victoria, Australia).

2.3.4 Tetramerization

The amount of Phycoerythin (PE), Allophycocyanin (APC) or Saporin conjugated Streptavidin to add was calculated to give a 1:1 ratio of biotinylated MHC class I molecules: biotin binding sites. This was added in 1/10th volumes waiting 10 minutes between additions. Tetramerized complexes were stored at 4°C.

2.4 Cell preparation and cell Separation in vitro

2.4.1 Isolations of lymphocytes

Spleens were harvested in PBS and disintegrated using 70µm plastic net strainer. The resulting cell suspension was washed and peleted by centrifugation. The pellet

was resuspended in ACK lysis buffer for red cell lysis. The pellets were resuspended in RPMI-5%.

To isolate lymphocytes from the lung tissue; lungs were harvested in PBS, dissected into small cubes and digested with collagenase and DNAse for 1 hour at 37°C. Organs were passed through a 70µm nylon filter, washed in PBS, pelleted and resuspended in ACK lysis buffer, then washed in PBS and resuspended in FACS buffer.

Bone marrow was isolated by washing the femur shaft with FACS buffer and passing it through a 70µm nylon filter, pelleted and resuspended in ACK lysis buffer, then washed in PBS and resuspended in FACS buffer.

For isolating cells from the liver, tissue was perfused via the hepatic artery with ice cold PBS and organs harvested into PBS. Livers were disintegrated using a 70µm filter and pelleted by centrifugation. The pellet was resuspended in 5ml 30% Percoll (Amersham Biosciences) and layered on a 70% Percoll solution in a 15ml Falcon tube. Samples were centrifuged (300g) for 25 minutes without brakes and the leukocyte population at the interface recovered, washed in PBS and resuspended in FACS Buffer.

Blood was harvested into 5ml round bottomed Falcon tubes (BD Biosciences) containing 4ml of FACS buffer either by bleeding from the tail vein or aspiration from the left ventricle post mortem.

2.4.2 Sorting cells by MACS

$CD8^+$ T cells were isolated from spleens. Single cell suspensions were obtained. Cells were resuspended and filtered in FACS buffer at a concentration of 10^7/90ul

cells. Cells were purified by negative selection using $CD8^+$ T cell selection kit (Miltenyi) adding the appropriate antibody and incubating at 4°C for 10 minutes. The magnetic beads were then added and cells incubated for a further 10 minutes in the fridge. Cells were washed and resuspended in 1ml FACS buffer and sorted using the AutoMACS (Miltenyi).

2.4.3 Cell sorting by MoFLO

Four spleens were pooled per group. Lymphocytes were harvested as described above and $CD8^+$ T cells were negatively sorted using MACS beads, described above. Cells were pelleted at 300g for 5 minutes and resuspended in 1ml FACS buffer and 10ul of appropriate antibody and tetramer added, cells were incubated for 1 hour on a rolling platform at 4°C; cells were washed, filtered through a 20µm nylon filter and resuspended in 3ml FACS buffer. Cells were sorted using MoFlo (BechmanCoulter) in FACS buffer. Cells were pelleted at 300g for 10 minutes and snap frozen using methanol and dry ice.

2.4.4 Peptide restimulation

Lymphocytes were isolated as described above and added at a concentration of $1x10^6$ cells/well in a 96 well plate. Cells were stimulated for 2 hours at 37°C with either 10^{-4}M peptide. As a positive control cells were stimulated with phorbol myristate acetate (PMA) (50 ng/ml) and ionomycin (500 ng/ml) or left untreated as a negative control. GolgiPlug (1µl/1ml final concentration) from BD Bioscience (Oxford, UK) was added to each well and cells incubated for a further 4 hours at 37°C. Plates were centrifuged at 300gfor 5 minutes and resuspended in 150ul FACS buffer

2.5 Flow Cytometry

Cells were analysed by flow cytometry using a BD LSR II flow cytometer and FlowJo software, gated on viable leukocytes using the live/dead fixable near-IR dead cell stain kit from Invitrogen (Paisley, UK).

2.5.1 Tetramer staining

Tetramer staining was performed on 50ul of whole blood or $1x10^6$ cells in a 96 well plate. Samples were pelleted and resuspended 50µl FACS buffer and the appropriate tetramers and incubated at 37°C for 15 minutes. Plates were centrifuged at 300g for 5 minutes and washed with FACS buffer. The samples were then stained with the relevant surface antibodies.

2.5.2 Extracellular antibody staining

For staining of surface molecules, $1x10^6$ cells were pelleted in a 96 well plate, then resuspended in 50µl FACS buffer containing the appropriate antibodies and incubated for 30 minutes at 4 °C. Cells were washed in 150µl of FACS buffer and centrifuged at 300g for 5 minutes. The pellet was resuspended in 200µl of FACS buffer.

Antibody	Flourochrome	Manufacturer
Bcl2	FITC	Biolegend
BTLA	PE	eBioscience
CCL3/MIP-1	FITC	R&D
CCL4	-	R&D
CCL5	-	R&D
CCL9	-	R&D
CCR5	Alexa Fluor-488	Biolegend
CD107a (Lamp 1)	Alexa Fluor-647	Biolegend
CD122	Alexa Fluor-647	eBioscience
CD126 (IL-6R)	PE	eBioscience
CD127 (IL-7R)	PE-Cy7	eBioscience
CD160	PE	eBioscience
CD26	PerCp-Cy5.5	eBioscience
CD27	PerCp-Cy5.5	Biolegend
CD3	Alexa Fluor-700	eBioscience
CD44	FITC	BD
CD45.1	eFluor-450	eBioscience
CD54 (ICAM-1)	FITC	BD
CD62L	PE-Cy7	eBioscience
CD8	eFluor-450	eBioscience
CD8	PerCp-Cy5.5	eBioscience
CRACC/SLAMF7	FITC	R&D
CX3CR1	-	R&D
CXCR3 (CD183)	PerCP-Cy5.5	eBioscience
eomes	PerCP-eFluor-710	eBioscience
F(ab) donkey Anti Goat	FITC	Immunoresearch
GITR	PE-Cy7	eBioscience
ICOS1	PerCP-eFluor-710	eBioscience
IFNg	Efluor-450	eBioscience
IL-18Ra	FITC	R&D
Ki67	FITC	BD
KLRG1	PE-Cy7	eBioscience
LAG-3	PE	R&D
Ly-6C	PerCP-Cy5.5	eBioscience
NKG2A	PerCP-eFluor-710	eBioscience
NKG2D (CD314)	FITC	Biolegend
PD1 (CD279)	PE-Cy7	Biolegend
T-Bet	PE-Cy7	eBioscience
Tim3	FITC	R&D
TNF a	FITC	eBioscience
XCL1	-	R&D

Table 2-1. List of antibodies.

2.5.3 Intracellular antibody staining

Following the staining of surface as described above. Cells were fixed, permeabilized using FOXP3 Fixation/Permeabilisation Kit (ebioscience), the cells were permeabilised using 150ul ebioscience Fix/Perm buffer for 10 minutes at 4°C. The samples were pelleted at 300g for 5 minutes, washed with 150ul permeablisation buffer and pelleted at 300g for 5 minutes. The samples were then resuspended in permeablisation buffer containing the appropriate antibody for 30 minutes at 4°C, washed twice with permeablisation buffer and resuspended in 150ul FACS buffer.

2.6 *In vivo* assays

2.6.1 *In vivo* cytotoxicitiy assay (In vivo killing assay)

Splenocytes from naïve C57BL/6 mice were pulsed with 10^{-4} M of the relevant peptide in 500µl RPMI 5% FCS for 1 hour at 37°C, cells were washed twice with PBS. The cells were then labelled with either 5mM CellTrace Violet (Invitrogen) or 0.5mM CellTrace Violet (Invitrogen), incubated for 20 minutes at 37°C, then 5x volume RPMI 5% FCS was added and cells pelleted at 300g for 5 minutes. Cells were then washed twice with PBS and resuspended 10ml PBS.

The control population of unplulsed splenocytes from naïve C57BL/6 mice were labelled with 5mM carboxyflouresceindiacetate-succinimidyl ester (CFSE) for 5 minutes at 37°C, CFSE was neutralised by the addition of 1ml FCS, the cells were then at 300g for 5 minutes and washed with twice with PBS and resuspended in 10ml PBS.

Control and pulsed cells were then mixed at equal numbers and before being injected into the tail veins of naïve and MCMV infected mice. After 12hours the mice were bled, and the organs harvested. Samples were acquired on a LSRII and analysed with Flowjo (Tree star).

2.6.2 Adoptive transfer

Single cells suspensions from spleens, cells were washed were subjected to ACK lysis buffer, washed with PBS, counted and diluted to a concentration of $1x10^6$ cells/ml in PBS and incubated with 10μM Carboxyfluorescein succinimidyl ester (CFSE) for 5 minutes at 37°C, CFSE neutralised with the addition of 1ml FCS, cells were washed with FACS buffer and resuspended at a concentration of $6x10^7$ cells/ml, 500ul was injected per mouse.

2.7 Transcriptional analysis

2.7.1 RNA extraction amplification and hybridization

Total RNA was isolated from sorted cells using mirVana Kit (Ambion) according to manufactures instructions. RNA integrity was checked using Agilent 2100 Bioanalyzer, samples with a RIN value of 8 or more were used for amplification. cDNA was synthesized and cRNA made using Illumina Total Prep RNA amplification Kit (Ambion). Samples were hybridized to Illumina MouseWG-6 v2.0 at the Welcome Trust Centre for Human Genetics, University Of Oxford.

2.7.2 DNA extraction

Tissues were homogenised using MagNa Lyser instrument (Roche) and DNA was isolated using the High Pure PCR Template Preparation Kit (Roche) as per manufactures instructions.

2.7.3 Microarray data analysis

Gene expression data were obtained by hybridising a total of 12 samples from 4 experimental groups (n=3 per group) to Illumina MouseWG6 Expression BeadChips. Raw data were exported from the Illumina GenomeStudio software (v1.0.6) for further processing and analysis using R statistical software (v2.10) and BioConductor packages. Raw signal intensities were background corrected using array-specific measures of background intensity based on negative control probes, prior to being transformed and normalized using the 'vsn' package. Quality control analyses did not reveal any outlier samples. The dataset was then filtered to remove probes not detected (detection score <0.95) in any of the samples.

Statistical analysis was performed using the Linear Models for Microarray Analysis (limma) package. Differential expression between the experimental groups was assessed by generating relevant contrasts corresponding to the various two-group comparisons. Raw p-values were corrected for multiple testing using the false discovery rate controlling procedure of Benjamini and Hochberg, adjusted p-values below 0.01 were considered significant. Significant probe lists were then annotated using the relevant annotation file (MouseWG6_V2_0_R0_11278593_A) that was downloaded from the Illumina website (http://www.illumina.com) for further biological investigation.

2.7.4 Further methods for gene transcriptional analysis

Only genes, which were at least two fold differently expressed compared to naïve $CD8^+$ T cells were used for the following analysis. Gene clustering was performed using comparative marker selection from genepattern (www.genepattern.broad.institute.org/gp/pages/index.jsf). Genecodis (www. Genecodis.cnb.csic.es) was used to execute gene ontology analysis on clusters. To compare MCMV-specific and bgal-specific inflationary $CD8^+$ T cells genes were ranked according to the p-values and gene set enrichment analysis (GSEA) was run (www.broadinstitute.org/gsea/index.jsp).

2.7.5 Quantitative real-time PCR for selected genes

Quantitative real-time PCR was performed using a Light cycler 480 Real-Time PCR System (Roche Diagnostics) and the LightCycler 480 probes master reaction mix (Roche Diagnostics) following the manufacturer's protocol. Data analysis was performed with LightCycler 480 Software (Roche Diagnostics). Oligonucleotides were purchased from Eurofins MWG Operon (Ebersberg, Germany). Oligonucleotides sequences used as primers for quantitative real-time PCR and corresponding probes from the Universal Probelibrary from Roche applied Science are shown in table 2. Thermal cycling started with HotStarTaq activation during 10 min at 95°C. Thereafter 45 cycles of amplification were run consisting of 10 s at 95°C, 30 s 60°C, and 20 s of 72°C. A negative control, containing reagents only, and serial dilutions of cDNA were included in each run. Each sample was measured as a triplicate and the average concentration was used. For LightCycler analysis, expression of hypoxanthine phosphoribosyltransferase gene (HPRT) was used for normalization. Relative expression of samples from naive and MCMV-infected or Ad-

LacZ immunized mice was calculated by the comparative cycling threshold method ($\Delta\Delta C_T$).

Oligoname	Sequence
ZEB2_P42_for	ccagaggaaacaaggatttcag
ZEB2_P42_rev	aggcctgacatgtagtcttgtg
ROG_P019_for	tccggcctcaagatcaga
ROG_P109_rev	gggaaaagatcctggagtgg
KLRE1_P26_for	gggaagaccattcggttctac
KLRE1_P26_rev	tgcacagaagtttttcatattagctt
IL10Ra_P19_for	gctcccattcctcgtcac
IL10Ra_P19_rev	aagggcttggcagttctgt
ID2_P89_for	gacagaaccaggcgtcca
ID2_P89_rev	agctcagaagggaattcagatg
HPRT_P95_for	tcctcctcagaccgctttt
HPRT_P95_rev	cctggttcatcatcgctaatc
FOXM1_P11_for	actttaagcacattgccaagc
FOXM1_P11_rev	ggagagaaaggttgtgacgaa
CISH_P1_for	gacatggtcctttgcgtaca
CISH_P1_rev	atgccccagtgggtaagg
Blimp1_P80_for	tgcggagaggctccacta
Blimp1_P80_rev	tgggttgctttccgtttg
Birc5_P71_for	cccgatgacaacccgata
Birc5_P71_rev	catctgcttcttgacagtgagg
MCMV_gB_For	agggcttggagaggacctaca
MCMV_gB_Rev	gcccgtcggcagtctagtc
MCMV_Probe1	gctctattgatactccgcgcgtta
MCMV_Probe2	aacagctagacgacagccaacgcaccg

Table 2-2 . List of probes used in qRT-PCR

3 CD8+ T-cell memory inflation induced by MCMV

3.1 Introduction

Following viral infection, naive $CD8^+$ T-cells are activated upon encounter with specific antigen, proliferate, acquire effector functions and differentiate into effector $CD8^+$ T-cells. Most effector $CD8^+$ T-cells die by apoptosis after viral clearance but about 5% survive and differentiate into memory cells. These memory cells down-regulate some properties of effector $CD8^+$ T-cells but retain the capacity to rapidly reactivate effector function upon antigen encounter. Depending on their phenotype they can be broadly categorized into one of two memory populations, central memory $CD8^+$ T-cells (T_{CM}) and effector $CD8^+$ T-cells (T_{EM}). T_{CM} are distinguished by the re-expression of homing markers such as CD62L and CCR7 allowing them to migrate to secondary lymphoid organs and are maintained by homeostatic proliferation responding to cytokines IL7 and IL-15(170). Furthermore these cells appear to have enhanced sensitivity to antigen that leads to a rapid recall response(39) and due to these properties they provide long term protection(17). T_{EM} are memory cells that have lost the constitutive expression of CCR7 and CD62L and a display characteristic set of chemokine and cytokine receptors and adhesion molecules that are required for homing to inflamed tissue, residing in the periphery(27). When compared to T_{CM}, T_{EM} are characterized by rapid effector function, producing large amounts of perforin, granzymes, IFNγ and TNFα. It is thought that T_{EM} require the presence of antigen to persist due to the lack of IL-7R and IL-15R expression; however this has been challenged by the finding of long term maintenance of effector cells in organs such as the skin(171,172).

The $CD8^+$ T-cell responses to MCMV are extremely large and broadly directed. Viral infection leads to an disseminated acute lytic replication followed by life long latency, with sporadic low level replication(117). As the virus establishes latency, a small number of immunodominant epitopes arise. These CMV-specific cells accumulate over time and are eventually stabilized at a high frequency, In chronic infection a $CD8^+$ T-cell response specific for one epitope can compose up to 20% of $CD8^+$ T-cells(112). This phenomenon has been termed “memory inflation”, in contrast to the immunodominant epitope specific $CD8^+$ T cell response from the acute phase (M45) that shows a classical memory response. The key defining feature of memory inflation was initially dynamic – a quantitative increase in the memory pool over time. However, subsequently it has been extended to include populations which are sustained but do not further increase and possess similar “effector memory” phenotypes(119)

Inflationary $CD8^+$ T-cells show a T_{EM} phenotype suggesting that their accumulation and maintenance is driven by viral antigen. It has been postulated that during MCMV latency low levels of viral gene expression in latently infected cells, would constantly stimulate inflationary $CD8^+$ T-cells which in turn would prematurely terminate such viral reactivation attempts(117). However in chronic LCMV infection $CD8^+$ T-cells become exhausted due to repetitive stimulation; they up-regulate the exhaustion marker PD1 and are no longer able to produce IFNγ(166). This is apparently not the case with inflationary $CD8^+$ T-cells that are still functional during chronic infection.

Here we analyzed the molecular profile of inflationary $CD8^+$ T-cells in a well-characterized model of MCMV infection. We compared M38-speciifc inflationary $CD8^+$ T-cells to non-inflationary M45-specific $CD8^+$ T-cells and to acute effector

$CD8^+$ T-cells generated. This approach has revealed a subset of genes that is uniquely expressed in inflationary cells. Many genes encoding cytokine and chemokine receptors are differentially expressed. The fractalkine receptor CX3CR1 is up-regulated and while they are low in Bcl-2 expression compared to M45-specific $CD8^+$ T-cells they express the apoptotic inhibitor Bcl-X_L and have a unique transcription factor expression profile.

3.1.1 Key questions in this chapter

1. What are the key transcriptional features of memory inflation?

2. How do they compare to the transcriptional signature of T-cell exhaustion?

3. Do the transcriptional changes translate into functional and phenotypic changes in inflationary T-cells?

3.2 Results

3.2.1 MCMV-specific $CD8^+$ T-cells are maintained at a high frequency and remain functional

Infection of C57BL/6 mice with MCMV induced two different $CD8^+$ T-cell responses. Using MHC class I tetramers, $CD8^+$ T-cell responses to the M38 and M45 epitope were tracked longitudinally. Lymphocytes were harvested from organs from spleen, blood, liver, lung and bone marrow (BM). M38-specific $CD8^+$ T-cells showed robust memory inflation with up to 7.8% of specific $CD8^+$ T-cells in the spleen 50 days post infection (Figure 3-1.A/B) and more than 15% in organs such as liver or lung (Figure 3-2). M45-specific $CD8^+$ T-cells showed a standard memory response peaking at 7 days post infection with a frequency of approximately 9% of $CD8^+$ T-cells. This was followed by a rapid decline to a stable level of around 0.7% M45-specific $CD8^+$ T-cells, which was maintained over time. While M45-specific $CD8^+$ T-cells are immunodominant in acute infection, M38-specific $CD8^+$ T-cells become immunodominant in the memory phase(119).

To check whether these cells were functional, cytokine secretion assays were performed after six hours of stimulation with either the M38 or M45 peptide (Figure 3-1.C/D). Their secretion profile followed that of tetramer staining. At 7 days post infection, stimulation with the M45 peptide induced secretion of IFNγ in 12% of $CD8^+$ T-cells and TNFα in 8% of $CD8^+$ T-cells, declining to around 0.9% and 0.7% of $CD8^+$ T-cells secreting IFNγ and TNFα respectively in the memory phase. Stimulation with the M38 peptide showed an inflationary response. In response to peptide stimulation, 5% of the $CD8^+$ T-cells secreted IFNγ and 2.9% secreted TNFα at 7 days post

infection, increasing to 5.8 % IFNγ and 4.8% TNFα secreting $CD8^+$ T-cells at 50 days post infection (Figure 3-1.C/D).

To assess whether memory inflation was restricted to the spleen, and to see if different organs displayed different proliferation kinetics, lymphocytes from blood, liver, lung and bone marrow, and kidney (data not shown), were analysed for M38- and M45-specific $CD8^+$ T-cells over time. All organs displayed the same profile as seen in the spleen (Figure 3-2). M45-specific $CD8^+$ T-cells rapidly proliferated to 7-14% of $CD8^+$ T-cells, then declining and were maintained at a low frequency of 0.7% $CD8^+$ T-cells. Interestingly in the bone marrow they were maintained at a higher frequency (1.6%). M38-specific $CD8^+$ T-cells increased until 21 days post infection and were maintained at a high frequency of 9-18% across all organs, with the lung showing the highest frequency of 18% M38-specific $CD8^+$ T-cells (Figure 3-2).

In summary, the accumulation of virus-specific $CD8^+$ T-cells following MCMV infection was not restricted to the spleen and a similar inflationary pattern was observed in other organs. The frequency of M38-specific $CD8^+$ T-cells in the spleen, liver, lungs, blood and in the bone marrow increased over time and was maintained at a high frequency. Inflationary M38-specific $CD8^+$ T-cells retained their functionality. They dominated IFNγ and TNFα secretion after peptide stimulation in the memory phase.

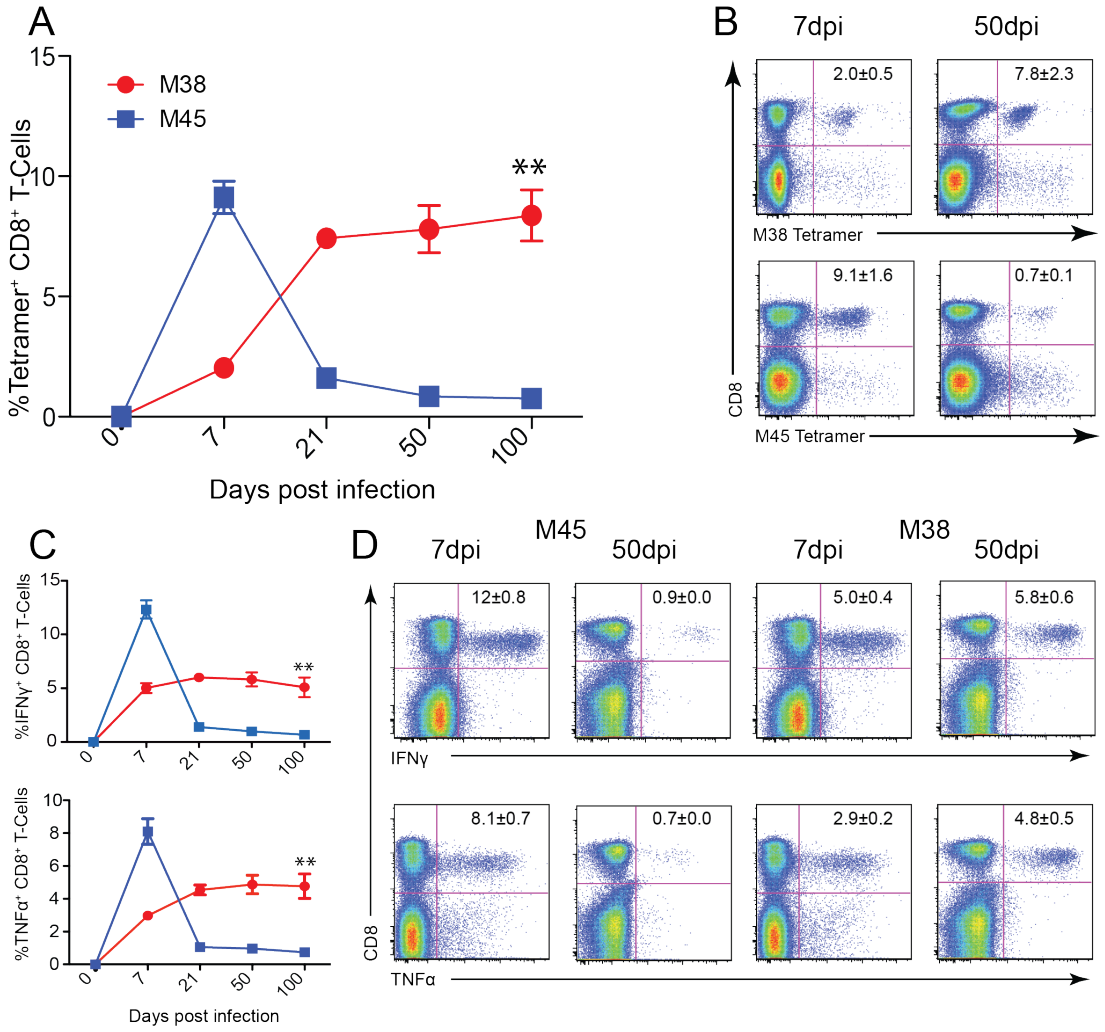


Figure 3-1 **Frequency and function of MCMV-specific CD8$^+$ T-cells.** C57BL/6 mice were infected intravenously (i.v.) with 1x10^6 pfu MCMV. (A) Time course for M38- (red) and M45- (blue) specific CD8$^+$ T-cells. Splenocytes from 0, 7, 21, 50 and 100 days post infection mice were stained with tetramers, and analysed by flow cytometry. Mean percentages of live tetramer$^+$ CD8$^+$ lymphocytes are indicated (n=8, mean±SEM). (B) Tetramer staining for M38 and M45-specific CD8$^+$ T-cells on 7 and 50 days post infection in spleen. Mean percentages of live tetramer$^+$ CD8$^+$ lymphocytes are indicated (n=8, mean±SEM). (C) Time course plotting the percentage of M38- (red) or M45- (blue) specific CD8$^+$ T-cells from the spleen producing IFNγ and TNFα after stimulation with either the M38 or M45 peptide. Mean percentage of IFNγ and TNFα producing cells within the CD8$^+$ T-cell compartment as indicated (n=8, mean±SEM). (D) Representative flow cytometry plots of splenocytes producing IFNγ or TNFα stimulated with either M38 or M45 peptide in mice 7 and 50 days post infection. Gated on live lymphocytes. Numbers indicate the percentage of IFNγ and TNFα positive CD8$^+$ T-cells (n=8, mean±SEM).

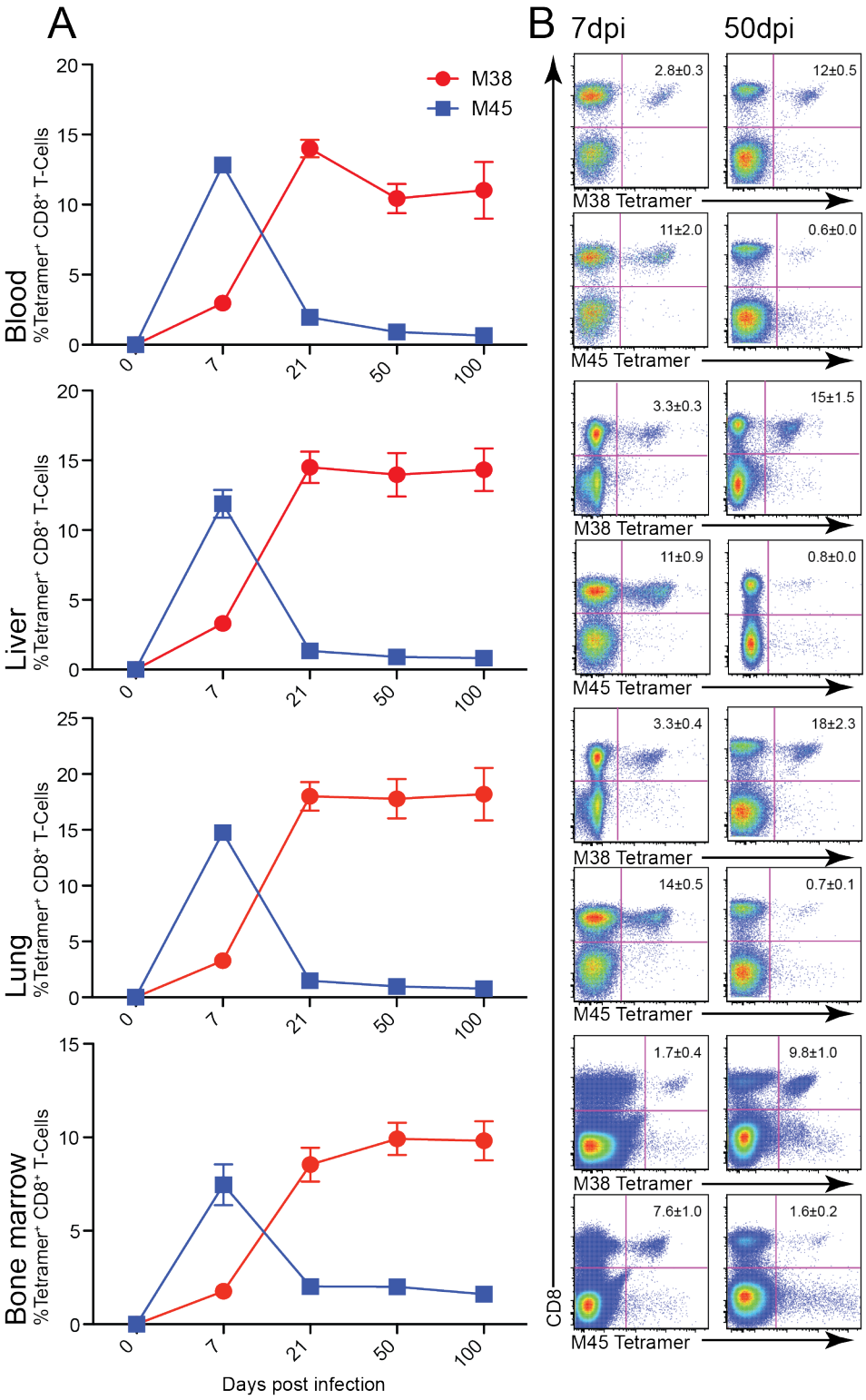


Figure 3-2 **Inflation is not restricted to the spleen.** C57BL/6 mice were infected i.v. with 1x10^6 pfu MCMV and expansion of M38- and M45-specific CD8$^+$ T-cells measured. (A) Time course showing the percentage of M38- (red) and M45- (blue) specific CD8$^+$ T-cells in the blood, liver, lung and bone marrow at 0, 7, 21, 50 and 100 days post infection mice. Mean percentage of live tetramer$^+$ CD8$^+$ lymphocytes is indicated (n=8, mean±SEM). (B) Representative flow cytometry plots of M38 and M45 tetramer staining in the blood, liver, lung and bone marrow on 7 and 50 days post infection mice. Mean percentages of live tetramer$^+$ CD8$^+$ lymphocytes are indicated (n=8, mean±SEM)

3.2.2 Tetramer sorting of MCMV-specific $CD8^+$ T-cells and gene expression array analysis

In order to assess whether there is a transcriptional program supporting memory inflation and to analyse the molecular mechanisms of $CD8^+$ T-cell inflation, a gene expression analysis was performed. Expression profiles of M38-specific inflationary $CD8^+$ T-cells were compared to that of M45-specific $CD8^+$ T-cells that show a central memory phenotype. C57BL/6 mice were infected i.v. with MCMV. Spleens were harvested on 7 and 50 days post infection, lymphocytes were isolated and tetramer staining carried, sort the cells. Purities of >95% were achieved for all sorts (Figure 3-3.A). As a control $CD8^+$ T-cells from naïve mice were sorted ($CD8^+$, $CD3^+$, $CD62L^+$, $CD44^-$).

RNA was extracted from sorted cells, and cDNA run on an Illumina MouseRef-8 v2.0 Expression BeadChip. The gene expression profiles of effector, central memory and inflationary $CD8^+$ T-cells were each compared to naïve $CD8^+$ T-cells so that direct comparisons between the groups could be performed. At 7 days post infection 627 genes were up-regulated and 246 genes down-regulated in M45-specific $CD8^+$ T-cells compared to naïve $CD8^+$ T-cells. At 50 days post infection, in the memory phase, still 400 genes were up-regulated and 168 down-regulated, in M45-specific $CD8^+$ T-cells compared to naïve $CD8^+$ T-cells (Figure 3-3.C). Acute M38-specific $CD8^+$ T-cells (7d.p.i.) up-regulated 964 genes and down-regulated 667 genes. On 50 days post infection, in contrast, the number of up-regulated genes increased to 1088, whereas 553 were down-regulated in M38-specific $CD8^+$ T-cells compared to naïve $CD8^+$ T-cells. This high number of differentially expressed genes in inflationary $CD8^+$ T-cells, which was more than double that of M45-specific $CD8^+$ T-cells, indicates the divergent regulation of this population.

Furthermore, comparing the different $CD8^+$ T-cell populations, it is evident that M38-specific inflationary $CD8^+$ T-cells are neither effector $CD8^+$ T-cells nor are they highly comparable with M45-specific non-inflationary memory $CD8^+$ T-cells (Figure 3-3.D). There are more similarities between the M38-specific acute and memory $CD8^+$ T-cell populations, with 648 differentially expressed genes in common and being unique for M38-specific $CD8^+$ T-cells, than between the two different memory populations with 373 common genes differentially expressed, 302, being shared with all the populations (Figure 3-3.B).

This data indicates that MCMV clearly induced two completely distinct $CD8^+$ T-cell memory responses. The two memory populations share 373 differentially expressed genes. However, M45-specific memory $CD8^+$ T-cells have 118 uniquely differentially expressed genes and the M38-specific inflationary memory $CD8^+$ T-cells have 355 uniquely differentially expressed genes (Figure 3-3.B).

In Figure 3-3.B gene expression signatures that uniquely defined effector, memory and inflationary $CD8^+$ T-cells were also identified. The genes found in M38-specific effector $CD8^+$ T-cells were also partially up regulated in M38-specific inflationary $CD8^+$ T-cells. However the panel of genes that identify M38-specific inflationary $CD8^+$ T-cells was not present in M45-specific $CD8^+$ T-cells.

Overall, analysis of the gene array experiments has identified that the inflationary M38-specific $CD8^+$ T-cells (while being similar to acute M38-specific $CD8^+$ T-cells) have a unique gene expression profile. Inflationary M38-specific $CD8^+$ T-cells have an increased number of differentially expressed genes compared to acute M38-specific $CD8^+$ T-cells and are also distinct from the M45-specific $CD8^+$ T-cell population. M45-specific $CD8^+$ T-cells down-regulate a large number of genes from

the acute phase as they enter the memory phase and most closely resemble naïve $CD8^+$ T-cells, showing a resting memory $CD8^+$ T-cell profile. In contrast, M38-specific $CD8^+$ T-cells keep expressing many of their acute phase genes in addition to their inflationary-specific genes. This indicates that inflation is a distinct state of $CD8^+$ T-cell differentiation.

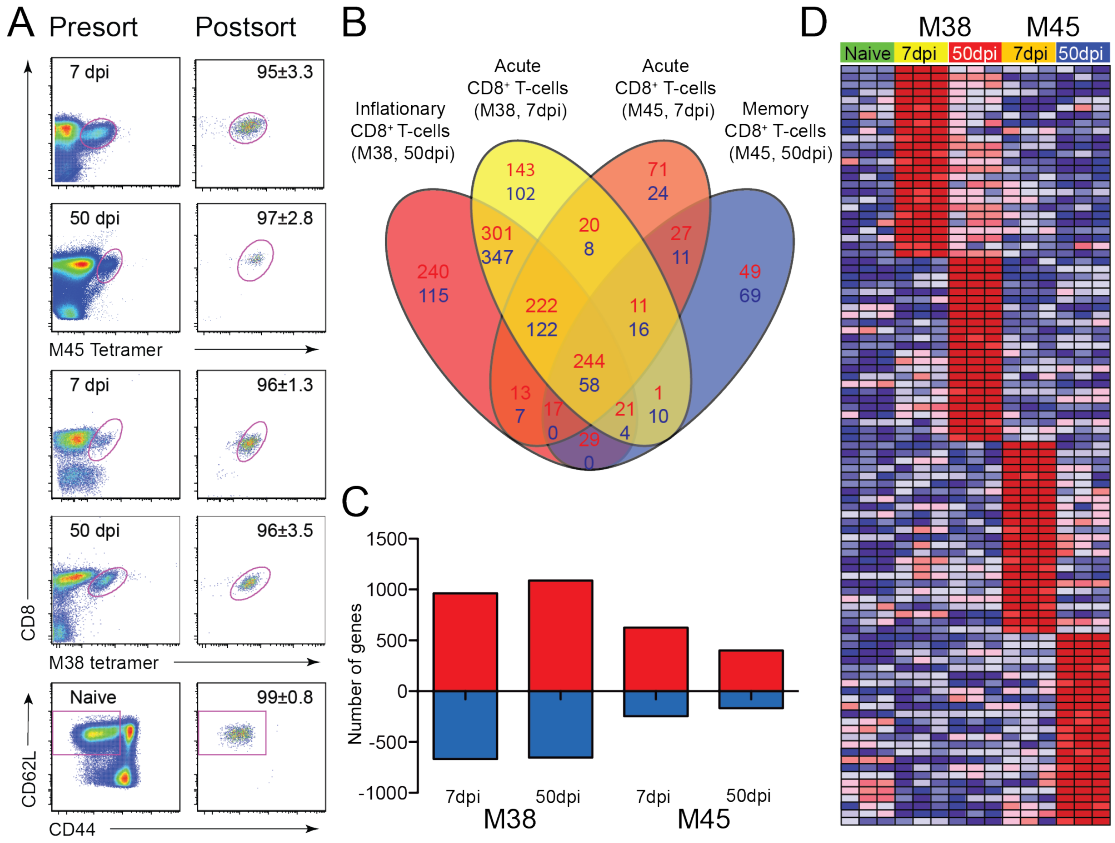


Figure 3-3 **Gene expression signature of MCMV-specific CD8$^+$ T-cells.** C57BL/6 mice were infected i.v. with 1x10^6 pfu MCMV. The expression level of mRNA was measured by microarray analysis of naive CD8$^+$ T-cells (CD62L^{Lo}, CD44^{Hi}), M38-specific CD8$^+$ T-cells 7 and 50 days post infection and M45-specific CD8$^+$ T-cells 7 and 50 days post infection. (A) Representative flow cytometry plots from cell sorts of naive CD8$^+$ T-cell and M38-, M45-specific CD8$^+$ T-cells 7 and 50 days post infection. Cell sorts were performed in triplicates; five mice were pooled per group. Mean percentage of live tetramer$^+$ CD8$^+$ lymphocytes is indicated (n=3, mean±SEM). (B) Venn diagram showing the number of differentially expressed genes between M38-specific CD8$^+$ T-cells 7 (yellow) and 50 (red) days post infection, M45-specific CD8$^+$ T-cells 7 (orange) 50 (blue) days post infection. Filter criteria of at least 2-fold change with P≤0.05 compared to naive CD8$^+$ T-cells. Up-regulated genes are indicated in red and down-regulated genes in blue. (C) Number of genes up-regulated (red) and down regulated (blue) in M38-specific CD8$^+$ T-cells from day 7 and 50 post infection and M45-specific CD8$^+$ T-cells 7 and 50 days post infection, compared to naive CD8$^+$ T-cell. (D) Heat map showing comparative marker selection taking the top 25 uniquely up-regulated genes for each population. Shades of red indicate up-regulated genes; shades of blue indicate down-regulated genes.

3.2.3 Gene ontology analysis of unique gene sets

To further dissect the results of the differentially expressed genes obtained with the gene array, the uniquely up-regulated genes of each population, in comparison to the others groups (Figure 3-3.B), were assessed for biological processes that were significantly enriched via gene ontology (Figure 3-4). In M38-specific inflationary $CD8^+$ T-cells, biological processes that were enriched are involved in metabolic processes (red), regulation of transcription (dark blue), transport (orange), phosphorylation (yellow), protein transport (light blue), cell cycle (dark red), mRNA processing (pink), regulation of catalytic activity (orange) and RNA splicing (green)(Figure 3-4.A).

In contrast, acute M38-specific $CD8^+$ T-cells are less enriched in biological processes. However, the cell cycle group (red) had the largest number of genes enriched (Figure 3-4.C). Further reduction of enriched biological processes was observed at 7 days post infection M45-specific $CD8^+$ T-cells, the cell adhesion group being the highest (Figure 3-4.C). No biological processes were significantly enriched in M45-specific $CD8^+$ T-cells at 50 days post infection

The enrichment of biological processes in acute M38-specific $CD8^+$ T-cells is consistent with the idea that these cells are highly proliferative in comparison to the other $CD8^+$ T-cell populations. Further, the M38-specific inflationary $CD8^+$ T-cells also have many genes enriched belonging to the cell cycle group, possibly indicating that the cells are still proliferating at 50 days post infection. However, M38-specific inflationary $CD8^+$ T-cells also have 26 genes enriched belonging to the group of regulation of transcription, suggesting that inflationary cells may have a distinct transcription factor profile.

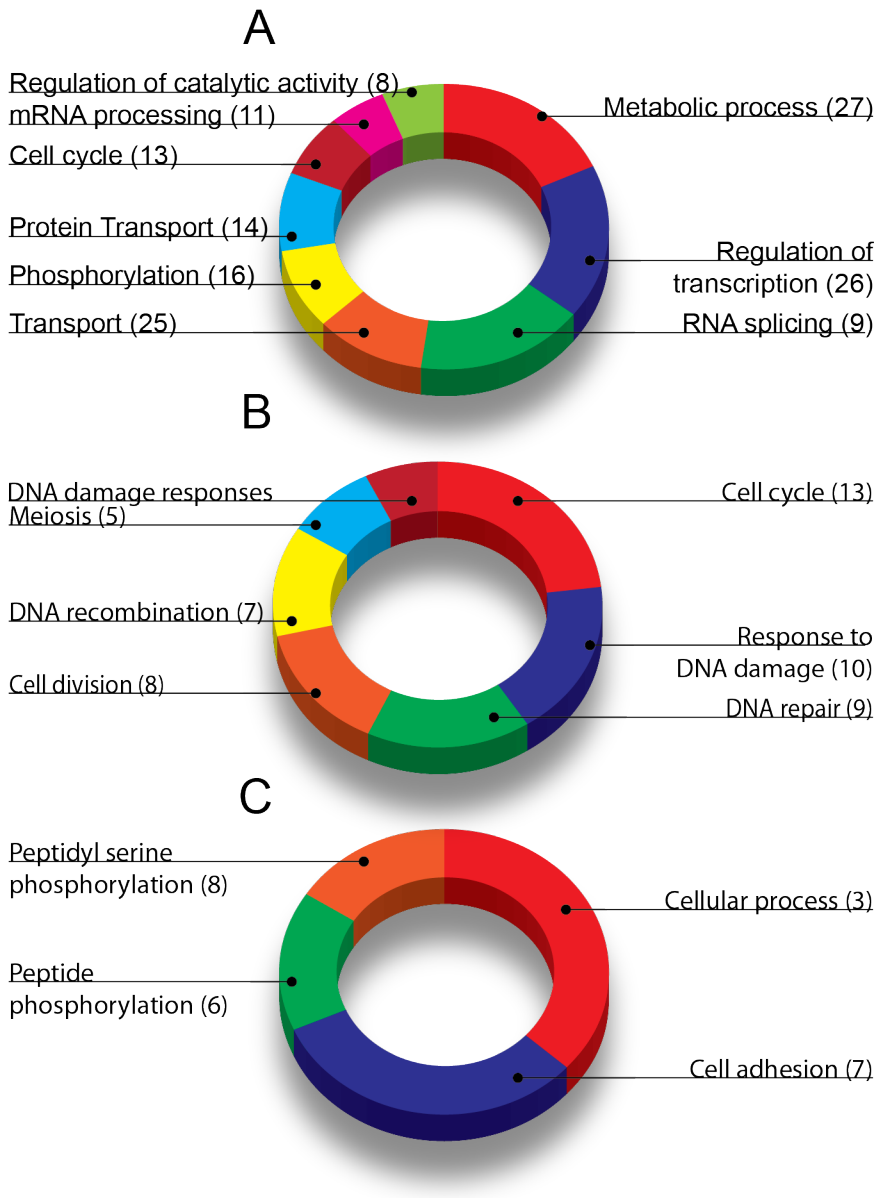


Figure 3-4. **Gene Ontology analysis of unique gene sets. Genes up-regulated in specific cell types were grouped by their function (Gene Ontology; GO) and represented by doughnuts, the larger the number of genes contained in a GO the larger the segment.** (A) GOs represented in M38-specific $CD8^+$ T-cells 7d.p.i, (B) 50d.p.i and (C) M45-specific $CD8^+$ T-cells 7d.p.i.. Genes up-regulated (>2 fold, P <0.05, compared to naïve $CD8^+$ T-cells) run on Genecodis. GO's enriched contain >3 genes, P≤0.001. No GO terms found to be significantly enriched in M45-specific $CD8^+$ T-cells at 50dpi.

3.2.4 K-means clustering and gene ontology analysis

K-means clustering was performed on the gene array results to find groups of genes that would cluster corresponding to their similarity in expression profiles across the different $CD8^+$ T-cell populations. This analysis aims to find groups of genes that distinguish antigen experienced, effector, memory and inflationary $CD8^+$ T-cells. To further analyse the individual clusters they were subjected to gene ontology analysis to study the functional properties by looking at the biological processes enriched in the gene sets. Clustering analysis (Figure 3-5) produced six clusters that identified gene sets differentially expressed in the different $CD8^+$ T-cell populations.

Cluster 1 was up-regulated in both M38- and M45-specific $CD8^+$ T-cells compared to naïve $CD8^+$ T-cells, showing the lowest expression in memory M45-specific $CD8^+$ T-cells. Cluster 1 contains the chemokines *Ccl3*, *Ccl4*, *Ccl5*, *Ccl9* and the cytokine *Ifng*, the granzymes A, K and M. Additionally seen were the chemokine receptors *Ccr5* and *Cx3cr1*, NK-cell receptors *Klrc1* , *Klre1*, *Klrg1*, *Klrk1* and the master transcription factor *Tbx21* (T-bet)(173). Analysis for enriched biological processes showed these genes were involved in processes such as the immune response, chemotaxis and cytolysis (Figure 3-6.A).

Cluster 2 showed a similar profile as cluster 1, with the cluster being highly expressed in the M38-specific $CD8^+$ T-cells - however expression levels decreased in acute M45-specific $CD8^+$ T-cells and further declined in memory M45-specific $CD8^+$ T-cells. The cluster consists of histones, cell cycle division genes (Cdc), antiapoptotic factors such as *Birc5* (*survivin*), the inhibitory receptor *Havcr2* (*Tim3*) and the master cell cycle regulator transcription factor *Foxm1*(174). Analysis of the clusters biological processes revealed that the genes high in cluster 2 were

predominately involved in cell cycle and its regulation and nucleosome assembly (Figure 3-6.B).

Cluster 3 was down regulated in M38-specific $CD8^+$ T-cells compared to naïve and M45-specific $CD8^+$ T-cells. This cluster contained genes known to be up-regulated in memory T-cells(175), such as the lymph node homing makers *Sell* (CD62L) and *Ccr7*, the anti-apoptotic *Bcl2*, and cytokine receptor *Il6ra* (CD126) and its signal transduction gene *Il6st* (CD130), the suppressor of cytokine 3 (*Socs3*) and the transcription factor *Znf238* (Rp58) which regulates neuron development and the expression of ID genes(176,177). By performing gene ontology analysis it could be demonstrated that the cluster was enriched with genes involved in signal transduction, neuropeptide signalling pathway, protein glycosylation, response to toxin and positive regulation of smooth muscle migration (Figure 3-6.C).

Cluster 4 shows a similar profile as cluster 2, having high expression in both M38-specific $CD8^+$ T-cell populations compared to naïve $CD8^+$ T-cells, and M45-specific $CD8^+$ T-cells. The cluster contains a group of histone genes, genes encoding centromere proteins, anti-apoptotic markers such as *Bcl2a1c* and *Bcl2a1d*(178), and the transcription factors *E2f1*, *E2f2* and *Zfp238* (Rog). The gene ontology analysis revealed the enriched biological processes were similar as in cluster 2 (cycle, cell division, nucleosome assembly and mitosis, chromosome segregation, response to DNA damage stimulus and DNA replication)(Figure 3-6.D).

Cluster 5 was up-regulated in M38- and M45-specific $CD8^+$ T-cells populations compared to naïve $CD8^+$ T-cells. The cluster contains genes such as *Il10ra*, *Il12rb1*, *Il18rap*, chemokine receptor *Ccr2* and *Cxcr3*, and the anti-apoptotic protein *Bag3*(179). There are several transcription factors of interest, for example *Prdm1*

(Blimp1), which is important in regulating T-cell responses (77), *Irf4* required for T-cell differentiation (180), the transcriptional inhibitor *Id2*, *Rora* and suppressor of cytokine 2 (*Socs2*). The most enriched biological process was the group of immune response followed by regulation of apoptotic processes (Figure 3-6.E).

Cluster 6 contains a set of genes that was uniquely up-regulated in M38-specific inflationary $CD8^+$ T-cells. This unique set of genes contains the transcription factors *Mkl1*, *Tle3*, *Rbbp7* and the cell cycle regulator, transcription factor, *Foxk1* (181). A further gene of interest is a member of the BH3 domain proteins, Bcl-2 like molecule, *Bcl2l1* (Bcl-x_L). By binding to *Bak* and *Bax* it inhibits mitochondrial-mediated apoptosis(182). This cluster further contains genes involved in cell differentiation, cell cycle, actin cytoskeleton organization, GTP catabolic processes and cyokinesis (Figure 3-6.F).

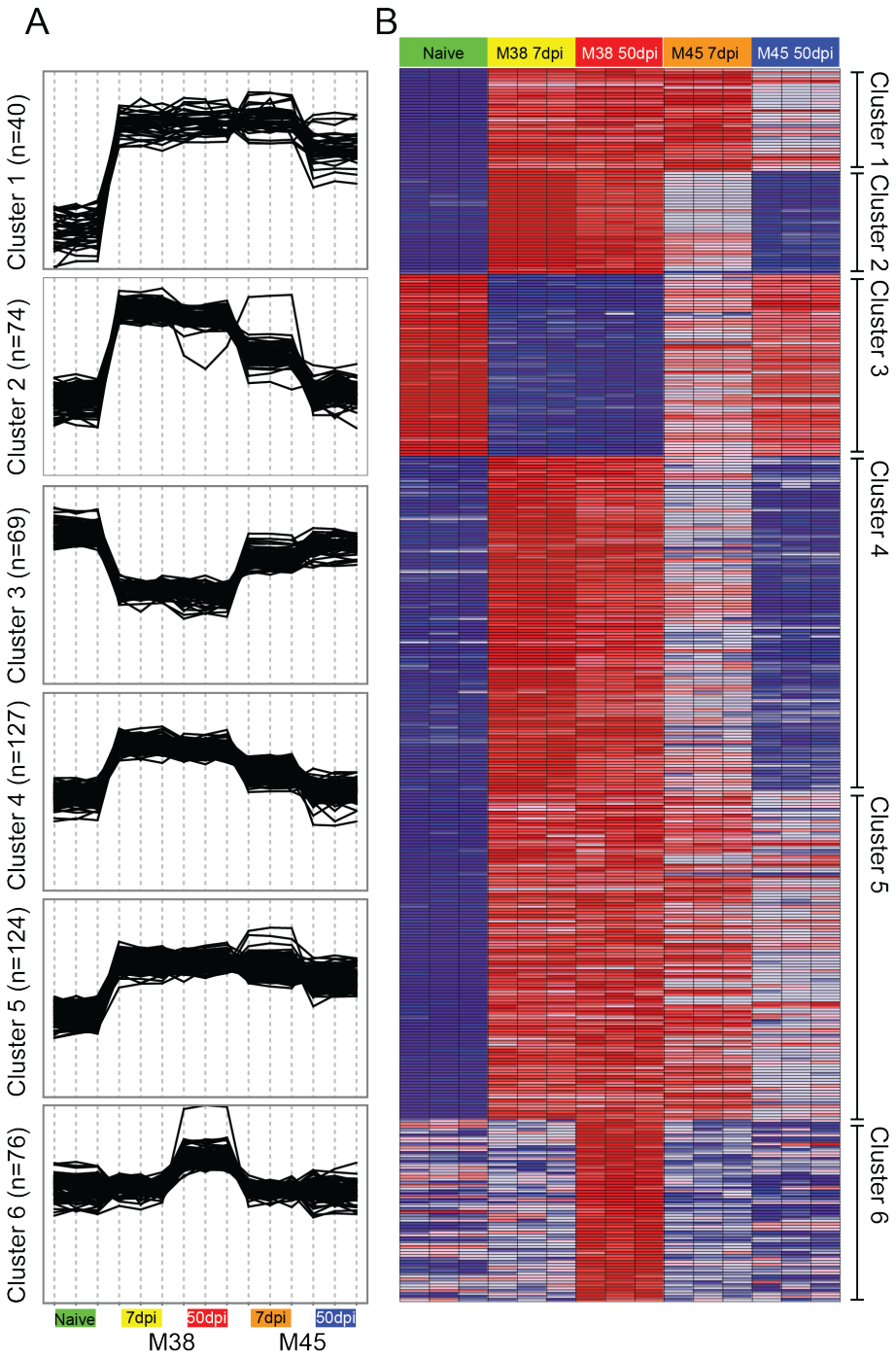


Figure 3-5 **K-means clustering of differentially expressed genes reveals unique subset of genes up-regulated in memory inflation.** A) Clustering of gene array results was performed by ExpressCluster with 100 iterations using genes differentially expressed (≥2 fold, P≤0.05, compared to naïve $CD8^+$ T-cells). The top six clusters are shown. B) Genes identified by K-means clustering were selected to produce a heat map showing the different pattern of expression across the cell populations. Shades of red indicate up-regulated genes and shades of blue indicate down-regulated genes.

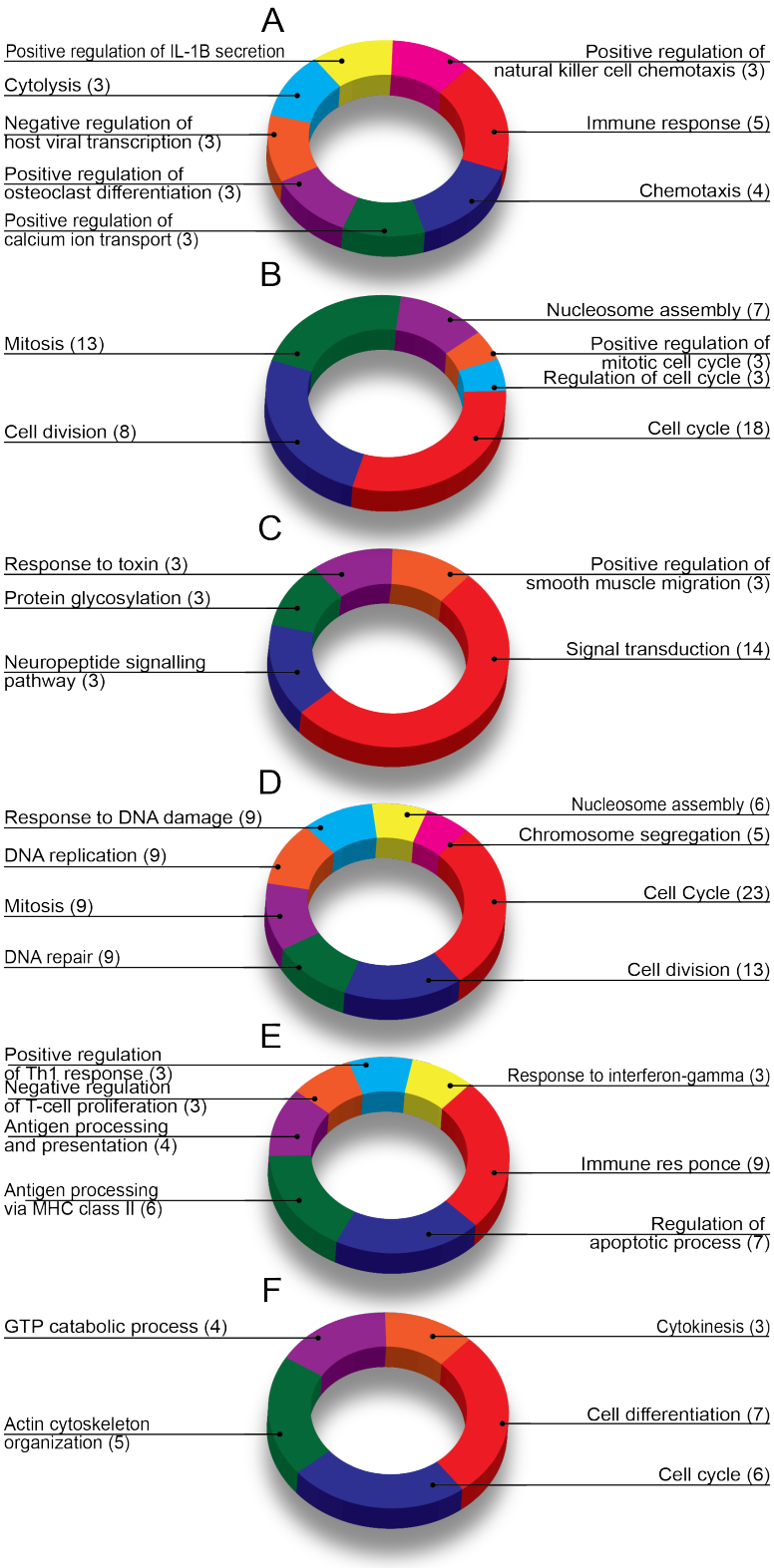


Figure 3-6 **Gene Ontology analysis of gene clusters.** Gene clusters identified by K-means clustering were run on Genecodis. Gene ontology (GO) biological processes (BP) that were enriched are shown (≥3 genes, P≤0.001). (A) Cluster 1, (B) cluster 2, (C) cluster 3, (D) cluster 4, (E) cluster 5, (F) and cluster 6.

By K-means clustering and gene ontology analysis, it has been possible to distinguish sets of genes that define different populations of $CD8^+$ T-cells in MCMV infection and to relate the biological processes that these gene clusters are involved in. Antigen experienced $CD8^+$ T-cells all express the genes in cluster 1, but they have differing expression levels. Both the M38- and M45-specific $CD8^+$ T-cells are functional, thus produce granzymes and an array of chemokines, with both expressing the Th1 transcription factor T-bet. M38-speciifc $CD8^+$ T-cells are highly proliferative compared to M45-specific $CD8^+$ T-cells at 50 days post infection and they have a unique set of genes up-regulated, containing transcription factors and the potentially important anti-apoptotic protein Bcl-X_L.

3.2.5 Cytokine and chemokine expression profile of MCMV-specific $CD8^+$ T-cells

To examine the gene expression profile in more detail, genes were grouped according their function. In the first group a set of chemokine and cytokine receptors, which were up-regulated more than 2-fold compared to naïve mice are listed. Chemokine receptors are induced to guide homing towards sites of inflammation. Cytokines participate in the differentiation of naïve $CD8^+$ T-cells to memory cells and act as growth and survival factors. Some are also required for maintenance of memory T-cells. By analysing the cytokine receptor expression profile the specific requirements for inflationary $CD8^+$ T-cells can be assessed.

The heat map (Figure 3-7.A) shows changes in chemokine and cytokine receptor expression in the different $CD8^+$ T-cell populations compared to naïve $CD8^+$ T-cells. M38-specific $CD8^+$ T-cells from 7 and 50 days post infection, showed a similar profile in the in chemokine and cytokine receptor expression. The same is true for M45-

specific $CD8^+$ T-cells from 7 and 50 days post infection. There are however vast differences if M38- and M45-specific $CD8^+$ T-cells are compared.

Ccr6, *Ccr7* and *Ccr9* for example were down-regulated in M38-specific $CD8^+$ T-cells compared to naïve $CD8^+$ T-cells; in contrast M45-specific $CD8^+$ T-cells (gradually) increased expression of these receptors over time (peaking in memory M45-specific $CD8^+$ T-cells). *Ccr5* and *Ccr2* were up-regulated in M38-specific $CD8^+$ T-cells and M45-specific $CD8^+$ T-cells but to a lesser extent, compared to naïve $CD8^+$ T-cells. Furthermore the chemokine receptors *Cxcr3* and *Cx3cr1* were up-regulated in both the M38- and M45-specific $CD8^+$ T-cells.

M38-specific $CD8^+$ T-cells down-regulated *Cd127* (*Il7ra*), *Cd124* (*Il4ra*) and *Cd126* (*Il6ra*) compared to naïve $CD8^+$ T-cells, but these molecules were highly expressed on M45-specific $CD8^+$ T-cells. Furthermore, the cytokine receptors *Il20rb*, *Cd123* (*Il3ra*), and *Il31ra* were uniquely up-regulated in M38-specific $CD8^+$ T-cells. Cytokine receptors *Cd210* (*Il10ra*), *Cd218a* (*Il18rb1*), *Cd215* (*Il15ra*), *Cd212* (*Il2rb*) and *Cd25* (*Il2ra*) were up-regulated in both M38- and M45-specific $CD8^+$ T-cells in comparison to naïve $CD8^+$ T-cells.

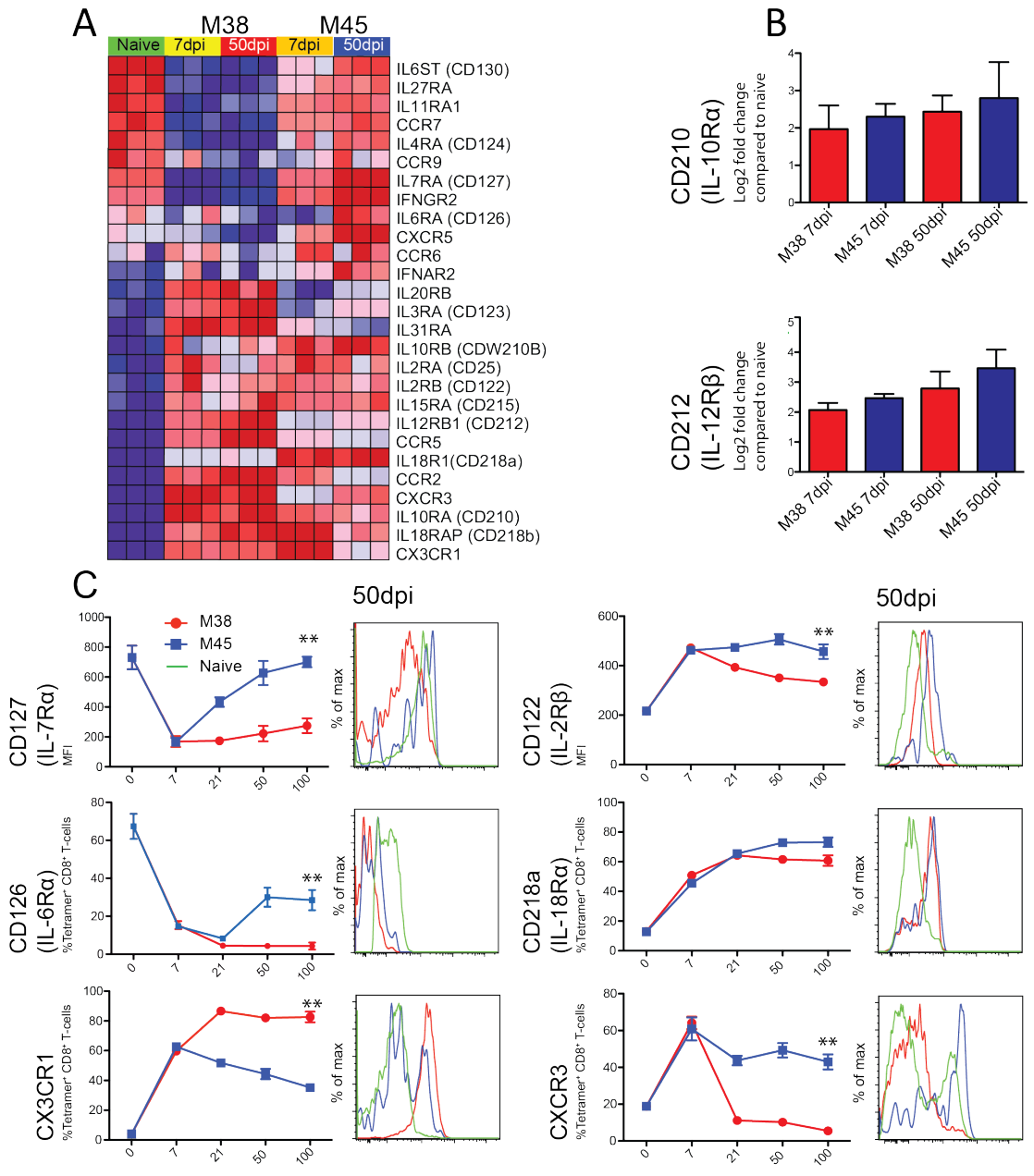


Figure 3-7 **Cytokine and chemokine receptor expression profile on MCMV specific CD8$^+$ T-cells** A) Heat map showing mRNA expression levels for cytokine and chemokine receptors measured by microarray analysis of naive CD8$^+$ T-cells, M38-specific CD8$^+$ T-cells 7 and 50 days post infection and M45-specific CD8$^+$ T-cells 7 and 50 days post infection. Shades of red indicate up-regulated genes and shades of blue indicate down-regulated genes. Filter criteria of at least 2-fold change with P≤0.05, compared to naïve CD8$^+$ T-cells. B) CD212 and CD210 expression after MCMV infection in spleens. CD212 and CD210 mRNA expression was determined by qRT-PCR in M38- and M45-specific CD8$^+$ T-cells at 7 and 50 days post infection. Five mice were pooled for each group; real-time analysis, performed in triplicates. Data presented as Log2 fold change compared to naive CD8$^+$ T-cells after normalization against the internal control gene HPRT. C) Flow cytometry analysis showing the percentage of cells or mean fluorescence intensity (MFI) of indicated markers expressed on M38-specific CD8$^+$ T-cells (red) and M45-specific CD8$^+$ T-cells (blue) in spleen in comparison with naive CD8$^+$ T-cells (d=0)(n=8, mean±SEM). Histograms show expression of indicated markers and are gated on live naive CD8$^+$ T-cells (green), M38-specific CD8$^+$ T-cells (red) and M45-specific CD8$^+$ T-cells (blue).

To confirm expression of *Il12rb* and *Il10ra* mRNA quantitative real-time PCR (qRT-PCR) was performed. To confirm expression of some of chemokine and cytokine receptors at the protein level flow cytometry analysis was performed. Flow cytometry allowed us to track the specific $CD8^+$ T-cells over the course of infection allowing us to distinguish the different stages of $CD8^+$ T-cell differentiation and the $CD8^+$ T-cells' cytokine requirements.

IL-10 is an immune regulatory cytokine that suppresses T-cell responses, and has been shown to be an important cytokine in limiting the expansion of M38-specific inflationary $CD8^+$ T-cells, knockout studies showed an expansion of inflationary $CD8^+$ T-cells(139). We confirmed the up-regulation of *Cd210* (*Il10ra*) mRNA by qRT-PCR, *Cd210* was expressed in M38- and M45-specific $CD8^+$ T-cells, in the acute and memory phase (Figure 3-7.B).

IL-12 can provide the 3rd signal, essential for efficient memory formation(14,53). *Cd212* (*IL12rb*) mRNA expression was confirmed by qRT-PCR to be up-regulated in both M38- and M45-specific $CD8^+$ T-cells, expressed on 7 and 50 days post infection (Figure 3-7.B).

The importance of cytokines, in particular IL-7 and IL-15 in the maintenance and homeostasis of memory T-cells is well recognized(25). Analysis by flow cytometry showed that CD122 was up-regulated in both M38- and M45-specific $CD8^+$ T-cells in the acute phase, compare to naïve $CD8^+$ T-cells. However, memory M45-specific $CD8^+$ T-cells maintained high expression of CD122, while M38-specific inflationary $CD8^+$ T-cells showed reduced expression compared to non-inflationary $CD8^+$ T-cells.

However, it was maintained at higher levels than in naïve $CD8^+$ T-cells (Figure 3-7.C).

The receptor for cytokine IL-7, involved in homeostasis, promoting the survival of memory $CD8^+$ T-cells(19) was also assessed by flow cytometry (Figure 3-1.C). Acute M38- and M45-specific $CD8^+$ T-cells down-regulate CD127 (IL-7Rα), compared to naïve $CD8^+$ T-cells. Inflationary M38-specific $CD8^+$ T-cells down-regulate CD127 expression compared to naive and memory M45-specific $CD8^+$ T-cells.

IL-6 high affinity receptor is composed of CD126 (IL-6Rα) and the common CD130 (IL-6ST) chain(183). As for many cytokines, IL-6 has pleiotropic actions on different cell types of the immune system. Specifically on $CD8^+$ T-cells, IL-6 is reported to promote the survival of naïve $CD8^+$ T-cells(184,185), to enhance the proliferation of $CD8^+$ T-cells following TCR triggering(186) and to synergize with IL-7 and IL-15 to induce antigen independent proliferation of $CD8^+$ T-cells(187). To confirm IL-6Rα expression at the protein level flow cytometry analysis was performed. Upon MCMV-infection specific $CD8^+$ T-cells down-regulate CD126 expression in comparison to naïve $CD8^+$ T-cells. M38-specific inflationary $CD8^+$ T-cells maintained down-regulation, whereas memory M45-specific $CD8^+$ T-cells start to re-express CD126 with approximately 20% expressing CD126 at 100 days post infection (Figure 3-7.C).

IL-18, a cytokine secreted by antigen APCs induces production of IFNγ in primed T-cells and NK-cells in synergy with IL-12(186,188,189). FACS analysis of IL-18 receptor (CD218a, IL-18Rα) expression shows up-regulation on specific $CD8^+$ T-cells upon infection with MCMV. CD218a expression levels continued to rise on both

the memory M45-specific $CD8^+$ T-cells and the inflationary M38-specific $CD8^+$ T-cells with nearly 80% of cells being positive for CD218a (Figure 3-7.C).

The homing of antigen experienced T-cells to sites of inflammation is key in combating viral infection. The chemokine receptor CXCR3 binds to CXCL9, CXCL10, and CXCL11. Shortly after recognition of antigen on DCs in the central lymphoid organs, activated T-cells up-regulate the inflammatory cytokine, CXCR3, allowing them to enter peripheral tissue(190). CXCR3 has been shown to regulate trafficking of activated inflammatory $CD8^+$ T-cells(190), and contributes to shaping the balance between effector and memory $CD8^+$ T-cell generation. Flow cytometry analysis for CXCR3 showed up-regulation on MCMV-specific $CD8^+$ T-cells in the acute phase, compared to naïve $CD8^+$ T-cells. After 7 days post infection M38-specific inflationary $CD8^+$ T-cells start to down-regulate CXCR3 expression and memory M45-specific $CD8^+$ T-cells maintain CXCR3 expression at a high level of about 50% of the M45-specific $CD8^+$ T-cells(Figure 3-7.C).

The fractalkine receptor CX3CR1 was shown to be up-regulated on human $CD8^+$ T-cells after CMV infection(123). We showed that CX3CR1 is up-regulated on both M38 and M45-specific $CD8^+$ T-cells, compared to naïve $CD8^+$ T-cells in the acute phase. After 7 days post infection, memory M45-specific $CD8^+$ T-cells down-regulate CX3CR1 expression to about 30%, while M38-specific inflationary $CD8^+$ T-cells further increased CX3CR1 expression with up to 80% on 100 days post infection (Figure 3-7.C).

To assess whether this expression profile of cytokine and chemokine receptors on M38-specific inflationary $CD8^+$ T-cells was specific to lymphocytes in the spleen we

performed flow cytometry analysis on lymphocytes extracted from lungs, livers and blood (Figure 3-8).

All organs showed a similar profile for CD122, CD127, CD218a (Figure 3-8). CX3CR1 expression in liver and blood showed a similar expression pattern as in the spleen. However the percentage of M45-specific $CD8^+$ T-cells expressing CX3CR1 in the lung did not decrease after day 7 post infection, but was maintained at the same level, which was nevertheless lower compared to M38-specific inflationary $CD8^+$ T-cells.

CXCR3 (Figure 3-8) in blood displayed a different profile, compared to the spleen. The specific $CD8^+$ T-cells increased expression, in comparison to naive $CD8^+$ T-cells. After 7 days post infection expression decreased in both M45- and M38-specific $CD8^+$ T-cells. However, M38-specific $CD8^+$ T-cells continued to decrease expression over time. In the lung M45-specific $CD8^+$ T-cell populations increased expression of CXCR3, in comparison to naïve $CD8^+$ T-cells, but with a lower magnitude to that seen in the spleen.

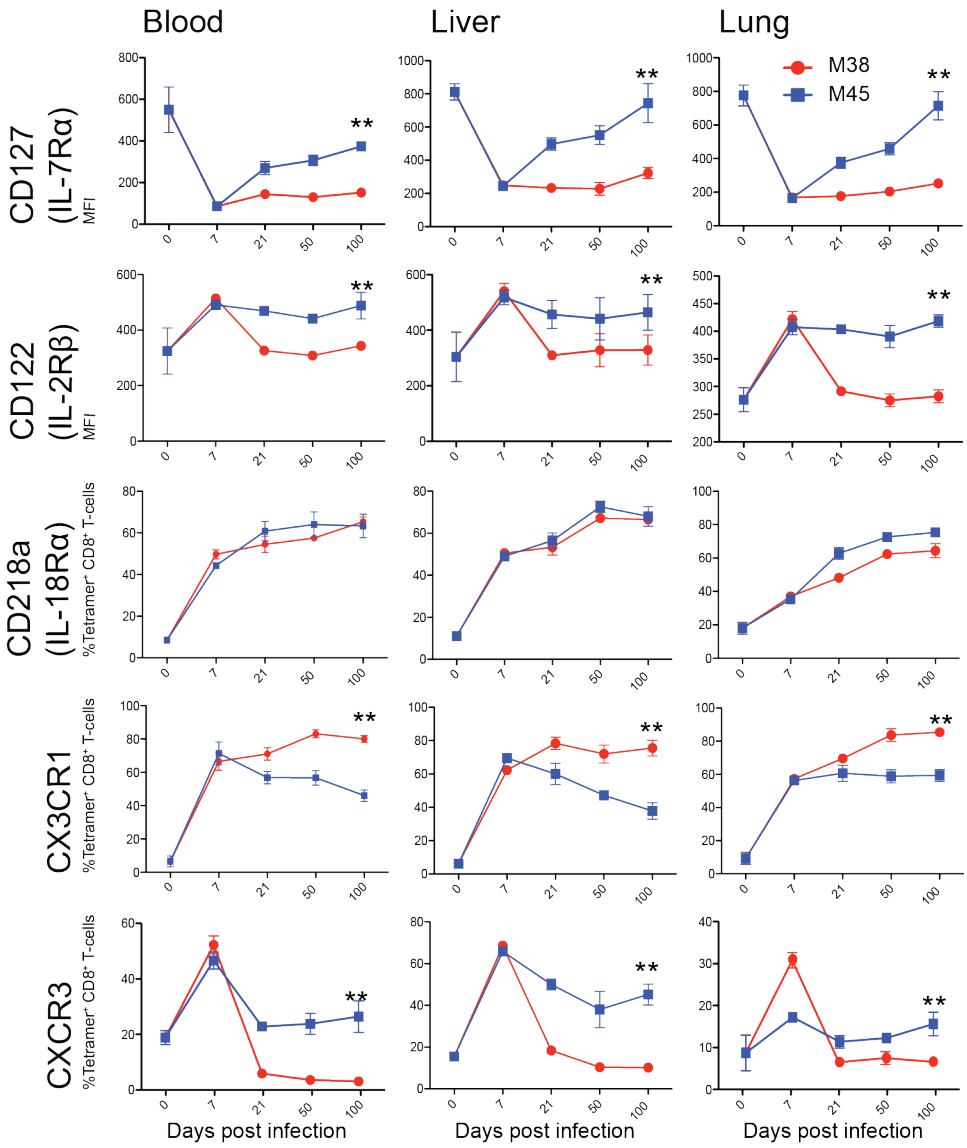


Figure 3-8 **Cytokine and chemokine receptor expression profile in blood, liver and lung of MCMV-specific CD8$^+$ T-cells.** A) Time course showing the percentage of cells or MFI of the indicated markers expressed on M38-specific CD8$^+$ T-cells (red) and M45-specific CD8$^+$ T-cells (blue), in blood, liver and lung on 0, 7, 21, 50 and 100 days post infection (n=8, mean±SEM).

3.2.6 Expression of NK-cell receptors on inflationary CD8$^+$ T-cells

Previous studies had identified the up-regulation of NK-cell receptors on M38-specific CD8$^+$ T-cells(113). The heat map (Figure 3-9.A) shows changes in CD8$^+$ T-cell NK-cell receptor expression in the different CD8$^+$ T-cell populations compared to naïve CD8$^+$ T-cells. M38-specific CD8$^+$ T-cells from 7 and 50 days post infection, show similar profile receptor expression, having high expression levels of *Nkg2a, Klrg1, Klre1* and *Nkg2d*. However, *Ly49c* was uniquely expressed on M38-specific CD8$^+$ T-cells. In contrast, memory M45-specific CD8$^+$ T-cells maintained expression of *Klre1* and *Nkg2d*, and down-regulated *Klrg1* and *Nkg2a*, and they uniquely expressed the inhibitory receptor *Ly49a*.

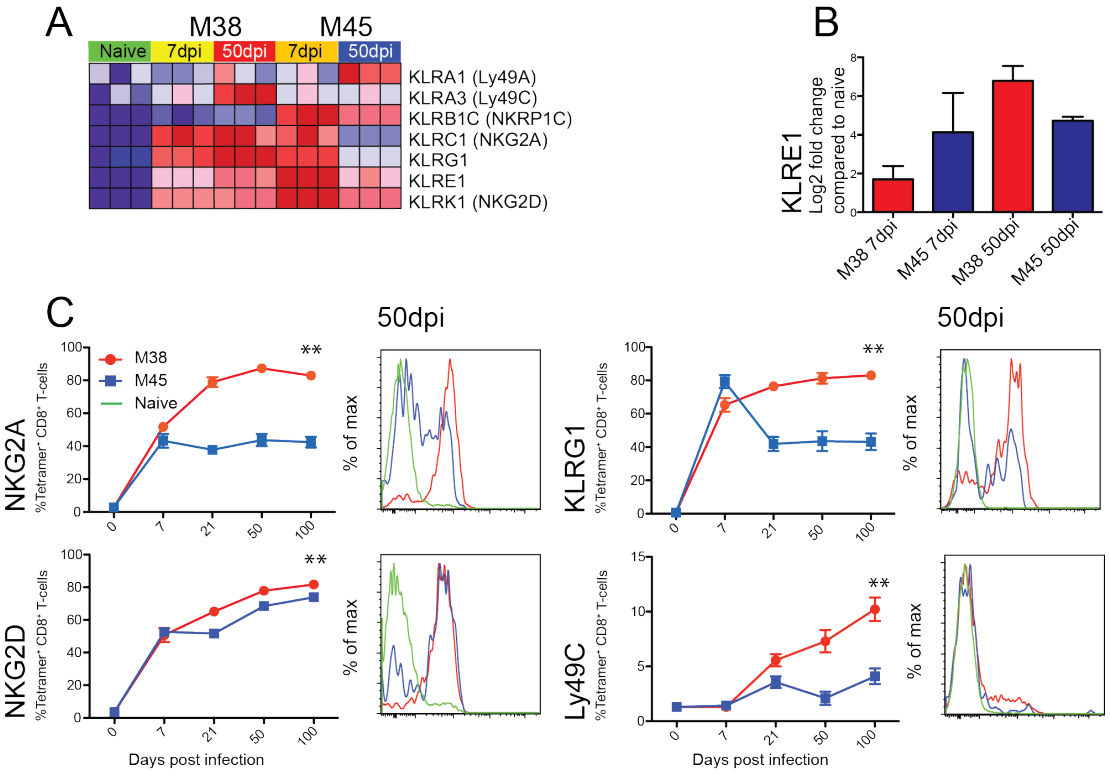


Figure 3-9 **Increased NK-cell receptor expression in inflationary cells** A) Heat map showing mRNA expression level for NK-cell receptors measured by microarray analysis of naïve $CD8^+$ T-cells, M38-specific $CD8^+$ T-cells 7 and 50 days post infection and M45-specific $CD8^+$ T-cells 7 and 50 days post infection. Shades of red indicate up-regulated genes and shades of blue indicate down-regulated genes. Filter criteria of at least 2-fold change with $P \leq 0.05$, compared to naïve $CD8^+$ T-cells. B) Expression of KLRE1 mRNA expression was determined with quantitative real-time PCR in M38- and M45-specific $CD8^+$ T-cells at 7 and 50 days post infection. Five mice were pooled for each group; real-time analysis was performed in triplicates. Data presented as Log2 fold change compared to naive $CD8^+$ T-cells after normalization against the internal control gene HPRT. C) Flow cytometry analysis showing the percentage of cells expressing the indicated markers on M38-specific $CD8^+$ T-cells (red) and M45-specific $CD8^+$ T-cells (blue) in the spleen (n=8, mean±SEM). Histograms show expression of indicated markers and are gated on live naïve $CD8^+$ T -cells (green) M38-specific $CD8^+$ T-cells (red) and M45-specific $CD8^+$ T-cells (blue).

Klre1 receptor has been shown to regulate NK-cell mediated cytotoxicity, capable of inducing both inhibitory and stimulatory signals(191). Its function on $CD8^+$ T-cells has not yet been assessed. To confirm the expression of *Klre1* mRNA, qRT-PCR was performed (Figure 3-9.B). M45-specific $CD8^+$ T-cells up-regulated *Klre1* receptor to a higher degree than M38-specific $CD8^+$ T-cells in the acute phase, in comparison to naïve $CD8^+$ T-cells. This level of expression is maintained in memory M45-specific $CD8^+$ T-cells. However, inflationary M38-specific $CD8^+$ T-cells increased expression of *Klre1* over time.

To assess expression of NKG2A, KLRG1, NKG2D and Ly49C at the protein level and time of infection, flow cytometry analysis was performed. NKG2A was up-regulated on both M38- and M45-specific $CD8^+$ T-cells to the same level at 7 days post infection, in comparison to naïve $CD8^+$ T-cells. M45-specific $CD8^+$ T-cells maintained this level of expression till day 100. In contrast, inflationary M38-specific $CD8^+$ T-cells increased expression over time.

The inhibitory receptor KLRG1 was up-regulated on both specific $CD8^+$ T-cells at 7 days post infection to comparable levels, in comparison to naïve $CD8^+$ T-cells (Figure 3-9.C). They then diverge, M45-specific $CD8^+$ T-cells decrease expression and M38-specific $CD8^+$ T-cells increase expression of KLRG1 in the memory phase. Both specific $CD8^+$ T-cells up-regulated NKG2D to equivalent levels in the acute phase, in comparison to naïve $CD8^+$ T-cells. After day 7, both further up-regulated NKG2D expression - however, inflationary M38-specific $CD8^+$ T-cells display a significantly higher expression compared to M45-specific memory $CD8^+$ T-cells.

Inhibitory receptor Ly-49C was not expressed in the acute phase on either specificity of $CD8^+$ T-cell, however there was a small percentage of M38-specific $CD8^+$ T-cells than did up-regulate expression of the receptor in the memory phase.

We further assessed the expression levels of NK-cell receptors, NKG2A, NKG2D and KLRG1 in the blood, liver, lung and bone marrow. The expression profiles were comparable with those seen in the spleen (Figure 3-10).

Overall, both M38- and M45-specific $CD8^+$ T-cells express inhibitory and stimulatory NK-cell receptors to similar levels in the acute phase after which M38-specific $CD8^+$ T-cells increase expression. This increase in expression of the NK-cell receptors on M38-specific $CD8^+$ T-cells could help control viral infection, due to “missing self” and/or limiting stimulation of the $CD8^+$ T-cells so that they do not become exhausted.

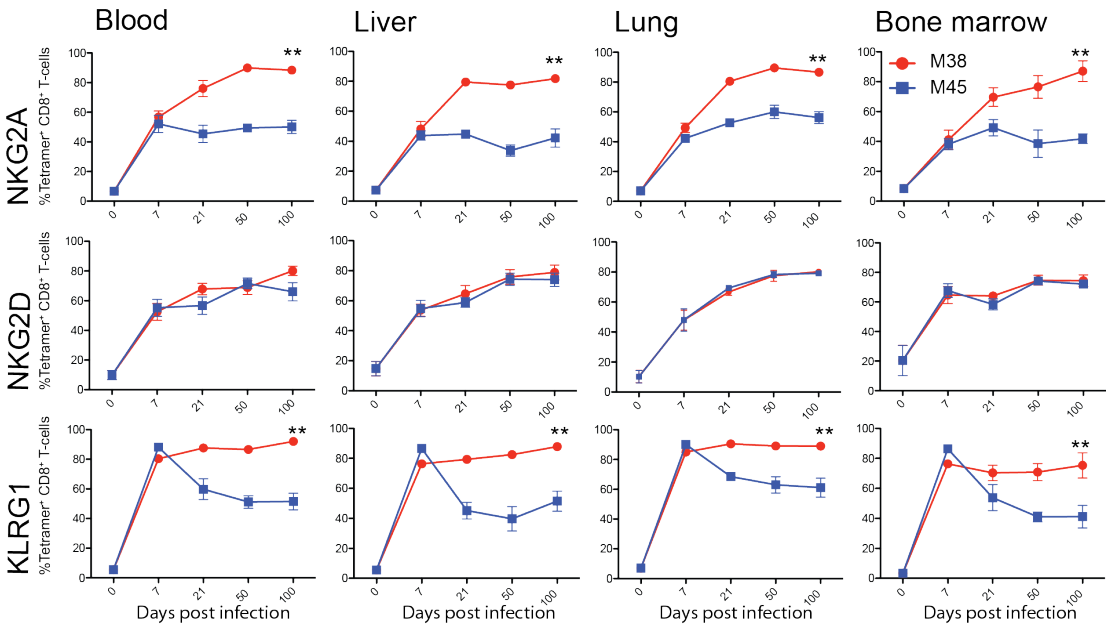


Figure 3-10 **NK-cell receptor expression in blood, liver, lung and bone marrow** A) Time course showing the percentage of cells expressing the indicated markers on M38-specific $CD8^+$ T-cells (red) and M45-specific $CD8^+$ T-cells (blue), in the blood, liver, lung and bone marrow (n=8, mean±SEM).

3.2.7 Cell cycle analysis

It has been suggested that inflationary M38-specific $CD8^+$ T-cells are maintained by continuous production of short lived function T-cells(113). Therefore, we assed the proliferation state of the specific $CD8^+$ T-cells looking at a group of genes controlling the cell cycle.

The heat map in Figure 3-11 shows genes involved in cell cycle. These genes were all highly up-regulated in M38-specific $CD8^+$ T-cells in acute infection, as well as at 50 days post infection (Figure 3-11.A). Already at 7 days post infection there is a remarkable difference between M38- and M45-specific $CD8^+$ T-cells. At 50 days post infection, M45-specific $CD8^+$ T-cells have a comparable expression profile as naïve $CD8^+$ T-cells, confirming their resting state.

The difference between M38- and M45-specific $CD8^+$ T-cells on day 7 as well as on day 50 could be due to the earlier contraction of M45- specific $CD8^+$ T-cells. An earlier time point may have allowed a more equal comparison between the two effector populations.

To confirm the replication state of inflationary cells, qRT-PCR was performed for *Foxm1*, a master regulator of cell cycle(174). M38-and M45-specific $CD8^+$ T-cells at 7 days post infection both have high levels of *Foxm1* mRNA expression, in comparison to naive $CD8^+$ T-cells. Levels of expression decreased in both specific $CD8^+$ T-cells in the memory phase.

To further confirm expression at the protein level and to follow the proliferation state of M38- and M45-specific $CD8^+$ T-cells over time, we measured expression of Ki67 in the spleen by flow cytometry. Ki67 is a marker of proliferation. Both M38- and M45-specific $CD8^+$ T-cells were highly proliferative at 7 days post infection, with

almost 100% of the tetramer-positive $CD8^+$ T-cells expressing Ki67. M45-specific $CD8^+$ T-cell expression levels of Ki67 decreased to about 10% at 21 days post infection, which was maintained till 100 days post infection. In distinction, M38-specific $CD8^+$ T-cells kept a higher proliferation state, with 30% Ki67 positive cells at 21 days post infection. This gradually declined to similar levels as M45-specific $CD8^+$ T-cells by 100 days post infection.

Taken together M45-specific $CD8^+$ T-cells rapidly proliferated in the acute phase, but had reached a stable rate of proliferation by day 21. M38-specific $CD8^+$ T-cells also rapidly proliferated in the acute stage, but a large percentage of the specific $CD8^+$ T-cells were still Ki67 or *Foxm1* positive on day 50 post infection. This increased/sustained proliferation could account for the increased frequency and total numbers seen.

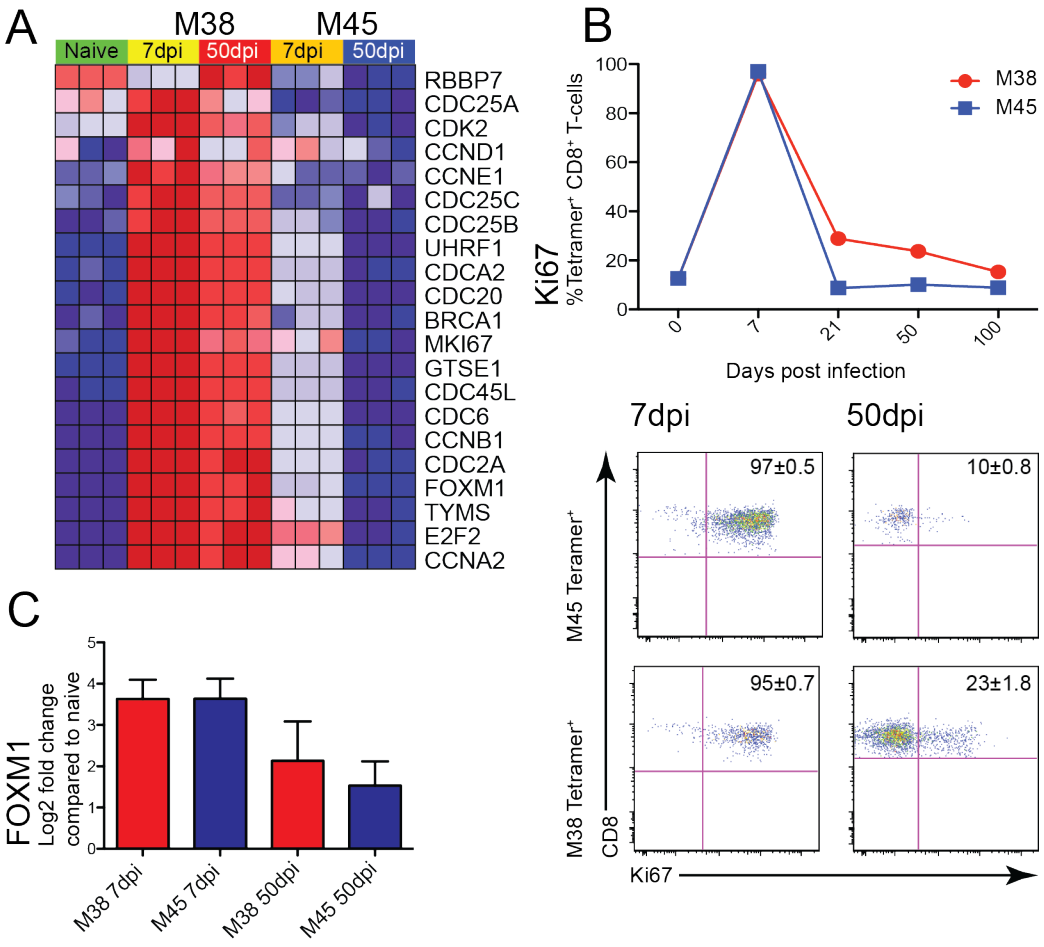


Figure 3-11 **Analysis of genes associated with proliferative state of specific CD8$^+$ T-cells after MCMV infection.** (A) Heat map showing mRNA expression levels for proliferation markers measured by microarray analysis of naive CD8$^+$ T-cells, M38-specific CD8$^+$ T-cells 7 and 50 days post infection and M45-specific CD8$^+$ T-cells 7 and 50 days post infection. Shades of red indicate up-regulated genes and shades of blue indicate down-regulated genes. Filter criteria of at least 2-fold changes with P≤0.05, compared to naive CD8$^+$ T-cells. (B) Time course showing the percentage of cells expressing Ki67 on M38-specific CD8$^+$ T-cells (red) and M45-specific CD8$^+$ T-cells (blue), in the spleen at 0, 7, 21, 50 and 100 days post infection (n=8, mean±SEM). Representative flow cytometry plots show the expression of Ki67 in the spleen at 7 and 50 days post infection, gated on live M38-specific CD8$^+$ T-cells or M45-specific CD8$^+$ T-cells. C) Expression of FOXM1 mRNA was determined with quantitative real-time PCR in M38- and M45-specific CD8$^+$ T-cells at 7 and 50 days post infection. Five mice were pooled for each group; real-time analysis was performed in triplicates. Data presented as Log2 fold change compared to naive CD8$^+$ T-cells after normalization against the internal control gene HPRT.

3.2.8 Receptors of the SLAM family are up-regulated on MCMV-specific CD8$^+$ T-cells

The signalling lymphocytic activation molecule (SLAM) family of receptors is expressed on a wide range of immune cells. They signal through their cytoplasmic domain, via SLAM-associated protein (SAP). They have diverse roles including the regulation of co-stimulation, cytokine production and reactivation induced cell death(192,193).

Several members of the SLAM family were highly up-regulated on M38-specific CD8$^+$ T-cells in comparison to naïve CD8$^+$ T-cells (Figure 3-12.A). M38-specific CD8$^+$ T-cells up-regulated *Cd319*, *Cd48* and *Cd150*, and the signalling molecule *Sap*, having comparable levels of expression in the acute and memory phase. Interestingly, inflationary M38-specific CD8$^+$ T-cells uniquely up-regulated *Cd84*. M45-specific CD8$^+$ T-cells in contrast, only expressed *Cd352* at 50 days post infection.

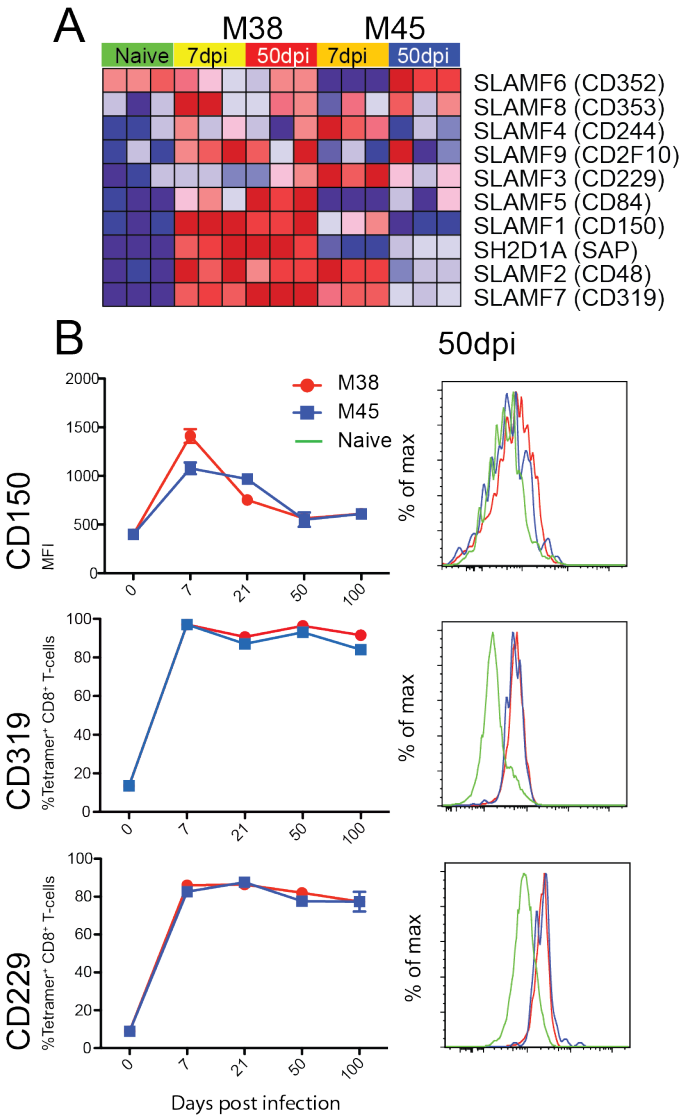


Figure 3-12. **Up-regulation of SLAM family receptors.** A) Heat map showing mRNA expression levels for the SLAM family receptors and the signalling molecule SAP, measured by microarray analysis of naive CD8$^+$ T-cells, M38-specific CD8$^+$ T-cells 7 and 50 days post infection and M45-specific CD8$^+$ T-cells 7 and 50 days post infection. Shades of red indicate up-regulated genes and shades of blue indicate down-regulated genes. Filter criteria of at least 2-fold changes with P≤0.05, compared to naïve CD8$^+$ T-cells. B) Time course showing the percentage of cells or mean fluorescence intensity (MFI) of the indicated markers expressed on M38-specific CD8$^+$ T-cells (red) and M45-specific CD8$^+$ T-cells (blue) in spleen at 0, 7, 21, 50 and 100 days post infection (n=8, mean±SEM). Histograms show expression of indicated markers, gated on live naïve CD8$^+$ T-cells (green) M38-specific CD8$^+$ T-cell (red) and M45-specific CD8$^+$ T-cell (blue).

To confirm whether the levels of mRNA expression correspond to protein expression, we performed flow cytometry analysis for CD229, CD319 and CD150. Both M38- and M45-specific $CD8^+$ T-cell populations increased expression of CD150 at 7 days post infection, in comparison to naïve $CD8^+$ T-cells. After day 7 both populations slowly decreased CD150 expression to the same levels as naïve $CD8^+$ T-cells at 50 days post infection (Figure 3-12.B). CD229 and CD319 showed the same expression profile after activation, in M38- and M45-specific $CD8^+$ T-cells. They both up-regulated their expression, and expression was maintained at high levels over time, in comparison to naïve $CD8^+$ T-cells.

The discrepancies between the array and FACS data at 50 days post infection, could be that M45-specific $CD8^+$ T-cells at 7 days post infection up-regulate SLAM receptors, but at 50 days the cells are slowly turning over so require very little mRNA expression to maintain protein expression on the surface of cells and thus appear negative for SLAM expression at 50 day post infection. Both M38- and M45-specific $CD8^+$ T-cells show the same protein expression levels of the SLAM family receptors, allowing them to receive the correct stimulus to become activated and combat viral infection.

3.2.9 Expression of other cellular receptors

Following activation with antigen, naïve $CD8^+$ T-cells differentiate, and up-regulate expression of adhesion markers, and decrease expression of lymph node homing receptors such as CD62L and disseminate throughout the body. Different migratory patterns indicate that cell surface molecules must regulate the entry of $CD8^+$ T-cells into peripheral sites.

The heat map (Figure 3-13.A) shows the expression levels of adhesion molecules from the gene array. Both M38- and M45-specific $CD8^+$ T-cells up-regulated the receptors *Ly6c*, *Ly6a*, *Cd44* and *Cd29* on 7 and 50 days post infection, in comparison to naïve $CD8^+$ T-cells. M38-specific $CD8^+$ T-cells from 7 and 50 days post infection showed a similar expression profile for most receptors, except for *Maea*, *Cd49d* and *Cd54*, which were up-regulated at 50 days post infection in comparison to day 7 and naïve $CD8^+$ T-cells.

M45-specific memory $CD8^+$ T-cells up-regulated the adhesion molecules *Cd31*, *Cd103*, *Cd62L*, *Cd26* and *Cd73* two ectoenzyme, and has similar expression to naïve $CD8^+$ T-cells. Furthermore, M45-specific memory $CD8^+$ T-cells down-regulated *Cs54, Cd11d, Notch3*, *Cd166* and *Cd11c*.

To confirm expression of CD44, CD73, CD54, Ly6C, CD26 and CD62L at the protein level a time course using flow cytometry was performed (Figure 3-13.B). The adhesion molecules CD44 and Ly6C were both up-regulated on M38- and M45-specific $CD8^+$ T-cells after infection with MCMV, and stayed up-regulated during the memory phase. Both receptors are markers of antigen-experienced cells.

CD54 (ICAM1) was up-regulated on M38- and M45-specific $CD8^+$ T-cells at 7 days post infection, in comparison to naïve $CD8^+$ T-cells. Expression of CD54 decreased on M45-specific $CD8^+$ T-cells in the memory phase, in comparison to M38-specific $CD8^+$ T-cells, where it was maintained at high expression levels. CD54 binds to LFA1 and has been shown to have significant roles in leukocyte adhesion and signalling by stabilizing the TCR synapses (194).

The lymph node homing marker CD62L, binds to GlyCam-1, found in the high endothelial venules of the lymph node. It is down-regulated on M38- and M45-specific $CD8^+$ T-cells following antigen stimulation, in comparison to naïve $CD8^+$ T-cells. M45-specific $CD8^+$ T-cells gradually up-regulated CD62L expression after the acute phase, whereas M38-specific $CD8^+$ T-cells stayed low in expression.

Two ectoenzymes CD73 and CD26 were differentially expressed between M38- and M45-specific $CD8^+$ T-cells. CD73 catalyzes the generation of adenosine, a potent immunosuppressive host nucleoside(195,196). CD26 forms a complex with adenosine deaminase (ADA) on the cell surface, blocking the inhibitory effects of adenosine(197). Working in conjunction with CD39 they control the suppressive effects of adenosine.

Both ectoenzymes were down-regulated on M38- and M45-specific $CD8^+$ T-cells, at 7 days post infection, in comparison to naïve $CD8^+$ T-cells (Figure 3-13.C). CD73 increases on M38- and M45-specific $CD8^+$ T-cells until 21 days post infection, when expression level has reached the same as naïve $CD8^+$ T-cells. This level of expression is maintained on M38-specific $CD8^+$ T-cells in the memory phase; however, M45-specific $CD8^+$ T-cells further increased expression in the memory phase. The population of cells expressing CD26 is maintained low in inflationary M38-specific $CD8^+$ T-cells, while the percentage of memory M45-specific $CD8^+$ T-cells increased CD26 expression over time.

The expression of adhesion molecules on M38-specific $CD8^+$ T-cells in the case of CD54 could allow for increased stimulation when antigen is encountered, stabilizing the TCR synapses. The difference between M38- and M45-specific $CD8^+$ T-cells suggests different migration patterns, while the lack of CD62L allows them to patrol

the peripheral regions. The balance of ectoenzyme on inflationary cells has not been documented before and their roles not defined, they could maintain the balance of proliferation by controlling the levels of external adenosine. This is discussed further in Chapter 6.

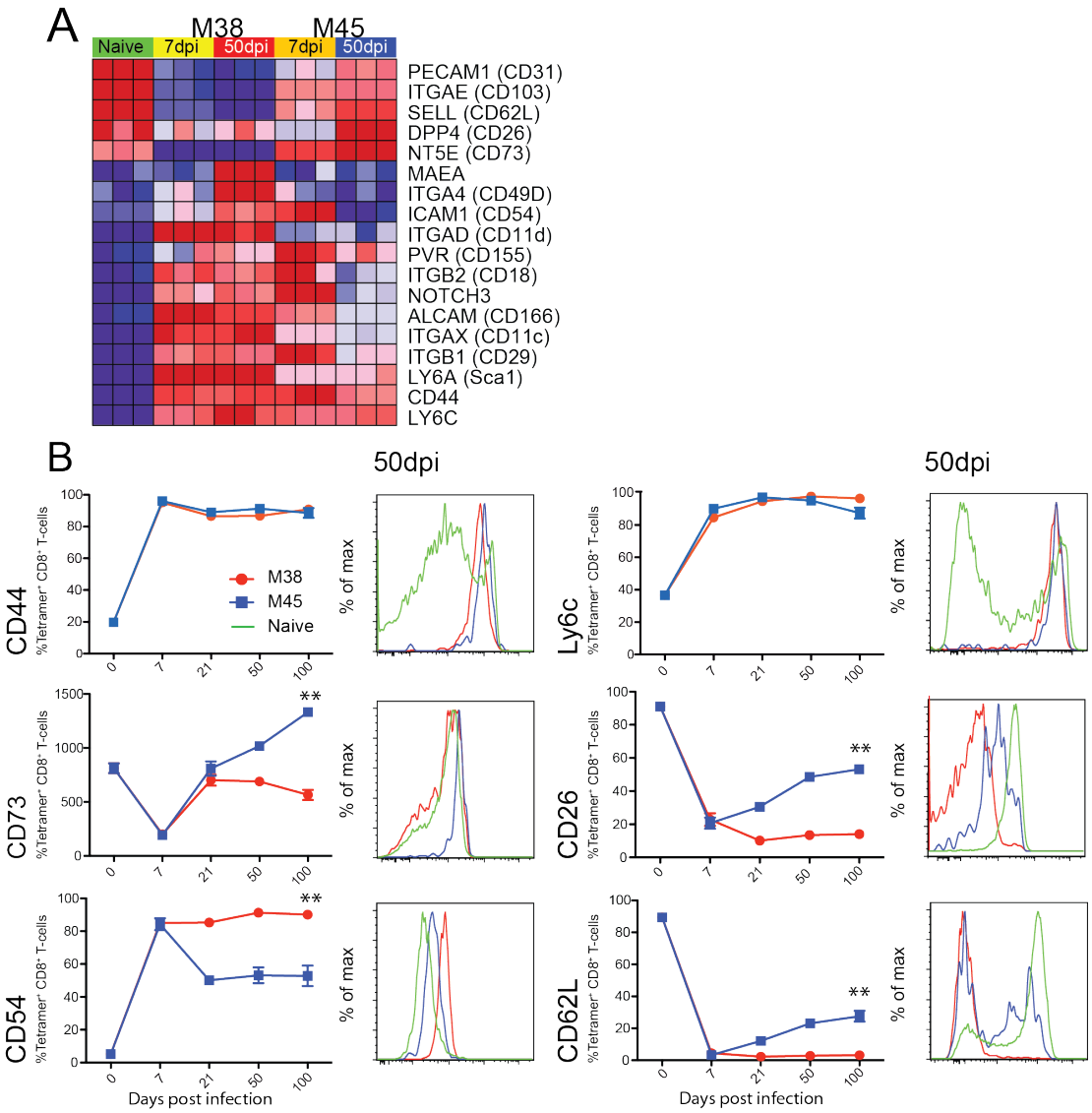


Figure 3-13. **Differential expression of cell surface molecules on MCMV specific CD8$^+$ T-cells.** A) Heat map showing mRNA expression levels for surface receptors measured by microarray analysis of naive CD8$^+$ T-cells, M38-specific CD8$^+$ T-cells 7 and 50 days post infection and M45-specific CD8$^+$ T-cells 7 and 50 days post infection. Shades of red indicate up-regulated genes and shades of blue indicate down-regulated genes. Filter criteria of at least 2-fold changes with P≤0.05, compared to naïve CD8$^+$ T-cells. B) Time course showing the percentage of cells or mean fluorescence intensity (MFI) of the indicated markers expressed on M38-specific CD8$^+$ T-cells (red) and M45-specific CD8$^+$ T-cells (blue) in spleen at 0, 7, 21, 50 and 100 days post infection (n=8, mean±SEM). Histograms show expression of indicated markers and are gated on live naïve CD8$^+$ T-cells (green) M38-specific CD8$^+$ T-cells (red) and M45-specific CD8$^+$ T-cells (blue).

3.2.10 Exhaustion-associated surface inhibitory receptors

Studies have well documented the roles of inhibitory receptors in exhaustion, induced by LCMV infection(166,198). Gene array results have shown that *Pdcd1* (*Pd1)*, *Tim3*, *Cd160* and *Lag3* were up-regulated in M38-specific $CD8^+$ T-cells on 7 and 50 days post infection, but not *Btla*, in comparison to naïve $CD8^+$ T-cells (Figure 3-14.A). M45-specific $CD8^+$ T-cells, in contrast, had intermediate expression levels of *Pdcd1*, *Tim3*, *Cd160*, *Lag3* and up-regulated *Btla* at 50 days post infection. M45-specific memory $CD8^+$ T-cells had a similar expression profiles to that of naïve $CD8^+$ T-cells, only expressing the inhibitory receptor *Btla*.

However, performing flow cytometry analysis for all exhaustion markers shown on M38- and M45-specific $CD8^+$ T-cells revealed similar expression profiles for LAG3, TIM3, CD160 and PD1, with high expression in the acute phase and then a gradual decrease, in the memory phase to the same levels of naïve $CD8^+$ T-cells.

Interestingly, the inhibitory receptor BTLA, showed a different expression profile. Here, gene array data was confirmed at the protein level with low level expression on M38-specific inflationary $CD8^+$ T-cells and significantly higher expression on M45-specific $CD8^+$ T-cells.

The expression levels of these inhibitory receptors, shows that both M38- and M45-specific $CD8^+$ T-cells are still capable of proliferating and are not exhausted. It is interesting to note that the levels of PD1 on M38- and M45-specific $CD8^+$ T-cells are similar; PD1 is not just a maker of exhaustion but also for proliferating/activated cells. The low levels of BTLA expression is also of interest because it not only restricts T-cell cytotoxic activity but controls proliferation and survival(199,200).

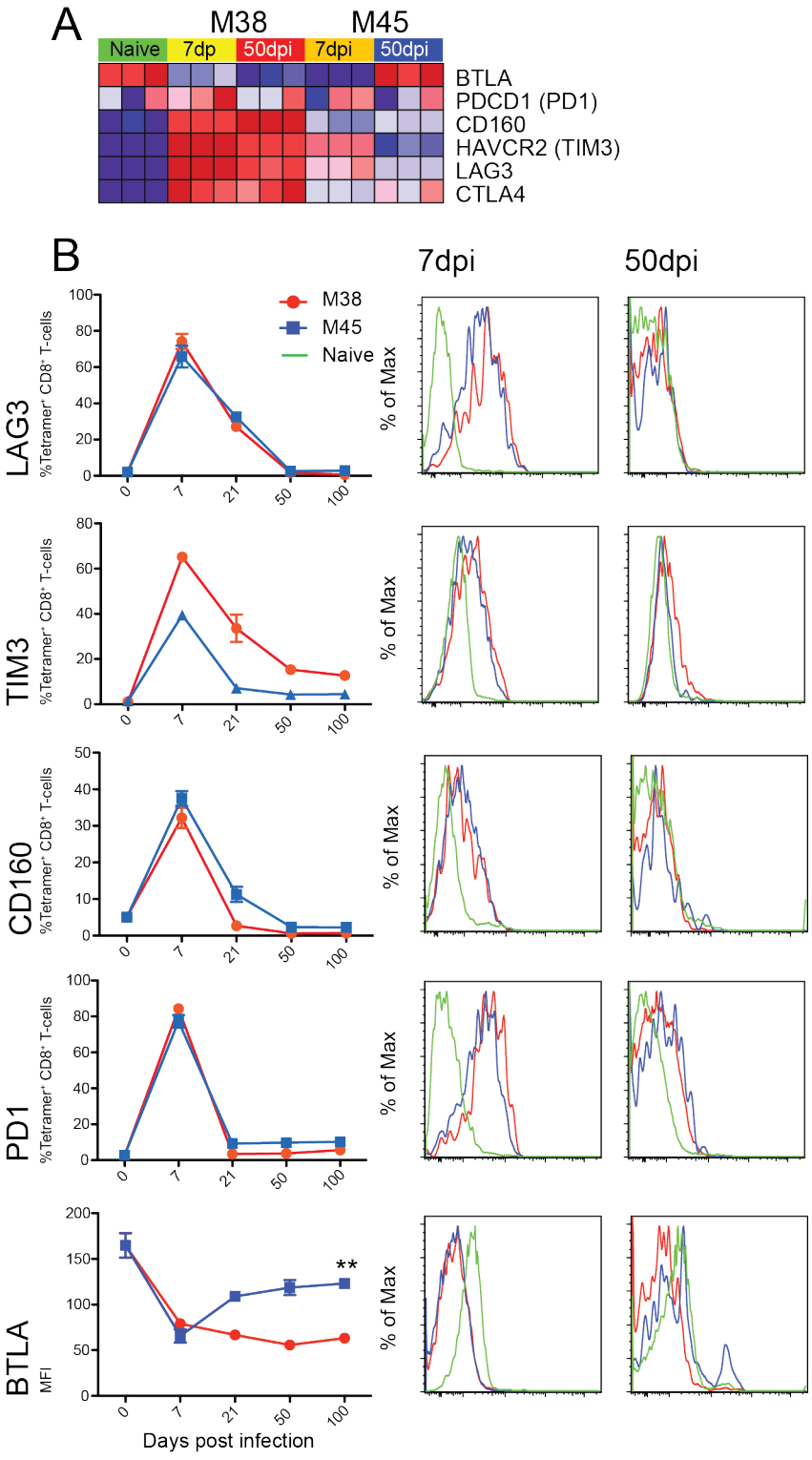


Figure 3-14. **Changes in exhaustion markers over the course of infection on MCMV specific CD8$^+$ T-cells.** A) Heat map showing mRNA expression levels of exhaustion markers measured by microarray analysis of naive CD8$^+$ T-cells, M38-specific CD8$^+$ T-cells 7 and 50 days post infection and M45-specific CD8$^+$ T-cells 7 and 50 days post infection. Shades of red indicate up-regulated genes and shades of indicate blue down-regulated genes respectively. Filter criteria of at least 2-fold changes with P≤0.05, compared to naïve CD8$^+$ T-cells. B) Time course showing the percentage of cells expressing or the MFI of the indicated markers on M38-specific CD8$^+$ T-cell (red) and M45-specific CD8$^+$ T-cell (blue) in the spleen (n=8, mean±SEM). Histograms show expression of indicated markers and are gated on live naïve CD8$^+$ T-cells (green) M38-specific CD8$^+$ T-cell (red) and M45-specific CD8$^+$ T-cell (blue).

3.2.11 Profiling apoptotic proteins in MCMV-specific $CD8^+$ T-cells

Programmed cell death is crucial for normal lymphocyte development and function. Defects in the control of lymphocytes can lead to a variety of disease, the death of too many can lead to immunodeficiency and too many can lead to lymphoma(201,202) It is essential for homeostasis of antigen specific T-cell pool that there is a balance between pro and anti-apoptotic genes of the Bcl-2 family.

The heat plot shows genes involved in the regulation of apoptosis , which are differentially expressed in M38- and M45-specific $CD8^+$ T-cells, in comparison to naïve $CD8^+$ T-cells (Figure 3-15.A). The anti-apoptotic protein-encoding gene *Bcl2* was down regulated in the acute phase in M38 and M45-specific $CD8^+$ T-cells, as well as in inflationary M38-specific $CD8^+$ T-cells. M45-specific memory $CD8^+$ T-cells up-regulated *Bcl2*, reaching similar levels to that of naïve $CD8^+$ T-cells.

A mixture of pro-apoptotic (*Bad*, *Bak*, *Bcl-2-rambo*) and anti-apoptotic (*Bag3*, *Birc5*, *Bcl2l1* (*Bclxl*) mRNAs were up-regulated in the acute and memory phase in M38-specific $CD8^+$ T-cells, in comparison to naïve $CD8^+$ T-cells. Memory M45-specific $CD8^+$ T-cells showed a similar expression profile to that of naïve $CD8^+$ T-cells, whereas M38-specific $CD8^+$ T-cells showed a distinct expression profile uniquely expressing the gene for the anti-apoptotic protein Bcl-x_L(203).

Analysis by flow cytometry confirmed the expression of Bcl-2 in M38- and M45-specific $CD8^+$ T-cells over time in spleen liver and lung (Figure 3-15.B). Bcl-2 expression was down-regulated at 7 days post infection in both MCMV-specific $CD8^+$ T-cells. It stayed low in M38-specific $CD8^+$ T-cells over time. However. M45-specific $CD8^+$ T-cells gradually increased Bcl-2 expression over time.

To confirm the expression levels of antiapoptotic *Bicr5* (*survivin*) (204), I performed qRT-PCR (Figure 3-15.C). Both M38- and M45-specific $CD8^+$ T-cells up-regulated *Birc5* expression in the acute phase. M38-specific $CD8^+$ T-cells maintained high expression of *Birc5*, while memory M45-speciific $CD8^+$ T-cells decreased its expression.

The role of pro-apoptotic and anti-apoptotic proteins has not been assessed in inflationary $CD8^+$ T-cells. In comparison to memory M45-specific $CD8^+$ T-cells, the reduction of *Bim* and the increase in *Bclxl* in inflationary M38-speciifc $CD8^+$ T-cells could reduce apoptosis and allow these cells to be maintained at a higher frequency, avoiding the contraction phase.

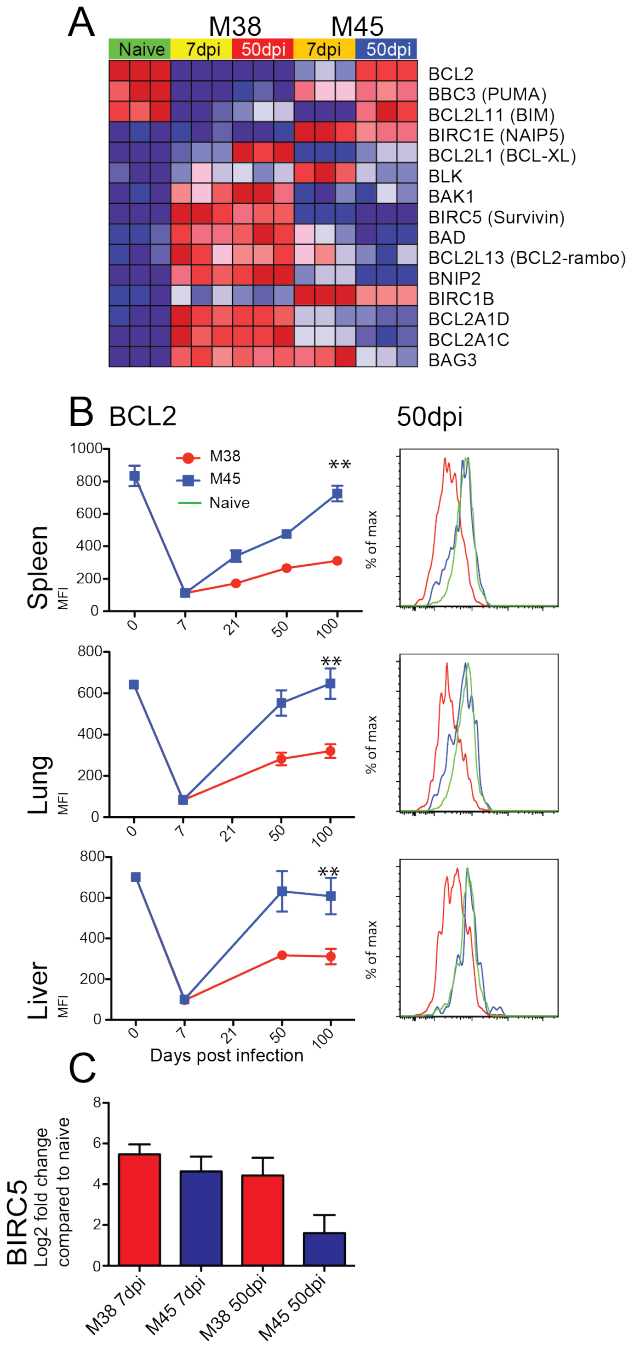


Figure 3-15 **Expression of apoptotic related proteins in MCMV-specific CD8$^+$ T-cells.** A) Heat map showing mRNA expression levels of proteins involved apoptosis measured by microarray analysis of naïve CD8$^+$ T-cells, M38-specific CD8$^+$ T-cells 7 and 50 days post infection and M45-specific CD8$^+$ T-cells 7 and 50 days post infection. Shades of red indicate up-regulated genes and shades of blue indicate down-regulated genes. Filter criteria of at least 2-fold changes with P≤0.05, compared to naïve CD8$^+$ T-cells. B) Time course showing MFI of Bcl2 in M38-specific CD8$^+$ T-cells (red) and M45-specific CD8$^+$ T-cells (blue), in the spleen, lung and liver at day 0, 7, 21, 50 and 100 post infection (n=8, mean±SEM). Histograms show expression of Bcl2, gated on live naïve CD8$^+$ T-cells (green) M38-specific CD8$^+$ T-cells (red) and M45-specific CD8$^+$ T-cells (blue). C) Expression of BIRC5 mRNA expression was determined with quantitative real-time PCR in M38- and M45-specific CD8$^+$ T-cells at 7 and 50 days post infection. Five mice were pooled for each group; real-time analysis was performed in triplicates. Data presented as Log2 fold change compared to naive CD8$^+$ T-cells after normalization against the internal control gene HPRT.

3.2.12 Differential expression of co-stimulatory molecules

To achieve maximal expansion $CD8^+$ T-cells need to integrate multiple signals, including the TCR, costimulatory signals and inflammatory cytokines. Many members of the TNFR family such as CD27 and OX-40 deliver important co-stimulatory signals(205).

The heat map shows the expression profile of *mRNA* encoding stimulatory receptors on M38- and M45-specific $CD8^+$ T-cells, in comparison to naïve $CD8^+$ T-cells (Figure 3-16.A). In the acute and memory phase M38-speciifc $CD8^+$ T-cells show a similar expression profile, being high in *Cd226*, *Cd278*, *Cd268*, *Cd120a*, *Cd28* and *Cd258*, while being low in *Tnfrsf26*, *Cd27*, *Cd134*, and *Cd257*, in comparison to naïve $CD8^+$ T-cells. M45-specific $CD8^+$ T-cells in contrast, change their expression profile from 7 to 50 days post infection. Compared to M38-specific $CD8^+$ T-cells, M45-specific $CD8^+$ T-cells have higher expression of *Tnfrsf26*, *Cd27*, *Cd134* and *Cd357*.

Expression levels of CD226, CD27 and CD357 were measured over a time course by flow cytometry analysis (Figure 3-16.C). CD27 expression was slightly down-regulated on 7 days post infection in M38 and M45-specific $CD8^+$ T-cells. M45-specific memory $CD8^+$ T-cells maintained this level of expression; in contrast inflationary M38-specific $CD8^+$ T-cells further decreased expression of CD27.

CD357, another member of the TNFR family, showed a similar expression profile to CD27. Memory M45-specific $CD8^+$ T-cells increased expression of this stimulatory receptor over time, to levels similar to that of naïve $CD8^+$ T-cells, while M38-specific $CD8^+$ T-cells continued to decrease the level of expression and stayed low in expression in the memory phase. The CD357 receptor delivers pro-survival signals to effector $CD8^+$ T-cells to promote expansion(206), In knockout studies GITR-/- T-

cells were hyper-proliferative when stimulated with anti CD3 compared to wild type cells(207), suggesting that CD357 may play an important role in inflation.

The expression profile of CD226 showed up-regulation in the acute phase on M38- and M45-specific $CD8^+$ T-cells, in comparison to naïve $CD8^+$ T-cells. Memory M45-specific $CD8^+$ T-cells down-regulated the receptor, and M38-specific $CD8^+$ T-cells maintained high expression in the chronic phase. CD226 binds to CD155; CD155 is expressed on many tissue cells such as fibroblasts, epithelia and endothelia and on a variety of hematopoietic cells types. CD226 is a co-stimulatory molecule involved in differentiation, cytotoxicity and migration(208-211).

Observations using $CD155^{-/-}$ cells in the role of DCs in priming T-cells reported that transgenic $CD8^+$ T-cells lacking CD226 are stimulated like WT cells when DC's were used to activate them. Intriguingly, when non-professional antigen presenting cells was used for this purpose, CD226 deficient cells were much less efficiently stimulated compared to WT(212). Therefore, CD226 is probably dispensable when DCs prime T-cells, it should be noted that DCs modulate the levels of CD226 on the surface of T-cells, down-regulating CD226 through binding of CD155(213), so the effect of CD226 levels on $CD8^+$ T-cells may become apparent only in pathways bypassing DCs.

We showed that the expression profile of stimulatory receptors on inflationary M38-specific $CD8^+$ T-cells is distinct to M45-specific memory $CD8^+$ T-cells. While having low expression levels of CD27, M38-specific inflationary $CD8^+$ T-cells still express CD258 and CD28; their roles in inflation have yet to be studied.

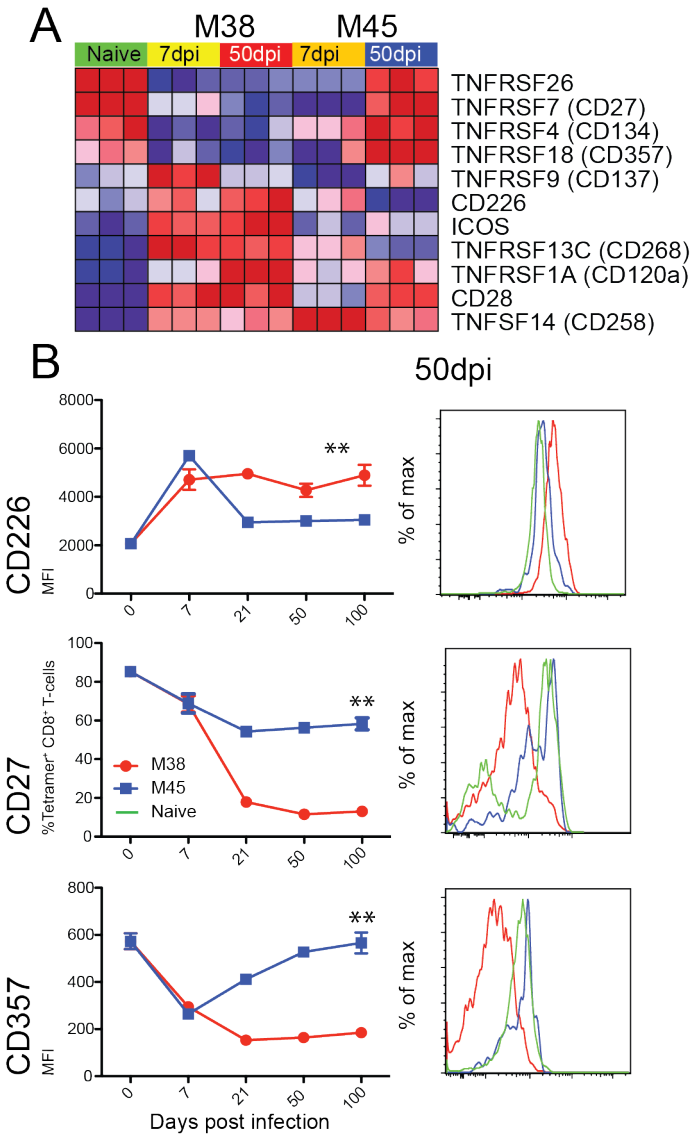


Figure 3-16. **Expression of co-stimulatory receptors in MCMV-specific CD8+ T-cells.** (A) Heat map showing mRNA expression levels of stimulatory receptors measured by microarray analysis of naïve CD8$^+$ T-cells, M38-specific CD8$^+$ T-cells 7 and 50 days post infection and M45-specific CD8$^+$ T-cells 7 and 50 days post infection. Shades of red indicate up-regulated genes and shades of blue indicate down-regulated genes. Filter criteria of at least 2-fold changes with P≤0.05, compared to naïve CD8+ T-cells. (B) Time course showing the percentage of cells or MFI of indicated markers expressed on M38 specific CD8+ T-cells (red) and M45 specific CD8$^+$ T-cells (blue), in the spleen at 0, 7, 21, 50 and 100 days post infection (n=8, mean±SEM). Histograms show expression of indicated markers, gated on live naïve CD8$^+$ T-cells (green) M38-specific CD8$^+$ T-cells (red) and M45-specific CD8+ T-cells (blue).

3.2.13 Production of effector molecules in M38- and M45-specific CD8$^+$ T-cells

Inflationary CD8$^+$ T-cells are known to be able to induce large amounts of IFNγ and TNFα. We wanted to further assess their cytokine secretion and their killing capacity.

The heat map shows mRNA levels of chemokines, cytokines and granzymes in M38- and M45-specific CD8$^+$ T-cells, compared to naïve CD8$^+$ T-cells from array data (Figure 3-17.A). M38-specific inflationary CD8$^+$ T-cells showed a similar expression profile to M38-specific CD8$^+$ T-cells in acute infection. They up-regulated expression of *Il18*, *IFNg*, chemokines (*Ccl3, Ccl4, Ccl5, Ccl9*), granzymes (*Gzma, Gzmb, Gzmm Gzmk)* in comparison to naïve CD8$^+$ T-cells.

The chemokine *Clcf1* mRNA was only up-regulated in M38- and M45-specific CD8$^+$ T-cells in the memory phase. Memory M45-specific CD8$^+$ T-cells, down-regulated *IFNg, Gzma, Gzmk, Ccl3 and Ccl9* while up-regulating *Xcl1, Prf1 Tnfa* and *Lta* (TNFβ), in comparison to inflationary M38-specific CD8$^+$ T-cells.

The levels of *Gzmm* and *Gzmk* mRNA expression were confirmed by qRT-PCR. Similar levels of both granzymes were seen in M38- and M45-specific CD8$^+$ T-cells in the acute and memory phase (Figure 3-17.B).

To assess the specific CD8$^+$ T-cells' ability to produce these chemokines, they were stimulated with peptide and intracellular staining (ICS) performed. Both M38- and M45-specific CD8$^+$ T-cells were capable of producing XCL1, CCL3, CCL4, CCL5 and CCL9 (Figure 3-17.C). They retained the ability to recruit antiviral T-cells and naïve CD8$^+$ T-cells through CCL3, CCL4 and CCL5(214), macrophages by CCL9 and DC cells by XCL1 to the site of infection (215).

The degranulation marker LAMP1, was also measured by flow cytometry. Both M38- and M45-specific $CD8^+$ T-cells, degranulated, indicating they are able to release effector proteins such as granzymes.

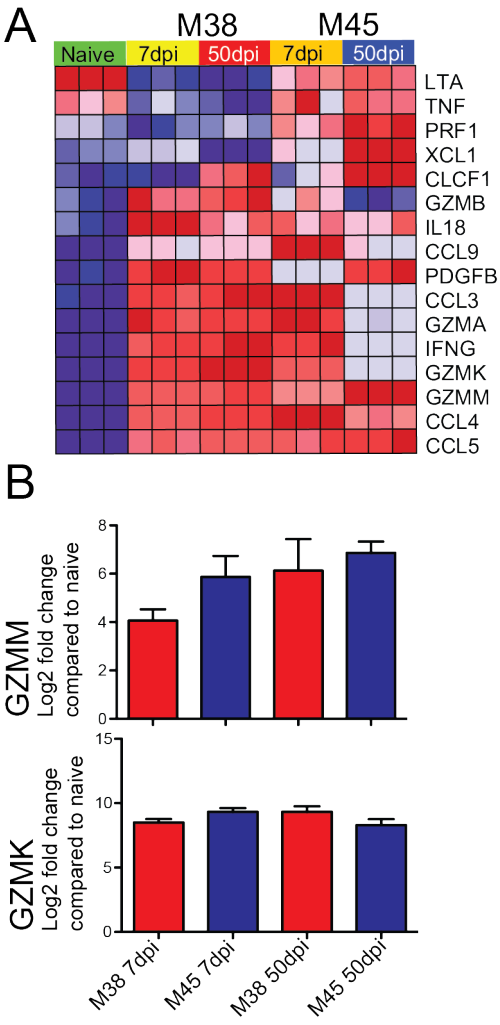
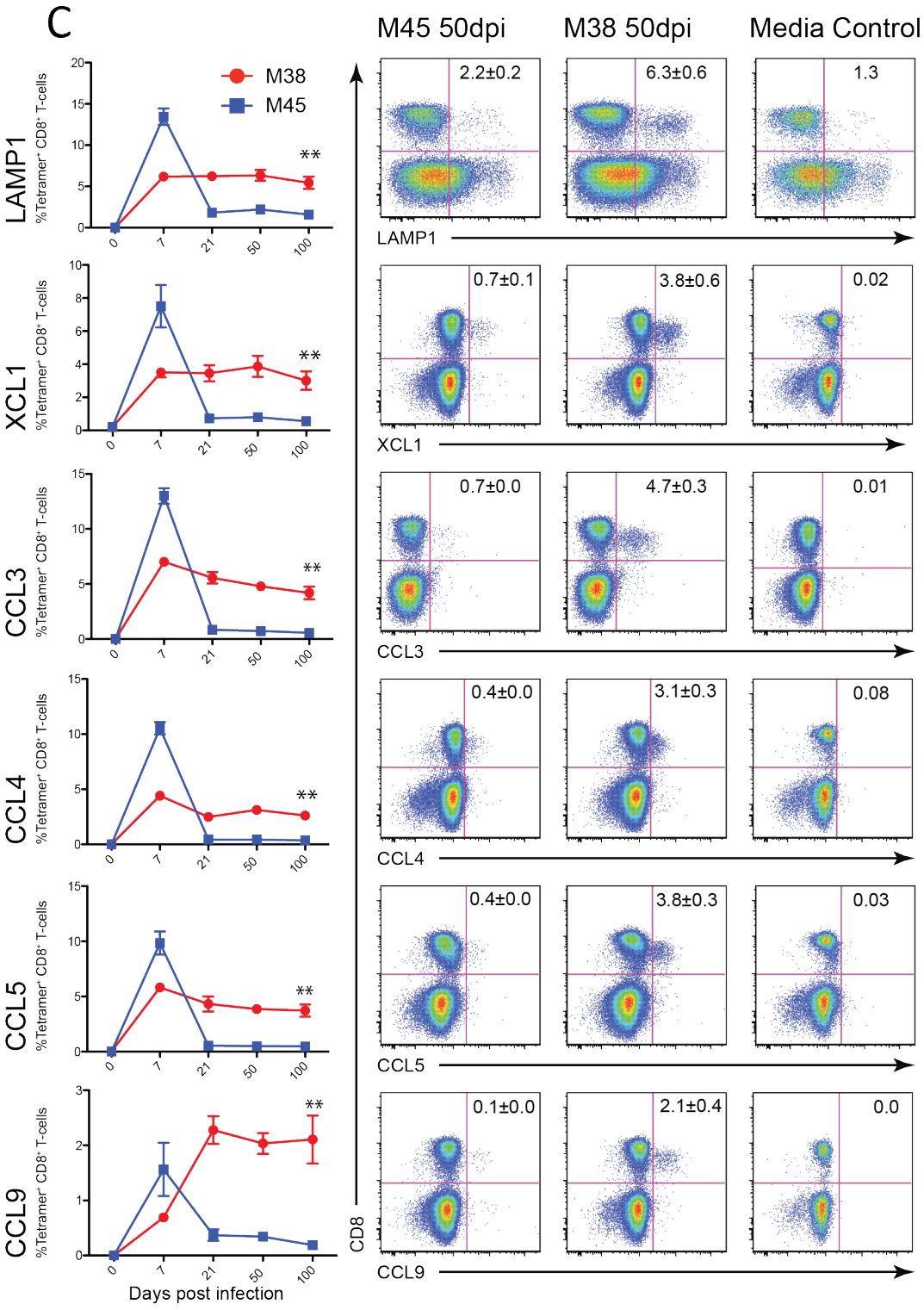


Figure 3-17. **Effector function of MCMV-specific CD8$^+$ T-cells. (**A) Heat map showing mRNA expression levels of effector molecules measured by microarray analysis of naive CD8$^+$ T-cells, M38-specific CD8$^+$ T-cells 7 and 50 days post infection and M45-specific CD8$^+$ T-cells 7 and 50 days post infection. Shades of red indicate up-regulated genes and shades of blue indicate down-regulated genes. Filter criteria of at least 2-fold changes with P≤0.05, compared to naïve CD8$^+$ T-cells. (B) Expression of Granzyme M and K mRNA expression was determined with quantitative real-time PCR in M38- and M45-specific CD8$^+$ T-cells at 7 and 50 days post infection. Five mice were pooled for each group; real-time analysis was performed in triplicates Data presented as Log2 fold change compared to naive CD8$^+$ T-cells after normalization against the internal control gene HPRT. (C) Time course plotting the percentage of M38- (red) or M45- (blue) specific CD8$^+$ T-cells from the spleen producing effector molecules after stimulation with either the M38 or M45 peptide. Mean percentage of LAMP1, XCL1, CCL3, CCL4, CCL5, and CCL9 positive cells within the CD8$^+$ T-cell compartment as indicated (n=8, mean±SEM). Representative flow cytometry plots of splenocytes producing effector molecules stimulated with either M38 or M45 peptide in mice 7 and 50 days post infection. Gated on live lymphocytes, (n=8, mean±SEM).


C
M45 50dpi
M38 50dpi
Media Control
M38
M45
LAMP1
XCL1
CCL3
CCL4
CCL5
CCL9
%Tetramer+ CD8+ T-cells
Days post infection
CD8
2.2±0.2
6.3±0.6
1.3
0.7±0.1
3.8±0.6
0.02
0.7±0.0
4.7±0.3
0.01
0.4±0.0
3.1±0.3
0.08
0.4±0.0
3.8±0.3
0.03
0.1±0.0
2.1±0.4
0.0

3.2.14 Transcription factor expression profile of M38-inflationary CD8$^+$ cells

Much focus has recently been placed on the transcriptional control of specific lymphocytes. In particular which “marker” transcription factor controls the phenotype and cytokine secretion profile. I wanted to assess inflationary CD8$^+$ T-cells to see if they display a specific set of transcription factors allowing inflation.

A heat map was generated from the array data showing transcription factors in M38- and M45-specific CD8$^+$ T-cells, in comparison to naïve CD8$^+$ T-cells (Figure 3-18.A). M38-specific CD8$^+$ T-cells in the acute and memory phase displayed a similar expression profile, having high expression levels of *Tbx21, Zeb2, Id2, Rora, Blimp1, Rog*, and eomes, in comparison to naive CD8$^+$ T-cells. M38-specific inflationary CD8$^+$ T-cells uniquely up-regulated *Zfp313*, *Foxk1* and *Zfp386* in comparison to naïve CD8$^+$ T-cells.

In the memory phase, M38- and M45-specific CD8$^+$ T-cells widely differed. M45-specific CD8$^+$ T-cells down-regulating *Tbx21, Zeb2, Blimp1, Id2, Rora,* and *Rog* and up-regulated expression of *Foxo1, Id3, Samd1, Smad5 and Bcl6*.

The expression levels of T-bet and eomes was confirmed by flow cytometry analysis over time (Figure 3-18.B). Both T-bet and eomes were up-regulated on specific CD8$^+$ T-cells in the acute phase in comparison to naïve CD8$^+$ T-cells. Eomes then decreased in the memory phase with M38-specific inflationary CD8$^+$ T-cells having a level of expression similar to that of naïve CD8$^+$ T-cells, while, M45-specific CD8$^+$ T-cells maintained a higher level of expression. T-bet showed the inverse level of expression in the memory phase, with M45-specific CD8$^+$ T-cells being low and M38-specific CD8$^+$ T-cells having high expression levels.

ID2 protein is required for maintenance of $CD8^+$ T-cells(88). Although ID2 is required for maintained levels of $CD8^+$ T-cells, the ID3 repressor is required for long lived memory cells(87). *Id2* mRNA levels were confirmed by qRT-PCR, *Id2* was up-regulated in specific $CD8^+$ T-cells compared to naïve $CD8^+$ T-cells in the acute and memory phase.

Blimp-1 is a transcriptional repressor involved in the transcriptional network guiding effector and memory T-cell homoeostasis(73). *Blimp1* mRNA levels were confirmed by qRT-PCR, *Blimp1* was up-regulated in M38- and M45-specific $CD8^+$ T-cells compared to naïve $CD8^+$ T-cells in the acute and memory phase (Figure 3-17.C).

Repressor of GATA (ROG) mRNA levels were also confirmed by qRT-PCR, *Rog* was up-regulated in M38- and M45-specific $CD8^+$ T-cells compared to naïve $CD8^+$ T-cells in the acute phase (Figure 3-17.C). In M45-specific memory $CD8^+$ T-cells *Rog* expression decreased, whereas inflationary M38-specific $CD8^+$ T-cells maintained high levels of *Rog* expression. ROG has been shown to dimerize with PLFF proteins and to repress GATA-3 dependent transactivation on cytokine promoters(216). Knock out studies showed that ROG induced inhibition of T-cell activation and proliferation(217).

The transcriptional repressor Bcl6 is in inhibited by Blimp-1; this repressor is up-regulated in M38- and M45-specific $CD8^+$ T-cells in the acute and memory phase, compared to naïve $CD8^+$ T-cells. This was confirmed by qRT-PCR, *Bcl6* has been shown to be required for the generation and maintenance of memory $CD8^+$ T-cells(80) (Figure 3-17.C).

RORα has previously been shown to be specifically expressed in T_H17 cells and to synergize with RORγt to promote the differentiation of T_H17 cells in mice(218). In

MCMV *Rora* mRNA was up-regulated in M38- and M45-specific $CD8^+$ T-cells in specific $CD8^+$ T-cells, qRT-PCR, revealed increased *Rora* expression in memory $CD8^+$ T-cells (Figure 3-17.C).

The transcription repress ZEB2 is a member of the ZFH1 family of 2-handed zinc finger/homeodomain protein and is associated inhibition of proliferation and migration(219). We confirmed the mRNA expression levels of *Zeb2* by qRT-PCR. M38- and M45-specific $CD8^+$ T-cells up-regulate expression, in comparison to naive $CD8^+$ T-cells, there is further increase as the cells enter the memory phase.

Inflationary $CD8^+$ T-cells displayed a unique set of transcription factors in comparison to memory M45-specific $CD8^+$ T-cells. This transcription profile induced by cytokines such as IL-12 is of importance in understanding the regulation of inflation.

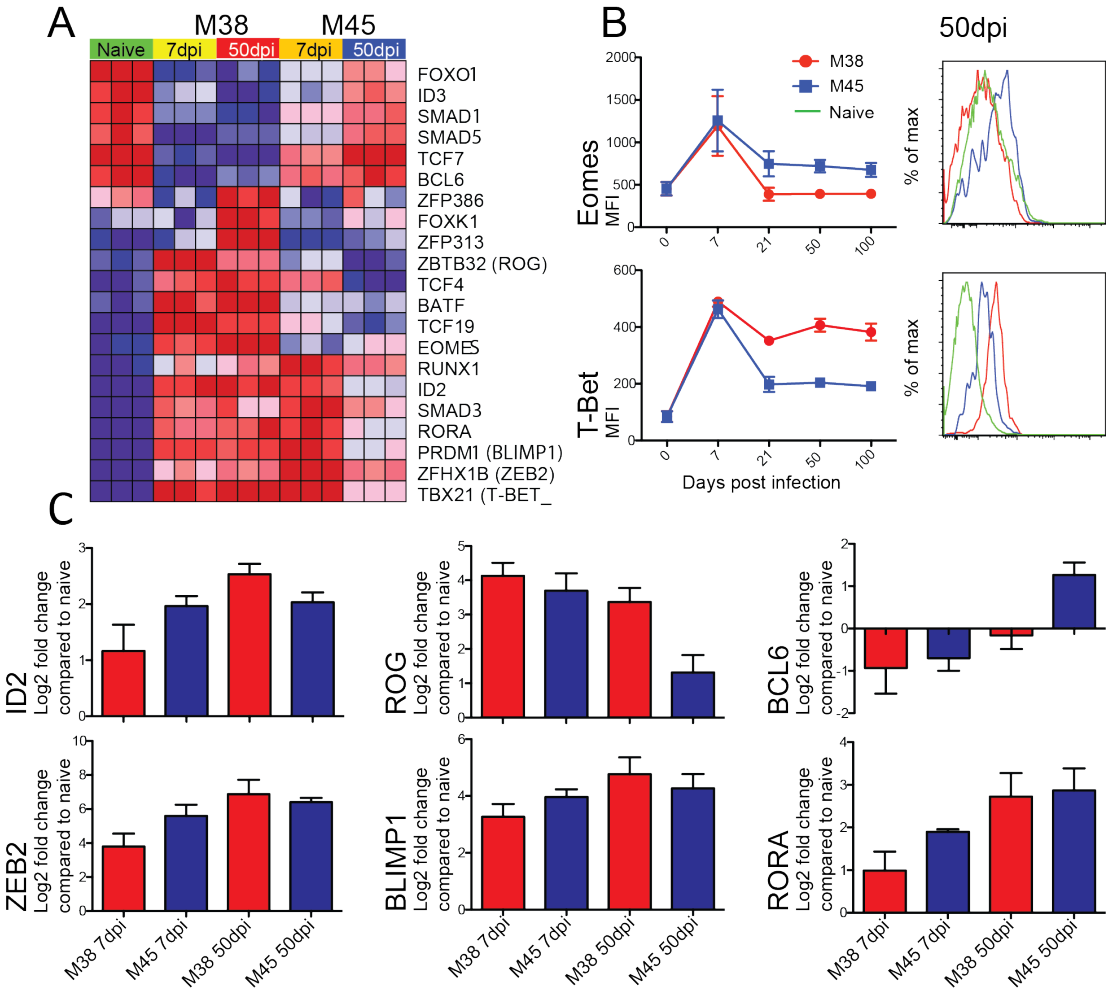


Figure 3-18. **M38-specific inflationary CD8$^+$ T-cells display a distinct transcription regulator profile compared to M45 specific memory CD8$^+$ T-cells**. (A) Heat map showing mRNA expression levels of transcriptional factors measured by microarray analysis of naive CD8$^+$ T-cells, M38-specific CD8$^+$ T-cells day 7 and 50 post infection and M45-specific CD8$^+$ T-cells 7 and 50 days post infection. Shades of red indicate up-regulated genes and shades of blue indicate down-regulated genes. Filter criteria of at least 2-fold changes with P≤0.05, compared to naïve CD8$^+$ T-cells. (B) Time course showing the MFI of the indicated markers on M38-specific CD8$^+$ T-cells (red) and M45-specific CD8$^+$ T-cells (blue) in the spleen at 0, 7, 21, 50 and 100 days post infection (n=8, mean±SEM). Histograms show expression of indicated markers, gated on live naïve CD8$^+$ T-cells (green) M38-specific CD8$^+$ T-cells (red) and M45-specific CD8$^+$ T-cells (blue). (C) mRNA expression of the transcription factors, ID2, ROG, BCL6, ZEB2, BLIMP1 and RORA was determined with quantitative real-time PCR in M38- and M45-specific CD8$^+$ T-cells at 7 and 50 days post infection. Five mice were pooled for each group; real-time analysis was performed in triplicates. Data presented as Log2 fold change compared to naive CD8$^+$ T-cells after normalization against the internal control gene HPRT.

3.2.15 Suppression of the Jak-Stat pathway in inflationary cells

The JAK-STAT pathway is a major signalling pathway involved in the homeostasis of lymphocytes. While none of the STAT genes were differentially expressed on the gene array, the Suppressor of cytokines (SOCS) family was differentially expressed in comparison to $CD8^+$ T-cells (Figure 3-19.A). The M38-specific $CD8^+$ T-cells showed a similar expression profile in the acute and memory phase. In the memory phase M38- and M45-specific $CD8^+$ T-cells displayed strikingly different expression profiles. *Socs2* and *Socs4* were up-regulated in M38 specific $CD8^+$ T-cells, in comparison to naive $CD8^+$ T-cells, while M45-specific $CD8^+$ T-cells down regulated *Socs2* and Socs4 and up-regulated *Socs3*, *Socs5*, *Socs1*, in comparison to M38-specific $CD8^+$ T-cells.

The family of repressors might have a role in determining $CD8^+$ T-cells maturation. Cytokine signaling drives the maturation of $CD8^+$ T-cells, and the SOCS family members suppress the signaling, therefore halting the maturation process.

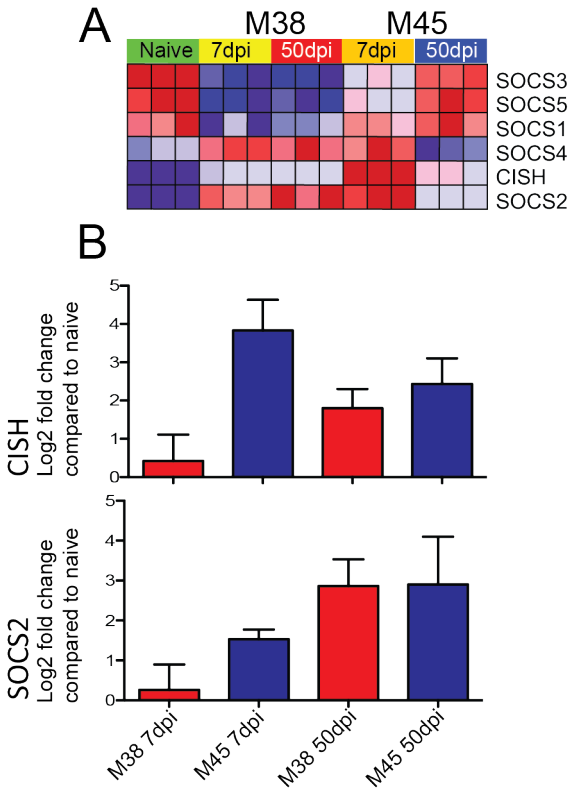


Figure 3-19. **Expression of SOCS family in MCMV-specific CD8$^+$ T-cells.** A) Heat map showing mRNA expression levels of SOCS family, measured by microarray analysis of naive CD8$^+$ T-cells, M38-specific CD8$^+$ T-cells day 7 and 50 post infection and M45-specific CD8$^+$ T-cell 7 and 50 days post infection. Shades of red and blue indicate up-regulated genes down-regulated genes respectively. Filter criteria of at least 2-fold changes with P≤0.05, compared to naïve CD8$^+$ T-cells. B) Expression of CISH and SOCS2 mRNA expression was determined with quantitative real-time PCR in M38- and M45-specific CD8$^+$ T-cells at 7 and 50 days post infection. Five mice were pooled for each group; real-time analysis was performed in triplicates. Data presented as Log2 fold change compared to naive CD8$^+$ T-cells after normalization against the internal control gene HPRT.

3.3 Discussion

MCMV infection produces a population of epitope-specific $CD8^+$ T-cells that gradually inflates over the course of 21 days and then is stably maintained at a high frequency. These were shown to be functional, and to have the phenotype of terminally differentiated effector memory cells, being $KLRG1^{high}$, $CD127^{low}$, $CD122^{low}$, and $CD27l^{ow}$ and expressing high levels of T-Bet and low levels of eomes (Table 3-1).

Previous research has focused on CD127 (IL-7Rα) and CD122 (IL-2Rβ); it has been shown that T_{EM}, while being low in CD122, are reliant on IL-15 for their maintenance(62). The expression levels of receptors can sometimes be misinterpreted in representing the level of the cells' reliance on the interleukin. Inflationary cells are also low in CD124 (IL-4Rα) and CD126 (IL-6Rα) compared to T_{CM} cells. They do however express CD218 (IL-18Rα), CD210 (IL-10Rα), CD215 (IL-15Rα) and CD212 (IL12Rβ1); it would be of interest to see the role IL-12 plays on inflationary cells. Its stimulation would account for the differential expression of T-bet and eomes(68,113).

There are many possible receptors that could be involved in the regulation of inflation, and the loss of the chemokine receptor CXCR3 could be just one possible explanation. Knockout studies showed that CXCR3 was important in regulating effector $CD8^+$ T-cell contraction and memory generation in influenza virus infection(174,220) The fractalkine receptor CX3CR1 was up-regulated on inflationary cells. Fractalkine receptor is induced by $CD8^+$ T-cells after infection, and in addition to its role in chemotaxis and adhesion, it supports survival and homeostasis(221).

Inflationary cells have high expression of the KLR receptors, both stimulatory and inhibitory. These are potentially involved in protecting the cells from destroying self while targeting MCMV-infected cells that have down regulated MHC Class I molecules. The activation threshold and downstream functions of the CD8+ T cells will be modulated by the complex of signals arising from these activatory and inhibitory receptors and this will depend in turn on the ligand expression on APC or target.

By following the replication state of inflationary $CD8^+$ T-cells with Ki67 over the course of infection we can see that these cells were still proliferating at higher rate than T_{CM} cells up to day 100 post infection. This is also confirmed by the expression of the exhaustion markers, which are in this context possibly more correctly makers of proliferation. Due to this decrease in replication there must be homeostasis to allow the cells to be stably maintained at such a high frequency, otherwise after 50 days post infection there would be a geadual decline in number.

The increase in frequency of inflationary $CD8^+$ T-cells could also hinge upon the expression of Bcl-x_L, which was uniquely expressed in the inflationary $CD8^+$ T-cells. Expression of this molecule inhibits apoptosis in $CD8^+$ T-cells, and has been reported to be induced by CX3CR1 triggering making this receptor a important target for future research(222)

	Naïve	M38 7dpi	M45 7dpi	M38 100dpi	M45 100dpi
CD127	++	-	-	-	++
CD126	++	-	-	-	+
CD122	-	++	++	+	++
CD218	-	+	+	++	++
CX3CR1	-	+	+	++	+/-
CXCR3	-	++	++	-	++
KLRC1	-	+	+	++	+
KLRG1	-	+	+	++	+
KLRK1	-	+	+	++	++
KLRE1	-	+	+	++	+
KLRA3	-	-	+	+	-
CD229	-	++	++	++	++
CD319	-	++	++	++	++
CD73	+	-	-	+	++
CD26	++	-	-	-	+
CD54	-	++	++	++	+
PD1	-	++	++	-	-
BTLA	+	-	-	-	+
BCL2	++	-	-	+	++
CD226	+	++	++	++	+
CD27	++	++	++	-	++
CD357	++	-	-	-	++
Eomes	-	++	++	-	+
T-Bet	-	++	++	++	+

Table 3-1. Differential expression of phenotypic markers on MCVM epitope specific $CD8^+$ T-cells. Levels of expression indicated by ++(high expression) and – (low expression).

3.3.1 Chapter summary

1) I have identified a number of different pathways that have been altered in $CD8^+$ T-cells memory inflation when comparing these cells to naïve $CD8^+$ T cells, effector $CD8^+$ T-cells and to the T_{CM} pool of cells, such as chemokine and cytokine receptors. They display a distinct set of genes that are up-regulated (KLR receptors and CX3CR1), some of which are uniquely associated with memory inflation Elucidating the roles these genes have in regulating the inflationary CD8 T-cells will be a key next step.
2) The inflationary CD8 T-cell gene profile is distinct from that seen in T cell exhaustion.
3) Largely but not uniformly, the transcriptional changes are mirrored in phenotypic and functional assays.

4 $CD8^+$ T-cell memory inflation induced by adenovirus

4.1 Introduction

The $CD8^+$ T-cell responses to acutely cleared viral infections are characterized by rapid expansion followed by contraction and differentiation into memory cells that self renew in a cytokine dependent, Ag-independent manner. In contrast $CD8^+$ T-cells in persistent infections have been described as acquiring defects in homeostatic proliferation; the maintenance of antiviral memory $CD8^+$ T-cell in high level systemic chronic lymphocytic choriomeningitis Virus (LCMV) infection requires cognate Ag but not IL-7 and IL-15(223). This dysfunction is associated with the level, duration and pathogenesis of the infection, as well as $CD4^+$ T cell help. However, low-level systemic viral infections induce different antiviral $CD8^+$ T-cell responses. As described in the previous chapters, depending on the epitope specificity, antiviral $CD8^+$ T-cell numbers in murine CMV (MCMV) increase over the course of infection and stabilize at a high frequency - the phenomenon of “memory inflation”(112).

Memory inflation occurs in other herpes viruses. Herpes simplex virus 1 establishes life long latency in sensory neurons with spontaneous events of virus reactivation. Antiviral $CD8^+$ T-cells accumulate upon ocular HSV-1 infection and infection induces $CD8^+$ T-cells persisting in the skin upon resolution of primary infection in the absence of antigen(199,200,224-226). Epstein-Barr virus (EBV) infection in adolescence causes prolonged high levels of virus shedding, persisting for the life of the host as asymptomatic latent infection, with $CD8^+$ T-cells specific for latent proteins increasing in frequency upon establishment of latency(201,202,227-229).

The induction of memory inflation has been harnessed to produce protective vaccines. A replicating CMV vaccine encoding a single Ebola virus nucleoprotein

induced large population of functional $CD8^+$ T-cells which proved to be protective(114,203). This method was also shown to induce protection against SIV, when inserting SIV epitopes into RhCMV(115,204).

These vaccines utilized replication-competent CMV strains, however it has been show that some degree of memory inflation can occur with a single cycle CMV virus(126,205). Furthermore, we have shown that using a replication incompetent adenovirus vector encoding β-galactosidase (Ad-LacZ) induces memory inflation to one of two immunodominant epitopes (Bolinger et al., submitted). Adenovirus vectors transduce a wide range of cell types, and have been used for a number of vaccine studies. They are attractive vectors due to ability to induce a broad immune response, including $CD8^+$ T cells, and their inability to integrate into the host genome (and good safety record)(230).

There are many questions about memory inflation still to be answered. Further analysis of specific transcriptional programmes may provide clues to understanding the control of memory inflation By analysing memory inflation induced by Ad-lacZ and comparing it to memory inflation induced by MCMV at the level of T cell transcriptomes I aimed to dissect out the unique gene profile that is distinct for inflationary $CD8^+$ T-cells, compared with effector and central memory $CD8^+$ T-cells.

4.1.1 Key questions in this chapter

1. To define the transcriptional changes associated with memory inflation using the novel adenovirus model.
2. To compare inflationary responses with conventional (non-inflationary) $CD8^+$ T cell memory responses in this model at the level of transcription, phenotype and function.

3. To identify a core set of transcriptional modifications associated with memory inflation in both the MCMV and adenoviral models.

4.2 Results

4.2.1 Epitope specific CD8+ T-cell memory inflation induced by adenovirus vector

Immunization of C57BL/6 mice with replication incompetent Ad-LacZ induces two types of $CD8^+$ T-cell responses to βgal epitopes (βgal_{96} and βgal_{497}) (Figure 4-1). Using MHC class I tetramers, $CD8^+$ T-cell responses were tracked longitudally. Lymphocytes from the spleen were isolated at different time points and βgal-specific $CD8^+$ T-cells quantified. At 21 days post immunization, βgal_{96}-specific $CD8^+$ T-cells have expanded, making up 8.6% of total $CD8^+$ T-cells. βgal_{96}-specific $CD8^+$ T-cells show an inflationary profile and carry on expanding until 50 days post immunization, then slightly decreasing at 100 days post immunization where they make up 13% of total $CD8^+$ T-cells. In contrast, βgal_{497}-specific $CD8^+$ T-cells show a standard "central" memory response. These peak at 21 days post immunization, making up 4.9% of total $CD8^+$ T-cells, then contract, being stabily maintained at a low frequency of 0.6% of total $CD8^+$ T-cells.

These data show memory inflation is not unique to MCMV infection; immunization with replication incompetent adenovirus containing β-galactosidase induces an inflationary $CD8^+$ T-cell profile. This novel induction of inflation provides a novel and tractable model to uncover the key requirements of inflation – in particular by avoiding the issue with the complex replication cycle of herpes viruses.

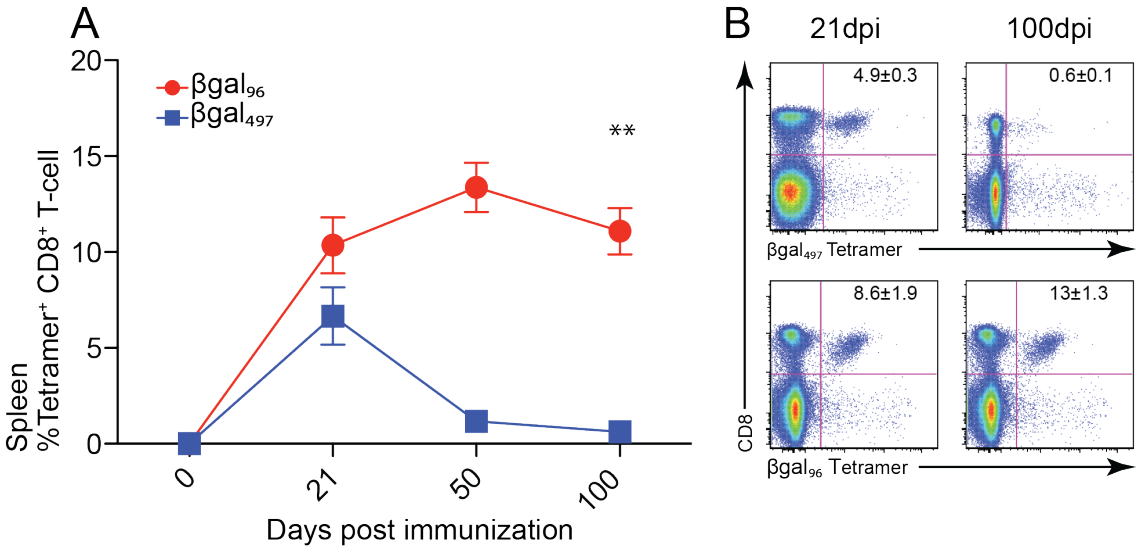


Figure 4-1 **Frequency of Ad-LacZ specific CD8$^+$ T-cells**. C57BL/6 mice were immunized intravenously (i.v) with 1x10^9 pfu Ad-LacZ. A) Time course for βgal$_{96}$ (red) and βgal$_{497}$ (blue) specific CD8$^+$ T-cells. Splenocytes from at 0, 21, 50 and 100 days post immunization were stained with tetramers and analysed by flow cytometry. Mean percentages of live tetramer CD8$^+$ lymphocytes are indicated (n=5, mean±SEM). B) Representative flow cytometry plots of tetramer staining for βgal$_{96}$ and βgal$_{497}$ CD8$^+$ T-cells on 21 and 100 days post immunization in the spleen. Mean percentage of live tetramer CD8$^+$ lymphocytes is indicated (n=10, mean±SEM).

4.2.2 Tetramer sorting of Ad-LacZ-specific $CD8^+$ T-cells and gene expression analysis

In order to assess whether there is a transcriptional program supporting memory inflation and to analyse the molecular mechanisms of $CD8^+$ T-cell inflation, gene expression array analysis was performed. Expression profiles of inflationary βgal_{96}-specific $CD8^+$ T-cells were compared to that of βgal_{497}-specific $CD8^+$ T-cells, that show a standard central memory response. C57BL/6 mice were immunized i.v with Ad-LacZ. Spleens were harvested on 21 and 100 days post immunization. Lymphocytes were isolated and tetramer stained, and tetramer-specific $CD8^+$ T-cells cells sorted. Purities of >85% were achieved for cell sorts (Figure 4-2). As a control $CD8^+$ T-cells from naïve mice were sorted ($CD8^+$, $CD3^+$, $CD62L^+$, $CD44^+$).

Numbers of up-regulated/down-regulated genes in effector and memory populations: RNA was extracted from sorted cells and cDNA run on an Illumina MouseRef-8 v2.0 Expression BeadChip. The gene expression profiles of effector, central memory and inflationary $CD8^+$ T-cells were each compared to naïve $CD8^+$ T-cells so that direct comparisons between the groups could be performed (Figure 4-2.C).

At 21 days post immunization 850 genes were up-regulated and 246 down-regulated in βgal_{96}- specific (inflationary) $CD8^+$ T-cells compared to naïve $CD8^+$ T-cells. On 100 days post immunization, in contrast the number of up-regulated genes increased to 937, whereas 403 were down-regulated in βgal_{96}- specific $CD8^+$ T-cells compared to naïve $CD8^+$ T-cells.

βgal_{497}-specific $CD8^+$ T-cells showed a similar profile in the number of genes expressed. At 21 days post immunization 746 genes were up-regulated and 424 down-regulated in βgal_{497}-specific $CD8^+$ T-cells compared to naïve $CD8^+$ T-cells.

However, on 100 days post immunization 953 genes were up-regulated and 441 down-regulated in βgal_{497}-specific $CD8^+$ T-cells compared to naïve $CD8^+$ T-cells.

While the different $CD8^+$ T-cell populations showed a similar number of genes differentially expressed at 21 and 100 days post immunization, by directly comparing the different $CD8^+$ T-cell populations it is evident that inflationary βgal_{96}- specific $CD8^+$ T-cells are neither identical to effector $CD8^+$ T-cells nor are they comparable with memory βgal_{497}-specific $CD8^+$ T-cells (Figure 4-2.D).

There are similarities between the different $CD8^+$ T-cell populations, sharing 377 differentially expressed genes (Figure 4-2.B). Adenovirus clearly induced two distinct $CD8^+$ T-cell memory responses. The two memory populations have the largest number of uniquely differentially expressed genes, inflationary βgal_{96}- specific $CD8^+$ T-cells contain 445 uniquely differentially expressed genes, in comparison, βgal_{497}-specific $CD8^+$ T-cells contain 669 uniquely differentially expressed genes.

Overall, analysis of the gene array identified that the inflationary βgal_{96}- specific $CD8^+$ T-cells have a distinct gene expression profile: they have an increased number of differentially expressed genes compared to that of acute βgal_{96}- specific $CD8^+$ T-cells and are also distinct to that of βgal_{497}-specific $CD8^+$ T-cells. I next went on to define the significance of the specific genes modulated in memory inflation.

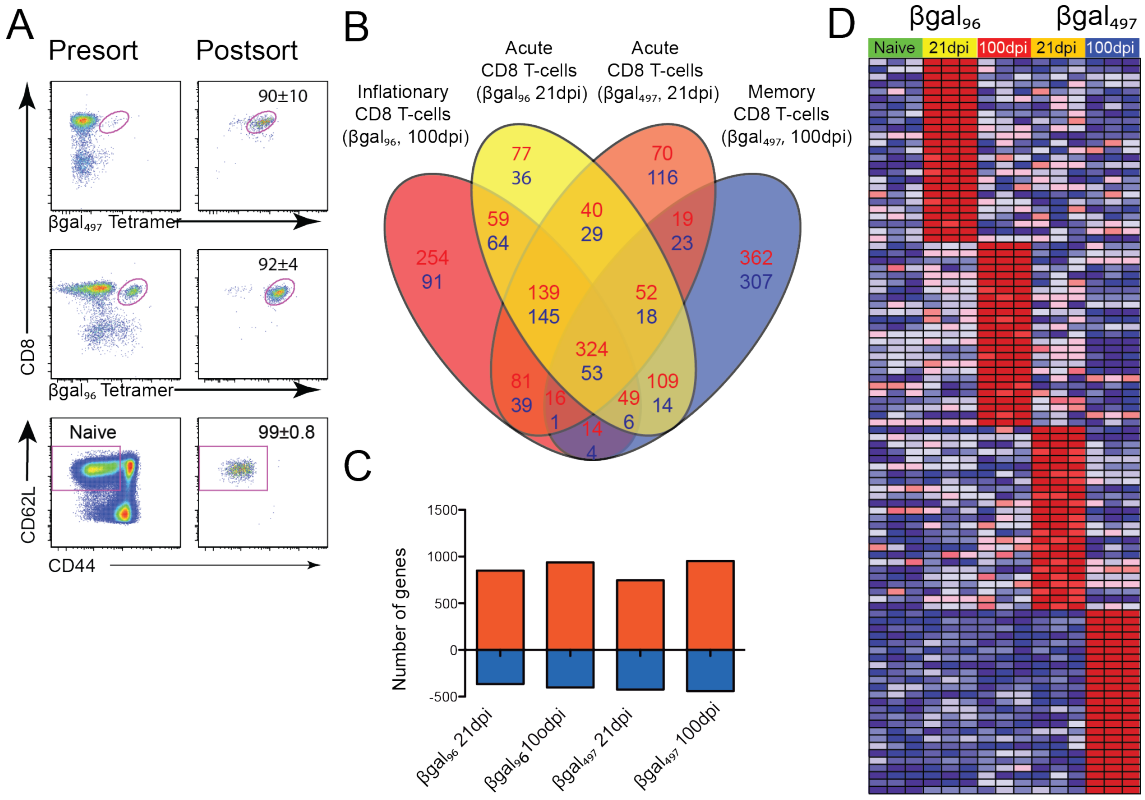


Figure 4-2 **Gene expression signature of Ad-LacZ specific CD8$^+$ T-cells.** C57BL/6 mice were immunized (i.v) with 1x10^9 pfu Ad-LacZ. Expression level of mRNA was measured by microarray analysis of naïve CD8$^+$ T-cells (CD62L$^-$, Cd44$^+$), βgal$_{96}$- specific CD8$^+$ T-cells and βgal$_{497}$-specific CD8$^+$ T-cells 21 and 100 days post immunization. (A) Representative flow cytometry plots from cell sorts of naïve CD8$^+$ T-cells and βgal$_{96}$- specific CD8$^+$ T-cells and βgal$_{497}$-specific CD8$^+$ T-cells 100 days post immunization. Cell sorts were performed in triplicate, five mice pooled per group. Mean percentage of live tetramer$^+$ CD8$^+$ lymphocytes is indicated (n=3, mean±SEM). (B) Venn diagram showing the number of differentially expressed genes between βgal$_{96}$- specific CD8$^+$ T-cells 21 (yellow) and 100 (red) days post infection, βgal$_{497}$-specific CD8$^+$ T-cells 21 (orange) and 100 (blue) days post immunization. Filter criteria of at least 2 fold change with P≤0.05 compared to naïve CD8$^+$ T-cells. Up-regulated genes are indicated in red and down-regulated genes in blue. (C) Number of genes up-regulated (red) and down-regulated (blue) in βgal$_{96}$- specific CD8$^+$ T-cells and βgal$_{497}$-specific CD8$^+$ T-cells, 21 and 100 days post immunization compared with naïve CD8$^+$ T-cells. . Filter criteria of at least 2 fold change with P≤0.05 compared to naïve CD8$^+$ T-cells. (D) Heat map showing comparative marker selection taking the top 25 up-regulated genes for each population. Shades of red indicate up-regulated genes; shades of blue indicate down-regulated genes.

4.2.3 Gene ontology analysis of unique gene sets

To further dissect the results of the differentially expressed genes obtained with the gene array, the uniquely up-regulated genes of each population were assessed for biological processes that were significantly enriched via gene ontology (Figure 4-3). No enrichment was found in acute βgal_{497}-specific $CD8^+$ T-cells. In inflationary βgal_{96}- specific $CD8^+$ T-cells, biological process that were enriched are involved in regulation of transcription (DNA-dependent) (red), transcription (yellow), transport (green), cell cycle (light blue), apoptosis (dark blue), regulation of transcription from RNA polymerase (pink), cell division (dark red), regulation of RNA splicing (green) and cellular processes (orange)(Figure 4-3.A).

In contrast, acute βgal_{96}-specific $CD8^+$ T-cells are less enriched in biological processes. Those enriched are cell cycle (red), negative regulation of cell cycle (yellow), induction of apoptosis (green) and endocytosis (blue).

However, memory βgal_{497}-specific $CD8^+$ T-cells had an increased number of biological processes enriched. In decreasing order of enrichment, transport (red), phosphorylation (yellow), proteolysis (green), protein phosphorylation (light blue), inflammatory response (dark blue), protein autophosphorylation (pink), innate immune response (dark red), cytokine mediated signalling pathway (dark green), positive regulation of IL-12 production (orange), and positive regulation of mast cell degranulation (purple).

The enrichment of biological processes in inflationary βgal_{96}-specific $CD8^+$ T-cells appear to relate to the cell cycle and survival, and appear highly relevant to cells which are still proliferating and maintained at high levels at 100 days post immunization. They contain 35 genes enriched belonging to the group regulation of

transcription, (DNA-dependent), suggesting that inflationary cells might have a distinct transcription factor profile. In contrast, in memory βgal_{497}-specific $CD8^+$ T-cells, the majority of biological processes enriched are involved in transport and regulation of protein function. To address these differences further, I next analysed individual gene expression.

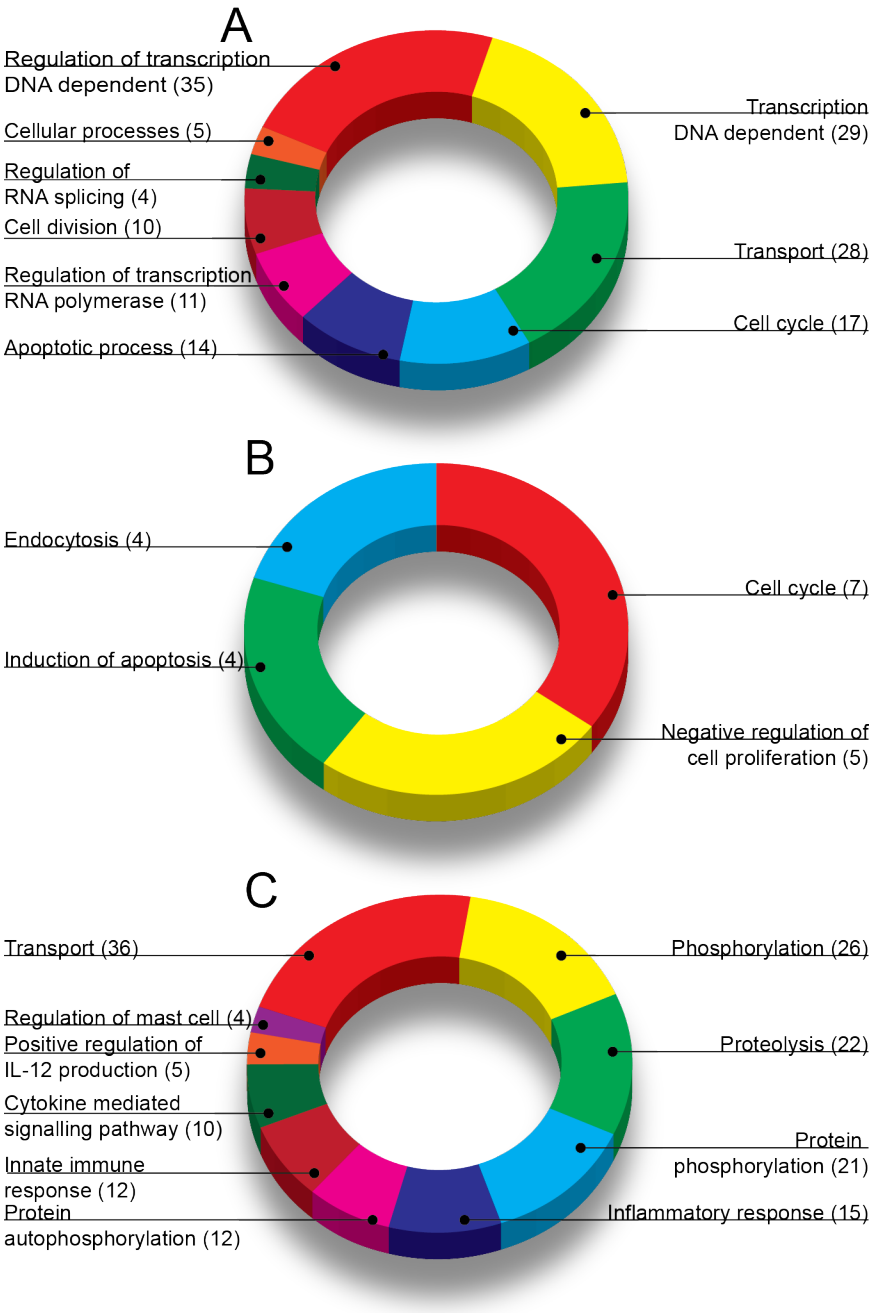


Figure 4-3 **Gene ontology analysis of unique gene sets.** Gene groups that are unique for specific Ad-LacZ CD8+ T-cell populations, up-regulated (≥2 fold, p-value ≤0.05, compared to naïve CD8+ T-cells were run on Genecodis. Gene ontology (GO), biological processes (BP) enriched are shown (≥4 genes, p-value ≤0.001). (A) βgal96-specific $CD8^+$ T-cells, 100dpi. (B) βgal96-specific $CD8^+$ T-cells, 21dpi. (C) βgal96-specific $CD8^+$ T-cells, 100dpi.

4.2.4 Expression of NK-cell receptors on inflationary CD8$^+$ T-cells

I have previously shown that the KLR family of receptors are up-regulated on inflationary βgal_{96}-specific CD8$^+$ T-cells, compared to naive CD8$^+$ T-cells. The heat map (Figure 4-4.A) shows the KLR family of receptor expression in different CD8$^+$ T-cell populations compared to naïve CD8$^+$ T-cells. In the acute phase βgal_{96}- and βgal_{497}-specific CD8$^+$ T-cells up-regulate the expression of inhibitory (*Nkg2a*, *Klrg1*, *Klre1*) and stimulatory receptors (*Nkg2d*) compared to naïve CD8$^+$ T-cells. Inflationary βgal_{96}-specific CD8$^+$ T-cells maintain high expression; in contrast, memory βgal_{497}-specific CD8$^+$ T-cells decreases expression of *Klre1*, *Klrg1* and *Nkg2a* in comparison to the acute phase.

This increased expression of inhibitory KLR receptors on inflationary βgal_{96}-specific CD8$^+$ T-cells is interesting in relation to adenovirus immunity. Adenoviruses are capable of down-regulating MHC class I molecules(207,231,232); thus by removing MHC class I glycoproteins from the cell surface of infected cells, βgal_{96}-specific CD8$^+$ T-cells may be primed to target viral infected cells.

4.2.5 Induction of effector molecules in βgal_{96}- and βgal_{497}-specific CD8$^+$ T-cells

Previous work has shown that inflationary βgal_{96}-specific CD8$^+$ T-cells are still functional and capable of producing large amounts of IFNγ and TNFα. I wanted to further assess their cytokine production and their killing capacity.

The heat map shows the mRNA levels of chemokine, cytokines and granzymes in βgal_{96}- and βgal_{497}-specific CD8$^+$ T-cells, in comparison to naïve CD8$^+$ T-cells

(Figure 4-4.B). Acute and inflationary βgal_{96}-specific $CD8^+$ T-cells show a similar expression profile, having high expression of *Ccl3, Ccl4, Ccl5, Ccl9*, *Gzma, Gzmm, Gzmk, Il15, Il18* and *IFNg* in comparison to naïve $CD8^+$ T-cells. The chemokine *Clcf1* was up-regulated in inflationary βgal_{96}-specific $CD8^+$ T-cells compared to the acute phase. In comparison memory βgal_{497}-specific $CD8^+$ T-cells down-regulate *Gzma*, *Gzmk*, *Ccl3* and *IFNg*, up-regulate *Xcl1*, *Prf1, Lta*, and *Tnfa* in comparison to the acute phase.

Based on these profiles, inflationary βgal_{96}-specific $CD8^+$ T-cells appear capable of killing virally infected cells through the production of granzymes, recruit $CD8^+$ T-cells by CCL3, CCL4, CCL5, macrophages by CCL9 and DCs by XCL1. They thus appear polyfunctional and capable of producing a wide range of effector molecules.

Further work by my colleague Dr Beatrice Bolinger has confirmed many of these features at the phenotypic and functional level, using assays as described in the previous chapter for MCMV.

4.2.6 Transcription factor profile of βgal_{96}-specific $CD8^+$ T-cells

Recently focus has been placed on the transcriptional control of lymphocytes. We wanted to assess inflationary $CD8^+$ T-cells to see if they display a specific set of transcription factors allowing inflation.

A heat map was generated from the array data showing transcription factors in βgal_{96}- and βgal_{497}-specific $CD8^+$ T-cells (Figure 4-1.C). βgal_{96}-specific $CD8^+$ T-cells in the acute and memory phase display a similar expression prolife, having high expression levels of *Tbx21, Zeb2, Id2, Rora*, *Prdm1*, *Rog* and *Eomes* in comparison

to naïve $CD8^+$ T-cells. Inflationary βgal_{96}-specific $CD8^+$ T-cells uniquely up-regulate three defined genes, *Zfp313, Foxk1* and *Zfp386* in comparison to naive $CD8^+$ T-cells.

In stark contrast, memory βgal_{497}-specific $CD8^+$ T-cells, down-regulate the transcription factors from the acute phase and up-regulate *Id3, Foxo1, Smad1*. *Smad5, Tcf7, Tcf4 and Bcl6*.

Thus, inflationary βgal_{96}-specific $CD8^+$ T-cells displayed up-regulation of a unique set of transcription factors in comparison to memory βgal_{497}-specific $CD8^+$ T-cells. This transcription profile is induced by cytokines such as IL-12 (see discussion) and is important in trying to understand the regulation of inflation.

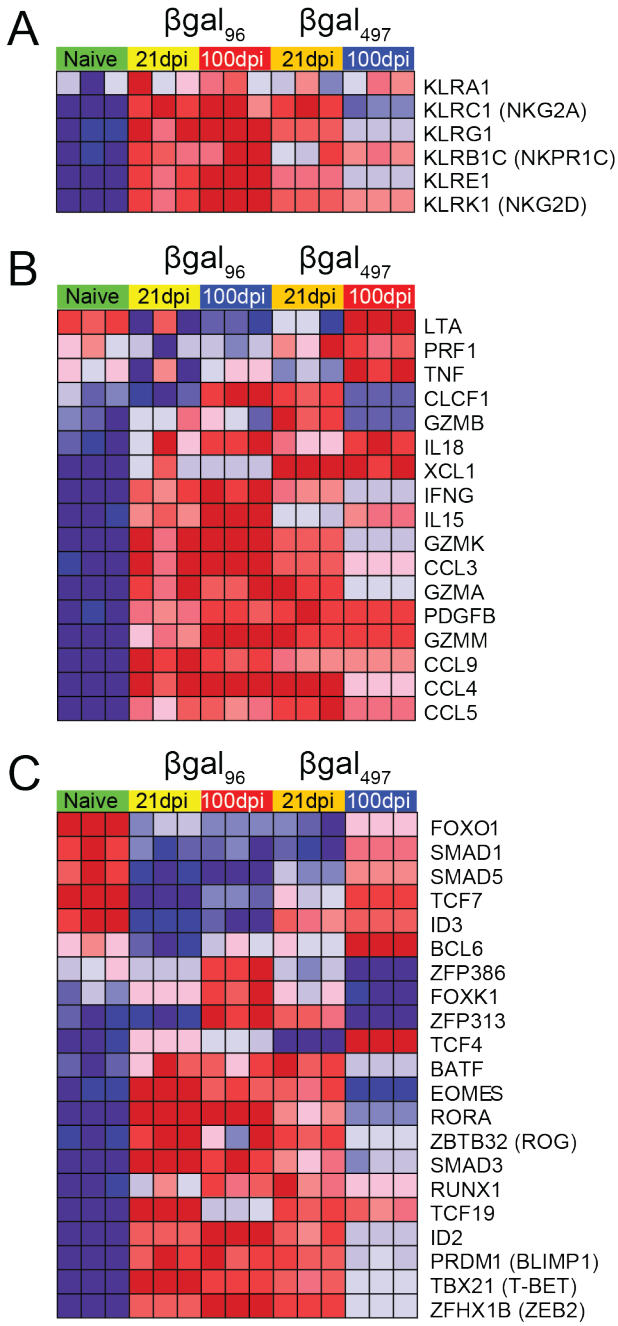


Figure 4-4 **NK-cell receptor, effector function and transcription factor expression profile of inflationary βgal$_{96}$-specific CD8$^+$ T-cells**. Heat maps showing mRNA expression levels of indicated genes measured by microarray analysis of naïve CD8$^+$ T-cells, βgal$_{96}$- and βgal$_{497}$-specific CD8$^+$ T-cells 21 and 100 days post immunization. Shades of red indicate up-regulated genes and shades of blue indicate down-regulated genes. Filter criteria of at least 2-fold changes with p-value≤0.05, compared to naïve CD8$^+$ T-cells. (A) NK-cell receptor expression of Ad-LacZ specific CD8$^+$ T-cells. (B) Effector function of Ad-LacZ specific CD8$^+$ T-cells. (C) Transcriptional profile of Ad-LacZ specific CD8$^+$ T-cells

4.2.7 Cell cycle analysis

We showed that inflationary M38-specific $CD8^+$ T-cells after MCMV infection have increased proliferation until 50 days post infection in comparison to memory M45-specific $CD8^+$ T-cells; by 100 days post infections they show the same profile. To check the proliferation kinetics of inflationary βgal_{96}-specific $CD8^+$ T-cells and memory βgal_{497}-specific $CD8^+$ T-cells I analysed a subset of genes involved in proliferation, shown in the heat map (Figure 4-5.A). Acute βgal_{96}-and βgal_{497}-specific $CD8^+$ T-cells up-regulate genes involved in proliferation compared to naïve CD8+ T cells. In contrast, inflationary βgal_{96}-specific $CD8^+$ T-cells then down regulate cell cycle genes. However, memory βgal_{497}-specific $CD8^+$ T-cells maintain high expression of some cell cycle genes and down-regulate a few, of interest the proliferation marker *Mki67*.

To follow the proliferation state of βgal_{96}- and βgal_{497}-specific $CD8^+$ T-cells, over time, I measured expression of Ki67 in the spleen by flow cytometry (Figure 4-5.B). Both βgal_{96}- and βgal_{497}-specific $CD8^+$ T-cells were highly proliferative at 21 days post immunization, with up to 85% of the tetramer-specific $CD8^+$ T-cells expressing Ki67. After this both peptide-specific $CD8^+$ T-cell populations decreased expression to about 15% at 50 days post immunization, a level that was maintained till 100 days post immunization.

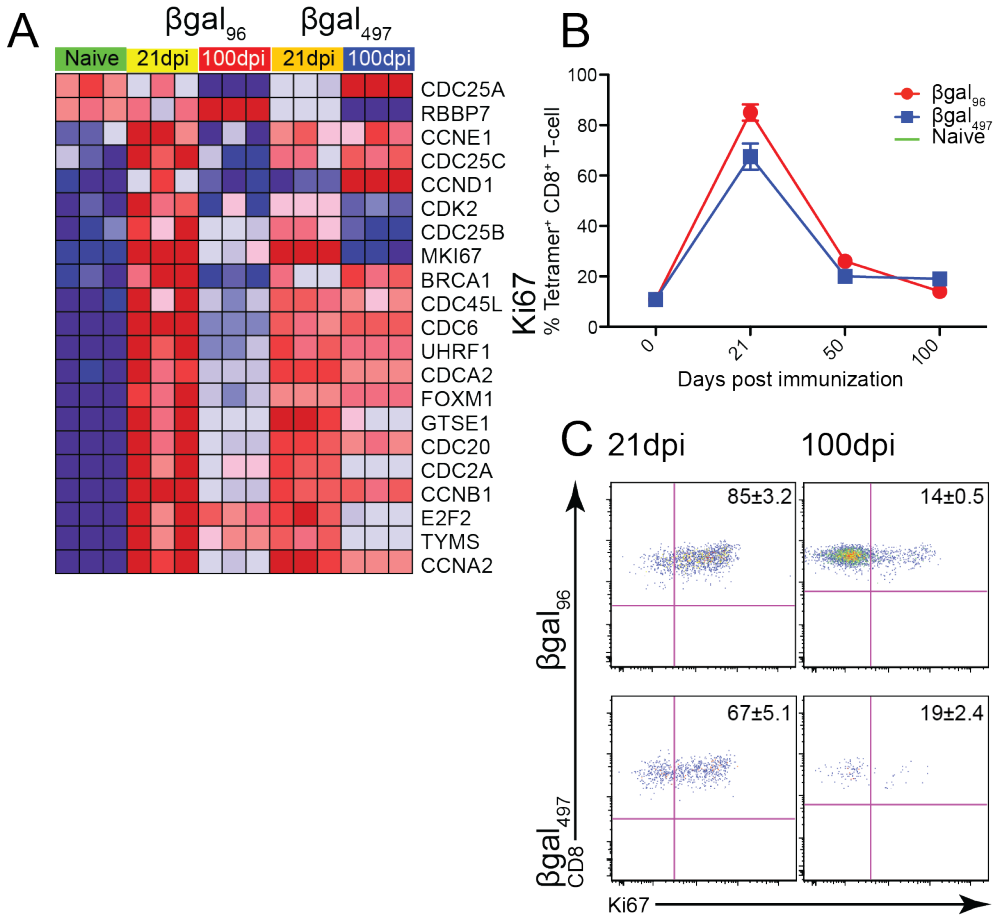


Figure 4-5 **Analysis of genes associated with the proliferation state of specific CD8$^+$ T-cells after Ad-LacZ immunization.** (A) Heat map showing the mRNA expression levels of proliferation markers measured by microarray analysis of naïve CD8$^+$ T-cells, βgal96- and βgal497-specific CD8$^+$ T-cells 21 and 100 days post immunization. Shades or red indicate up-regulated genes and shades of blue indicate down-regulated genes. Filter criteria of at least 2-fold change with P≤005, compared to naïve CD8$^+$ T-cells, (B) Time course showing the percentage of cells expressing Ki67 in βgal96- (red) and βgal497- (blue) specific CD8+ T-cells in the spleen on 0, 21, 50 and 100 days post immunization (n=10, mean±SEM). (C) Representative flow cytometry plots show the expression of Ki67 in the spleen on 21 and 100 days post immunization, gated on live βgal96- (red) and βgal497- (blue) specific CD8$^+$ T-cells. Numbers indicate the mean percentage expressing the marker (n=5, mean±SEM).

The heat plot shows genes involved in the regulation of apoptosis, which are differentially expressed in βgal_{96}- and βgal_{497}-specific $CD8^+$ T-cells, in comparison to naïve $CD8^+$ T-cells (Figure 4-6.A). The antiapoptotic protein Bcl-2 was down-regulated in the acute phase in both βgal_{96}- and βgal_{497}-specific $CD8^+$ T-cells, as well as in inflationary βgal_{96}-specific $CD8^+$ T-cells. However in contrast, memory βgal_{497}-specific $CD8^+$ T-cells up-regulate Bcl-2.

A mixture of pro-apoptotic (BAK) and anti-apoptotic (Bag3, Bcl-X_L) proteins are up-regulated in inflationary βgal_{96}-specific $CD8^+$ T-cells, in comparison to naïve $CD8^+$ T-cells. Interestingly, the anti-apoptotic protein Bcl-X_L is uniquely expressed in inflationary βgal_{96}-specific $CD8^+$ T-cells. Memory βgal_{497}-specific $CD8^+$ T-cells, showed a distinct profile, up-regulating pro-apoptotic proteins (BIM, PUMA, BID, BAD and Bcl-G) and anti-apoptotic proteins (BLK, Bcl-2) understanding the balance these play in the maintenance of inflationary cells and memory cells could provide further insight into the stability of both populations.

Analysis by flow cytometry: Analysis by flow cytometry confirmed the expression of Bcl-2 in βgal_{96}- and βgal_{497}- specific $CD8^+$ T-cells in the spleen (Figure 4-6.B). Bcl-2 expression was down-regulated at day 21 post immunization in both Ad-LacZ-specific $CD8^+$ T-cells. It gradually increased in both populations over time, although to a higher degree in memory βgal_{497}-specific $CD8^+$ T-cells.

In terms of apoptotic markers, inflationary βgal_{96}-specific $CD8^+$ T-cells showed a similar expression profile to inflationary M38-specific $CD8^+$ T-cells. In comparison to memory βgal_{497}- and M45-specific $CD8^+$ T-cells, they have reduced expression levels of BIM and increased expression in Bcl-X_L. This could profile could reduce

apoptosis and account for the maintenance of inflationary $CD8^+$ T-cells, at a high frequency.

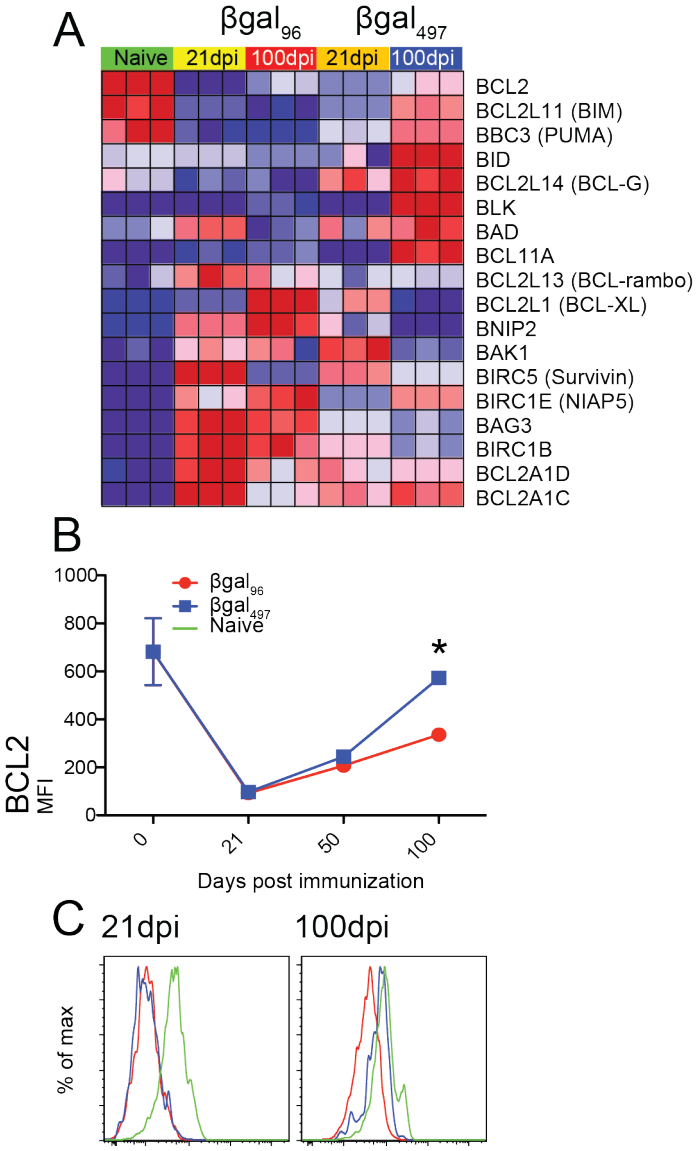


Figure 4-6 **Expression of apoptotic related protein in Ad-LacZ specific CD8$^+$ T-cells.** (A) Heat map showing mRNA expression levels of proteins involved in apoptosis measured by microarray analysis of naïve CD8$^+$ T-cell, βgal96-and βgal497-specific CD8$^+$ T-cells day 21 and 100 post immunization. Shades or red indicate up-regulated genes and shades of blue indicate down-regulated genes. Filter criteria of at least 2-fold with P≤0.05, compared with naïve CD8$^+$ T-cells. (B) Time course showing (MFI) of Bcl-2 in βgal96- (red) and βgal497- (blue) specific CD8$^+$ T-cells in the spleen day 0, 21, 50 and 100 post immunization (n=5, mean±SEM). (C) Representative histograms show the expression of Bcl-2 in the spleen on day 21 and 100 post immunization, gated on live βgal96- (red) and βgal497- (blue) specific CD8$^+$ T-cells, compared to naive CD8$^+$ T-cells (green).

4.2.8 Cytokine and chemokine receptor profile of Ad-LacZ-specific $CD8^+$ T-cells

Chemokine receptors are induced to guide homing towards sites of inflammation(208-211,233,234). Cytokines participate in the differentiation of naïve $CD8^+$ T-cells, to memory cells and act as growth and survival factors, as well as effector molecules. By comparing the cytokine and chemokine receptor expression profile of βgal_{96}- and βgal_{497}-specific $CD8^+$ T-cells I aimed to identify the specific cytokine and chemokine requirements of inflationary $CD8^+$ T-cells.

The heat map (Figure 4-7.A) shows the changes in chemokine and cytokine receptor expression in the different $CD8^+$ T-cell populations, compared to naïve $CD8^+$ T-cells. βgal_{96}-specific $CD8^+$ T-cells day 21 and 100 post immunization, showed a similar profile in their chemokine and cytokine receptor expression. However, βgal_{497}-specific $CD8^+$ T-cells, differ markedly between day 21 and 100 post immunization.

Chemokine receptors, CCR7, CCR6, and CCR9 were down-regulated in βgal_{96}-specific $CD8^+$ T-cells, in comparison to naïve $CD8^+$ T-cells; in contrast memory βgal_{96}-specific $CD8^+$ T-cells had increased expression of these receptors. CCR5 and CCR2 were up-regulated in βgal_{96}-specific $CD8^+$ T-cells and down-regulated in memory βgal_{497}-specific $CD8^+$ T-cells to levels similar to that of naïve $CD8^+$ T-cells. Moreover, CXCR3 and CX3CR1 were up-regulated in βgal_{96}-specific $CD8^+$ T-cells and to a lesser extent in memory βgal_{497}-specific $CD8^+$ T-cells, compared to naïve $CD8^+$ T-cells.

Importantly, βgal_{96}-specific $CD8^+$ T-cells down-regulated CD127 (IL-7Rα), CD124 (IL-4Rα) and CD126 (IL-6Rα) compared to naïve $CD8^+$ T-cell, but these molecules

were highly up-regulated on memory βgal_{497}-specific $CD8^+$ T-cells. IL-7 is a key cytokine in antigen-independent memory maintenance(19,235-237).

Confirmation by flow cytometry: To confirm expression of CXCR3, flow cytometry analysis was performed (Figure 4-7.B). CXCR3 was up-regulated in the acute phase on βgal_{96}-specific $CD8^+$ T-cells, in comparison to naïve $CD8^+$ T-cells, decreasing expression in the memory phase. In contrast, βgal_{497}-specific $CD8^+$ T-cells over the course of 100 days increased expression of CXCR3. Although the expression patterns are broadly consistent with the gene expression compared to naïve cells, the pattern of increase of CXCR3 in non-inflationary cells over time was not predicted from the array data.

CX3CR1 was up-regulated in the acute phase on βgal_{497}- and βgal_{96}-specific $CD8^+$ T-cells, in comparison to naïve $CD8^+$ T-cells. There was decreasing expression in the memory phase on βgal_{96}-specific $CD8^+$ T-cells. In contrast βgal_{497}-specific $CD8^+$ T-cells, over the course of 100 days maintained high expression of CX3CR1. Overall, the expression patterns are broadly consistent with the gene expression compared to naïve cells.

IL-6R was down-regulated in the acute phase on βgal_{497}- and βgal_{96}-specific $CD8^+$ T-cells, in comparison to naïve $CD8^+$ T-cells. There was increasing expression in the memory phase on βgal_{96}-specific $CD8^+$ T-cells, staying low in expression on βgal_{497}-specific $CD8^+$ T-cells in the memory phase.

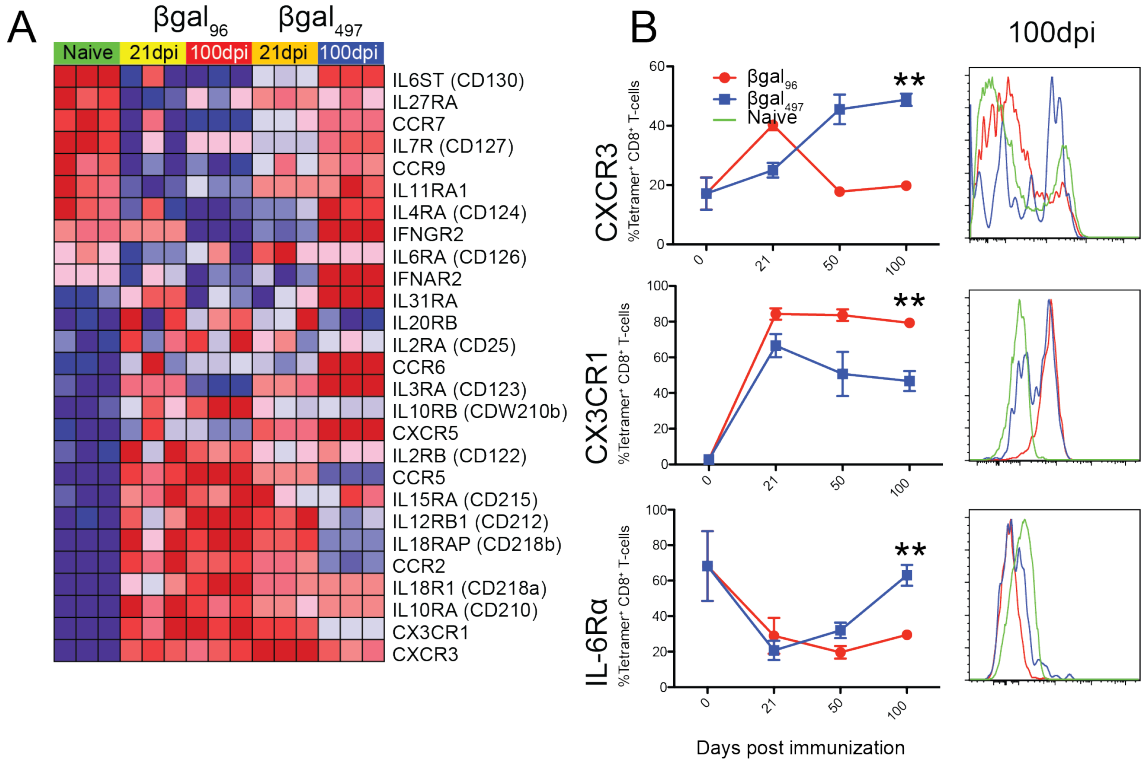


Figure 4-7 **Cytokine and chemokine receptor expression profile on Ad-LacZ-specific CD8$^+$ T-cells**. (A) Heat map showing the mRNA expression levels of cytokine and chemokine receptors measured by microarray analysis of naïve CD8+ T-cells, βgal96- and βgal497-specific CD8$^+$ T-cells 21 and 100 days post immunization. Shades or red indicate up-regulated genes and shades of blue indicate down-regulated genes. Filter criteria of at least 2-fold change with P≤005, compared to naïve CD8$^+$ T-cells, (B) Time course showing the percentage of cells expressing indicated markers on βgal96- (red) and βgal497- (blue) specific CD8+ T-cells in the spleen at 0, 21, 50 and 100 days post immunization (n=10, mean±SEM). (C) Representative histograms show the expression of CXCR3 in the spleen on 21 and 100 days post immunization, gated on live naïve CD8$^+$ T-cells (green) βgal96- (red) and βgal497- (blue) specific CD8$^+$ T-cells.

4.2.9 Receptors of the SLAM family up-regulated on Ad-LacZ-specific CD8+ T-cells

The SLAM family of receptors are involved in co-stimulation and cytokine production of NK-cells and $CD8^+$ T-cells(212,238). βgal_{96}-specific $CD8^+$ T-cells in the acute and memory phase showed the same expression profile, up-regulating *Cd229*, *Cd150*, *Cd48*, *Cd244* and *Cd319* and *Sap*, in comparison to naïve $CD8^+$ T-cells (Figure 4-8.A). Non-inflationary βgal_{497}-specific $CD8^+$ T-cells down regulate *Cd150*, *Cd48*, *Cd84* and up-regulate *Cd2f10*, *Cd353* and *Cd229* in comparison to βgal_{497}-specific $CD8^+$ T-cells in the acute phase.

To confirm expression of CD319, flow cytometry analysis was performed (Figure 4-8.B). Both βgal_{96}- and βgal_{497}-specific $CD8^+$ T-cells up-regulated CD319 in the acute phase, in comparison to naïve $CD8^+$ T-cells, maintain high expression of the receptor in the memory phase. The increase in SLAM receptors may allow the $CD8^+$ T-cells to be efficient killers of virally infected cells.

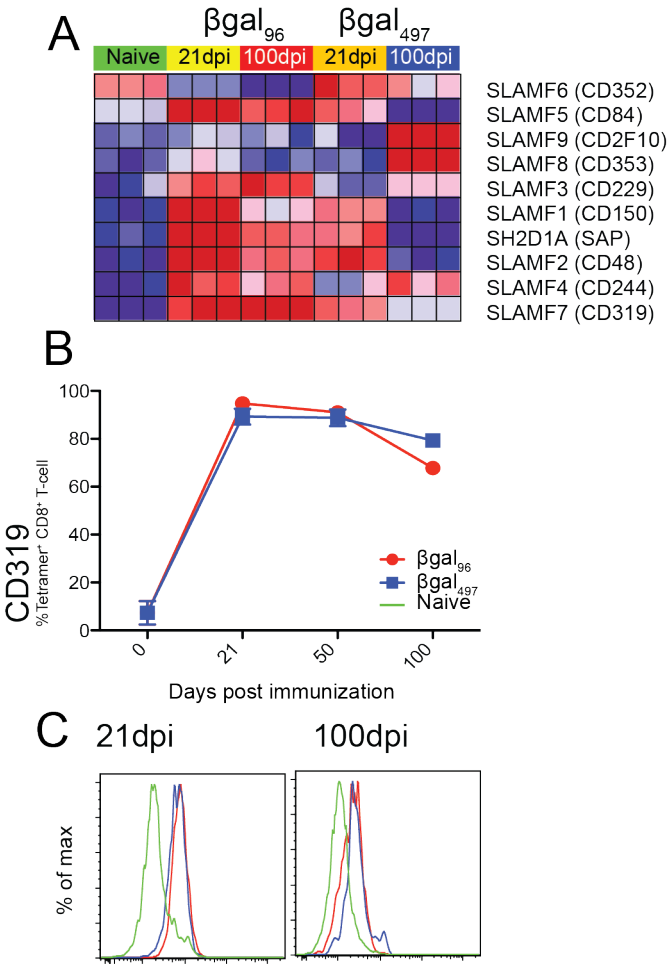


Figure 4-8 **Up-regulation of the SLAM family receptors on Ad-LacZ-specific CD8$^+$ T-cells**. (A) Heat map showing the mRNA expression levels of the SLAM family receptors measured by microarray analysis of naïve CD8$^+$ T-cells, βgal96- and βgal497-specific CD8+ T-cells 21 and 100 days post immunization. Shades or red indicate up-regulated genes and shades of blue indicate down-regulated genes. Filter criteria of at least 2-fold change with P≤005, compared to naïve CD8+ T-cells, (B) Time course showing the percentage of cells expressing CD319 in βgal96- (red) and βgal497- (blue) specific CD8+ T-cells in the spleen at 0, 21, 50 and 100 days post immunization (n=5, mean±SEM). (C) Representative histograms show the expression of CD319 in the spleen on 21 and 100 days post immunization, gated on live, naïve CD8+ T-cells (green) and βgal96- (red) and βgal497- (blue) specific CD8$^+$ T-cells.

4.2.10 Expression of exhaustion markers on Ad-LacZ specific $CD8^+$ T-cells

$CD8^+$ T-cell exhaustion in LCMV infection is identified by up-regulation of inhibitory receptors(166,213). Gene array results have shown that TIM3 and CD160 were up-regulated on βgal_{96}-specific $CD8^+$ T-cells in the acute and memory phase, in comparison to naive $CD8^+$ T-cells (Figure 4-9.A), surprisingly βgal_{497}-specific $CD8^+$ T-cells in the acute and memory phase also up-regulated PD1, CTLA4 and LAG3, in comparison to naive $CD8^+$ T-cells, suggesting an exhausted phenotype.

To confirm the array data, flow cytometry analysis was performed for PD1 and Tim3 (Figure 4-9.B). Both βgal_{96}- and βgal_{497}-specific $CD8^+$ T-cells showed the same expression profile, up-regulating both PD1 and Tim3 in the acute phase and then gradually declining in expression levels as they enter into the memory phase. This was not as predicted from the array data, although is broadly consistent; however, it shows that neither βgal_{96}- or βgal_{497}-specific $CD8^+$ T-cells are exhausted by these criteria.

In contrast BLTA was down-regulated on both βgal_{96}- and βgal_{497}-specific $CD8^+$ T-cells in the acute phase. Then gradually increased in expression on βgal_{497}-specific $CD8^+$ T-cells, however expression stayed low on βgal_{96}- specific $CD8^+$ T-cells in the memory phase, confirming the results seen with the array data.

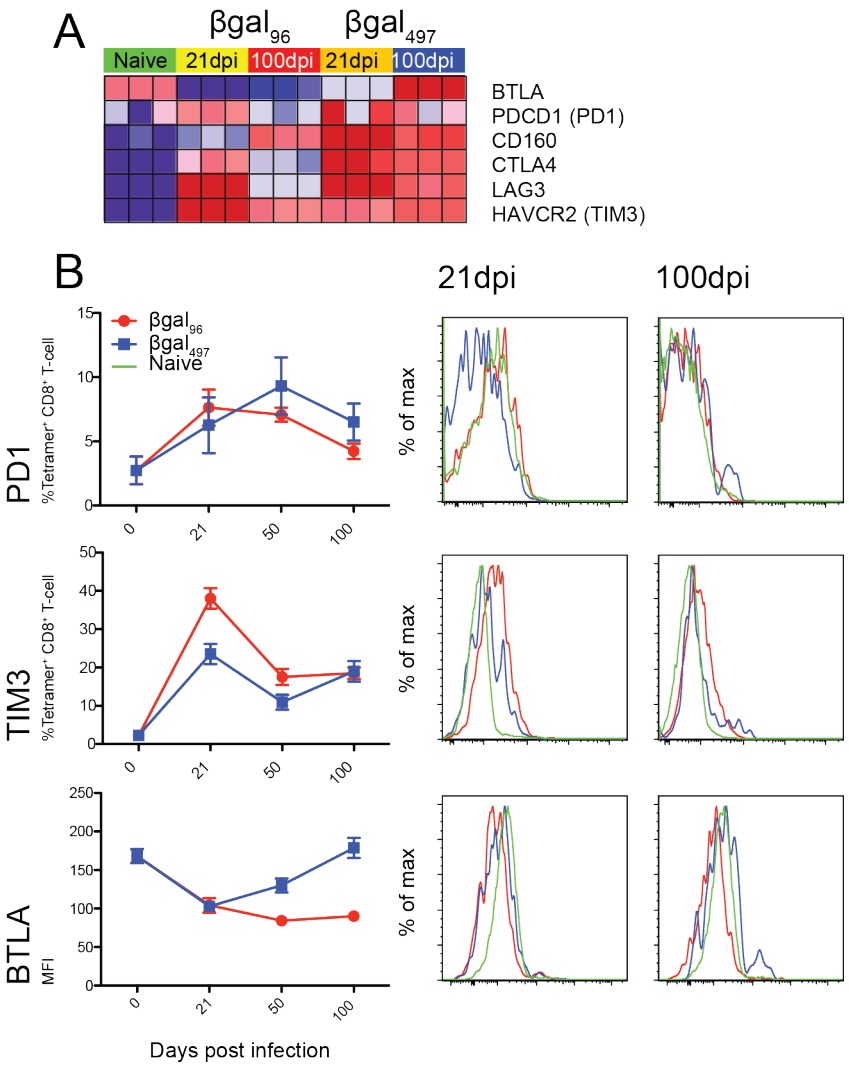


Figure 4-9 **Changes in exhaustion markers on Ad-LacZ-specific CD8$^+$ T-cells.** (A) Heat map showing the mRNA expression levels of the exhaustion markers measured by microarray analysis of naïve CD8$^+$ T-cells, βgal96- and βgal497-specific CD8$^+$ T-cells 21 and 100 days post immunization. Shades or red indicate up-regulated genes and shades of blue indicate down-regulated genes. Filter criteria of at least 2-fold change with P≤005, compared to naïve CD8+ T-cells, (B) Time course showing the percentage of cells expressing PD1 and TIM3 in βgal96- (red) and βgal497- (blue) specific CD8$^+$ T-cells in the spleen at 0, 21, 50 and 100 days post immunization (n=5, mean±SEM). Representative histograms show the expression of PD1, TIM3 and BTLA in the spleen at 21 and 100 days post immunization, gated on live, naïve CD8$^+$ T-cells (green) and βgal96- (red) and βgal497- (blue) specific CD8$^+$ T-cells.

4.2.11 Differential expression of co-stimulatory receptors on Ad-LacZ-specific $CD8^+$ T-cells

Stimulatory receptors provide the second signal and are important in achieving maximal expansion of $CD8^+$ T-cells. The heat map shows the changes in expression profile of stimulatory receptors in βgal_{96}- and βgal_{497}-specific $CD8^+$ T-cells (Figure 4-10.A). In the acute phase, βgal_{96}- specific $CD8^+$ T-cells up-regulate ICOS, a marker of activation, in comparison to naïve $CD8^+$ T-cells, decreasing expression in the memory phase. βgal_{96}- and βgal_{497}-specific $CD8^+$ T-cells in the memory phase differ widely, with the latter increasing expression of *Cd27, CD357* (*Tnfrf18/Gitr*) and *Cd134*.

Expression levels of CD357 was measured over a time course by flow cytometry (Figure 4-10.B). Both βgal_{96}- and βgal_{497}-specific $CD8^+$ T-cells down-regulated expression in the acute phase, in comparison to naïve $CD8^+$ T-cells. While βgal_{96}-specific $CD8^+$ T-cells stayed low in expression, βgal_{497}-specific $CD8^+$ T-cells increased expression in the memory phase.

The implications of these co-stimulatory receptors on inflationary $CD8^+$ T-cells with the exception of CD28(134,214) has not been assessed, and may be of interest in future research.

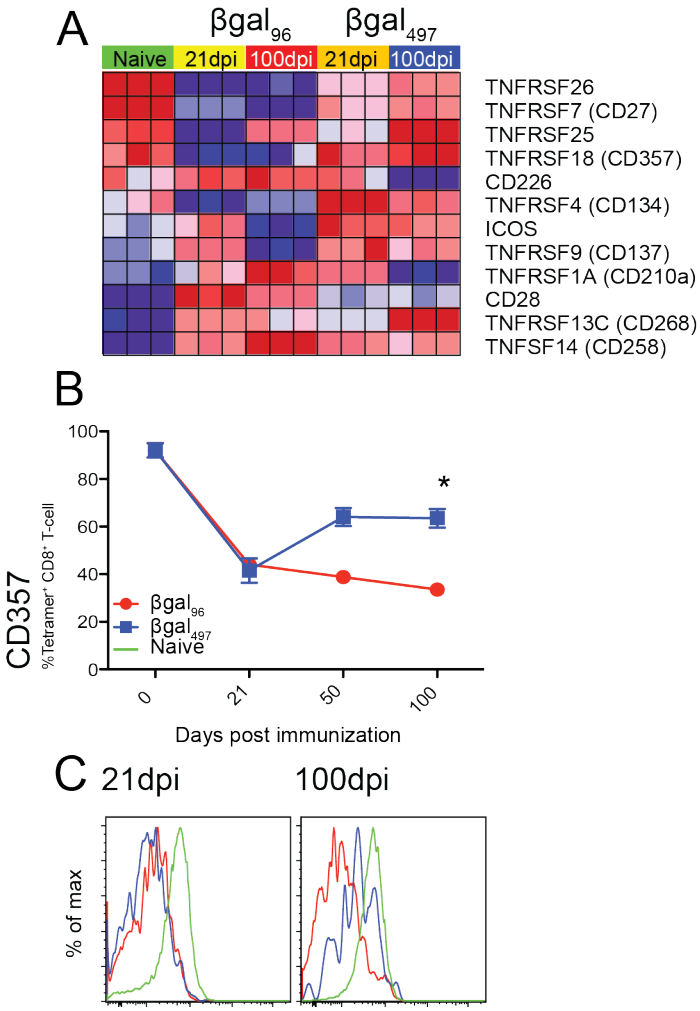


Figure 4-10 **Expression of stimulatory receptors on Ad-LacZ-specific CD8$^+$ T-cells. (**A) Heat map showing the mRNA expression levels of the stimulatory receptors measured by microarray analysis of naïve CD8$^+$ T-cells, βgal96- and βgal497-specific CD8$^+$ T-cells 21 and 100 days post immunization. Shades or red indicate up-regulated genes and shades of blue indicate down-regulated genes. Filter criteria of at least 2-fold change with P≤005, compared to naïve CD8$^+$ T-cells, (B) Time course showing the percentage of cells expressing CD357 on βgal96- (red) and βgal497- (blue) specific CD8+ T-cells in the spleen at 0, 21, 50 and 100 days post immunization (n=5, mean±SEM). (C) Representative histograms show the expression of CD357 in the spleen at 21 and 100 days post immunization, gated on live, naïve CD8$^+$ T-cells (green) and βgal96- (red) and βgal497- (blue) specific CD8$^+$ T-cells.

4.2.12 Expression of adhesion molecules on Ad-LacZ- specific $CD8^+$ T-cells

Differentiated $CD8^+$ T-cells express adhesion molecules allowing them to enter specific sites and in the case of CD62L home to the lymph node. The heat map shows the expression levels of adhesion molecules from the gene array (Figure 4-11.A). Both βgal_{96}- and βgal_{497}-specific $CD8^+$ T-cells up-regulate *Ly6c*, *Cd44*, and *Cd11a* in the acute and memory phase, in comparison to naïve $CD8^+$ T-cells; these receptors are markers of antigen-experienced $CD8^+$ T-cells.

In the acute and memory phase βgal_{96}-specific $CD8^+$ T-cells show a similar expression, however, inflationary βgal_{96}-specific $CD8^+$ T-cells uniquely up-regulate *Cd73*, *Cd49d* and *Maea*. Memory βgal_{497}-specific $CD8^+$ T-cells differ from inflationary βgal_{96}-specific $CD8^+$ T-cells, decreasing expression of *Cd26*, *Cd73, Ly6c* and *Icam1* and up-regulating *Pecam1, Cd103, Cd26* and *Cd62L*.

To confirm expression of CD26 and Ly6C at the protein expression level a time course using flow cytometry was performed (Figure 4-11.B). The adhesion molecule Ly6C was up-regulated on βgal_{96}- and βgal_{497}-specific $CD8^+$ T-cells in the acute phase, in comparison to naïve $CD8^+$ T-cells. In the memory phase, inflationary βgal_{96}-specific $CD8^+$ T-cells showed a small increase in expression; in contrast memory βgal_{497}-specific $CD8^+$ T-cells decreased expression of Ly6C.

The adhesion and ecotoenzyme molecule CD26 expression decreased on βgal_{96}- and βgal_{497}-specific $CD8^+$ T-cells in the acute phase, in comparison to naïve $CD8^+$ T-cells. In the memory phase, inflationary βgal_{96}-specific $CD8^+$ T-cells stayed low in expression; however, memory βgal_{497}-specific $CD8^+$ T-cells increased expression of CD26.

ICAM1 expression increases on βgal_{96}- and βgal_{497}-specific $CD8^+$ T-cells in the acute phase. βgal_{96}-specific $CD8^+$ T-cells maintained expression into the memory phase, while βgal_{497}-specific $CD8^+$ T-cells gradually decreased expression of ICAM1.

The expression profile of CD26, Ly6C and ICAM1 on βgal_{96}- and βgal_{497}-specific $CD8^+$ T-cells is comparable with that of M38- and M45-specific $CD8^+$ T-cells.

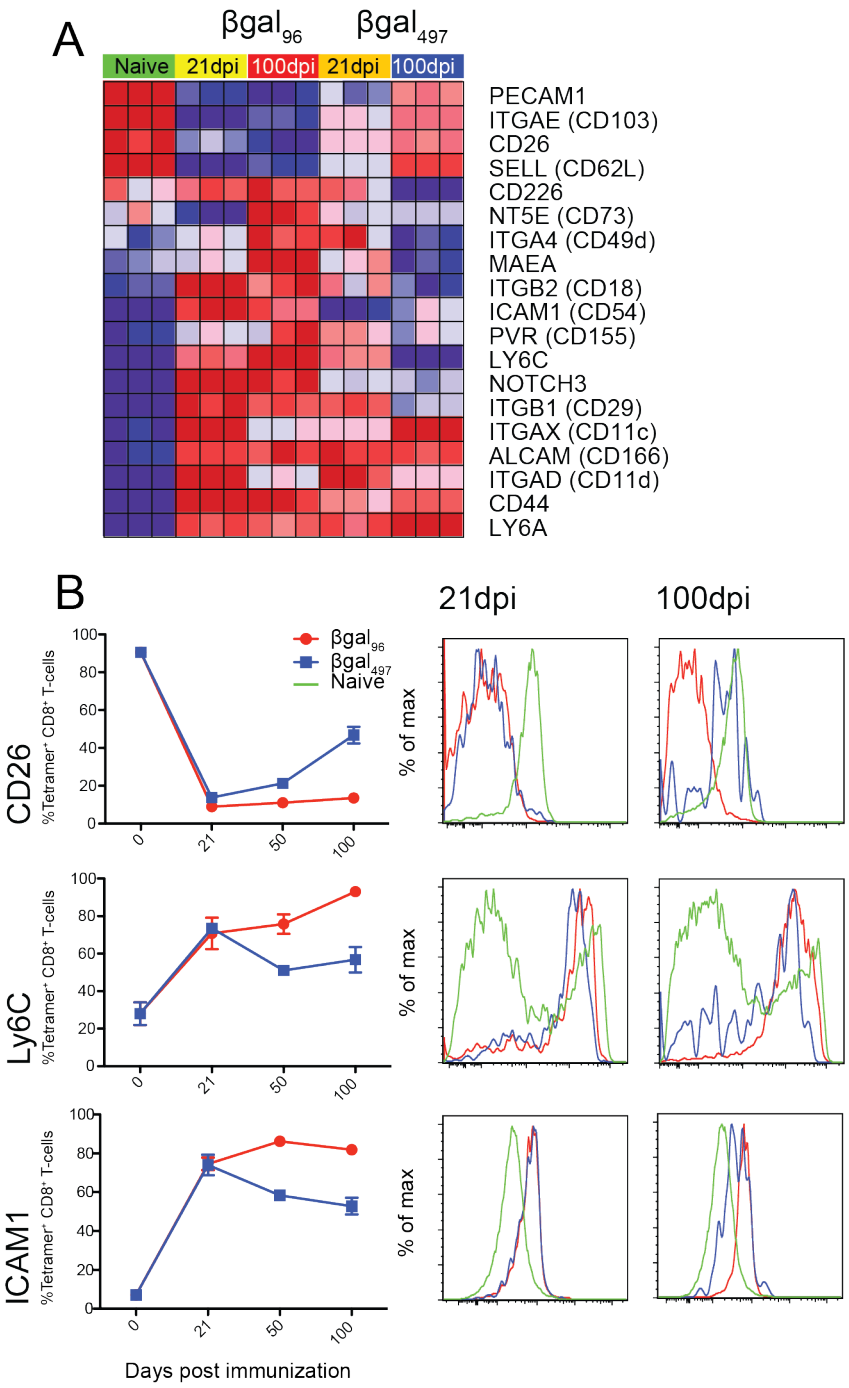


Figure 4-11 **Differential expression of adhesion molecules on Ad-LacZ-specific CD8+ T-cells**. (A) Heat map showing the mRNA expression levels of the adhesion molecules measured by microarray analysis of naïve $CD8^+$ T-cells, βgal96- and βgal497-specific CD8+ T-cells 21 and 100 days post immunization. Shades or red indicate up-regulated genes and shades of blue indicate down-regulated genes. Filter criteria of at least 2-fold change with P≤005, compared to naïve $CD8^+$ T-cells, (B) Time course showing the percentage of cells expressing CD26, Ly6C and ICAM1 on βgal96- (red) and βgal497- (blue) specific $CD8^+$ T-cells in the spleen at 0, 21, 50 and 100 days post immunization (n=5, mean±SEM). Representative histograms show the expression of CD26, Ly6C and ICAM1 in the spleen at 21 and 100 days post immunization, gated on live, naïve $CD8^+$ T-cells (green) and βgal96- (red) and βgal497- (blue) specific $CD8^+$ T-cells.

4.2.13 K-means clustering and gene ontology analysis of MCMV- and Ad-LacZ-specific CD8$^+$ T-cells

There are many similarities between inflationary M38- and βgal_{96}- specific CD8$^+$ T-cells, such as high expression of KLR receptors and low expression of CD26. To further analyse inflationary CD8$^+$ T-cells cells, K-means clustering was performed on gene array results from both MCMV- and Ad-LacZ-specific CD8$^+$ T-cells. This analysis aims to find groups of genes that distinguish antigen experienced, effector, memory and inflationary CD8$^+$ T-cells. To further our understanding of the functional properties of these genes groups we looked for biological processes that were enriched. Clustering analysis produced five clusters that identified gene sets differentially expressed in the different CD8$^+$ T-cell populations (Figure 4-12).

Cluster 1 was up-regulated in acute phase and inflationary CD8$^+$ T-cells, in comparison to naïve CD8$^+$ T-cells, decreasing in memory CD8$^+$ T-cells. Cluster 1 contains the chemokines *Ccl3, Ccl4, Ccl5, Ccl9* the cytokine *IFNg*, granzymes A and K. Additionally the chemokine receptors *Ccr5* and *Cx3Cr1*, NK-cell receptors (*Klrc1, Klre1, Klrg1*) and the transcription factors *Zeb2* and *Tbx21*. Analysis of enriched biological processes showed these genes were involved in processes such as the immune response and chemotaxis (Figure 4-13.A).

Cluster 2 showed a similar profile as Cluster 1, with the cluster being highly expressed in the acute phase and inflationary CD8$^+$ T-cell, in comparison to naïve CD8$^+$ T-cell, and decreasing in memory CD8$^+$ T-cells. The cluster consists of genes involved in biological processes such as apoptotic processes (*Bag3* and CASP's) and cell adhesion (*Alcam, Cd11c* and *Cd44*) and transcription factors (*eomes*, *Rora, Rog* and *Prdm1*) (Figure 4-13.B).

Cluster 3 was up-regulated in the acute phase, in comparison to naïve $CD8^+$ T-cell, and then decreased in both MCMV- and Ad-LacZ-specific $CD8^+$ T-cells in the memory phase. Genes in the cluster are involved in controlling the cell cycle and DNA repair (Figure 4-13.C).

Cluster 4 was up-regulated in naïve $CD8^+$ T-cells and memory M45- and βgal_{497}-specific $CD8^+$ T-cells. The cluster consists of genes involved in biological processes such as regulation of transcription (*Tcf7, Lef1, Irf6* and *Smad1*) signal transduction (*IL6st, Socs3* and *Ccr7*) and transcription (*Id3* and *Zfp238*)(Figure 4-13.D).

Cluster 5 is unique to inflationary cells; it contains genes up-regulated to the highest degree in inflationary M38- and βgal_{96}-specific $CD8^+$ T-cells, in comparison to naïve $CD8^+$ T-cells. This cluster consists of genes involved in biological processes such as regulation of transcription (Foxk1, Rbbp7 and *Bmi1*) and positive regulation of apoptosis (*Bcl-x_L*)(Figure 4-13.E).

By K-means clustering it has been possible to find a set of genes that define populations of $CD8^+$ T-cells in both MCMV and Ad-LacZ infection. Both infections induce inflationary and memory $CD8^+$ T-cells with a similar gene expression profile. Moreover, I found a specific set of genes that are uniquely up-regulated in inflationary $CD8^+$ T-cells. This set of genes may contain specific genes that may allow inflation to occur such as the anti-apoptotic protein Bcl-X_L, the transcription factor Foxk1, and the epigenetic control molecule RBBP7.

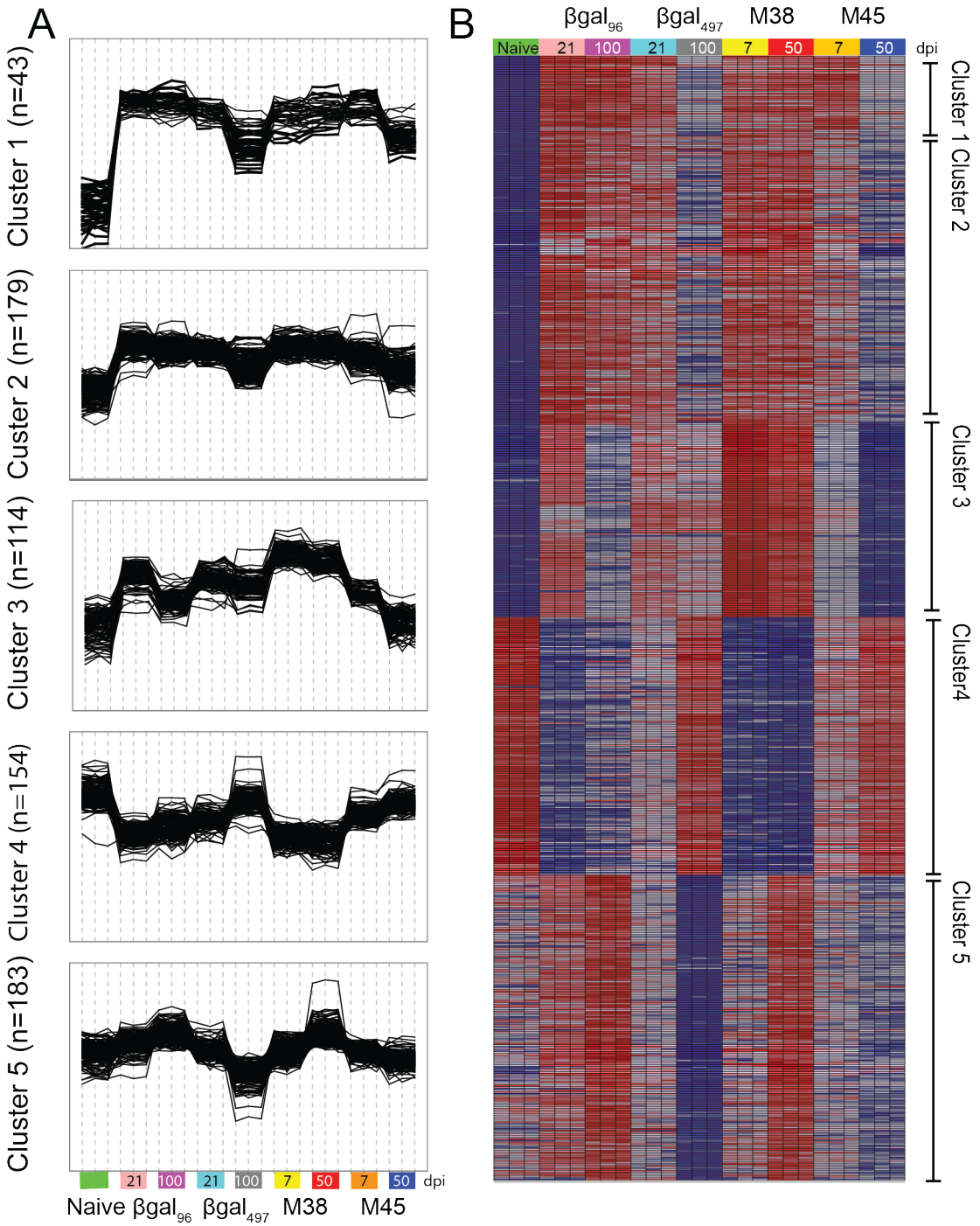


Figure 4-12 **K-means clustering of differentially expressed gens from MCMV- and Ad-LacZ-specific CD8$^+$ T-cells.** (A) Clustering of gene results for naïve CD8+ T-cells, MCMV- and Ad-LacZ-specific CD8$^+$ T-cells, performed by ExpressCluster with 100 iterations using genes differentially expressed (≥2 fold, P≤0.05, compared to naïve CD8$^+$ T-cells). The top five clusters are shown. (B) Genes identified by K-means clustering were selected to produce a heat map showing the different pattern of expression across the cell populations. Shades of red indicate up-regulated genes and shades of blue indicate down-regulated genes

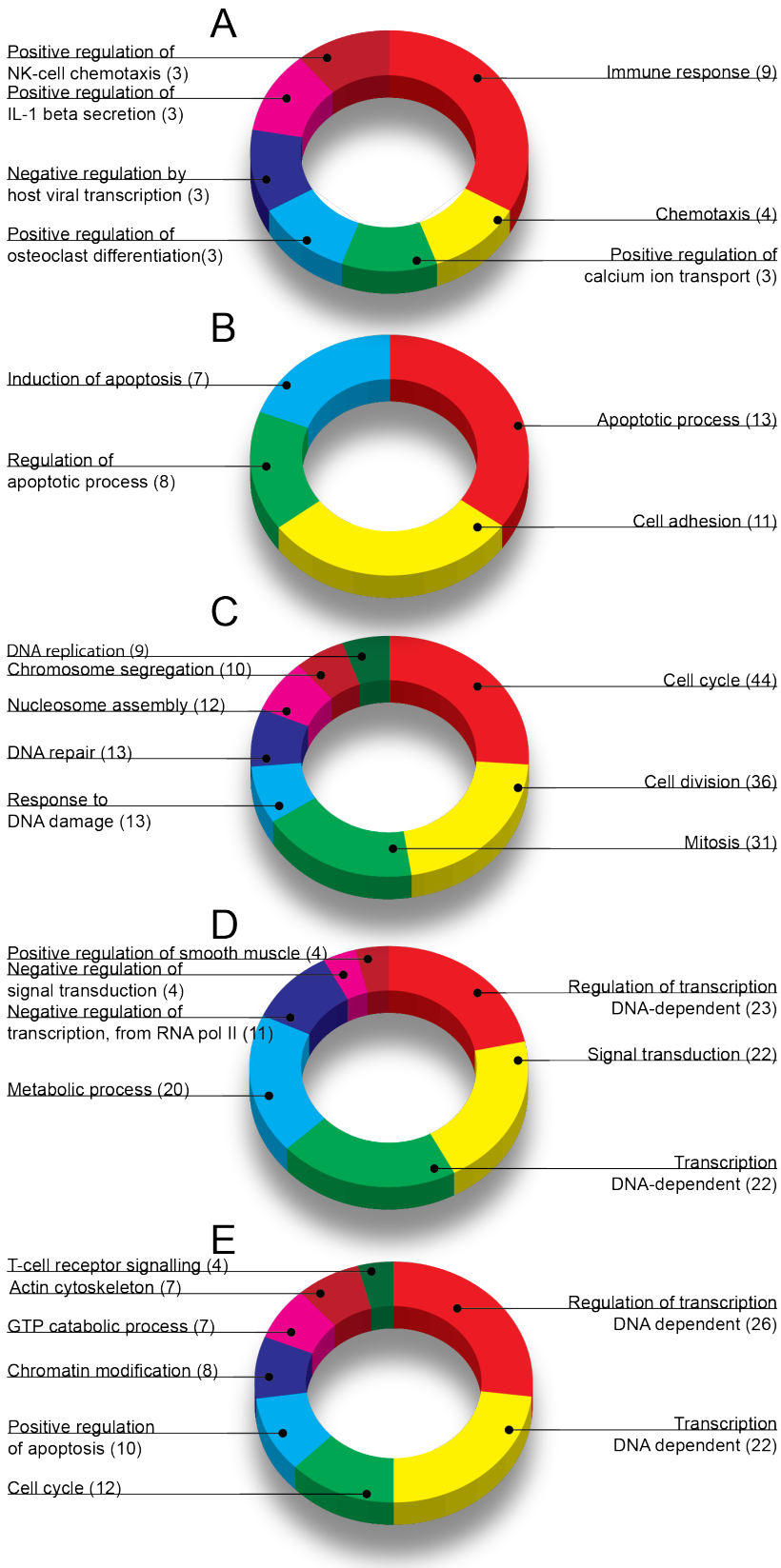


Figure 4-13 **Gene ontology analysis of gene clusters.** Gene clusters identified by K-means clustering were run on Genecodis. Gene ontology (GO) biological processes (BP) that were enriched are shown (≥3 genes, P≤0.001). A: Cluster 1, B: Cluster 2, C: Cluster 3, D: Cluster 4 and E: Cluster 5.

4.2.14 Comparison between M38- and βgal$_{96}$-specific CD8$^+$ T-cells

Inflationary CD8$^+$ T-cells from MCMV infection and Ad-LacZ immunization, showed a similar gene expression profile. Comparing both gene sets directly reveals they share 663 up-regulated and 290 enriched in biological processes such as cell cycle, transcription, phosphorylation, apoptosis and immune response.

Up-regulated genes of interest are chemokine receptors (*Cx3cr1, Ccr5*), chemokines (*Ccl3, Ccl4, Ccl5, Ccl9*), Cytokine receptors (*Il18rb1, Il12rb1, Il15ra, Il10ra* and *Il2rb*), KLR receptors (*Klrg1, Nkg2a, Nkg2d, Klre1*), Granzymes (A, K, M), transcription factors (*eomes, Tbet, Rog, Rora*, and *Prdm1*) and control of apoptosis (*Bag3, Bclxl*).

I have identified numerous genes that are up-regulated in both inflationary M38- and βgal$_{96}$ CD8$^+$ T-cells compared to T$_{CM}$, although the role these gene play in controlling inflation has yet to assessed. To evaluate how this group of genes relate to each other, in function, I constructed a network in the hope of finding a subset of genes that control inflation.

s.

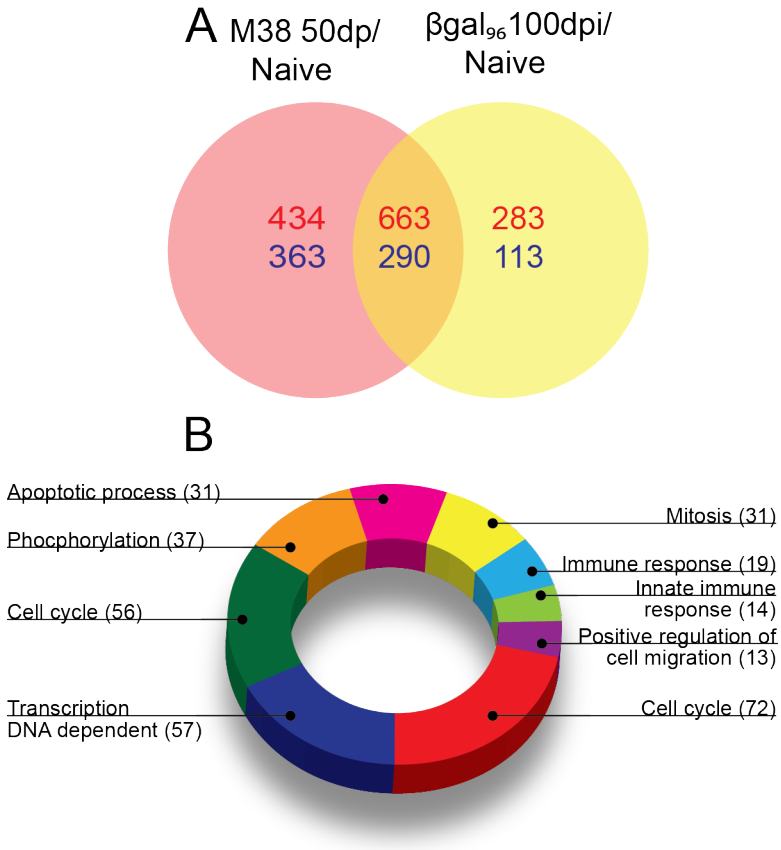


Figure 4-14 **Comparison of inflationary M38- and βgal96-specific CD8$^+$ T-cells**. (A) Venn diagram showing the number of differentially expressed genes between of inflationary M38- (red) and βgal96-(yellow) specific CD8$^+$ T-cells. Filter criteria of at least 2-fold change P≤0.05 compared to naïve CD8+ T-cells. Up-regulated genes are indicated in red and down-regulated in blue. (B) Genes up-regulated and shared between inflationary M38- (rand βgal96- specific CD8$^+$ T-cells were run on Genecodis. Gene ontology (GO) biological processes (BP) that were enriched are shown (≥3 genes, P≤0.001).

4.2.15 Gene network of inflationary $CD8^+$ T-cells

To try and understand their relationship to one another, we constructed a gene network (Figure 4-15). Genes differentially expressed in both inflationary $CD8^+$ T-cells from MCMV and adenovirus infection, in comparison to naïve were analysed for their protein-protein interactions. Lines indicated protein interactions and colour of circle indicates fold change expression (red=increase, blue=decrease), genes were clustered according to their interactions. The two major clusters were analysed for their GO (Gene Ontology) function circled in green are genes involved in cell cycle and circled in yellow are genes involved in the immune system.

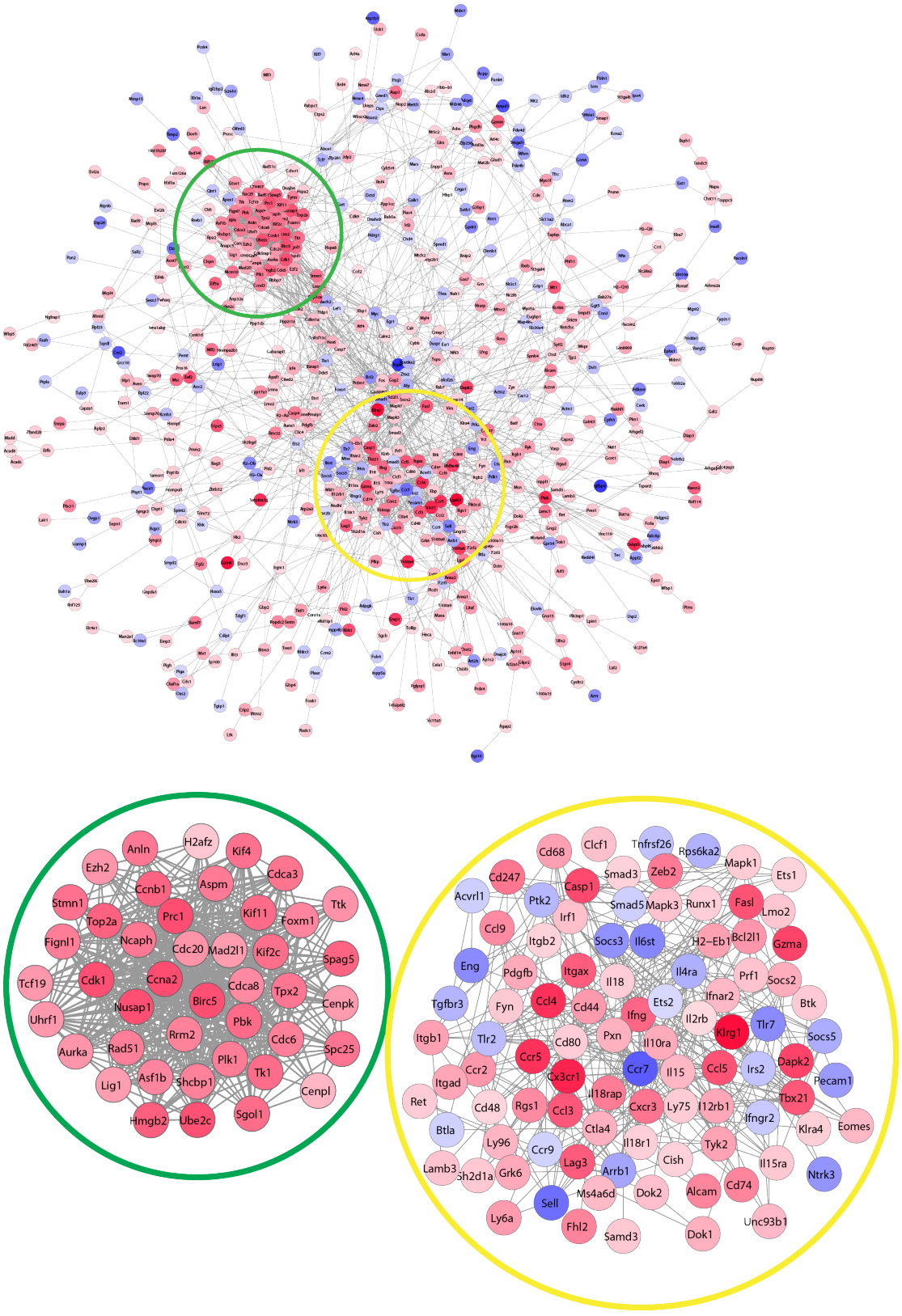


Figure 4-15 **Inflationary CD8+ T-cell gene network**. Genes differentially expressed (≥2-fold, P≤0.05) in M38- and βgal96-specific CD8$^+$ T-cells, in comparison to naïve CD8$^+$ T-cells, were assessed with STRING 9.0, the network produced was analysed by cytoscape. Clusters of genes were assessed for biological processes enriched by BiNGO, genes involved in cell cycle (Green circle) and immune system (yellow circle) are highlighted. Shades of red indicate up-regulated genes and shades of blue indicate down regulated genes.

4.3 Discussion

Immunization with Ad-LacZ induces a population of epitope specific $CD8^+$ T-cells that increases in frequency over the course of 50 days and is stably maintained at a high frequency. These inflationary βgal_{96}-specific $CD8^+$ T-cells are distinct from central memory $CD8^+$ T-cells, expressing a unique set of genes. They have a phenotype regarded as terminally differentiated effector memory cells, being $KLRG1^{Hi}$, $CD127^{Lo}$, $CD27^{Lo}$ and expressing high levels of T-bet.

These inflationary βgal_{96}-specific $CD8^+$ T cell populations show a similar phenotype as to that seen in inflationary $CD8^+$ T-cells in MCMV infection, expressing several members of KLR and SLAM family receptors. The cytokine receptor profile is distinctive for inflationary $CD8^+$ T-cells being $CD216^{Hi}$, $CD210^{Hi}$, $CD215^{Hi}$, $CD212^{Hi}$, $CD124^{Lo}$, $CD126^{Lo}$, $CD127^{Lo}$, this profile would suggest that that the cells are able to respond and proliferate in response to IL-12 and IL-15, but not IL7.

What stimulatory requirements inflationary $CD8^+$ T-cells require to achieve expansion has only been partially assessed(134,135). Here we see that inflationary $CD8^+$ T-cells are $CD258^{Hi}$, $CD226^{Hi}$, $CD27^{Lo}$ and $CD357^{Lo}$. Of interest is CD226 which binds to CD155, expressed on a epithelial and hematopoietic cells, CD226 is required for efficient stimulation of $CD8^+$ T-cells by non-professional antigen presenting cells(212,215), these have been shown be essential for the maintenance of memory inflation(88,239).

Inflationary $CD8^+$ T-cells also have a unique chemokine receptor expression prolife, being $CXCR3^{Lo}$ and $CX3CR1^{Hi}$. The up-regulation of fractalkine receptor supports the idea that it plays a role both in inflationary $CD8^+$ T-cell survival, and chemotaxis to epithelial cells that are latently infected(87,240). Interestingly, CX3CR1 has been

shown to induce expression of Bcl-X_L (73,221): this anti-apoptotic protein is uniquely expressed in inflationary cells and future work will be carried out to assess its role in maintaining inflationary $CD8^+$ T-cells.

K-means clustering showed inflationary M38- and βgal_{96}-specific $CD8^+$ T-cells express a unique set of genes that identified inflationary $CD8^+$ T-cells. Genes in this group consisted of the master cell cycle regulator FOXK1 and the anti-apoptotic gene Bcl-X_L. Understanding the roles this group of genes plays in the regulation of inflation could be key in being able to induce inflationary $CD8^+$ T-cells.

4.3.1 Chapter summary

1. I have identified the transcriptional changes associated with memory inflation using the novel adenovirus model.
2. The inflationary $CD8^+$ T-cell gene profile is distinct from that from central memory $CD8^+$ T-cells.
3. Inflationary cells induced by both MCMV and adenovirus express a shared set of genes that are not expressed in effector or memory $CD8^+$ T-cells.

5 Function and stability of inflationary CD8$^+$ T-cells

5.1 Introduction

Infection with MCMV induces both classical “central memory CD8$^+$ T-cell responses and a unique CD8+ T-cell response termed “memory inflation. As seen in chapter 3 MCMV-specific CD8+ T-cells proliferate during acute infection, then contract in the memory phase and are maintained at a low frequency by homeostatic proliferation. Memory inflating CD8+ T-cells develop at high frequency during the acute MCMV infection however these populations do not contract and are stably maintained at a high frequency when MCMV is quiescent.

Immune control of MCMV is achieved by utilizing by utilizing a concerted and redundant contribution from different components of the innate and adaptive immune system. Primary infection is mainly controlled by the innate arm of the immune system, by the action of Type I and type II IFN and by NK cells(241). NK cells act via the activating receptor Ly49H, which recognizes infected cells by binding to the m157 gene product of MCMV(242). However, CD8$^+$ T-cells have no effect on the control on primary infection, whereas the depletion of CD4$^+$ T-cells impaired control in the salivary glands(243). However CD8$^+$ T-cells have been shown to control infection in immunocompromised hosts, when MCMV-specific CD8$^+$ T-cells were adoptively transferred and prevented disease(244,245).

During latent infection, infection of B-cell deficient mice revealed that CD8$^+$, CD4$^+$ T-cells and NK cells play a hierarchical and redundant role in controlling latent infection, induction of viral reactivation required removal of two subsets(246). Evidence of CD8$^+$ T-cell protection during latency, was revealed in a study using a mutated MCMV stain which abrogates MHC class I binding of the immunodominant

epitope pp89, derived from the immediate early gene IE1, infected mice showed a 5-fold increase in IE1 transcripts in the lungs compared to WT mice(247).

While I have shown that inflationary $CD8^+$ T-cells are functional *in vitro* I wanted to see if they are still functional *in vivo.* Data in chapter 3 illustrates that M38-specific memory inflating $CD8^+$ T-cells produce cytokines such as IFNγ and TNFα in a standard intracellular cytokine staining assay - however, this may not necessarily correlate with *in vivo* function nor with cytotoxicity. Given the high frequency of M38-specifc $CD8^+$ T-cells encountered long after peak MCMV viremia it could be postulated memory inflating T-cells play a role in control of latent MCMV infection. In order to elicit whether M38-specific $CD8^+$ T-cells play a role in vivo it is necessary to clearly delineate whether they have a direct action *in vivo* – by performing an in vivo killer assay. These assays are widely used to examine the efficiency of destruction of specifically labelled target cells in vivo. Clearance or disappearance of sensitized targets (typically splenocytes, pulsed with peptide) compared to that of control targets provides a quantitative assessment of the activity of peptide-specific $CD8^+$ T cell pools. Interestingly the mechanism of clearance has not been fully defined but is likely due to granzyme mediated cytotoxicity(248).

It has previously been suggested that inflationary $CD8^+$ T-cells are maintained by the recruitment of precursors and also naïve $CD8^+$ T-cells(113,241). Mice three months post-MCMV infection were injected with the cytotoxic agent busulfan followed by naïve CD45.1 bone marrow to create chimeric mice. Tracking the recruitment of naïve $CD8^+$ T-cells to MCMV-specific $CD8^+$ T-cell population pools, it was shown over time that the percentage of CD45.1 $CD8^+$ T-cells present in the inflationary $CD8^+$ T-cell pools increased. However, thymectomised mice infected with MCMV

generate identical $CD8^+$ T-cell responses compared to C57BL/6 mice. Thus the requirement for naïve precursors to maintain memory inflation is not yet clear(242,249).

Questions still therefore remain as to how long these inflationary $CD8^+$ T-cells are maintained, whether their phenotype is stable, and what the kinetics of turnover rate are. To fully address these questions adoptive transfer of M38-specific $CD8^+$ T-cells into naïve and immune mice was performed and both congenic markers and CFSE staining used to analyse whether inflationary $CD8^+$ T-cells are maintained by homeostatic proliferation.

To analyse how quickly inflationary M38-specific $CD8^+$ T-cells are replaced (or turnover) I used a new method to specifically delete M38-specific $CD8^+$ T-cells *in vivo*. This method involves conjugating the potent type I ribosomal inactivating toxin (RIP) saporin, Type I RIP's are relatively nontoxic because of their inability to bind to and enter mammalian cells, bound to streptavidin, to MHC class I monomers.

Saporin is a plant enzyme of 30 kDa with N-glycosidase activity that specifically depurinates ribosomal RNA (rRNA) 28s(243,250), irreversibly blocking protein synthesis. It has been used as a potent immunotoxin when bound to antibodies that recognize cell surface receptors(244,245,251). MHC class I tetramers, which provide the specific delivery of the toxin, are regularly used for visualization of antigen specific T-cells, and are produced by coupling biotinylated MHC class I monomers with streptavidin bound to a flourochrome. Studies have used streptavidin-Saporin conjugate instead of the fluorochrome to produce a T-cell specific immunotoxin(246,252). The T-cell receptor (TCR) is internalized upon binding the MHC class I(247,253), thus the tetramer-saporin is internalized upon binding the

TCR. In the lysosomal compartment the tetramer-saporin will disassociate, thus saporin is free to bind ribosomes, deactivating them and leading to cell death of the specific $CD8^+$ T-cell (Fig 5.1). This specific killing has been used to delay or prevent T-cell mediated disease(248,254).

In this chapter I show the specific killing of M38- and M45-specific $CD8^+$ T-cells. Specific $CD8^+$ T-cells were killed 24 hours after injection of tetramer saporin. Surprisingly I found that a) the inflationary $CD8^+$ T-cells rebound six days post injection to a higher frequency and b) this is associated with a transient loss of control over the viral load.

5.1.1 Key questions in this chapter

1. What is the in vivo function of the antiviral (inflationary and non-inflationary) $CD8^+$ T cell populations as judged by in vivo killer assays?
2. What is the turnover of antiviral (inflationary and non-inflationary) $CD8^+$ T cells as measured by survival and division upon adoptive transfer?
3. What is the stability of the phenotype of antiviral (inflationary and non-inflationary) $CD8^+$ T cells upon adoptive transfer?
4. Is it possible to delete such populations in vivo using tetramer-saporin technology?
5. What is the turnover of such cell populations upon depletion?
6. What is the impact of specific $CD8^+$ T cell depletion on viral load?

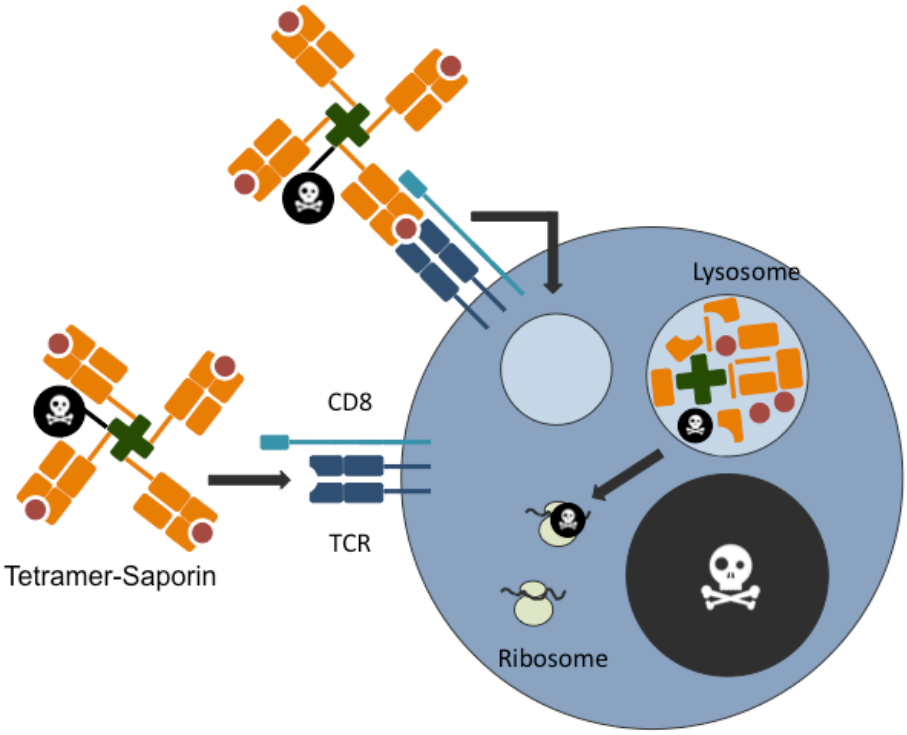


Figure 5-1 **Representation of the killing of specific CD8$^+$ T-cells by tetramer conjugated saporin.** MHC class I monomers were conjugated to streptavidin-saporin. Saporin is a ribonuclease inactivating protein. Upon binding of the MHC class I tetramer to the TCR on a CD8$^+$ T-cell, the tetramer will be internalized. In the lysosomal compartment it will dissociate and the saporin will travel to the ribosomes, leading to inactivation and death of the specific CD8$^+$ T-cell.

5.2 Results

5.2.1 In vivo killer assay

In chapter three data was presented showing that inflationary $CD8^+$ T-cells after stimulation with peptide, are polyfunctional, producing both and IFNγ and TNFα. This however does not give a clear indication of their killing potential, especially in an in vivo setting. I assessed the killing capacity of M38- and M45-specific $CD8^+$ T-cells from the acute and memory phase of MCMV infection using an *in vivo* cytotoxicity assay. Naïve splenocytes were pulsed with M38 or M45 peptide and stained with low and high concentrations of cell trace violet; unpulsed cells were stained with CFSE and acted as controls. These were mixed and injected intravenously into naïve control mice and MCMV-infected mice 7 and 50 days post infection. The mice were euthanised 12 hrs after transfer to measure the proportions of cells remaining in blood and tissues, allowing measurement of specific killing capacity.

I measured the killing potential of peptide-specific cells in the blood, liver, lung, spleen and lymph nodes. Unpulsed, stained cells were visible in all organs at 7 and 50 days post infection (Fig 5.2). Naïve mice showed no specific killing. At 7 days post infection all M38 and M45 peptide pulsed cells were killed over 12 hours, i.e. both M38- and M48-specific cells show 100% killing capacity. At 50 days post infection in the blood around 40% of M38 peptide pulsed cells were killed and 80% of M45 peptide pulsed cells were killed (Fig 5.2). A similar killing potential was seen in the liver, lung and spleen. In the lymph node we see the same killing potential of M38-specific $CD8^+$ T-cells and a reduced killing potential of M45-specific $CD8^+$ T-cells, with around 60% pulsed cells killed.

Thus both effector and inflationary M38-specific $CD8^+$ T-cells are able to kill, with inflationary M38-specific $CD8^+$ T-cells at a reduced capacity. Surprisingly, memory M45-specific $CD8^+$ T-cells are highly effective killers.

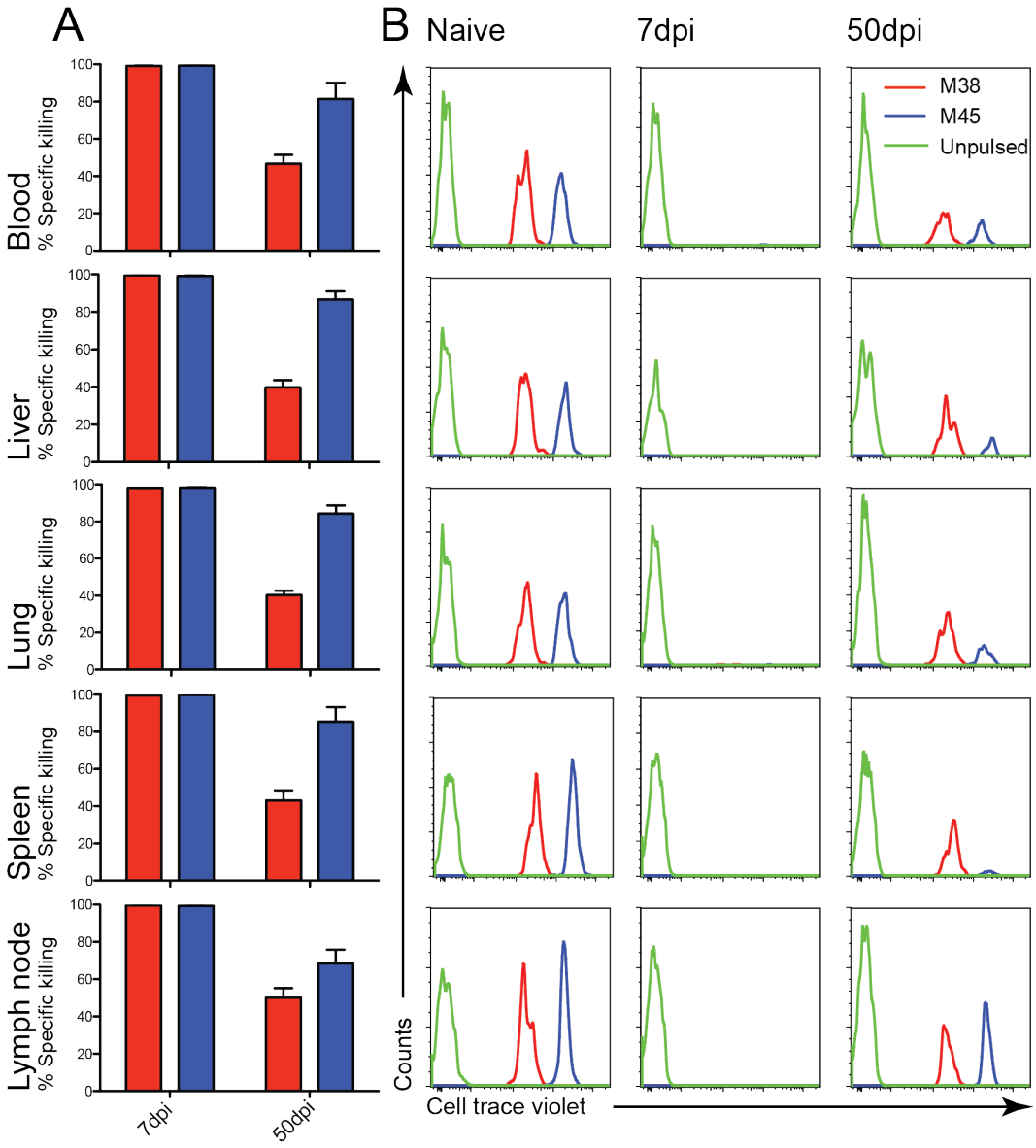


Figure 5-2 **In vivo killing capacity of specific CD8$^+$ T-cells**. Naïve C57BL/6 splenocytes were stained with CFSE (green), or peptide loaded with either M38 (red) or M45 (blue) peptide and stained with low or high concentrations of cell trace violet repetitively, these were mixed in equal proportions and transferred i.v into naïve or mice previously immunized (i.v) with 1x10^6 pfu MCMV. At 7 and 50 days post infection Flow cytometry analysis was performed 12 hours after transfer, measuring the surviving donor cells in the blood, liver, lung, spleen, and lymph node in recipient mice, mean percentage of specific is indicated (A) (n=3, mean±SEM), representative histograms shown (B), gated on live lymphocytes.

5.2.2 Adoptive transfer

Too assess the turnover of inflationary and non-inflationary $CD8^+$ T-cells through homeostatic proliferation, I performed adoptive transfer experiments, of CFSE labelled bulk splenocytes from CD45.1 mice 50 days post MCMV infection, into naïve mice and mice 50 days post MCMV infection. The use of the congenic CD45.1 marker and CFSE allowed tracking of the transferred cells and characterization of their proliferative history.

Analysis of frequency: The number of M45-specific $CD8^+$ T-cells transferred were to low for accurate quantification after 21 days post adoptive transfer. In blood the percentage of $CD45.1^+$ M38-specific $CD8^+$ T-cells shows a slight decrease over the course of 140 days post adoptive transfer in naïve mice (Fig 5.3). However in chronically infected mice the transferred M38-specific $CD8^+$ T-cells appear to be maintained. The data from naïve mice suggest prolonged survival and/or turnover of the inflationary CD8+ T cell populations in the absence of antigen. The enhanced survival in MCMV-infected mice suggests improved survival and/or proliferation in the presence of antigen/virus-specific immunity (e.g. helper T cell populations).

Analysis of CFSE dilution: To assess if the inflationary cells were capable of division *in vivo*, and if maintenance of the populations requires division *in vivo*, the percentage of $CFSE^+$ cells were analysed. At 7 days post adoptive transfer in the blood all $CD45.1^+$ M38-specific $CD8^+$ T-cells in naïve and immune infected mice are $CFSE^+$, i.e. surprisingly no division has taken place. At 140 days post adoptive transfer there is a decrease in the percentage of $CFSE^+$ cells in both naïve and MCMV infected mice at an increased frequency in the chronically infected mice. These data show that the inflationary cells are capable of proliferation in vivo and this is enhanced in the presence of antigen.

Surprisingly, there is a difference in the maintenance of inflationary cell populations between the blood and spleen, liver and lung (Fig 5.4). In the spleen the percentage of CD45.1$^+$ M38-specific CD8$^+$ T-cells in naïve and MCMV infected mice decayed at the same rate even though there has been a higher rate of division in chronically infected mice (Fig 5.5). However, in the liver and lung adoptively transferred cells were maintained at a higher frequency than that of the spleen in both naïve and immune mice. In particular in immune mice, the levels diverge substantially from those of naïve mice, with no apparent decay over time. Additionally, while in the blood and spleen, the M38-specific population appears to undergo a similar rate of proliferation compared to that seen in naïve mice, in lung and liver there were obvious differences. M38-specific populations are maintained with higher levels of CFSE dilution in MCMV-infected compared to naïve mice. This data suggest different mechanisms of memory maintenance are active in the spleen and in peripheral organs.

Analysis of phenotype: To ascertain whether the phenotype of M38-specific CD8$^+$ T-cells is stable, flow cytometry analysis was performed (Fig 5.6). M38-specific CD8$^+$ T-cells in naïve and immune mice, stay high in expression for the KLR receptors, NKG2A and KLRG1. The co-stimulatory molecule CD27 shows a small increase on M38-specific CD8$^+$ T-cells in both naïve and immune recipients, as does the lymph node homing maker CD62L gradually increases over the course of 140 days post adoptive transfer in naïve mice, while staying low in immune mice. Broadly, the phenotype of M38-specific inflationary CD8$^+$ T-cells is maintained in naïve mice i.e. without the presence of antigen.

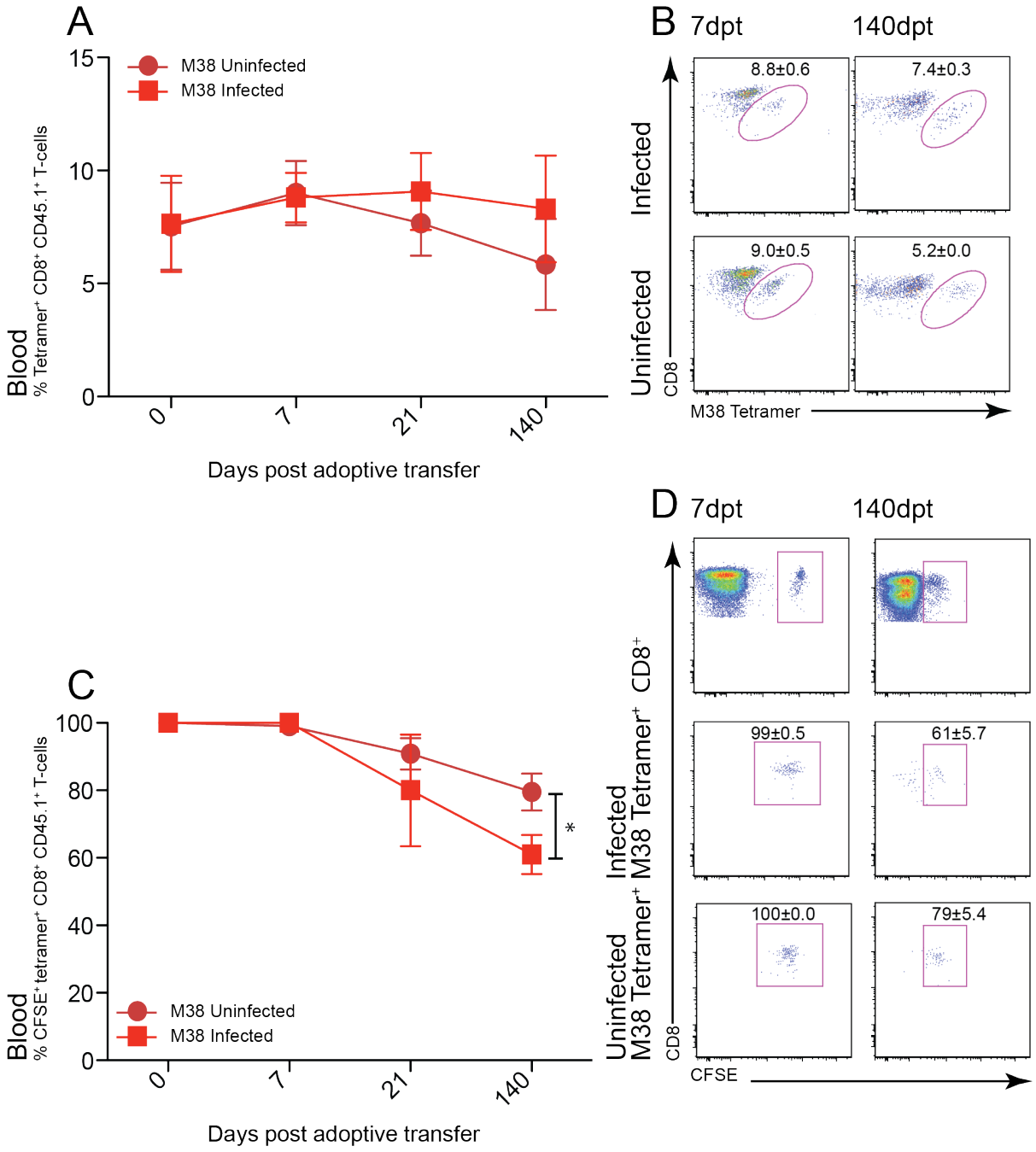


Figure 5-3 **Percentage of adoptive transferred of M38-specific CD8$^+$ T-cells in the blood**. CD45.1 congenic mice were infected (i.v) with 1x10^6 pfu MCMV, 50 days post infection; splenocytes were harvested and stained with CFSE and transferred into C57BL/6 naïve or C57BL/6 50 days post MCMV infection. (A) Time course for the percentage of CD45.1$^+$ M38-specific CD8$^+$ T-cells in naïve and immune mice. Blood was taken 7, 21 and 140 days post adoptive transfer and stained with tetramers. Mean percentages of live CD45.1$^+$ M38-specific CD8$^+$ T-cells are indicated (n=6, mean ±SEM). (B) Tetramer staining for CD45.1$^+$ M38-specific CD8$^+$ T-cells from the blood on 7 and 140 days post adoptive transfer in immune and naïve mice. Mean percentages of live tetramer$^+$ CD45.1$^+$ CD8$^+$ T-cells indicated (n=6, mean±SEM). (C) Time course for the percentage of CFSE$^+$ CD45.1$^+$ M38-specific CD8$^+$ T-cells in naïve and immune mice. Blood was taken 7, 21 and 140 days post adoptive transfer and stained with tetramers. Mean percentages of live CFSE$^+$ CD45.1$^+$ M38-specific CD8$^+$ T-cells are indicated (n=6, mean±SEM). (D) Representative flow cytometry plots, gated on live CD45.1$^+$ M38-specific CD8$^+$ T-cells. Mean percentages of live CFSE$^+$ tetramer$^+$ CD45.1$^+$ CD8$^+$ T-cells indicated (n=6, mean±SEM).

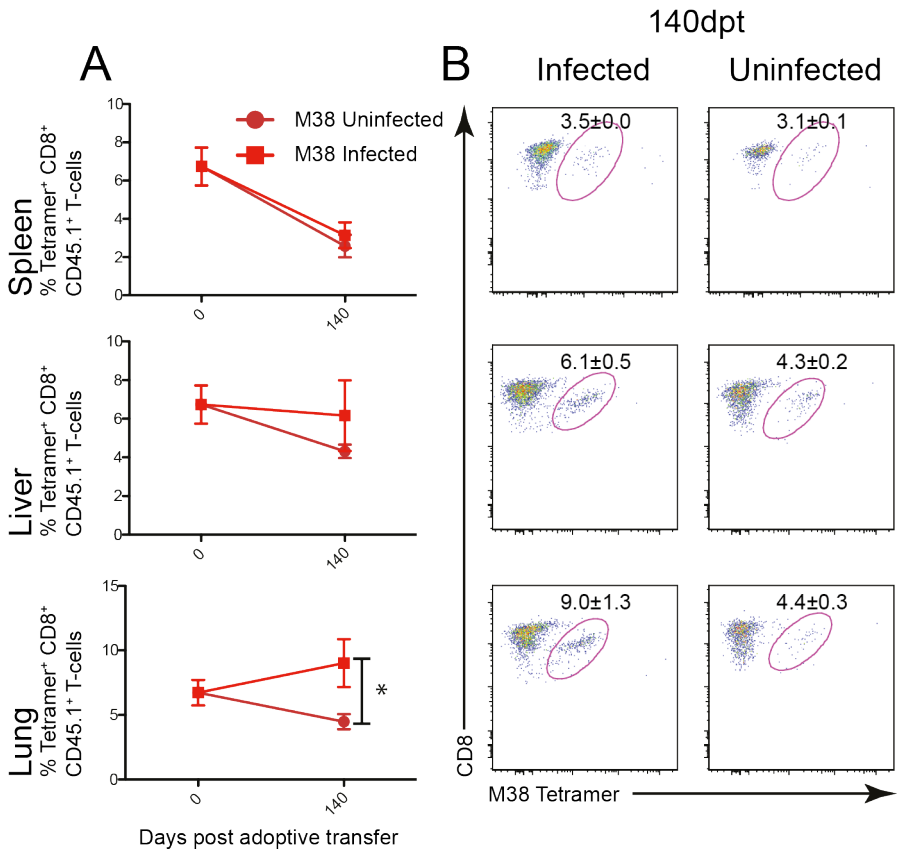


Figure 5-4 **Percentage of adoptive transferred of M38-specific CD8$^+$ T-cells in spleen, liver and lung**. CD45.1 congenic mice were infected (i.v) with 1x10^6 pfu MCMV, 50 days post infection, splenocytes were harvested and stained with CFSE and transferred into naïve C57BL/6 or C57BL/6 50 days post MCMV infection. (A) Percentage of CD45.1$^+$ M38-specific CD8$^+$ T-cells in naïve and immune mice in the spleen, lung and liver. Lymphocytes were harvested 140 days post adoptive transfer and stained with tetramers. Mean percentages of live CD45.1$^+$ M38-specific CD8$^+$ T-cells are indicated (n=6, mean±SEM). (B) Tetramer staining for CD45.1$^+$ M38-specific CD8$^+$ T-cells from the spleen, liver and lung 140 days post adoptive transfer in naïve and immune mice. Mean percentages of live tetramer$^+$ CD45.1$^+$ CD8$^+$ T-cells indicated (n=6, mean±SEM).

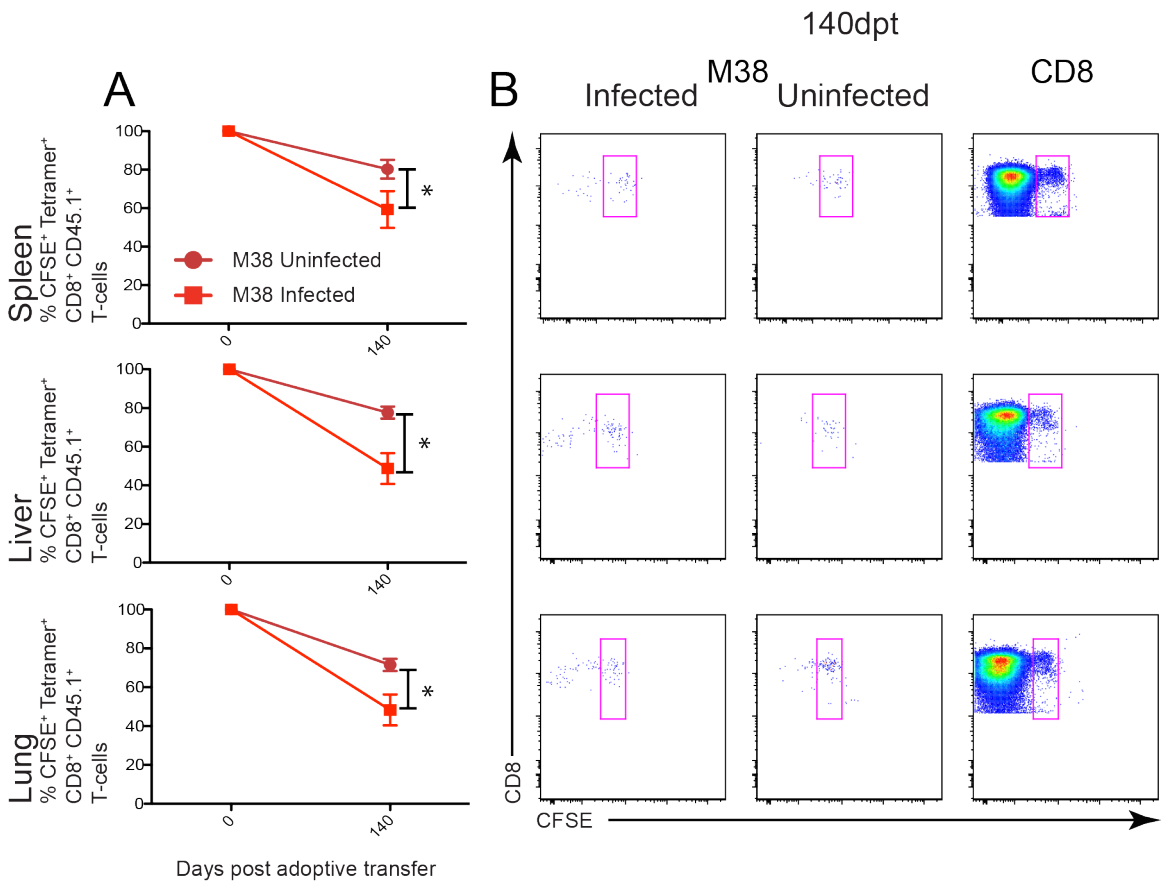


Figure 5-5 **Percentage of CFSE$^+$ CD45.1$^+$ M38-specific CD8$^+$ T-cells in the spleen, liver and lung**. CD45.1 congenic mice were infected (i.v) with 1x10^6 pfu MCMV, 50 days post infection, splenocytes were harvested and stained with CFSE and transferred into C57BL/6 naïve or C57BL/6 50 days post MCMV infection. (A) Time course for the percentage of CFSE$^+$ CD45.1$^+$ M38-specific CD8$^+$ T-cells in naïve and immune mice. Lymphocytes were harvested 140 days post adoptive transfer and stained with tetramers. Mean percentages of live CFSE$^+$ CD45.1$^+$ M38-specific CD8$^+$ T-cells are indicated (n=6, mean±SEM). (B) Representative flow cytometry plots from naïve and immune mice 140 days post infection, gated on live CD45.1$^+$ M38-specific CD8$^+$ T-cells.

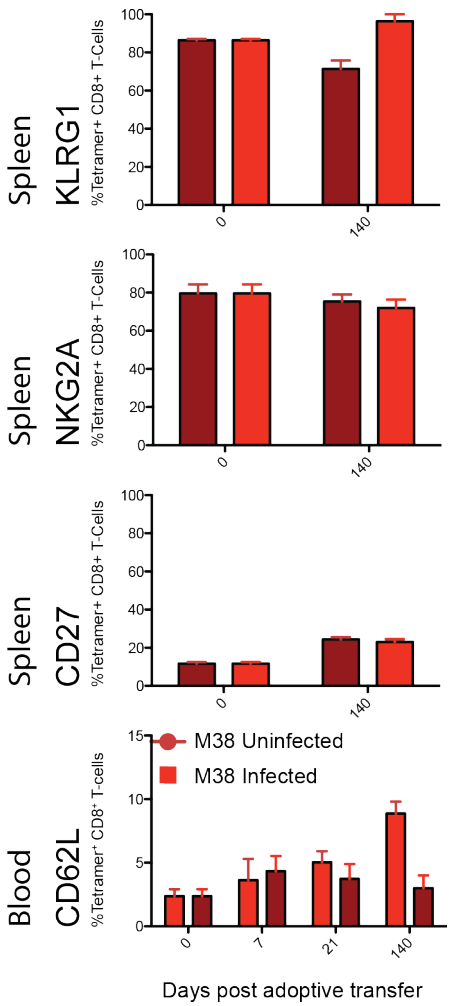


Figure 5-6 **Stable phenotype of inflationary M38-specific CD8$^+$ T-cells.** CD45.1 congenic mice were infected (i.v) with 1x10^6 pfu MCMV, 50 days post infection, splenocytes were harvested and stained with CFSE and transferred into C57BL/6 naïve or C57BL/6 50 days post MCMV infection. Time course showing the percentage of cells expression the indicated marker on CD45.1$^+$ M38-specific CD8$^+$ T-cells in naïve and immune mice from the blood and spleen. Gated on live CD45.1$^+$ M38-specific CD8$^+$ T-cells (n=6, mean±SEM).

5.2.3 Tetramer Saporin experiments

The adoptive transfer experiments show the inflationary cell pools are long-lived, still proliferating in chronically infected mice up to 140 days post infection, and are maintained in naïve hosts in the absence of antigen. To further investigate the stability of the inflationary $CD8^+$ T-cell population I injected mice infected with MCMV with M38- or M45-tetramer conjugated to saporin (SAP), to deplete these epitope specific $CD8^+$ T-cell populations. This experiment tests not only the turnover rate of the population, by allowing analysis of their re-population, but also their in vivo role in virus control.

Time course of depletion and recovery: 50 days post infection I injected mice with 44ρm of M38-tetramer conjugated to either PE or SAP and then bled mice over a time course (Fig 5. 7). After injection of M38-tetramer-SAP, one day post injection there was 88% specific killing of M38-specific $CD8^+$ T-cells, i.e. I achieved a decrease in M38-specific $CD8^+$ T-cells in the blood from 13% down to 1.4%. This reduction was maintained for a further 2 days. Surprisingly, after 6 days the percentage of M38-specific $CD8^+$ T-cells had returned and overshot the initial frequency, with 42% of $CD8^+$ T-cells specific for M38. The control M38-tetramer conjugated to PE showed a small increase in the percentage of M38-specific $CD8^+$ T-cells, increasing from 13 to 16% of $CD8^+$ T-cells. There was no further increase in the percentage of M38-specific $CD8^+$ T-cells. After infection with M38-tetramer-SAP there was also a small increase in M45-specific $CD8^+$ T-cells from 0.6% to 1.2% of $CD8^+$ T-cells.

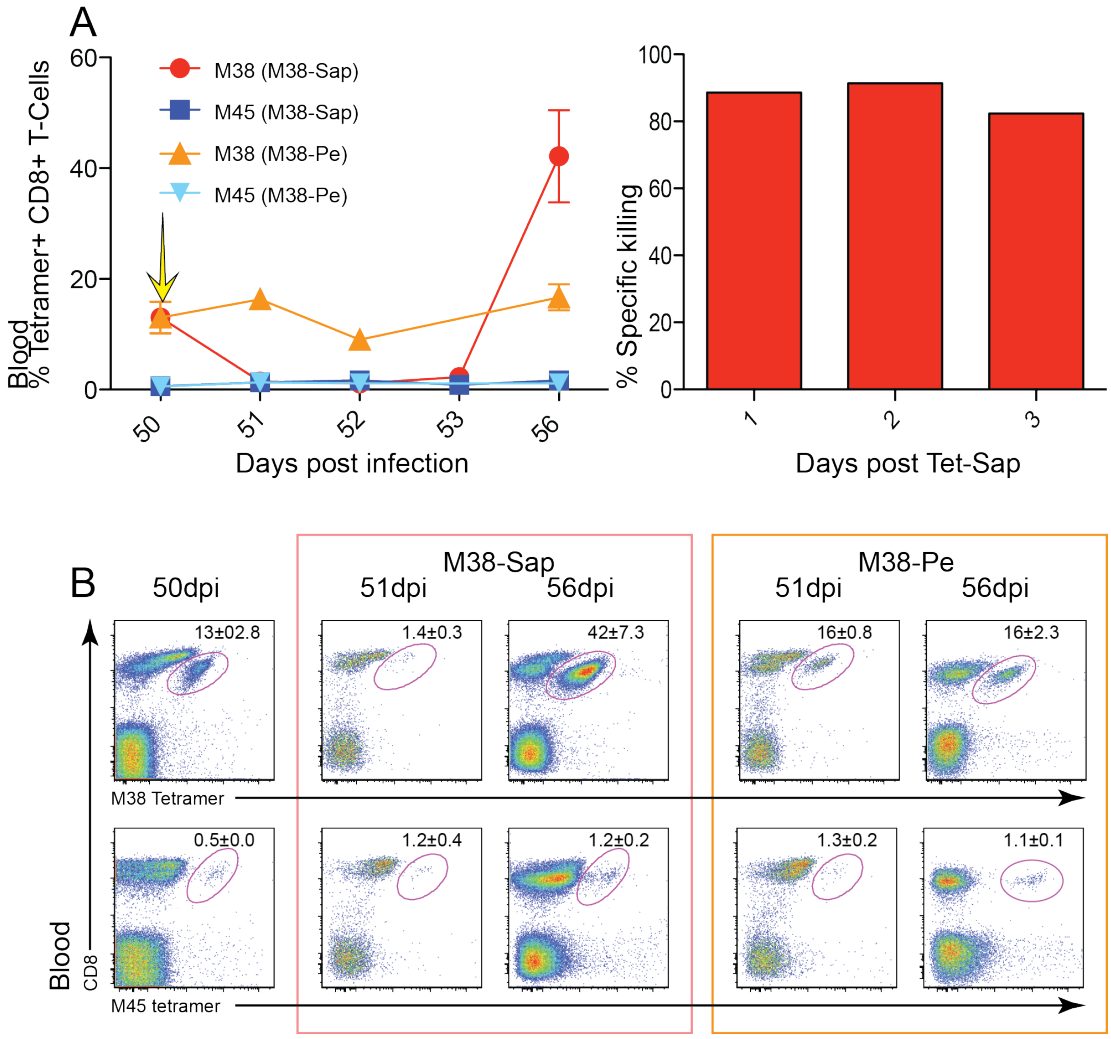


Figure 5-7 D**epletion of M38-specific CD8$^+$ T-cells.** C57BL/6 mice were infected (i.v) with 1x10^6 pfu MCMV; 50 days post infection, mice were injected with either M38-teramer-SAP or M38-teramer-PE, mice were bled over a time course. (A) Time course for M38- (red) and M45- (blue) specific CD8$^+$ T-cells after injection with M38-teramer-SAP, and M38- (orange) and M45- (light blue) specific CD8$^+$ T-cells after injection with M38-teramer-PE. Mice were bled 0, 1, 2, 3 and 6 days post injection, stained with tetramers, and analysed by flow cytometry. Mean percentages of live tetramer$^+$ CD8$^+$ lymphocytes are indicated (n=6, mean±SEM). (C) Representative flow cytometry plots of M38-specific CD8$^+$ T-cells and M45-specific CD8$^+$ T-cells 50 days after MCMV infection and 1 and 6 days after either M38-tetramer-SAP or M38-tetramer-Pe injection (n=6, mean±SEM). (C) Percentage of M38-specific CD8$^+$ T-cells killed at 0, 1, 6 days post injection with M38-tetramer-SAP (n=6, mean±SEM)

Depletion in organs: This deletion and subsequent increase in the percentage of M38-specific $CD8^+$ T-cells was not restricted to the blood. It was also observed in the spleen, liver and lung (Fig 5.8). Injection with M38-tetramer-SAP, achieved a reduction from 7.7% to 1% of M38-specific $CD8^+$ T-cells 1 day after infection, then 6 days after injection an increase to 14% of M38-specific $CD8^+$ T-cells in the spleen. In the lung there was a reduction from 16% to 2.3% then an increase to 51% M38-specific $CD8^+$ T-cells. In the liver there was a reduction from 15% to 2.1% and then an increase to 42% M38 specific-$CD8^+$ T-cells, 6 days after injection. There was no change in the percentage of M38-specific $CD8^+$ T-cells after the injection with M38-tetramer-PE in any of the organs.

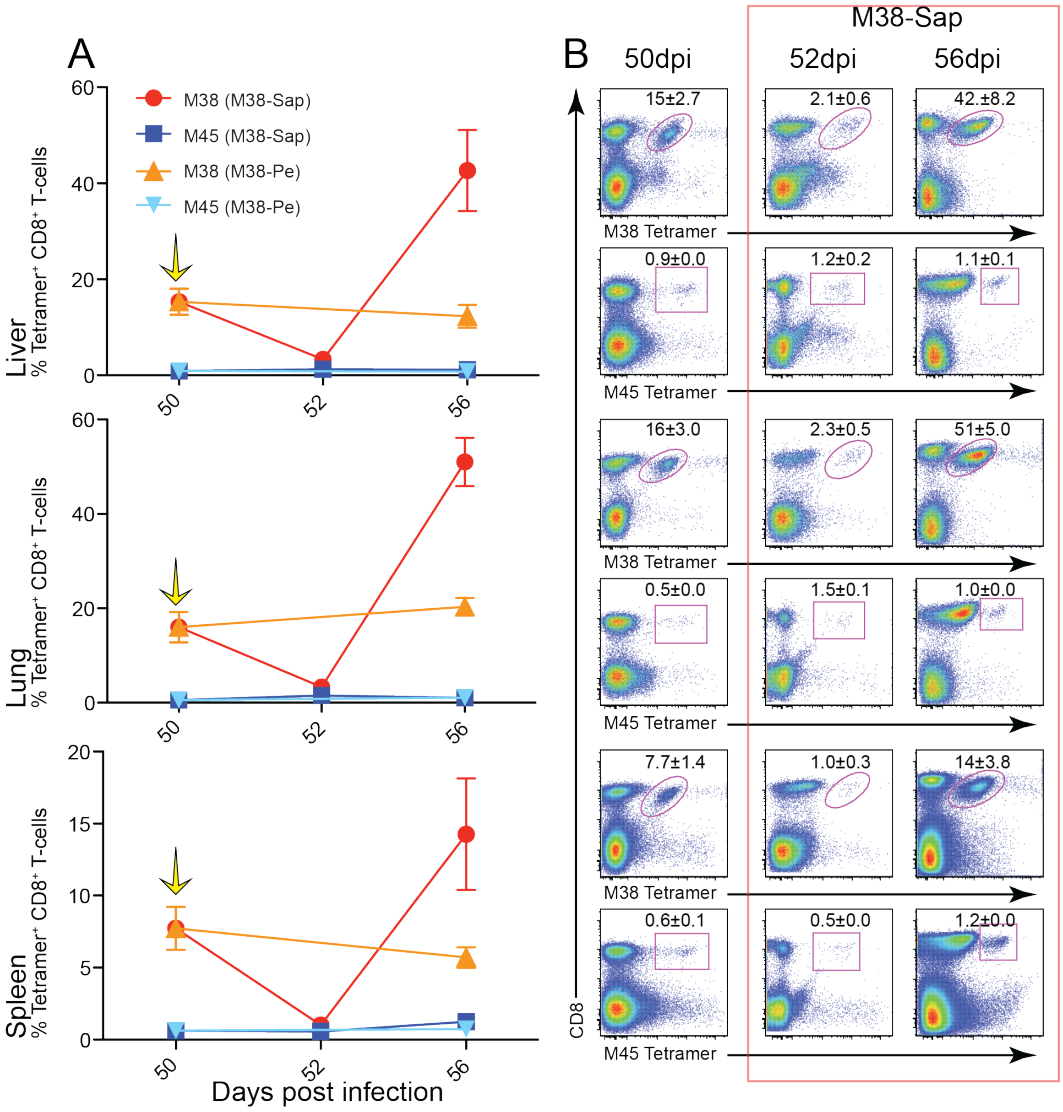


Figure 5-8 **Depletion of M38-specific CD8$^+$ T-cells in organs.** C57BL/6 mice were infected (i.v) with 1x10^6 pfu MCMV; 50 days post infection, mice were injected with either M38-teramer-SAP or M38-teramer-PE, lymphocytes harvested from the liver, lung and spleen. (A) Time course for M38- (red) and M45- (blue) specific CD8$^+$ T-cells after injection with M38-teramer-SAP, and M38- (orange) and M45- (light blue) specific CD8$^+$ T-cells after injection with M38-teramer-PE. Lymphocytes were harvested from the liver, lung and spleen 0, 2, and 6 days post injection, stained with tetramers, and analysed by flow cytometry. Mean percentages of live tetramer$^+$ CD8$^+$ lymphocytes are indicated (n=6, mean±SEM). (B) Representative flow cytometry plots of M38-specific CD8$^+$ T-cells and M45-specific CD8$^+$ T-cells 50 days after MCMV infection and 2 and 6 days after either M38-tetramer-SAP or M38-tetramer-Pe injection (n=6, mean±SEM).

Stability of M38-specific populations after Tet-SAP treatment: To determine whether the increased frequency of M38-specific $CD8^+$ T-cells after injection with M38-tetramer-SAP was stable, I injected mice 50 days post infection with 44ρM M38-tetramer-SAP, and sacrificed mice over a time course (Fig 5.9). I observed a dramatic decrease of M38-specific $CD8^+$ T-cells in all organs (blood, spleen, liver, lung and bone marrow) 2 days after injection. This was then followed by a doubling of the original percentage of M38-specific $CD8^+$ T-cells across all organs, which was maintained up to 90 days after M38-tetramer-SAP injection. I also observed an increase in the percentage of M45-specific $CD8^+$ T-cells after injection across all organs increasing from 0.6% to 1.5% of $CD8^+$ T-cells than a decrease to 0.6% of $CD8^+$ T-cells by 40 days after injection.

Proliferation analysis: The proliferative state of the tetramer specific $CD8^+$ T-cells was analysed by ICS staining for Ki67 (Fig 5.10). In the liver, lung and spleen almost 100% of M38-specific $CD8^+$ T-cells were positive for the proliferation marker 6 days after M38-tetramer-SAP injection, deceasing to 20% at 22 days post infection. This was followed by a further decrease to a level similar to that before infection, with 6% M38-specific $CD8^+$ T-cells being positive for Ki67, 40 days after injection.

We see a doubling of M45-specific $CD8^+$ T-cells after infection with M38-tetramer-SAP and we also see an increase in the percentage of M45-specific $CD8^+$ T-cells that are specific for the proliferation marker Ki67. There is an increase from 9% to 30% of M45-specific $CD8^+$ T-cells being positive for Ki67 at 6 days post injection, then a decrease to 15% at 21 days post injection and a further decrease to the same

level before injection to around 9% of M45-specific $CD8^+$ T-cells being positive for Ki67, 40 days after injection.

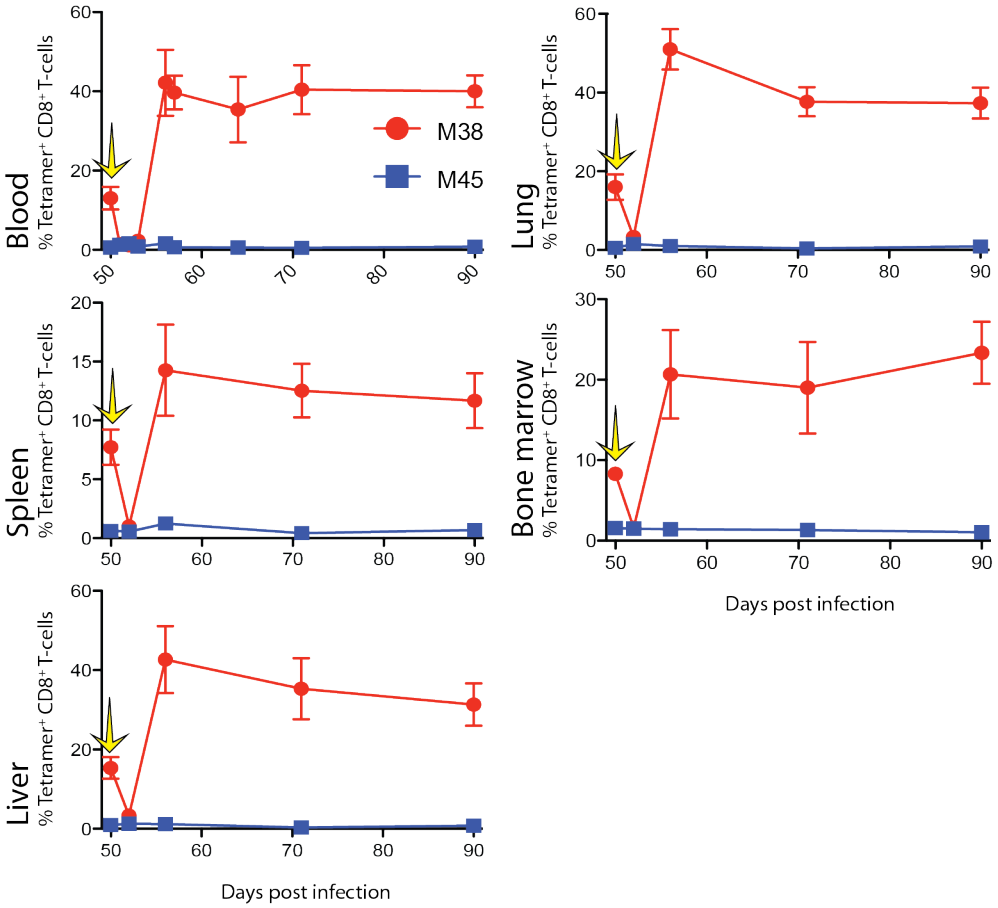


Figure 5-9 I**ncreased frequency of M38-specific CD8$^+$ T-cells after depletion.** C57BL/6 mice were infected (i.v) with 1x10^6 pfu MCMV, 50 days post infection, mice were injected with M38-teramer-SAP, lymphocytes harvest from the blood, liver, lung, spleen and bone marrow at 0, 2, 6 21 and 40 days post injection stained with tetramers, and analysed by flow cytometry. Mean percentages of live tetramer$^+$ CD8$^+$ lymphocytes are indicated (n=6, mean±SEM).

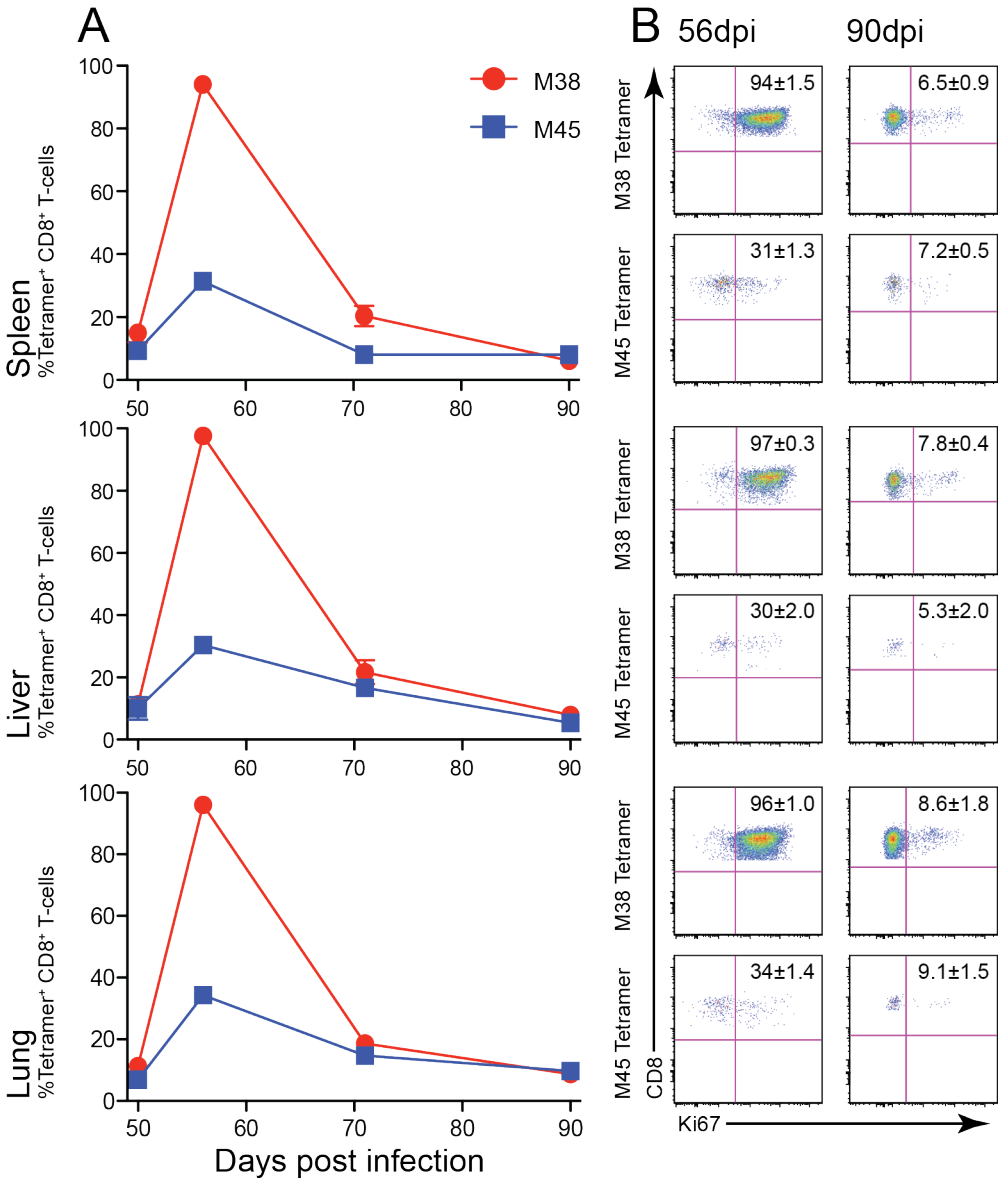


Figure 5-10 **Proliferative state of specific CD8$^+$ T-cells after M38-tetramer-Sap injection.** C57BL/6 mice were infected (i.v) with 1x10^6 pfu MCMV, 50 days post infection, mice were injected with M38-teramer-SAP lymphocyte harvested and stained with tetramers over a time course. (A) Time course showing the percentage of cells expressing Ki67 on M38- CD8$^+$ T-cells (red) and M45-specific CD8$^+$ T-cells (blue) in the spleen, liver and lung 0, 6, 21, and 40 days post injection with M38-tetramer-SAP, (n=6, mean±SEM). (B) Representative flow cytometry plots show the expression of Ki67 in the spleen, live and lung on 6 and 40 days after infection with M38-Tetramer-SAP, gated on live M38-specific CD8$^+$ T-cells or M45-specific CD8$^+$ T-cells (n=6, mean±SEM).

Functional analysis: To discover if these cells displayed any evidence of exhaustion, an ICS was performed on splenocytes. Cells were stimulated with either M38 or M45 peptide for 6 hours and stained with IFNγ and TNFα (Fig 5.11). The percentage of cells producing IFNγ rose from 4% before injection with M38-tetramer-SAP to 13%, 21 days after injection, there was no increase observed after M45 stimulation. The percentage of TNFα expressing cells after M38 peptide stimulation increased from 5% before injection with M38-tetramer-SAP to 10% 21 days after injection with M38-tetramer-SAP. The increase correlated with the increase in the percentage of M38-tetramer positive cells.

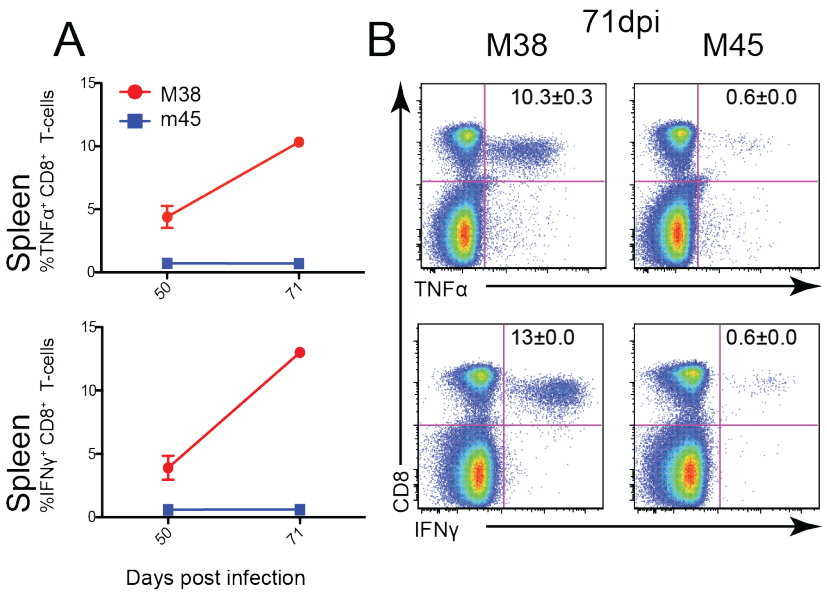


Figure 5-11 **Function of MCMV specific CD8$^+$ T-cells after M38-tetramer-SAP injection.** C57BL/6 mice were infected (i.v) with 1x10^6 pfu MCMV, 50 days post infection, mice were injected with M38-teramer-SAP, lymphocyte harvested and stimulated with either M38 or M45 peptide. ICS was performed. (A) Change in the percentage of cells expressing IFNγ, and TNFα before and 21 days after M38-tetramer-SAP injection; splenocytes were harvested and stimulated with either M38 or M45 peptide (n=6, mean±SEM). (B) Representative flow cytometry plots of splenocytes producing IFNγ, and TNFα stimulated with either M38 or M45 peptide in mice 21 days after M38-tetrame-SAP injection. Numbers indicate the percentage of IFNγ positive CD8$^+$ T-cells (n=6, mean±SEM)

The phenotype of M38-specific $CD8^+$ T-cells after M38-tetramer-SAP injection did not significantly change in the blood, spleen, liver and lung (Fig 5.12). They remained low in CD127 and CD122 expression in comparison to M45-specific $CD8^+$ T-cells. There was a subtle reduction in CD127 expression after injection and then it increased back to the initial baseline after 21 days. Expression of the NK cell receptors NKG2A and NKG2D did not alter on M38-specific $CD8^+$ T-cells, remaining for both markers. Surprisingly there was an increase in NKG2A expression on M45-specific $CD8^+$ T-cells 6 days after injection; this then decreased to the initial level after 21 days. The percentage of M38-specific $CD8^+$ T-cells expressing the exhaustion marker TIM3 increased, with nearly 100% of M38-specific cells expressing the maker 6 days after injection; this then gradually decreased over 40 days post injection to the same levels before injection.

Viral load analysis: The viral load of MCMV was measured by quantitative RT-PCR for number of DNA copies. Over the course of infection, 7, 21, 50 and 100 days post infection, the salivary glands, spleen, liver and lung were taken and viral load quantified (Fig 5.13). Here there is a gradual decrease in viral load over 100 days. To see if there was a change in viral load after M38-tetramer-SAP injection, I injected mice with tetramer saporin 100 days post infection. Two days later organs were harvested and viral load quantified. There was no change in the viral load observed (Figure 5.13).

Due to the kinetics of viral replication, a longer M38-tetramer-SAP injection time course was applied. 4 injections of 44pm over 8 days were performed, after which the organs were harvested and the viral load quantified. Here I observed a substantial increase in viral load across all organs. In the lung and liver there was an

increase of one log and in the spleen and salivary gland there was an increase of two logs (Figure 5.13).

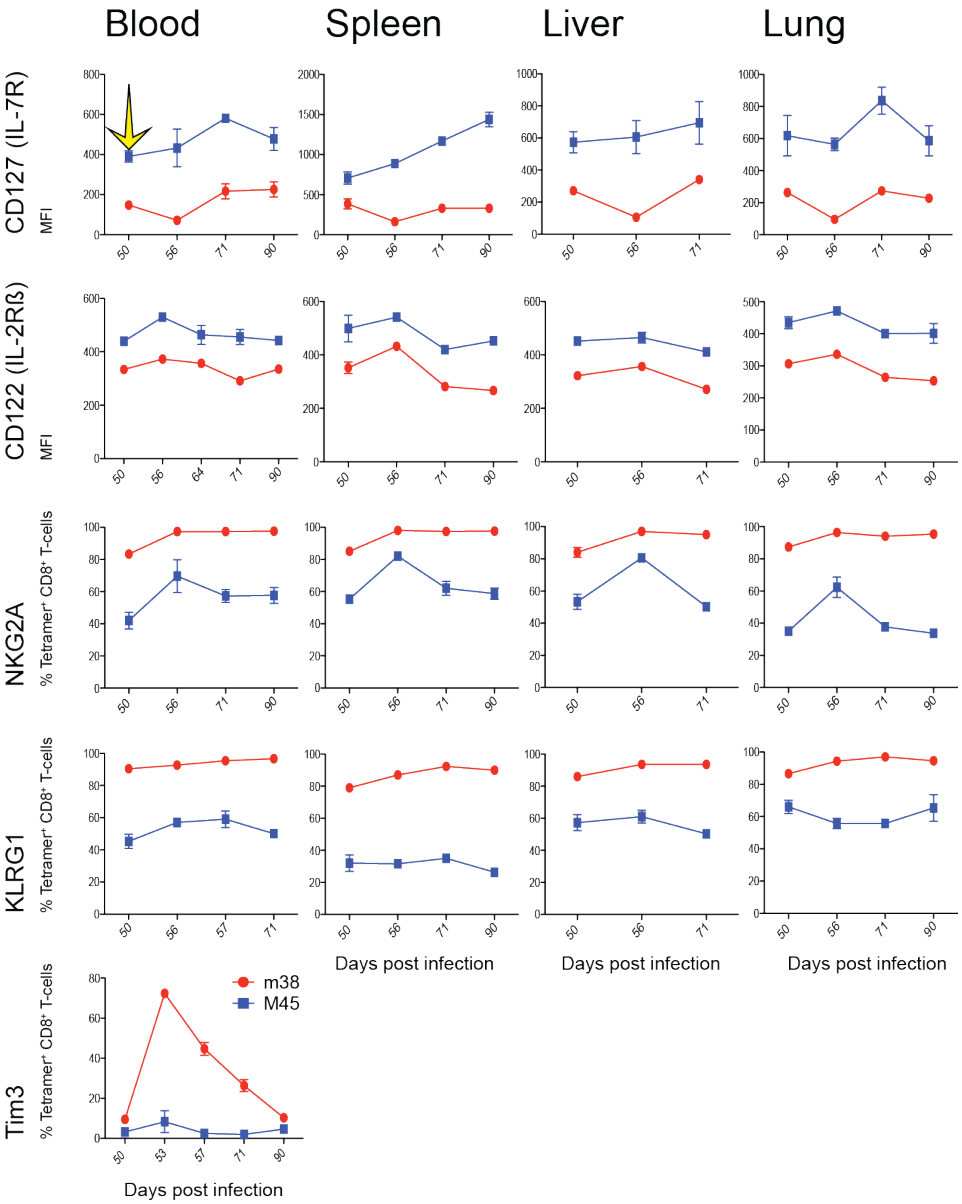


Figure 5-12 **Phenotype of specific CD8$^+$ T-cells after M38-tetramer-SAP injection.** C57BL/6 mice were infected (i.v) with 1x10^6 pfu MCMV: 50 days post infection. Mice were injected with M38-teramer-SAP, lymphocytes harvested from the spleen, liver, lung and blood, and stained with M38- and M45-Tetramer and the indicated marker (n=6, mean±SEM).

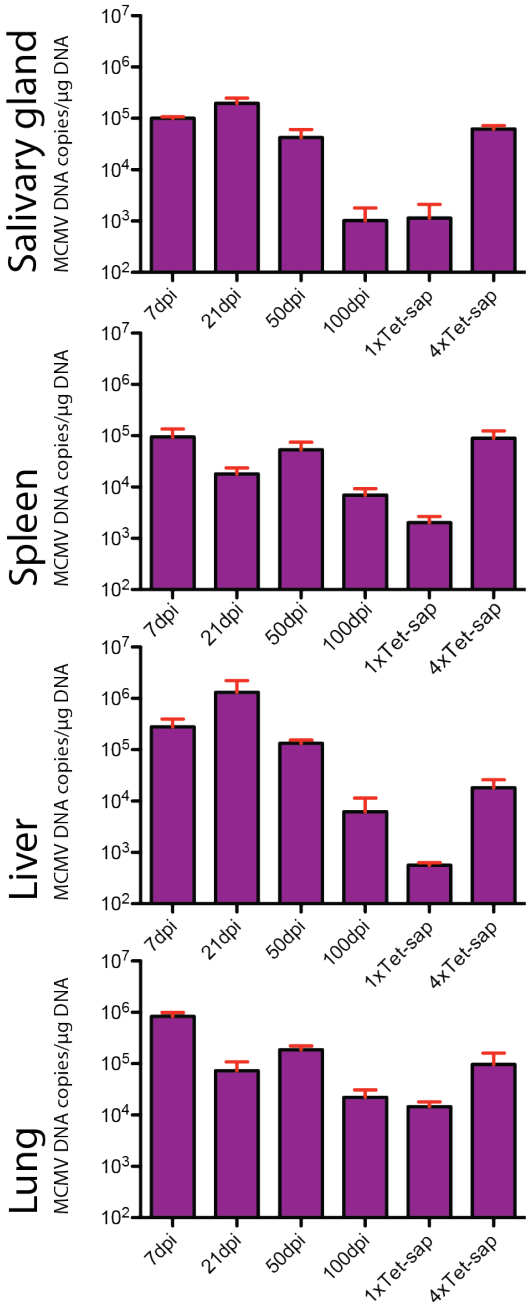


Figure 5-13 **Change in MCMV viral load after M38-tetramer-SAP injection.** C57BL/6 mice were infected (i.v) with $1x10^6$ pfu MCMV; organs were harvested 7,21, 50 and 100 days post injection. Mice 100 days post infection were injected 1x or 4x with 44ρM M38-teramer-SAP over 2 or 8 days respectively, organs harvested and qRT-PCR performed (n=3, mean±SEM).

Impact of M45 depletion: Since there was an increase in M38-specific $CD8^+$ T-cells after injection of M38-tetramer SAP, I injected M45-tetramer-SAP into mice 50 days post infection as a control. After injection there was a decrease in M45-specific $CD8^+$ T-cells from 0.6% to 0.1% of $CD8^+$ T-cells, 2 days post injection. After 6 days post injection the percentage of M45-specific $CD8^+$ T-cells returned to the same level as before injection and maintained at this level up to 21 days post injection (Fig 5.14).

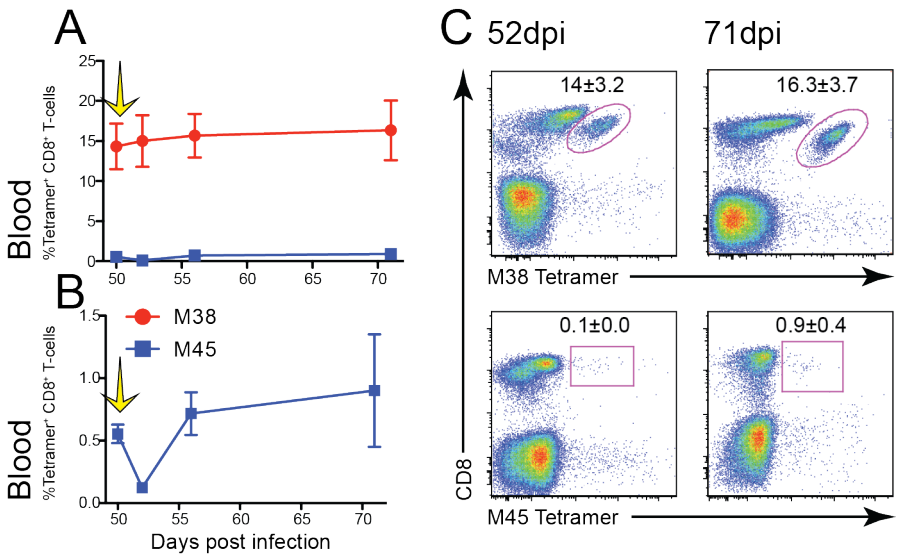


Figure 5-14 **Depletion of M45-specific CD8$^+$ T-cells.** C57BL/6 mice were infected (i.v) with 1x10^6 pfu MCMV; 50 days post infection, mice were injected with M45-teramer-SAP; mice were bled over a time course. (A) Time course for M38- (red) and M45- (blue) specific CD8$^+$ T-cells after injection with M45-teramer-SAP, Mice were bled post injection, stained with tetramers, and analysed by flow cytometry. Mean percentages of live tetramer$^+$ CD8$^+$ lymphocytes are indicated (n=6, mean±SEM). (B) Magnified graph of graph A, without M38$^+$ T-cells. (C)Representative flow cytometry plots of M38- and M45-specific CD8$^+$ T-cells 52 and 71 days after MCMV infection (2 and 11 days after M45-tetramer-SAP injection, respectively) (n=6, mean±SEM).

5.3 Discussion

The in vivo killing assay shows that inflationary M38-specific $CD8^+$ T-cells are still capable of killing but at a reduced capacity compared with effector $CD8^+$ T-cells and, unexpectedly, memory M45-specific $CD8^+$ T-cells. This reduced killing capacity may be an effect of the technique and not a true representation of the killing capacity of virally infected cells. For example, M38-specific $CD8^+$ T-cells express inhibitory KLR receptors such as NKG2A, these receptors prime the $CD8^+$ T-cells to kill cells that have down regulated MHC class I molecules and thus protect against killing self. I transferred splenocytes from naïve mice and will express MHC class I molecules potentially at higher levels than on virally infected cells. Likewise the $CD8^+$ T cell populations express high levels of NKG2D, whose activatory ligand (MICA) is expressed on virally infected cells. Thus using a more natural target may provide a slightly different result in such assays.

By adoptively transferring splenocytes 50 days post MCMV infection I have shown that inflationary M38-specific $CD8^+$ T-cells are maintained in a naive host and could undergo homeostatic proliferation. They gradually decrease over 140 days – this occurs at an increased rate in naive hosts compared to chronically infected mice. A likely explanation is that exposure to antigen is required to maintain the high frequency of inflationary M38-specific $CD8^+$ T-cells. An alternative or additional possibility is that CD4+ T helper populations present in the MCMV-infected mice contribute to memory maintenance. The inflationary M38-specific $CD8^+$ T-cells display a stable phenotype. Although this has been described as “terminally differentiated” they are capable of cell division as a population. The stability of the phenotype over time is strong supportive evidence for a defined transcriptional

signature as described in previous chapters and suggests the signature is a stable feature of the cells over time.

One caveat of the adoptive transfer experiments may be I did not use purified tetramer+ cells, but bulk splenocyte populations. This may have potentially led to transfer of virus or viral antigen, or may lead to unexpected impacts of co-transfer (e.g. of CD4+ T cell help) into naïve hosts. However, there were clear differences in transfer into naïve hosts compared to MCMV-infected mice and in the latter the population was very stable without high levels of turnover. The experimental transfer of labelled congenic cells into MCMV-infected hosts does not suffer from the same caveat, and these data indicate relatively stable populations, especially in the peripheral organs. Our data differ somewhat from those of Snyder et al, who used Busulphan to adoptively transfer in naïve cells into infected hosts(113). One explanation for this is that busulphan treatment modifies peripheral control over the virus, rather than just depleting bone marrow cells, leading to higher antigen-specific cell turnover and thus increased recruitment of naïve cells; this situation does not appear to be replicated in the unmodified steady state, as in these experiments, where turnover is slower.

I noted an interesting discrepancy between the maintenance of memory populations in lung and liver, compared to spleen and blood. In the peripheral organs the transferred M38-specific $CD8^+$ T cells were maintained at high levels in MCMV-infected hosts, with no apparent loss of transferred populations over time and with higher levels of proliferation than in naïve controls. This may represent local proliferation to maintain populations, although it could represent migration of cells, which have proliferated at a distant site such as the spleen, and migrated to the organs

To further analyse the turnover rate of the inflationary populations as well as their role in vivo, I injected chronically infected mice with M38-tetramer-SAP. I deleted M38-specific $CD8^+$ T-cells for up to three days after just one injection but the M38-specific $CD8^+$ T-cells returned at an increased frequency, suggesting this was due to viral rebound, and indicating therefore they were controlling viral replication. This was confirmed by measuring the viral load by quantitative RT-PCR after prolonged depletion of the cells. Rebound of virus was noted in all organs but was most obvious in salivary gland. The result is somewhat surprising given the specificity of the depletion. Previous data have suggested that depletion of $CD8^+$ T-cells on their own did not lead to viral rebound in MCMV-infected mice but required co-depletion of CD4+ T cells or NK cells(255). However these experiments were performed at a much earlier stage of infection. Other data in the BALB/c model suggest that inflationary $CD8^+$ T cells can provide a checkpoint by limiting viral reactivation(247). Our data indicate that at this stage of infection depletion of this single cell population appears critical. Further experiments to deplete other inflationary populations such as M39 could be of interest, as well as conventional plaque assays to assess viral load for confirmation.

The phenotype of inflationary populations did not change after depleting M38-specific $CD8^+$ T-cells. This is surprising since staining for Ki67 revealed the cell population is dividing rapidly in the rebound phase. This data is important as it reveals both the proliferative potential of the pool as well as the fact that the rebound seen is due to cell division rather than redistribution. As discussed above, the stable phenotype is further evidence of a stable transcriptional programme.

5.3.1 Chapter summary

1. In vivo killing experiments revealed functional inflationary populations, although interestingly superior killing was observed in these assays from the non-inflationary M45-specific cell population.
2. Adoptive transfer experiments revealed long term maintenance of transferred populations in MCMV-infected mice and in controls, with many cells surviving without CFSE dilution. The turnover and maintenance of antigen-specific populations in MCMV-infected mice was greater than in controls, especially in organs such as liver and lung
3. The transfer into MCMV-infected mice revealed a stable phenotype over time.
4. In contrast to the adoptive transfer experiments, which suggest a slowly dividing and stable population, depletion of $CD8^+$ T cells using tetramer-SAP led to rapid repopulation and overshoot, indicating a highly dynamic system
5. Depletion of M38-specific cells was associated with a marked increase in viral load in tissues, suggesting an important role in virus containment in the steady state.

6 CD73 - a potent suppressor of immune response - has no effect on generation of inflationary CD8$^+$ T-cells

6.1 Introduction

Circulating or locally released nucleotides are rapidly metabolized by ectoenzymes localised on the cell surface. Ecto-5'-nuceleotidase (CD73) is a glycosly phosphatidylinositol (GPI)-linked membrane bound glycoprotein which hydrolyzes extracellular nucleoside monophosphates into bioactive nucleoside intermediates(241,256). CD73 catalyzes the generation of adenosine, a potent immunosuppressive host nucleoside, from adenosine 5'-monophsopate (AMP). CD73 is expressed on a wide range of epithelial, endothelial, and lymphocytes and plays a role in maintaining barrier function, cardioprotection, and ion transport and suppressing the immune system (242,257).

For more than two decades it has been known that adenosine attenuates potentially harmful suspects of neutrophil activation. More recent studies using new reagents and previous insight into metabolic pathways to generate extracellular adenosine provide an opportunity to understand these pathways in more detail.

The metabolism of ATP into its metabolites ADP, AMP and adenosine is a tightly regulated process. These reactions are carried out by ectoenzymes of the NTPDase family and tissue non-specific alkaline phosphatases. The conversion of ATP into AMP is generated by CD39 (NTPDase1)(243,258), CD73 catalyses the conversion of AMP into adenosine. Thus CD73 and CD39 act to convert ATP into adenosine. Although CD73 is required for conversion of immune activating ATP into immunosuppressive adenosine, loss of function of CD73 lead to an increase in the

expression of tissue non-specific alkaline phosphatases. Alkaline phosphatases have the capacity to compensate for the lack of CD73. In addition, lymphocytes have high levels of extracellular adenosine deaminase bound to CD26 molecules at their surface, and this quickly degrades adenosine(244,245,259).

The balance of ATP and adenosine is crucial in immune homeostasis because ATP is a danger signal released by damaged cells and acts to prime the immune system by ligating to P_2X or P_2Y purinoreceptors, and is critical in activating dendritic cells (DCs) and the secretion of IL-1B and IL-18(246,260). However adenosine suppresses the immune response through the activation of G-protein coupled receptors. Adenosine has four receptors (A_1, A_3, A_{2A}, and A_{2B}), expressed on a variety of immune cells. Including T-cells, NK-cells, NKT-cells, macrophages, DCs, neutrophils and B-cells(247,261,262).

The effects of adenosine are wide ranging. T-cells, which may express A_{2A}, A_{2B} and A_3 receptors, up-regulate adenosine receptors upon TCR stimulation and then stimulation of the receptors by adenosine results in inhibition of proliferation, cytotoxicity and proinflammatory cytokine production(248,263,264). Stimulation of adenosine receptors on APCs, induces the differentiation of alternatively activated macrophages (AAMs). These macrophages secrete less IL-2 and TNFα but increased amounts of IL-10, and are immunosuppressive themselves. On DCs, adenosine inhibits maturation and proinflammatory cytokine production, impairing their ability to induce T_{H1} responses(265,266).

The role of CD73 and CMV in common variable immunodeficiency (CVID) has recently been studied(267). Patients with CVID have defective antibody production and increased susceptibility to infection and show and inflammatory phenotype.

CMV-specific $CD8^+$ T-cells were shown to be CD73 low in patients with CVID, it was postulated that the inflammation seen in patients was a likely effect of CMV infection resulting in inflationary $CD8^+$ T-cells.

To study the effect of CD73 on to inflationary $CD8^+$ T-cells, we analysed the frequency and phenotype of inflationary $CD8^+$ T-cells in CD73 knockout mice in comparison to C57BL/6 mice after MCMV infection. We found no significant difference in the CD73 knockout mice for inflationary $CD8^+$ T-cells. However there was a difference in the viral load - CD73 knockout mice did not reduce the viral load of MCMV over the course of 100 days, in comparison there was a gradual decreases in viral load in C57BL/6 mice.

.

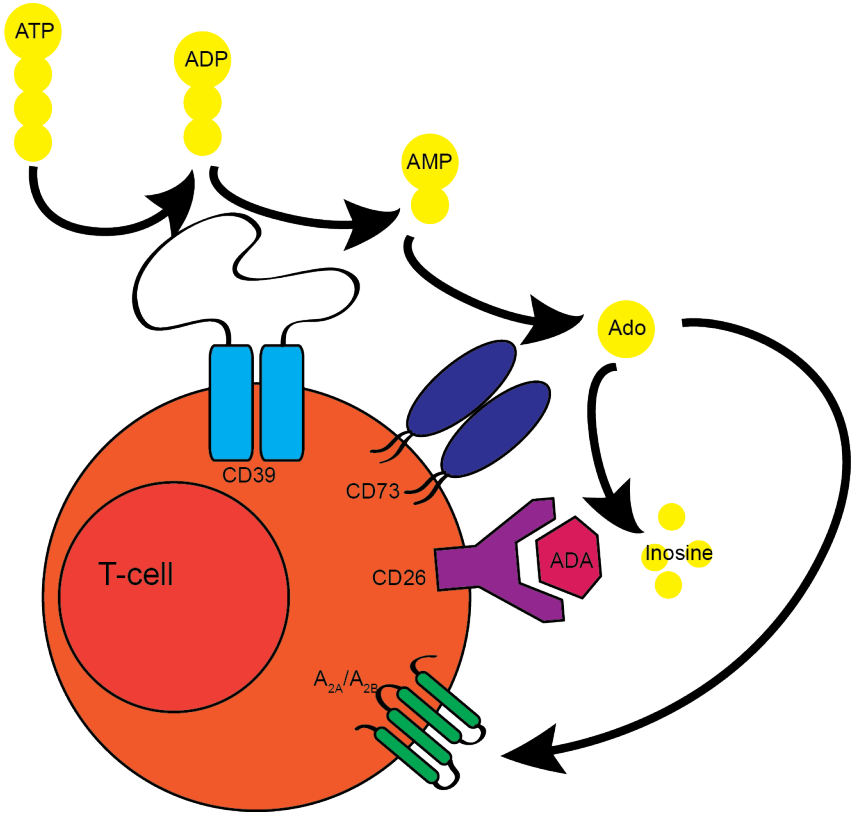


Figure 6-1 Extracellular ATP metabolism. ATP is dephosphorylated to ADP and to AMP by CD39. AMP is dephosphorylated to adenosine by CD73. ATP which binds to purinoceptors P2X and P2Y, is pro-inflammatory. By contrast, adenosine which binds purinoceptros of the P1 type, is anti-inflammatory. Adenosine is degraded to inosine by adenosine deaminase (ADA) that is bound to lymphocyte expressed CD26.

6.2 Results

6.2.1 Frequency of MCMV-specific $CD8^+$ T-cells.

Infection of C57BL/6 and $CD73^{-/-}$ mice with MCMV induced two different $CD8^+$ T-cell responses. As previously, we tracked the $CD8^+$ T-cells specific for M38 and M45 epitopes using MHC class I tetramers. Lymphocytes were harvested from the spleen, liver, lung and blood. M45-specific $CD8^+$ T-cells show standard memory responses in both mice, peaking at 7 days post infection with a frequency of 10-15% of $CD8^+$ T-cells; this was followed by a rapid decline to a stable level of 0.6-2% of $CD8^+$ T-cells and maintained over time. M38-specific $CD8^+$ T-cells showed an inflationary response, with a frequency of 5-15% of $CD8^+$ T-cells at 21 days post infection, this was maintained over time. At 100 days post infection; there was no significant difference between C57BL/6 and $CD73^{-/-}$ mice (Figure 6-2).

We did not see a change in the percentage of specific $CD8^+$ T-cells or in the total number of lymphocytes between C57BL/6 and $CD73^{-/-}$ mice (Figure 6-3). There was no change in the absolute number of virus-specific $CD8^+$ T-cells. This is in contrast with the expectation based on prior data, which suggests CD73 by production of adenosine is a potent immunosuppressor.

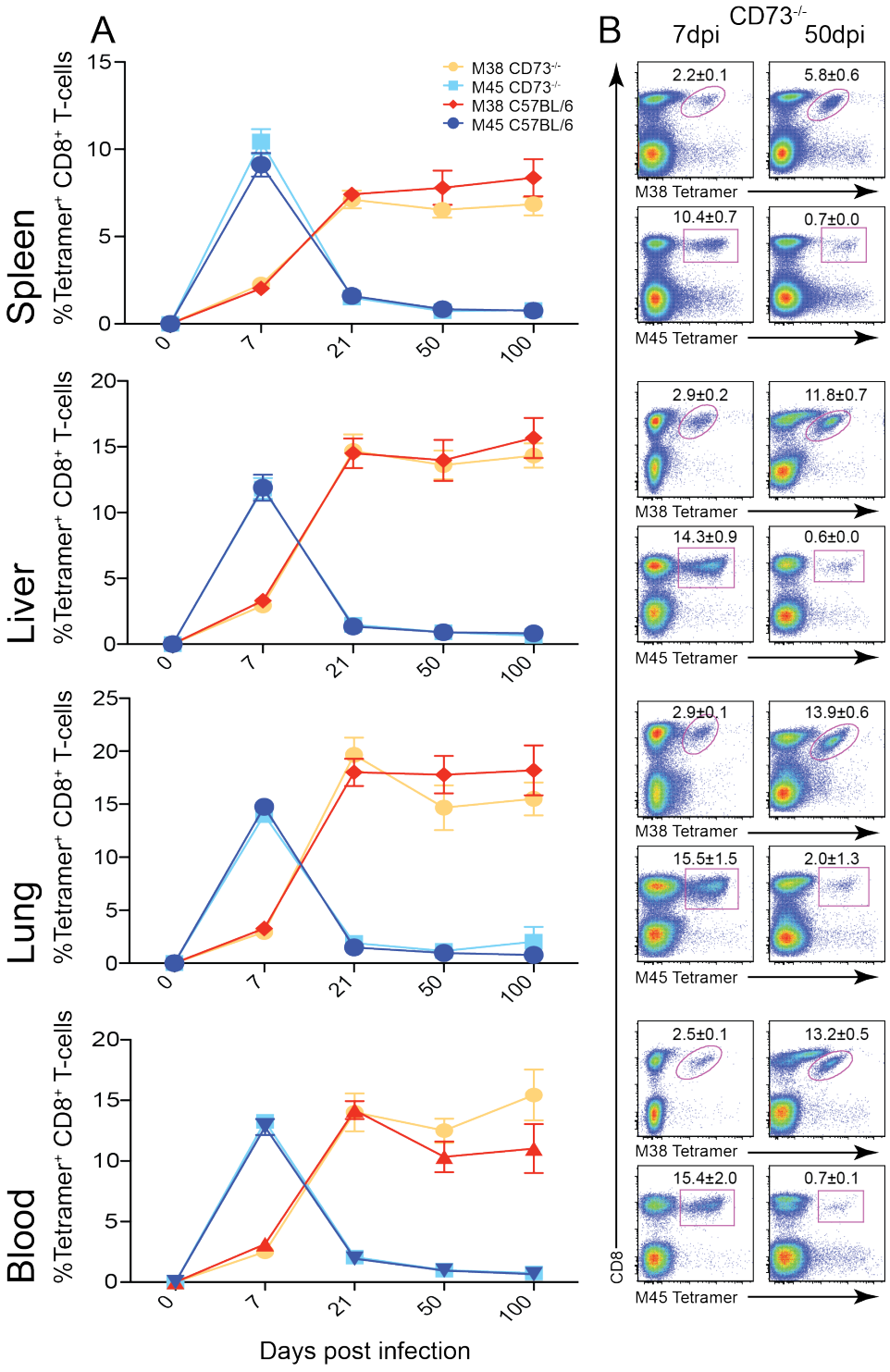


Figure 6-2 CD73 has no affect on inflation. C57BL/6 and CD73$^{-/-}$ mice were infected intravenously (i.v.) with 1x106 pfu MCMV and expansion of M38- and M45-specific CD8^{+} T-cells measured. (A) Time course showing the percentage of M38- (red/orange) and M45- (blue/light blue) specific CD8+ T-cells in the spleen, liver, lung and blood at 0, 7, 21, 50 and 100 days post infection mice. Mean percentage of live tetramer+ CD8^{+} lymphocytes is indicated (n=6, ±SEM). (B) Representative flow cytometry plots of M38 and M45 tetramer staining in the spleen, liver, lung and blood at 7 and 50 days post infection in CD73$^{-/-}$ mice. Mean percentages of live tetramer^{+} CD8^{+} lymphocytes are indicated (n=6, mean±SEM)

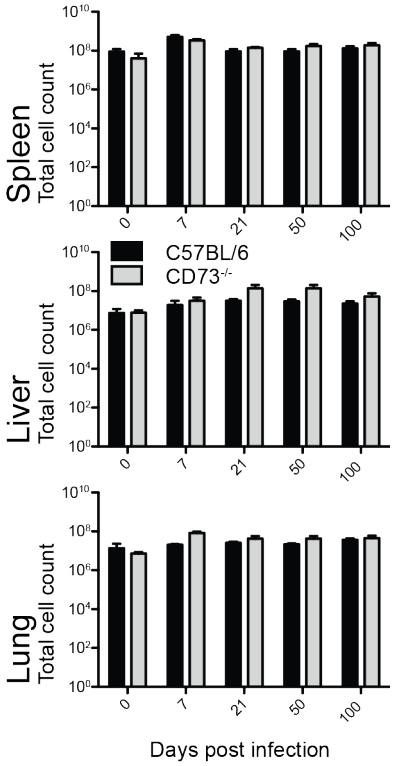


Figure 6-3 **Total number of lymphocytes in CD73$^{-/-}$ mice after MCMV infection.** C57BL/6 and CD73$^{-/-}$ mice were infected intravenously (i.v.) with 1x10^{6} pfu MCMV and total number of lymphocytes from the spleen, liver and lung calculated (n=6, mean±SEM).

6.2.2 Proliferation

To analyse the proliferation kinetics of MCMV-specific $CD8^+$ T-cells in $CD73^{-/-}$ mice we performed ICS staining for the proliferation marker Ki67 (Figure 6-4). Both M38- and M45-specific $CD8^+$ T-cells show a similar profile in the C57BL/6 and $CD73^{-/-}$ mice. At 7 days post infection nearly 100% of specific $CD8^+$ T-cells are expressing Ki67, and therefore proliferating. M45-specific $CD8^+$ T-cells expressing Ki67 decreases to 10% at 21 days post infection and this level of expression is maintained in the memory phase. However, 30% of M38-specfic $CD8^+$ T-cells express Ki67 at 21 days post infection and this then decreases to 15% at 100 days post infection. There is no significant difference at 100 days post infection between C57BL/6 and $CD73^{-/-}$ mice. This is in contrast with the hypothesis, which would suggest that the $CD73^{-/-}$ $CD8^+$ T-cells would show an increase in proliferation.

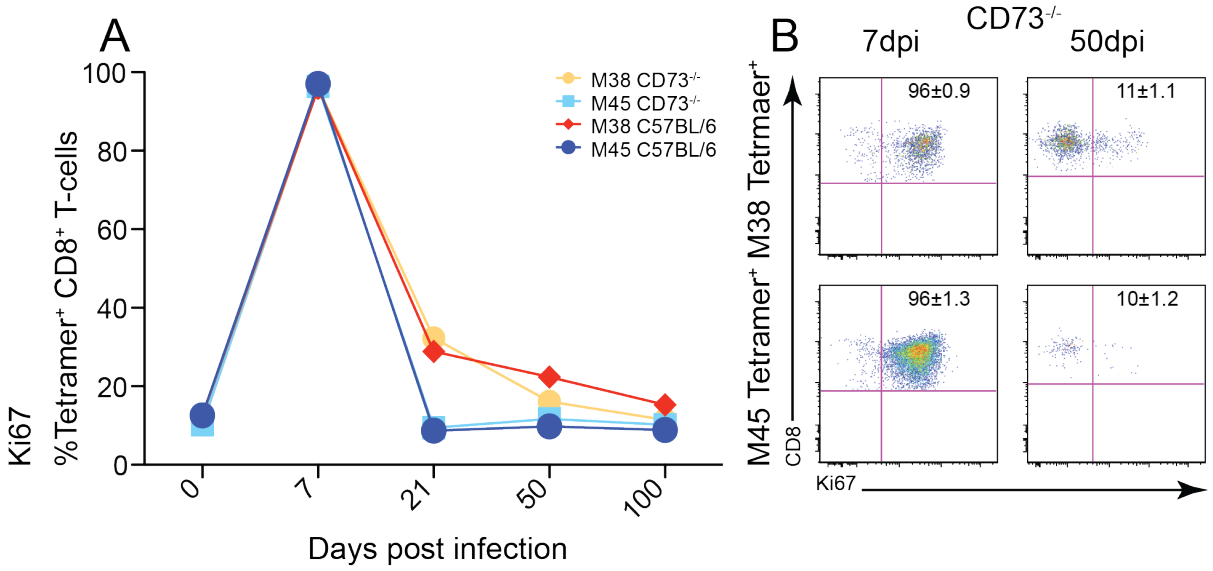


Figure 6-4 **Following the proliferative state of specific CD8$^+$ T-cells in CD73$^{-/-}$ mice after MCMV infection.** (A) Time course showing the percentage of cells expressing Ki67 on M38-specific CD8$^+$ T-cells (red/orange) and M45-specific CD8$^+$ T-cells (blue/light blue), in the spleen on 0, 7, 21, 50 and 100 days post infection (n=6, mean±SEM). (B) Representative flow cytometry plots show the expression of Ki67 in the spleen on 7 and 50 days post infection, gated on live M38-specific CD8$^+$ T-cells or M45-specific CD8$^+$ T-cells in CD73$^{-/-}$ mice (n=6, mean±SEM).

6.2.3 Cytotoxicity and cytokine secretion

It has been shown that adenosine reduces the cytotoxicity of T-cells. Therefore, I expected to see an increase in the production of TNFα and IFNγ in cells from $CD73^{-/-}$. I stimulated splenocytes with either M38 or M45 peptide and stained for LAMP-1 and performed an ICS for CCL3, TNFα and IFNγ (Figure 6-5). I did not see a difference in the production of CCL3, TNFα and IFNγ or the degranulation marker LAMP-1 between C57BL/6 and $CD73^{-/-}$ in the spleen and the secretion profile followed that of tetramer staining. This lack of difference could be due to looking at secretion in vitro, thus in the absence of adenosine. An in vivo killer assay may provide a better understanding of such function of the in vivo levels of adenosine.

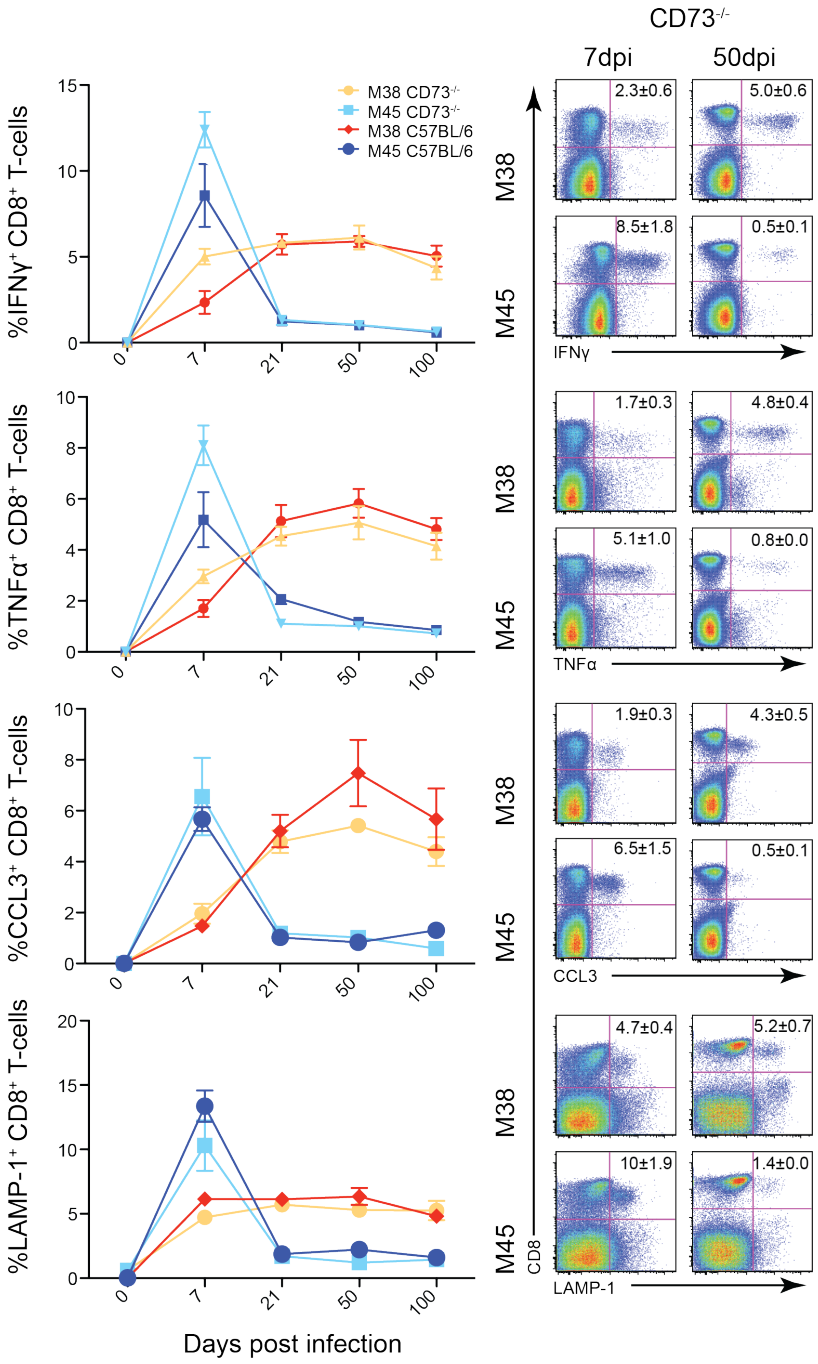


Figure 6-5 **Effector function of specific CD8+ T-cells in CD73-/- mice after MCMV infection**. (A) Time course plotting the percentage of M38- (red/orange) or M45- (blue/light blue) specific CD8+ T-cells from the spleen producing effector molecules after stimulation with either the M38 or M45 peptide. Mean percentage of producing cells within the CD8+ T-cell compartment as indicated (n=6, mean±SEM). (B) Representative flow cytometry plots of splenocytes producing effector molecules stimulated with either M38 or M45 peptide in mice 7 and 50 days post infection in CD73-/- mice. Gated on live lymphocytes, (n=6, mean±SEM).

6.2.4 Phenotype

I looked at the phenotype of the specific $CD8^+$ T-cells to give a better understanding of their activation (Figure 6-6Figure 6-7). Again, I did not see any clear differences between C57BL/6 and $CD73^{-/-}$mice. Lymphocytes were stained for M38- and M45-specific $CD8^+$ T-cells and KLR receptors (NKG2A, KLRG1, NKG2D), cytokine receptors CD122, CD127, co-stimulatory receptor CD27, homing receptors CXCR3, CCR5, CD62L, adhesion receptor ICAM1, exhaustion marker LAG3, and anti-apoptotic maker BCL-2. Specific $CD8^+$ T-cells in the spleen, liver, lung and blood showed the same expression profile in both C57BL/6 and $CD73^{-/-}$ mice. This would suggest that there is no reduction in the activation of M38-specific and M45-specific $CD8^+$ T-cells and remarkably their phenotype is exactly the same in both C57BL/6 and $CD73^{-/-}$ mice.

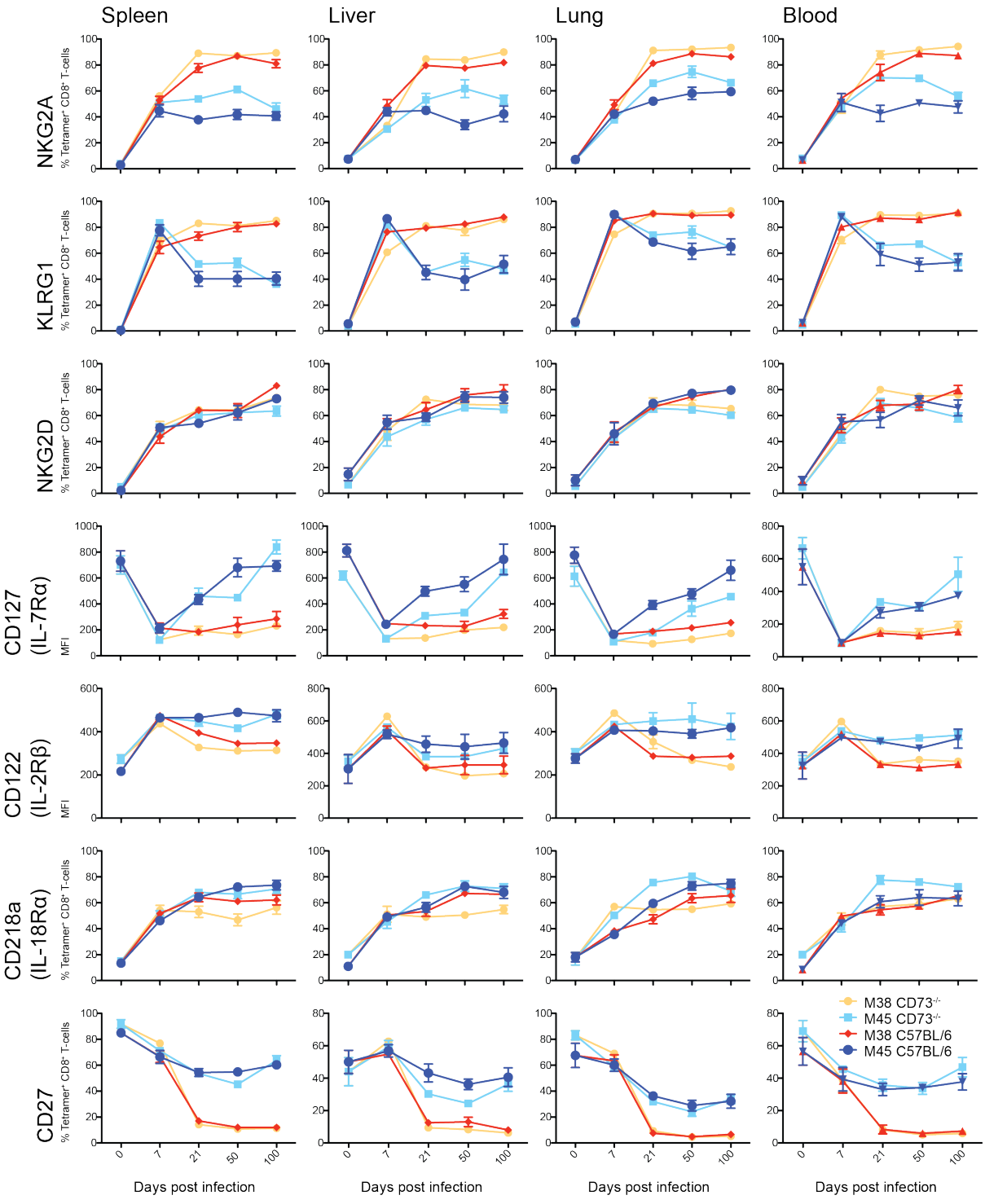


Figure 6-6 **Phenotype of specific CD8$^+$ T-cells in CD73$^{-/-}$ mice after MCMV infection.** Time course showing the percentage of cells expressing or MFI of the indicated markers on M38-specific CD8$^+$ T-cells (red/orange) and M45-specific CD8$^+$ T-cells (blue/light blue), in the spleen, liver, lung and blood in comparison with naive CD8 T cells (n=6, mean±SEM).

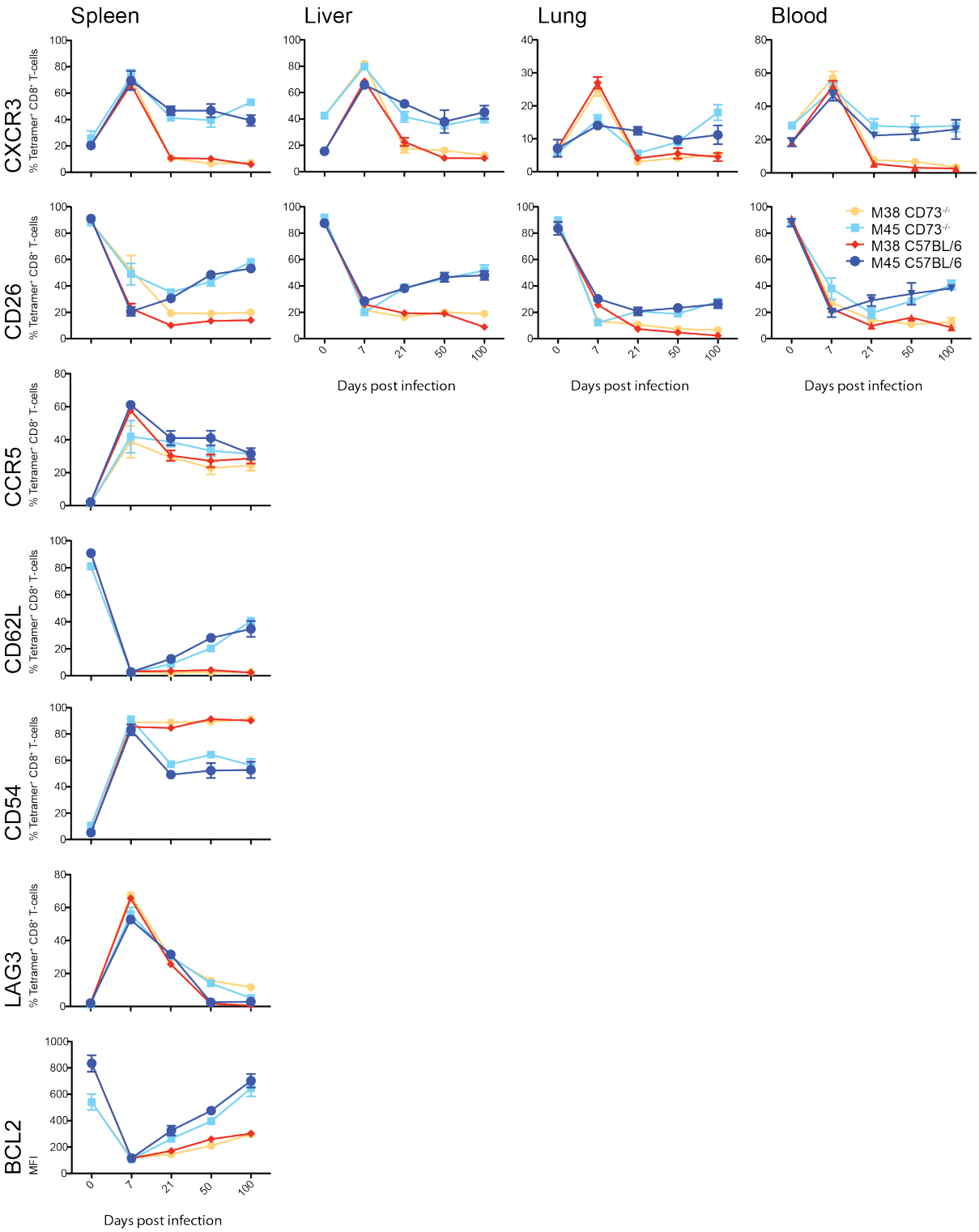


Figure 6-7 **Phenotype of specific CD8$^+$ T-cells in CD73$^{-/-}$ mice after MCMV infection.** Time course showing the percentage of cells expressing or MFI of the indicated markers on M38-specific CD8$^+$ T-cells (red/orange) and M45-specific CD8$^+$ T-cells (blue/light blue), in the spleen, liver, lung and blood in comparison with naive CD8 T cells (n=6, mean±SEM).

6.2.5 Viral loads

As mentioned before CD73 is expressed on many cell types of the immune system and the in vivo levels of adenosine may alter the killing potential of $CD8^+$ T-cells. I performed quantitative RT-PCR to determine the viral load in both C57BL/6 and $CD73^{-/-}$ mice over a time course (Figure 6-8). I expected that the $CD73^{-/-}$ would be more efficient killers of virally infected cells due to not being able to produce adenosine. To our surprise, C57BL/6 over the course of 100 days reduced the viral load in the salivary glands, spleen, liver and lung, while in the $CD73^{-/-}$ I did not see a reduction in any of the organs over the course of 100 days after infection.

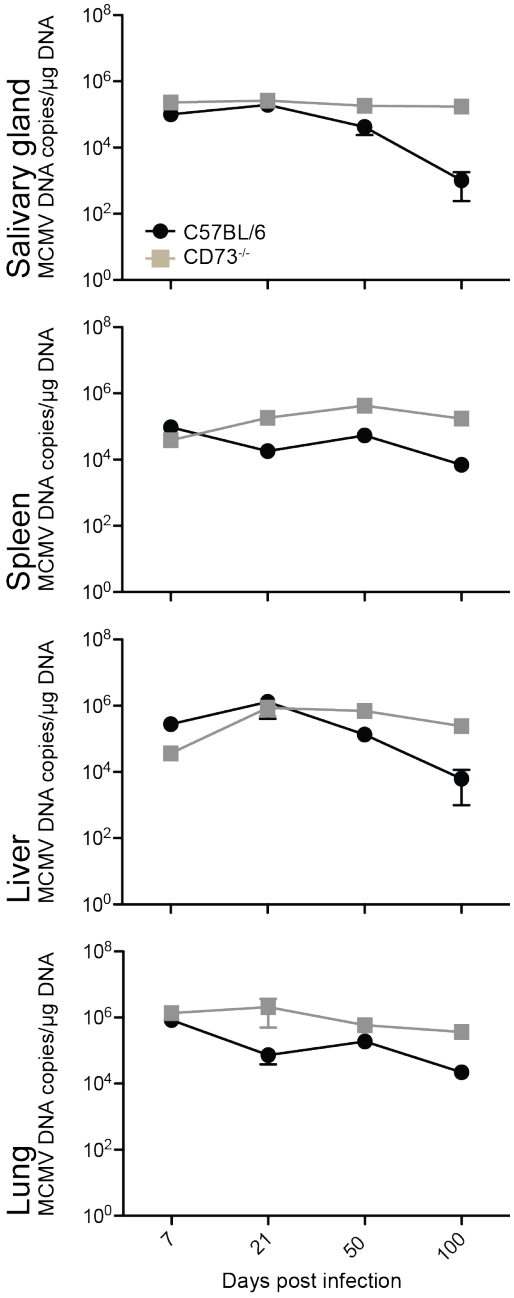


Figure 6-8 **MCMV Viral load in CD73$^{-/-}$ mice.** Time course showing MCMV viral load in CD73$^{-/-}$ and C57BL/6 mice 7, 21, 50 and 100 dpi. Viral load analysis performed by qRT-PCR (n=3, mean±SEM).

6.3 Discussion

I show that the expression of CD73 has no effect on the frequency of specific $CD8^+$ T-cells after MCMV infection and that they show the same proliferation kinetics, functionality and phenotype in C57BL/6 and $CD73^{-/-}$ mice. This could be due to an increase in the expression of tissue non-specific alkaline phosphatases. In contrast to what was expected, I also noted that $CD73^{-/-}$ were not able to reduce the viral load of MCMV over the course of 100 days.

That CD73 has on no effect on M38- and M45-specific $CD8^+$ T-cells could due to the expression levels of other receptors. M45-specific $CD8^+$ T-cells, while being high for CD73, are also high for CD26. Adenosine deaminase (ADA) bound to CD26 can degrade adenosine into inosine, thus abrogating its function. In contrast M38-specifc $CD8^+$ T-cells are low in CD73 and also low in CD26 - as they do not produce as much adenosine they may not require CD26 function.

An explanation for the lack of control of MCMV in $CD73^{-/-}$ mice could be due to regulatory T-cells (T-regs). T-regs suppress the immune system through the production of IL-10, these cells also express CD73 and produce adenosine which may in an autocrine manner inhibit their function(268,269). Thus, in $CD73^{-/-}$ mice T-regs could have increased activation and are limiting the function of specific cell types *in vivo.*

The viral load assay was only done once on three mice and are to be repeated, alongside a plaque assay. If this is in fact a true result then it could be due to CD73 production of adenosine having multiple functions, one of which is barrier formation. Studies have shown that inhibition of CD73 on leukocytes at cell-cell junctions

inhibited the resealing of endothelial and epithelial barriers, suggesting the necessity for extracellular nucleotide metabolism in this pathway.

The expression of CD73 is increased at sires of inflammation by IFNα and in hypoxic conditions. This leads to increased adenosine production and is one of the protective mechanisms that increase endothelial cell permeability. This limits leukocyte trafficking to the sites of inflammation, by limiting permeability in knockout studies may contribute to the lack of viral clearance.

6.3.1 Chapter summary

1. CD73 is not required for maintenance of antiviral $CD8^+$ T-cell population.
2. CD73 is not required for maintenance of memory inflation.
3. CD73-/- mice appear to have higher viral loads than WT C57BL/6 mice. This result requires confirmation and repeating.

7 Conclusion

Most of our knowledge about $CD8^+$ T-cell differentiation comes from primary infection. In this thesis I have predominantly studied the differentiation of $CD8^+$ T-cells in the context of chronic MCMV infection, in an attempt to improve the phenomenon “memory inflation”. This term refers to the increase in the frequency of epitope-specific $CD8^+$ T-cells during the course of infection that are stably maintained at a high frequency for the lifetime of the host(112).

The effect of antigen persistence on the differentiation of $CD8^+$ T-cells is poorly understood. Memory T-cells are considered to be long-lived cells that require little if any antigen re-encounter for survival. This is due to the fact that antigen-specific clones are long lived. However, continuous low-level stimulation is perhaps a more likely scenario given that lymphoid tissues are adapted for the long term maintenance of antigen - it can be stored for months and maybe years in complexes on the surface of follicular dendritic cells (FDCs)(270). In the context of viral infections, many viruses can persist in host tissue for years, such as LCMV, previously thought to be eradicated by the immune system(271). Would it not be advantageous to have a continuous access to low levels of antigen available to stimulate cells? It is this optimal quantity or concentration of available antigen that may be the determining factor in inducing a good immune response as high levels of epitope expression can induce exhaustion.

In MCMV infection, certainly in the case of $CD8^+$ T-cells, the system may achieve the optimal expression of specific epitopes. This is particularly relevant of in the context of vaccines. Although we do not know what frequency is required for the “best” response, by following the notion that more is better then MCMV may indeed be the

best. As many as 20% of $CD8^+$ T-cells can be specific for one epitope(119) (as shown in this thesis), a truly staggering number. However, although not discussed in depth in this thesis, this may have drawbacks in the elderly. Memory cells are continuously generated, however the overall size of the immune system is finite(272,273). With aging there is a loss of naïve T-cell numbers; acceleration of this loss can be attributed to infections such as MCMV/CMV with potential impairment of immune function such as reduced responses (and hence protection) to vaccines (274,275).

We have found that MCMV induces inflationary M38-specifc $CD8^+$ T-cells in the spleen, liver, lung, kidney, bone marrow and blood up to a frequency of 20% of total $CD8^+$ T-cells. These cells remain functional and capable of producing IFNγ and TNFα and the chemokines CXCL1, CCL3, CCL4, CCL5 and CCL9. The production of an array of chemokines is of interest, as it would allow for the $CD8^+$ T-cells to recruit DCs, macrophages and other $CD8^+$ T-cells to the site of infection, but is unlikely to be the reason for inflation as M45-specific $CD8^+$ T-cells are capable of producing the same array of chemokines. One additional chemokine that may be of future interest is CLCF1 as this was only produced by memory $CD8^+$ T-cells in our system and so far it has not been shown that $CD8^+$ T-cells are capable of producing this chemokine.

By comparing the transcriptional profile of M38- and M45-specific $CD8^+$ T-cells at 7 and 50 days post infection we have shown that inflationary M38-specific $CD8^+$ T-cells display a unique transcriptional profile that suggests that inflationary is a distinct state of $CD8^+$ T-cell differentiation. This state is different to exhaustion(166), as they do not up-regulate the inhibitory receptors PD1, Lag3, Tim3 but interestingly down-

regulate BTLA, which could be of interest as BTLA controls proliferation(276,277) and has been shown to increase survival of T-cells(200). Whether BTLA is down-regulated as a consequence of the $CD8^+$ T-cells being continuously stimulated by peptide or is terminally down-regulated and therefore allowing the inflation of these cells has yet to be determined. $CD8^+$ T-cells in CMV infection have been shown to down-regulate BTLA(278). CMV encodes the UL44 protein that has been shown to interact with BTLA to decrease T-cell activation(279). If MCMV encodes for a similar protein, or one with a similar function then M38-specific $CD8^+$ T-cells may have also avoided this inhibitory mechanism.

By analysing the expression kinetics of Ki67 upon M38- and M45-specific $CD8^+$ T-cells I have shown that inflationary cells display increased proliferation until 100 days post infection when compared to M45-specifc $CD8^+$ T-cells, after this timepoint they show a similar proliferation rate as M45-specifc $CD8^+$ T-cells. It is easy to speculate that this increase in proliferation could account for the increase in frequency in $CD8^+$ T-cells. However, the fact remains that as with M45-specfic $CD8^+$ T-cells, for M38-specific $CD8^+$ T-cells the rate of proliferation after 7 days post infection does decrease. So why do M38-specific $CD8^+$ T-cells not go through the contraction phase when M45-specfic $CD8^+$ T-cells do?

This becomes more interesting when examining mRNA expression levels for apoptotic and anti-apoptotic proteins. I have shown that M38-specific $CD8^+$ T-cells express lower levels of Bcl-2 than M45-specific $CD8^+$ T-cells; however after the acute phase M38-specific $CD8^+$ T-cells do increase expression of Bcl-2 expression. From the array we can see that M45-specifc $CD8^+$ T-cells also express mRNA for the apoptotic proteins PUMA and BIM while M38-specific $CD8^+$ T-cells express do not but they do express mRNA for anti-apoptotic proteins SURVIVIN and *Bcl-x_L*.

These proteins could account for inflation and require further analysis although I have not addressed the mechanism by which they are being induced.

Increased survival of M38-specific $CD8^+$ T-cells could be sustained by expression of CX3CR1, shown to induce the expression of Bcl-x_L. However, CX3CR1 is expressed in acute infection on M45-specific $CD8^+$ T-cells so CX3CR1 alone cannot account for the development of inflationary cells. It is likely that inflationary $CD8^+$ T-cells are maintained through continuous stimulation by antigen as they express low levels of the receptors CD122 and CD127, required for binding to IL-7 and IL-15 and maintaining homeostatic proliferation.

Inflationary $CD8^+$ T-cells also have reduced expression of stimulatory receptors CD27 and CD357, a sign of continuous antigen stimulation, while they do express higher levels of CD226 than M45-specific $CD8^+$ T-cells. This marker is of interest as it is important in priming $CD8^+$ T-cells by non-professional $CD8^+$ T-cells(212).

The transcriptional control of $CD8^+$ T-cells has recently gained much interest and here I show that inflationary $CD8^+$ T-cells express high levels of T-Bet and low levels of Eomes in comparison to central memory $CD8^+$ T-cells. Other transcription factors that have been shown to be important for innate lymphocytes (ILCs) such as RORA and ID2(280) are highly expressed in inflationary $CD8^+$ T-cells. Inflationary $CD8^+$ T-cells also uniquely express ZFP313 and FOXK1, which has not been described in T-cells before, but has been shown to promote proliferation of muscle progenitor cells(281).

Inflationary $CD8^+$ T-cells also express inhibitory and stimulatory NK-cell receptors. As MCMV down-regulates MHC class I molecules, inhibitory receptors may be important in killing cells by “non-self” mechanism. While it was known that they

express NKG2A, KLRG1 and NKG2D, I have shown for the first time that they express the inhibitory receptor KLRE1.

MCMV is a chronic infection and therefore it is difficult to determine if inflation is driven by viral replication alone or is a consequence of the $CD8^+$ T-cells being driven into a unique differentiation state. To address the replication question I used a replication incompetent adenovirus expressing LacZ. This virus induced two types of $CD8^+$ T-cell responses to βgal epitopes (βgal_{96} and βgal_{497}). βgal_{497}-specific $CD8^+$ T-cells showed a standard $CD8^+$ T-cell response, increasing until 21 days post immunization then contracting, being maintained at a low frequency. In contrast βgal_{96}-specific $CD8^+$ T-cells showed an inflationary response, increasing in frequency until 21 days post immunization and then being stably maintained at a high levels. These cells are functional, producing IFNα, TNFγ and an array of chemokines in a similar pattern to M38-specific $CD8^+$ T-cells.

Again βgal_{96}-specific $CD8^+$ T-cells inflationary cells showed a unique transcriptional profile, distinct from effector and central memory $CD8^+$ T-cells. They express the same NK-cell receptors and showed the same transcription factor expression profile as M38-specific $CD8^+$ T-cells. While βgal_{96}-specific $CD8^+$ T-cells were maintained at a high frequency their replication state was the same as βgal_{497}-specific $CD8^+$ T-cells, so the replication state of these cells was not the reason for inflation.

I further looked at the expression profile of apoptotic related proteins and as with inflationary M38-specific $CD8^+$ T-cells, βgal_{96}-specific $CD8^+$ T-cells had high expression of *Bcl-x_L* and low expression of *Bim* and *Puma*. The inflationary βgal_{96}-specific $CD8^+$ T-cells also showed the same expression profile of chemokine receptors being high for CX3CR1 and are low in CXCR3. Another similarity was the

low expression of the inhibitory reporter BTLA in βgal_{96}-specific $CD8^+$ T-cells in comparison to βgal_{497}-specific $CD8^+$ T-cells.

To further compare the inflationary cells from MCMV infection and adenovirus immunization I performed K-means clustering. Identifying 183 genes, that as a group were specifically up-regulated in inflationary cells, these genes were involved in gene ontology categories such as; regulation of transcription, cell cycle and apoptosis. Specific genes in this group of interest are the anti-apoptotic *Bcl-x*$_L$ inhibitory and the transcription factors *Foxk1*, *Bmi1* and *Rbbp7*. I have identified a set of genes that can be used to identify inflationary $CD8^+$ T-cells, but how these genes interact to control inflation has yet to be addressed.

I further wished to assess the stability and function of MCMV inflationary M38-specific $CD8^+$ T-cells. In the adoptive transfer experiments into naïve and infected recipients there was a decrease over the course of 140 days in the percentage of M38-specific $CD8^+$ T-cells. However there was no significant difference in the percentage of cells between those transferred into naïve and MCMV infected recipients, although M38-specific $CD8^+$ T-cells transferred into infected recipients did undergo a higher rate of proliferation. This would suggest that M38-specific $CD8^+$ T-cells are capable of undergoing homeostatic proliferation. However, as whole splenocytes were transferred there is the possibility that infected cells were transferred into the naïve recipients. Neverthless if this was true one may expect an increase in the percentage of M45-specific $CD8^+$ T-cells which I did not see - in fact 21 days after adoptive transfer they were below the limit of quantification.

To analyse the turnover, I performed tetramer-saporin experiments: here M38-specific $CD8^+$ T-cells were deleted from chronically infected mice. After one injection

of M38-Sap I achieved a 90% reduction in M38-specific $CD8^+$ T-cells. To my surprise 6 days post injection M38-specific $CD8^+$ T-cells had overshot their initial level and were now at around 40% of total $CD8^+$ T-cells. This could be due to the M38-MHC class I-monomer stimulating M38-specific $CD8^+$ T-cells that were not depleted. This is thought unlikely as when injecting with M38-PE I did not see any increase in the percentage of M38-specific $CD8^+$ T-cells. I tested the viral loads and after one injection of M38-Sap I did not see an increase in viral load. As MCMV is a slow replicating virus I injected 4 times with M38-Sap over 8 days and then measured the viral load. There was an increase in all organs: this was only performed once and needs to be repeated but suggests that MCMV is under constant immunological control and inflationary cells are responsible for control of viral replication.

Due to the differential expression of the ectoenzymes CD73 and CD26 on M38- and M45-specific $CD8^+$ T-cells, I wanted see if the levels of extracellular adenosine were involved in the control of inflation. Using $CD73^{-/-}$ mice and following inflation I found there was no difference between knock out mice and wild type in relation to M38-specific $CD8^+$ T-cells. However when it came to measuring the viral load I noticed that $CD73^{-/-}$ were not capable reducing the viral load over the course of 100 days, this experiment was done only once and needs to be repeated but could potentially be down to the overactivation of T_{reg} cells in the knockout mice.

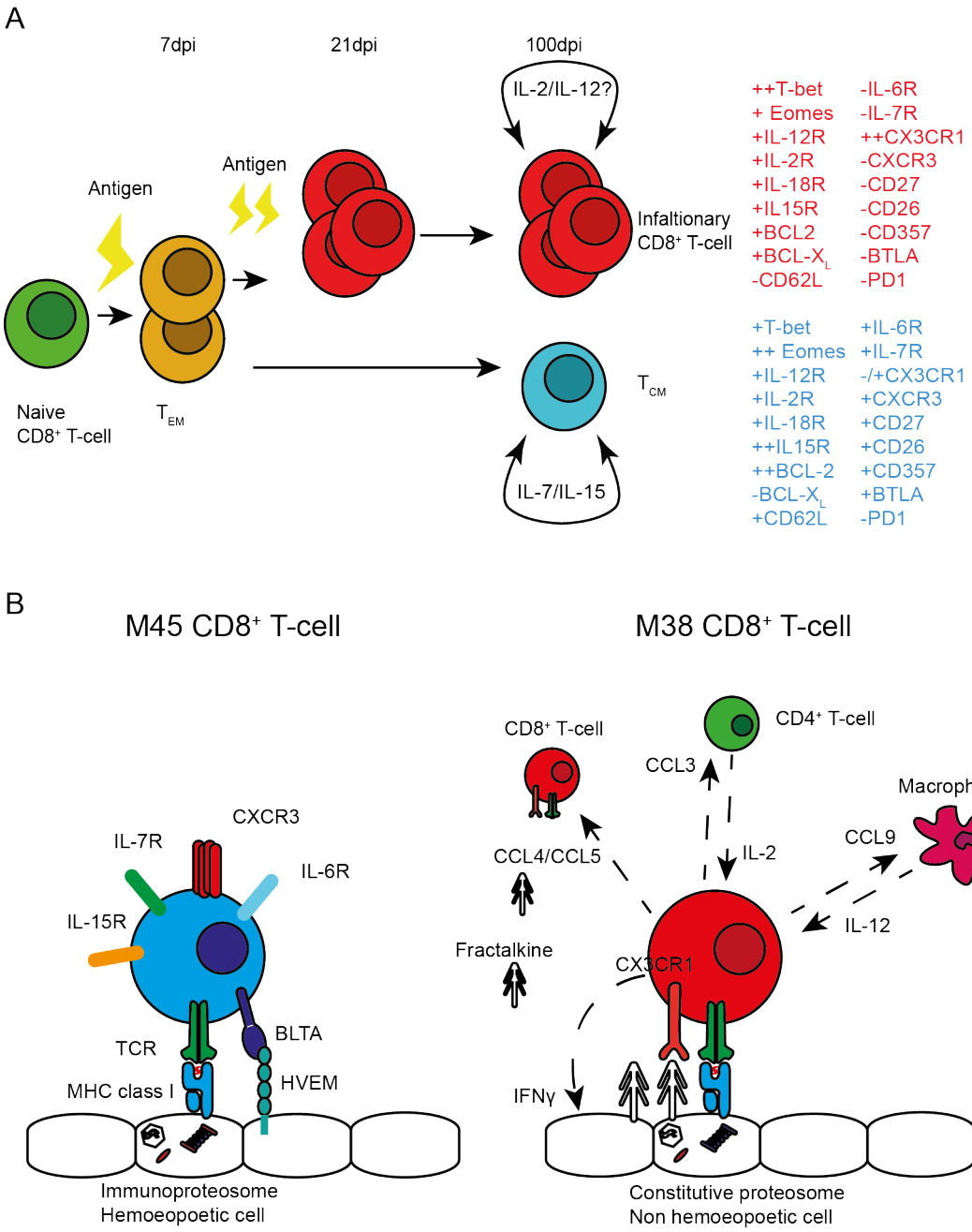


Figure 7-1 **Model of inflation in chronic infection**. (A) Inflationary MCMV-specific CD8$^+$ T-cells accumulate in peripheral tissues where they are maintained at high frequency with an effector memory phenotype. Inflation occurs due to prolonged antigen stimulation, inducing proliferation at a higher frequency than M45 CD8$^+$ T-cells up to 100dpi, after which the cells are maintained by homeostatic proliferation, possibly by IL-2, IL-15 and Il-12. (B) Memory CD8$^+$ T cell inflation is triggered by MCMV antigen recognition on latently infected non-hematopoietic cells, stimulation induces IFNα which in turn stimulates the expression of fractalkine. Binding of fractalkine up-regulates Bcl-X_L and are therefore able to avoid the contraction phase due to decreased apoptosis. Inflationary CD8$^+$ T-cells produce chemokines attracting CD8$^+$ T-cells and CD4$^+$ T-cells, providing IL-2, and macrophages, providing IL-12. Stimulation of IL-12 in turn induces up-regulation of T-Bet and down regulation of Eomes. Inflationary CD8$^+$ T-cells are immunoproteasome independent and have down regulated the inhibitory receptor BTLA. M45 CD8$^+$ T cell do not inflate partially due to the low expression of fractalkine and the expression of the inhibitory receptor BTLA.

7.1 Future work

1: The expression levels of gene involved in apoptosis could be the key to understanding how inflation is maintained. Two candidates for further research are the pro-apoptotic protein BIM, shown to be low in inflationary cells and high in T_{CM}. The other, anti-apoptotic Bcl-X_L is high in inflationary cells in comparison to $T_{CM.}$

2: Fractalkine receptor is highly expressed on inflationary cells, and it has been shown to induce the expression of Bcl-X_L. By Infecting CX3CR1 knock out mice with MCMV we hope to see a decrease in inflation compared to C57BL/6 due to a increase in apoptosis.

3: There has recently been a focus on the transcription factors controlling T-cell development. I have identified some unique transcription factors expressed in inflationary cells that have not been documented to have a function in T-cell development. I will first confirm the expression of transcription factors FOXK1 and RBBP7 and construct knock out mice for future MCMV infections.

4: The inhibitory receptor BTLA has been shown to inhibit T-cell replication, I have shown that this receptor is low on inflationary cells, I will further inject MCMV chronically infected mice with a BTLA blocking antibody to see if this inhibitory receptor is limiting the expansion of M45-specfic $CD8^+$ T-cells. And overexpress BTLA in T-cells using a lentivirus to confirm that BTLA is playing a role in inflation.

8 Papers during my DPhil period.

Defining the molecular signature of CD8+ T cells in memory inflation

Stuart Sims, Beatrice Bolinger, Geraldine O'Hara, Catherine de Lara, Natasha Saghal and Paul Klenerman

(in preparation – for submission January/Feb 2012)

A new model for CD8+ T cell memory inflation based upon a recombinant adenoviral vector

Beatrice Bolinger, Stuart Sims, Geraldine O'Hara, Catherine de Lara, Elma Tchilian, Sonja Firner, Daniel Engeler, Burkhard Ludewig and Paul Klenerman

Journal Immunology (resubmitted after revision December 2012)

Transient CD8-memory contraction: a potential contributor to latent cytomegalovirus reactivation.

Campbell J, Trgovcich J, Kincaid M, Zimmerman PD, Klenerman P, Sims S, Cook CH.

J. Leukoc. Biol. 2012 Jun 22.

Molecular footprints reveal the impact of the protective HLA-A*03 allele in hepatitis C virus infection.

Fitzmaurice K, Petrovic D, Ramamurthy N, Simmons R, Merani S, Gaudieri S, Sims S, Dempsey E, Freitas E, Lea S, McKiernan S, Norris S, Long A, Kelleher D, Klenerman P.

Gut. 2011 May 6.

High frequency, sustained T cell responses to PARV4 suggest viral persistence in vivo.

Simmons R, Sharp C, Sims S, Kloverpris H, Goulder P, Simmonds P, Bowness P, Klenerman P.

J. Infect. Dis. 2011 May 15;203(10):1378–87.

A dominant role for the immunoproteasome in CD8+ T cell responses to murine cytomegalovirus.

Hutchinson S, Sims S, O'Hara G, Silk J, Gileadi U, Cerundolo V, Klenerman P.

PLoS ONE. 2011;6(2):e14646.

HLArestrictor—a tool for patient-specific predictions of HLA restriction elements and optimal epitopes within peptides.

Malene Erup Larsen, Henrik Kloverpris, Anette Stryhn, Catherine K. Koofhethile, Stuart Sims, Thumbi Ndung'u, Philip Goulder, Søren Buus, Morten Nielsen.

Immunogenetics . 2010 Nov **63**, 43–55.

Efficacious early antiviral activity of HIV Gag- and Pol-specific HLA-B 2705-restricted CD8+ T cells.

Rebecca P. Payne, Henrik Kløverpris, Jonah B. Sacha, Zabrina Brumme, Chanson Brumme, Søren Buus, Stuart Sims, Stephen Hickling, Lynn Riddell, Fabian Chen, Graz Luzzi, Anne Edwards, Rodney Phillips, Julia G. Prado, and Philip J. R. Goulder

J. Virol. 2010 Oct;84(20):10543–57.

A genetic and functional relationship between T cells and cellular proliferation in the adult hippocampus.

Huang GJ, Smith AL, Gray DH, Cosgrove C, Singer BH, Edwards A, Sims S, Parent JM, Johnsen A, Mott R, Mathis D, Klenerman P, Benoist C, Flint J.

PLoS Biol. 2010;8(12):e1000561.

MHC-peptide tetramers for the analysis of antigen-specific T cells.

Sims S, Willberg C, Klenerman P.

Expert Rev Vaccines. 2010 Jul;9(7):765–74.

9 References

1. Kisselev AF, Akopian TN, Woo KM, Goldberg AL. The sizes of peptides generated from protein by mammalian 26 and 20 S proteasomes. Implications for understanding the degradative mechanism and antigen presentation. J. Biol. Chem. 1999 Feb 5;274(6):3363–71.

2. Goldberg AL, Rock KL. Proteolysis, proteasomes and antigen presentation. Nature. 1992 Jun 4;357(6377):375–9.

3. Rock KL, Gramm C, Rothstein L, Clark K, Stein R, Dick L, et al. Inhibitors of the proteasome block the degradation of most cell proteins and the generation of peptides presented on MHC class I molecules. Cell. 1994 Sep;78(5):761–71.

4. Yewdell JW, Reits E, Neefjes J. Making sense of mass destruction: quantitating MHC class I antigen presentation. Nat. Rev. Immunol. 2003 Dec;3(12):952–61.

5. Salio M, Cella M, Suter M, Lanzavecchia A. Inhibition of dendritic cell maturation by herpes simplex virus. Eur J Immunol. 1999 Oct;29(10):3245–53.

6. Sevilla N, Kunz S, Holz A, Lewicki H, Homann D, Yamada H, et al. Immunosuppression and resultant viral persistence by specific viral targeting of dendritic cells. J. Exp. Med. 2000 Nov 6;192(9):1249–60.

7. Bevan MJ. Antigen recognition. Class discrimination in the world of immunology. Nature. 1987 Jan;:192–4.

8. Nopora K, Bernhard CA, Ried C, Castello AA, Murphy KM, Marconi P, et al. MHC class I cross-presentation by dendritic cells counteracts viral immune evasion. Front Immunol. 2012;3:348.

9. Blattman JN. Estimating the Precursor Frequency of Naive Antigen-specific CD8 T Cells. Journal of Experimental Medicine. 2002 Mar 4;195(5):657–64.

10. Pewe LL, Netland JM, Heard SB, Perlman S. Very diverse CD8 T cell clonotypic responses after virus infections. J. Immunol. 2004 Mar 1;172(5):3151–6.

11. Kedzierska K, Day EB, Pi J, Heard SB, Doherty PC, Turner SJ, et al. Quantification of repertoire diversity of influenza-specific epitopes with predominant public or private TCR usage. J. Immunol. 2006 Nov 15;177(10):6705–12.

12. Probst HC, Lagnel J, Kollias G, van den Broek M. Inducible transgenic mice reveal resting dendritic cells as potent inducers of CD8+ T cell tolerance. Immunity. 2003 May;18(5):713–20.

13. Bousso P, Robey E. Dynamics of CD8+ T cell priming by dendritic cells in

intact lymph nodes. Nat. Immunol. 2003 Jun;4(6):579–85.

14. Mescher MF, Curtsinger JM, Agarwal P, Casey KA, Gerner M, Hammerbeck CD, et al. Signals required for programming effector and memory development by CD8+ T cells. Immunological Reviews. 2006 Jun;211:81–92.

15. Hou S, Hyland L, Ryan KW, Portner A, Doherty PC. Virus-specific CD8+ T-cell memory determined by clonal burst size. Nature. Nature Publishing Group; 1994 Jun 23;369(6482):652–4.

16. Murali-Krishna K, Altman JD, Suresh M, Sourdive DJ, Zajac AJ, Miller JD, et al. Counting antigen-specific CD8 T cells: a reevaluation of bystander activation during viral infection. Immunity. 1998 Feb;8(2):177–87.

17. Kaech SM, Tan JT, Wherry EJ, Konieczny BT, Surh CD, Ahmed R. Selective expression of the interleukin 7 receptor identifies effector CD8 T cells that give rise to long-lived memory cells. Nat. Immunol. 2003 Dec;4(12):1191–8.

18. Sarkar S, Kalia V, Haining WN, Konieczny BT, Subramaniam S, Ahmed R. Functional and genomic profiling of effector CD8 T cell subsets with distinct memory fates. Journal of Experimental Medicine. 2008 Mar 10;205(3):625–40.

19. Schluns KS, Kieper WC, Jameson SC. Interleukin-7 mediates the homeostasis of naïve and memory CD8 T cells in vivo - Nature Immunology. Nat. Immunol. 2000.

20. Croom HA, Denton AE, Valkenburg SA, Swan NG, Olson MR, Turner SJ, et al. Memory precursor phenotype of CD8+ T cells reflects early antigenic experience rather than memory numbers in a model of localized acute influenza infection. Eur J Immunol. 2011 Jan 25;41(3):682–93.

21. Obar JJ, Jellison ER, Sheridan BS, Blair DA, Pham Q-M, Zickovich JM, et al. Pathogen-induced inflammatory environment controls effector and memory CD8+ T cell differentiation. J. Immunol. 2011 Nov 15;187(10):4967–78.

22. Nolz JC, Harty JT. Protective Capacity of Memory CD8+ T Cells Is Dictated by Antigen Exposure History and Nature of the Infection. Immunity. 2011 May;34(5):781–93.

23. Masopust D, Ha S-J, Vezys V, Ahmed R. Stimulation History Dictates Memory CD8 T Cell Phenotype: Implications for Prime-Boost Vaccination. he Journal of Immunology. 2006.

24. Murali-Krishna K, Lau LL, Sambhara S, Lemonnier F. Persistence of Memory CD8 T Cells in MHC Class I-Deficient Mice. Science. 1999.

25. Surh CD, Sprent J. ScienceDirect.com - Immunity - Homeostasis of Naive and Memory T Cells. Immunity. 2008 Dec 19;29(6):848–62.

26. Jameson SC, Masopust D. Diversity in T cell memory: an embarrassment of riches. Immunity. 2009 Dec 18;31(6):859–71.

27. Masopust D, Vezys V, Marzo AL, Lefrançois L. Preferential localization of effector memory cells in nonlymphoid tissue. Science. 2001 Mar 23;291(5512):2413–7.

28. Jiang X, Clark RA, Liu L, Wagers AJ, Fuhlbrigge RC, Kupper TS. Skin infection generates non-migratory memory CD8+ TRM cells providing global skin immunity. Nature. Nature Publishing Group; 2012 Mar 1;483(7388):227–31.

29. Masopust D, Choo D, Vezys V, Wherry EJ, Duraiswamy J, Akondy R, et al. Dynamic T cell migration program provides resident memory within intestinal epithelium. Journal of Experimental Medicine. 2010 Mar 15;207(3):553–64.

30. Wakim LM, Woodward-Davis A, Bevan MJ. Memory T cells persisting within the brain after local infection show functional adaptations to their tissue of residence. Proceedings of the …. 2010.

31. Stemberger C, Huster KM, Koffler M, Anderl F, Schiemann M, Wagner H, et al. A single naive CD8+ T cell precursor can develop into diverse effector and memory subsets. Immunity. 2007 Dec;27(6):985–97.

32. Gerlach C, van Heijst JWJ, Swart E, Sie D, Armstrong N, Kerkhoven RM, et al. One naive T cell, multiple fates in CD8+ T cell differentiation. Journal of Experimental Medicine. 2010 Jun 7;207(6):1235–46.

33. Ahmed R, Gray D. Immunological memory and protective immunity: understanding their relation. Science. 1996 Apr 5;272(5258):54–60.

34. Badovinac VP, Messingham KAN, Jabbari A, Haring JS, Harty JT. Accelerated CD8+ T-cell memory and prime-boost response after dendritic-cell vaccination. Nat. Med. Nature Publishing Group; 2005 Jun 12;11(7):748–56.

35. Badovinac VP, Porter BB, Harty JT. CD8+ T cell contraction is controlled by early inflammation. Nat. Immunol. Nature Publishing Group; 2004 Jul 11;5(8):809–17.

36. D'Souza WN, Hedrick SM. Cutting Edge: Latecomer CD8 T Cells Are Imprinted with a Unique Differentiation Program. J. Immunol. 2006.

37. Gett AV, Sallusto F, Lanzavecchia A, Geginat J. T cell fitness determined by signal strength. Nat. Immunol. 2003 Apr;4(4):355–60.

38. van Stipdonk MJB, Hardenberg G, Bijker MS, Lemmens EE, Droin NM, Green DR, et al. Dynamic programming of CD8+ T lymphocyte responses. Nat. Immunol. 2003 Apr;4(4):361–5.

39. Lanzavecchia A, Sallusto F. Progressive differentiation and selection of the fittest in the immune response. Nat. Rev. Immunol. 2002 Dec;2(12):982–7.

40. Chang JT, Palanivel VR, Kinjyo I, Schambach F, Intlekofer AM, Banerjee A, et al. Asymmetric T lymphocyte division in the initiation of adaptive immune

responses. Science. 2007 Mar 23;315(5819):1687–91.

41. Ciocca ML, Barnett BE, Burkhardt JK, Chang JT, Reiner SL. Cutting edge: Asymmetric memory T cell division in response to rechallenge. J. Immunol. 2012 May 1;188(9):4145–8.

42. Oliaro J, Van Ham V, Sacirbegovic F, Pasam A, Bomzon Z, Pham K, et al. Asymmetric cell division of T cells upon antigen presentation uses multiple conserved mechanisms. J. Immunol. 2010 Jul 1;185(1):367–75.

43. Jabbari A, Harty JT. Secondary memory CD8+ T cells are more protective but slower to acquire a central–memory phenotype. J. Exp. Med. 2006.

44. Wirth TC, Xue H-H, Rai D, Sabel JT, Bair T, Harty JT, et al. Repetitive Antigen Stimulation Induces Stepwise Transcriptome Diversification but Preserves a Core Signature of Memory CD8+ T Cell Differentiation. Immunity. 2010 Jul;33(1):128–40.

45. Joshi NS, Cui W, Dominguez CX, Chen JH, Hand TW, Kaech SM. Increased Numbers of Preexisting Memory CD8 T Cells and Decreased T-bet Expression Can Restrain Terminal Differentiation of Secondary Effector and Memory CD8 T Cells. he Journal of Immunology. 2011.

46. Wirth TC, Martin MD, Starbeck-Miller G, Harty JT, Badovinac VP. Secondary CD8+ T-cell responses are controlled by systemic inflammation. Eur J Immunol. 2011 Mar 21;41(5):1321–33.

47. Voehringer D, Blaser C, Brawand P, Raulet DH, Hanke T, Pircher H. Viral Infections Induce Abundant Numbers of Senescent CD8 T Cells. he Journal of Immunology. 2001.

48. Vezys V, Yates A, Casey KA, Lanier G, Ahmed R, Antia R, et al. Memory CD8 T-cell compartment grows in size with immunological experience. Nature. 2008 Nov 12;457(7226):196–9.

49. Curtsinger JM, Schmidt CS, Mondino A, Lins DC, Kedl RM, Jenkins MK, et al. Inflammatory Cytokines Provide a Third Signal for Activation of Naive CD4+ and CD8+ T Cells. he Journal of Immunology. 1999.

50. Curtsinger JM, Valenzuela JO, Agarwal P, Lins D, Mescher MF. Cutting Edge: Type I IFNs Provide a Third Signal to CD8 T Cells to Stimulate Clonal Expansion and Differentiation. he Journal of Immunology. 2005.

51. Rolle CE, Carrio R, Malek TR. Modeling the CD8+ T Effector to Memory Transition in Adoptive T-Cell Antitumor Immunotherapy. Cancer Res. 2008.

52. Carrio R, Bathe OF, Malek TR. Initial Antigen Encounter Programs CD8+ T Cells Competent to Develop into Memory Cells That Are Activated in an Antigen-Free, IL-7- and IL-15-Rich Environment. J. Immunol. 2004.

53. Xiao Z, Casey KA, Jameson SC, Curtsinger JM, Mescher MF. Programming for CD8 T Cell Memory Development Requires IL-12 or Type I IFN. he

Journal of Immunology. 2009.

54. Kolumam GA, Thomas S, Thompson LJ, Sprent J, Murali-Krishna K. Type I interferons act directly on CD8 T cells to allow clonal expansion and memory formation in response to viral infection. J. Exp. Med. 2005 Sep 5;202(5):637–50.

55. Aichele P, Unsoeld H, Koschella M, Schweier O, Kalinke U, Vucikuja S. Cutting Edge: CD8 T Cells Specific for Lymphocytic Choriomeningitis Virus Require Type I IFN Receptor for Clonal Expansion. J. Immunol. 2006 Apr 15;176(8):4525–9.

56. Keppler SJ, Theil K, Vucikuja S, Aichele P. Effector T-cell differentiation during viral and bacterial infections: Role of direct IL-12 signals for cell fate decision of CD8(+) T cells. Eur J Immunol. 2009 Jul;39(7):1774–83.

57.

58. Casey KA, Mescher MF. IL-21 Promotes Differentiation of Naive CD8 T Cells to a Unique Effector Phenotype. J. Immunol. 2007.

59. Elsaesser H, Sauer K, Brooks DG. IL-21 is required to control chronic viral infection. Science. 2009 Jun 19;324(5934):1569–72.

60. Fröhlich A, Kisielow J, Schmitz I, Freigang S, Shamshiev AT, Weber J, et al. IL-21R on T cells is critical for sustained functionality and control of chronic viral infection. Science. 2009 Jun 19;324(5934):1576–80.

61. Yi JS, Du M, Zajac AJ. A vital role for interleukin-21 in the control of a chronic viral infection. Science. 2009 Jun 19;324(5934):1572–6.

62. Joshi NS, Cui W, Chandele A, Lee HK, Urso DR, Hagman J, et al. Inflammation Directs Memory Precursor and Short-Lived Effector CD8+ T Cell Fates via the Graded Expression of T-bet Transcription Factor. Immunity. 2007 Aug;27(2):281–95.

63. Joshi NS, Kaech SM. Effector CD8 T Cell Development: A Balancing Act between Memory Cell Potential and Terminal Differentiation. J. Immunol. 2008.

64. Intlekofer AM, Takemoto N, Wherry EJ, Longworth SA, Northrup JT, Palanivel VR, et al. Effector and memory CD8+ T cell fate coupled by T-bet and eomesodermin. Nat. Immunol. 2005 Dec;6(12):1236–44.

65. Banerjee A, Gordon SM, Intlekofer AM, Paley MA, Mooney EC, Lindsten T, et al. Cutting edge: The transcription factor eomesodermin enables CD8+ T cells to compete for the memory cell niche. J. Immunol. 2010 Nov 1;185(9):4988–92.

66. Intlekofer AM, Takemoto N, Kao C, Banerjee A, Schambach F, Northrop JK, et al. Requirement for T-bet in the aberrant differentiation of unhelped memory CD8+ T cells. he Journal of Immunology. 2007.

67. Rao RR, Li Q, Odunsi K, Shrikant PA. The mTOR kinase determines effector versus memory CD8+ T cell fate by regulating the expression of transcription factors T-bet and Eomesodermin. Immunity. 2010 Jan 29;32(1):67–78.

68. Takemoto N, Intlekofer AM, Northrup JT, Wherry EJ, Reiner SL. Cutting Edge: IL-12 inversely regulates T-bet and eomesodermin expression during pathogen-induced CD8+ T cell differentiation. J. Immunol. 2006 Dec 1;177(11):7515–9.

69. Cruz-Guilloty F, Pipkin ME, Djuretic IM, Levanon D, Lotem J, Lichtenheld MG, et al. Runx3 and T-box proteins cooperate to establish the transcriptional program of effector CTLs. Journal of Experimental Medicine. 2009 Jan 19;206(1):51–9.

70. Rao RR, Li Q, Bupp MRG, Shrikant PA. Transcription Factor Foxo1 Represses T-bet-Mediated Effector Functions and Promotes Memory CD8+ T Cell Differentiation. Immunity. 2012 Mar;36(3):374–87.

71. Pipkin ME, Sacks JA, Cruz-Guilloty F, Lichtenheld MG, Bevan MJ, Rao A. Interleukin-2 and Inflammation Induce Distinct Transcriptional Programs that Promote the Differentiation of Effector Cytolytic T Cells. Immunity. 2010 Jan;32(1):79–90.

72. Crotty S, Johnston RJ, Schoenberger SP. Effectors and memories: Bcl-6 and Blimp-1 in T and B lymphocyte differentiation. Nat. Immunol. 2010 Feb;11(2):114–20.

73. Gong D, Malek TR. Cytokine-dependent Blimp-1 expression in activated T cells inhibits IL-2 production. J. Immunol. 2007 Jan 1;178(1):242–52.

74. Kwon H, Thierry-Mieg D, Thierry-Mieg J, Kim H-P, Oh J, Tunyaplin C, et al. Analysis of Interleukin-21-Induced Prdm1 Gene Regulation Reveals Functional Cooperation of STAT3 and IRF4 Transcription Factors. Immunity. 2009 Dec;31(6):941–52.

75. Rutishauser RL, Martins GA, Kalachikov S, Chandele A, Parish IA, Meffre E, et al. Transcriptional Repressor Blimp-1 Promotes CD8+ T Cell Terminal Differentiation and Represses the Acquisition of Central Memory T Cell Properties. Immunity. 2009 Aug;31(2):296–308.

76. Shin H, Blackburn SD, Intlekofer AM, Kao C, Angelosanto JM, Reiner SL, et al. A Role for the Transcriptional Repressor Blimp-1 in CD8+ T Cell Exhaustion during Chronic Viral Infection. Immunity. Elsevier; 2009 Aug;31(2):309–20.

77. Kallies A, Hawkins ED, Belz GT, Metcalf D, Hommel M, Corcoran LM, et al. Transcriptional repressor Blimp-1 is essential for T cell homeostasis and self-tolerance. Nat. Immunol. 2006 May;7(5):466–74.

78. Kallies A, Xin A, Belz GT, Nutt SL. Blimp-1 Transcription Factor Is Required for the Differentiation of Effector CD8+ T Cells and Memory Responses.

Immunity. 2009 Aug;31(2):283–95.

79. Cui W, Liu Y, Weinstein JS, Craft J, Kaech SM. An Interleukin-21-Interleukin-10-STAT3 Pathway Is Critical for Functional Maturation of Memory CD8+ T Cells. Immunity. 2011 Nov;35(5):792–805.

80. Ichii H, Sakamoto A, Hatano M, Okada S, Toyama H, Taki S, et al. Role for Bcl-6 in the generation and maintenance of memory CD8+ T cells. Nat. Immunol. 2002 Jun;3(6):558–63.

81. Ichii H, Sakamoto A, Kuroda Y, Tokuhisa T. Bcl6 acts as an amplifier for the generation and proliferative capacity of central memory CD8+ T cells. J. Immunol. 2004 Jul 15;173(2):883–91.

82. Oestreich KJ, Huang AC, Weinmann AS. The lineage-defining factors T-bet and Bcl-6 collaborate to regulate Th1 gene expression patterns. Journal of Experimental Medicine. 2011 May 9;208(5):1001–13.

83. Oestreich KJ, Mohn SE, Weinmann AS. Molecular mechanisms that control the expression and activity of Bcl-6 in TH1 cells to regulate flexibility with a TFH-like gene profile. Nat. Immunol. 2012 Mar 11;13(4):405–11.

84. Oestreich KJ, Weinmann AS. T-bet employs diverse regulatory mechanisms to repress transcription. Trends Immunol. 2012 Feb;33(2):78–83.

85. Hara E, Hall M, Peters G. Cdk2-dependent phosphorylation of Id2 modulates activity of E2A-related transcription factors. The EMBO Journal. 1997 Jan 15;16(2):332–42.

86. Massari ME, Murre C. Helix-loop-helix proteins: regulators of transcription in eucaryotic organisms. Mol. Cell. Biol. 2000 Jan;20(2):429–40.

87. Yang CY, Best JA, Knell J, Yang E, Sheridan AD, Jesionek AK, et al. The transcriptional regulators Id2 and Id3 control the formation of distinct memory CD8+ T cell subsets. Nat Immunol. 2011 Nov 6;12(12):1221–9.

88. Cannarile MA, Lind NA, Rivera R, Sheridan AD, Camfield KA, Wu BB, et al. Transcriptional regulator Id2 mediates CD8+ T cell immunity. Nat. Immunol. Nature Publishing Group; 2006 Nov 5;7(12):1317–25.

89. Ji Y, Pos Z, Rao M, Klebanoff CA, Yu Z, Sukumar M, et al. Repression of the DNA-binding inhibitor Id3 by Blimp-1 limits the formation of memory CD8+ T cells. Nat. Immunol. 2011 Dec;12(12):1230–7.

90. Darnell JE Jr. STATs and Gene Regulation. Science. 1997 Sep 12;277(5332):1630–5.

91. Gil MP, Salomon R, Louten J, Biron CA. Modulation of STAT1 protein levels: a mechanism shaping CD8 T-cell responses in vivo. Blood. 2006.

92. Liao W, Lin J-X, Wang L, Li P, Leonard WJ. Modulation of cytokine receptors by IL-2 broadly regulates differentiation into helper T cell lineages. Nat.

Immunol. Nature Publishing Group; 2011 Apr 24;12(6):551–9.

93. Hand TW, Cui W, Jung YW, Sefik E, Joshi NS, Chandele A, et al. Differential effects of STAT5 and PI3K/AKT signaling on effector and memory CD8 T-cell survival. Proceedings of the …. 2010.

94. Palmer DC, Restifo NP. Suppressors of cytokine signaling (SOCS) in T cell differentiation, maturation, and function. Trends Immunol. 2009 Dec;30(12):592–602.

95. Kubo M, Hanada T, Yoshimura A. Suppressors of cytokine signaling and immunity. Nat. Immunol. 2003.

96. Chong MMW, Cornish AL, Darwiche R, Stanley EG, Purton JF, Godfrey DI, et al. Suppressor of Cytokine Signaling-1 Is a Critical Regulator of Interleukin-7-Dependent CD8+ T Cell Differentiation. Immunity. 2003 Apr;18(4):475–87.

97. Zhang Z, Bin Zeng, Zhang Z, Jiao G, Li H, Jing Z, et al. Suppressor of Cytokine Signaling 3 Promotes Bone Marrow Cells to Differentiate into CD8+ T Lymphocytes in Lung Tissue via Up-Regulating Notch1 Expression. Cancer Res. 2009.

98. Nosaka T. STAT5 as a molecular regulator of proliferation, differentiation and apoptosis in hematopoietic cells. The EMBO Journal. Nature Publishing Group; 1999 Sep 1;18(17):4754–65.

99. Ramanathan S, Gagnon J, Leblanc C, Rottapel R, Ilangumaran S. Suppressor of Cytokine Signaling 1 Stringently Regulates Distinct Functions of IL-7 and IL-15 In Vivo during T Lymphocyte Development and Homeostasis. he Journal of Immunology. 2006.

100. Cornish AL, Davey GM, Metcalf D, Purton JF, Corbin JE, Greenhalgh CJ, et al. Suppressor of Cytokine Signaling-1 Has IFN-γ-Independent Actions in T Cell Homeostasis. he Journal of Immunology. 2003.

101. Zeng R. Synergy of IL-21 and IL-15 in regulating CD8+ T cell expansion and function. Journal of Experimental Medicine. 2005 Jan 3;201(1):139–48.

102. Hinrichs CS, Spolski R, Paulos CM, Gattinoni L, Kerstann KW, Palmer DC, et al. IL-21 priming enhances T-cell immunotherapy. Blood. 2008 Jun 1;111(11):5268–9.

103. Gattinoni L, Zhong X-S, Palmer DC, Ji Y, Hinrichs CS, Yu Z, et al. Wnt signaling arrests effector T cell differentiation and generates CD8+ memory stem cells. Nat. Med. Nature Publishing Group; 2009 Jun 14;15(7):808–13.

104. Gagnon J, Ramanathan S, Leblanc C, Ilangumaran S. Regulation of IL-21 signaling by suppressor of cytokine signaling-1 (SOCS1) in CD8+ T lymphocytes. Cellular Signalling. 2007 Apr;19(4):806–16.

105. Marine J-C, Topham DJ, McKay C, Wang D, Parganas E, Stravopodis D, et

al. SOCS1 Deficiency Causes a Lymphocyte-Dependent Perinatal Lethality. Cell. 1999 Sep;98(5):609–16.

106. Davey GM, Starr R, Cornish AL, Burghardt JT, Alexander WS, Carbone FR, et al. SOCS-1 regulates IL-15-driven homeostatic proliferation of antigen-naive CD8 T cells, limiting their autoimmune potential. J. Exp. Med. 2005 Oct 17;202(8):1099–108.

107. Matsumoto A, Seki YI, Watanabe R, Hayashi K, Johnston JA, Harada Y, et al. A Role of Suppressor of Cytokine Signaling 3 (SOCS3/CIS3/SSI3) in CD28-mediated Interleukin 2 Production. Journal of Experimental Medicine. 2003 Feb 17;197(4):425–36.

108. Matsumoto A, Seki Y, Kubo M, Ohtsuka S, Suzuki A, Hayashi I, et al. Suppression of STAT5 functions in liver, mammary glands, and T cells in cytokine-inducible SH2-containing protein 1 transgenic mice. Mol Cell Biol. 1999 Sep;19(9):6396–407.

109. Tannahill GM, Elliott J, Barry AC, Hibbert L, Cacalano NA, Johnston JA. SOCS2 can enhance interleukin-2 (IL-2) and IL-3 signaling by accelerating SOCS3 degradation. Mol. Cell. Biol. 2005 Oct;25(20):9115–26.

110. Ilangumaran S, Rottapel R. Regulation of cytokine receptor signaling by SOCS1. Immunological Reviews. 2003 Apr;192(1):196–211.

111. Brender C, Tannahill GM, Jenkins BJ, Fletcher J, Columbus R, Saris CJM, et al. Suppressor of cytokine signaling 3 regulates CD8 T-cell proliferation by inhibition of interleukins 6 and 27. Blood. 2007 Oct 1;110(7):2528–36.

112. Karrer U, Sierro S, Wagner M, Oxenius A, Hengel H, Koszinowski UH, et al. Memory inflation: continuous accumulation of antiviral CD8+ T cells over time. J. Immunol. 2003 Feb 15;170(4):2022–9.

113. Snyder CM, Cho KS, Bonnett EL, van Dommelen S, Shellam GR, Hill AB. Memory inflation during chronic viral infection is maintained by continuous production of short-lived, functional T cells. Immunity. 2008 Oct 17;29(4):650–9.

114. Tsuda Y, Caposio P, Parkins CJ, Botto S, Messaoudi I, Cicin-Sain L, et al. A replicating cytomegalovirus-based vaccine encoding a single Ebola virus nucleoprotein CTL epitope confers protection against Ebola virus. PLoS Negl Trop Dis. 2011 Aug;5(8):e1275.

115. Hansen SG, Ford JC, Lewis MS, Ventura AB, Hughes CM, Coyne-Johnson L, et al. Profound early control of highly pathogenic SIV by an effector memory T-cell vaccine. Nature. 2011 May 26;473(7348):523–7.

116. McGeoch DJ, Cook S, Dolan A, Jamieson FE, Telford EA. Molecular phylogeny and evolutionary timescale for the family of mammalian herpesviruses. J. Mol. Biol. 1995 Mar 31;247(3):443–58.

117. Simon CO, Holtappels R, Tervo H-M, Böhm V, Däubner T, Oehrlein-Karpi

SA, et al. CD8 T cells control cytomegalovirus latency by epitope-specific sensing of transcriptional reactivation. J. Virol. 2006 Nov;80(21):10436–56.

118. Holtappels R, Pahl-Seibert MF, Thomas D, Reddehase MJ. Enrichment of immediate-early 1 (m123/pp89) peptide-specific CD8 T cells in a pulmonary CD62Llo memory-effector cell pool during latent murine cytomegalovirus infection of the lungs. J. Virol. Am Soc Microbiol; 2000;74(24):11495–503.

119. Munks MW, Cho KS, Pinto AK, Sierro S, Klenerman P, Hill AB. Four distinct patterns of memory CD8 T cell responses to chronic murine cytomegalovirus infection. J. Immunol. 2006 Jul 1;177(1):450–8.

120. Sierro S, Rothkopf R, Klenerman P. Evolution of diverse antiviral CD8+ T cell populations after murine cytomegalovirus infection. Eur J Immunol. 2005 Apr;35(4):1113–23.

121. Romero P, Zippelius A, Kurth I, Pittet MJ, Touvrey C, Iancu EM, et al. Four Functionally Distinct Populations of Human Effector-Memory CD8+ T Lymphocytes. he Journal of Immunology. 2007.

122. Gamadia LE, van Leeuwen EMM, Remmerswaal EBM, Yong S-L, Surachno S, Wertheim-van Dillen PME, et al. The size and phenotype of virus-specific T cell populations is determined by repetitive antigenic stimulation and environmental cytokines. J. Immunol. 2004 May 15;172(10):6107–14.

123. Hertoghs KML, Moerland PD, van Stijn A, Remmerswaal EBM, Yong SL, van de Berg PJEJ, et al. Molecular profiling of cytomegalovirus-induced human CD8+ T cell differentiation. J. Clin. Invest. 2010 Nov 1;120(11):4077–90.

124. Ibegbu CC, Xu Y-X, Harris W, Maggio D, Miller JD, Kourtis AP. Expression of killer cell lectin-like receptor G1 on antigen-specific human CD8+ T lymphocytes during active, latent, and resolved infection and its relation with CD57. J. Immunol. 2005 May 15;174(10):6088–94.

125. Thimme R, Appay V, Koschella M, Panther E, Roth E, Hislop AD, et al. Increased expression of the NK cell receptor KLRG1 by virus-specific CD8 T cells during persistent antigen stimulation. J. Virol. 2005 Sep;79(18):12112–6.

126. Snyder CM, Cho KS, Bonnett EL, Allan JE, Hill AB. Sustained CD8+ T cell memory inflation after infection with a single-cycle cytomegalovirus. PLoS Pathog. 2011 Oct;7(10):e1002295.

127. Hutchinson S, Sims S, O'Hara G, Silk J, Gileadi U, Cerundolo V, et al. A dominant role for the immunoproteasome in CD8+ T cell responses to murine cytomegalovirus. PLoS ONE. 2011;6(2):e14646.

128. Koffron AJ, Hummel M, Patterson BK, Yan S, Kaufman DB, Fryer JP, et al. Cellular localization of latent murine cytomegalovirus. J. Virol. 1998 Jan;72(1):95–103.

129. Torti N, Walton SM, Brocker T, Rülicke T, Oxenius A. Non-hematopoietic

cells in lymph nodes drive memory CD8 T cell inflation during murine cytomegalovirus infection. PLoS Pathog. 2011 Oct;7(10):e1002313.

130. Seckert CK, Renzaho A, Tervo H-M, Krause C, Deegen P, Kühnapfel B, et al. Liver sinusoidal endothelial cells are a site of murine cytomegalovirus latency and reactivation. J. Virol. 2009 Sep;83(17):8869–84.

131. Torti N, Walton SM, Murphy KM, Oxenius A. Batf3 transcription factor-dependent DC subsets in murine CMV infection: differential impact on T-cell priming and memory inflation. Eur J Immunol. 2011 Sep;41(9):2612–8.

132. Campbell AE, Cavanaugh VJ, Slater JS. The salivary glands as a privileged site of cytomegalovirus immune evasion and persistence. Med. Microbiol. Immunol. 2008 Jun;197(2):205–13.

133. Grzimek NK, Dreis D, Schmalz S, Reddehase MJ. Random, asynchronous, and asymmetric transcriptional activity of enhancer-flanking major immediate-early genes ie1/3 and ie2 during murine cytomegalovirus latency in the lungs. J. Virol. 2001 Mar;75(6):2692–705.

134. Arens R, Loewendorf A, Redeker A, Sierro S, Boon L, Klenerman P, et al. Differential B7-CD28 costimulatory requirements for stable and inflationary mouse cytomegalovirus-specific memory CD8 T cell populations. J. Immunol. 2011 Apr 1;186(7):3874–81.

135. Humphreys IR, Loewendorf A, de Trez C, Schneider K, Benedict CA, Munks MW, et al. OX40 Costimulation Promotes Persistence of Cytomegalovirus-Specific CD8 T Cells: A CD4-Dependent Mechanism. he Journal of Immunology. 2007.

136. Song J, So T, Cheng M, Tang X, Croft M. Sustained survivin expression from OX40 costimulatory signals drives T cell clonal expansion. Immunity. 2005 May;22(5):621–31.

137. Rogers PR, Song J, Gramaglia I, Killeen N, Croft M. OX40 promotes Bcl-xL and Bcl-2 expression and is essential for long-term survival of CD4 T cells. Immunity. 2001 Sep;15(3):445–55.

138. Humphreys IR, Lee S-W, Jones M, Loewendorf A, Gostick E, Price DA, et al. Biphasic role of 4-1BB in the regulation of mouse cytomegalovirus-specific CD8(+) T cells. Eur J Immunol. 2010 Oct;40(10):2762–8.

139. Jones M, Ladell K, Wynn KK, Stacey MA, Quigley MF, Gostick E, et al. IL-10 restricts memory T cell inflation during cytomegalovirus infection. J. Immunol. 2010 Sep 15;185(6):3583–92.

140. Bachmann MF, Wolint P, Walton S, Schwarz K, Oxenius A. Differential role of IL-2R signaling for CD8+ T cell responses in acute and chronic viral infections. Eur J Immunol. 2007 Jun;37(6):1502–12.

141. Arens R, Loewendorf A, Her MJ, Schneider-Ohrum K, Shellam GR, Janssen E, et al. B7-mediated costimulation of CD4 T cells constrains

cytomegalovirus persistence. J. Virol. 2011 Jan;85(1):390–6.

142. Snyder CM, Loewendorf A, Bonnett EL, Croft M, Benedict CA, Hill AB. CD4+ T cell help has an epitope-dependent impact on CD8+ T cell memory inflation during murine cytomegalovirus infection. J. Immunol. 2009 Sep 15;183(6):3932–41.

143. Walton SM, Torti N, Mandaric S, Oxenius A. T cell help permits memory CD8(+) T cell inflation during cytomegalovirus latency. Eur J Immunol. 2011 May 17.

144. Iancu EM, Corthesy P, Baumgaertner P, Devevre E, Voelter V, Romero P, et al. Clonotype selection and composition of human CD8 T cells specific for persistent herpes viruses varies with differentiation but is stable over time. J. Immunol. 2009 Jul 1;183(1):319–31.

145. Schepers K, Swart E, van Heijst JWJ, Gerlach C, Castrucci M, Sie D, et al. Dissecting T cell lineage relationships by cellular barcoding. Journal of Experimental Medicine. 2008 Sep 29;205(10):2309–18.

146. Day EK, Carmichael AJ, Berge ten IJM, Waller ECP, Sissons JGP, Wills MR. Rapid CD8+ T cell repertoire focusing and selection of high-affinity clones into memory following primary infection with a persistent human virus: human cytomegalovirus. J. Immunol. 2007 Sep 1;179(5):3203–13.

147. Wills MR, Carmichael AJ, Weekes MP, Mynard K, Okecha G, Hicks R, et al. Human virus-specific CD8+ CTL clones revert from CD45ROhigh to CD45RAhigh in vivo: CD45RAhighCD8+ T cells comprise both naive and memory cells. J. Immunol. 1999 Jun 15;162(12):7080–7.

148. Wills MR, Okecha G, Weekes MP, Gandhi MK, Sissons PJG, Carmichael AJ. Identification of Naive or Antigen-Experienced Human CD8+ T Cells by Expression of Costimulation and Chemokine Receptors: Analysis of the Human Cytomegalovirus-Specific CD8+ T Cell Response. he Journal of Immunology. 2002.

149. Kramer MF, Chen SH, Knipe DM, Coen DM. Accumulation of viral transcripts and DNA during establishment of latency by herpes simplex virus. J. Virol. 1998 Feb;72(2):1177–85.

150. Nicoll MP, Proença JT, Efstathiou S. The molecular basis of herpes simplex virus latency. FEMS Microbiol. Rev. 2012 May;36(3):684–705.

151. Simmons A, Tscharke DC. Anti-CD8 impairs clearance of herpes simplex virus from the nervous system: implications for the fate of virally infected neurons. J. Exp. Med. 1992 May 1;175(5):1337–44.

152. Lang A, Brien JD, Nikolich-Zugich J. Inflation and long-term maintenance of CD8 T cells responding to a latent herpesvirus depend upon establishment of latency and presence of viral antigens. J. Immunol. 2009 Dec 15;183(12):8077–87.

153. Liu T, Khanna KM, Chen X, Fink DJ, Hendricks RL. CD8(+) T cells can block herpes simplex virus type 1 (HSV-1) reactivation from latency in sensory neurons. J. Exp. Med. 2000 May 1;191(9):1459–66.

154. Swanson PA, Hofstetter AR, Wilson JJ, Lukacher AE. Cutting edge: shift in antigen dependence by an antiviral MHC class Ib-restricted CD8 T cell response during persistent viral infection. J. Immunol. 2009 May 1;182(9):5198–202.

155. Isa A, Kasprowicz V, Norbeck O, Loughry A, Jeffery K, Broliden K, et al. Prolonged activation of virus-specific CD8+T cells after acute B19 infection. PLoS Med. 2005 Dec;2(12):e343.

156. Simmons R, Sharp C, Sims S, Kloverpris H, Goulder P, Simmonds P, et al. High frequency, sustained T cell responses to PARV4 suggest viral persistence in vivo. J. Infect. Dis. 2011 May 15;203(10):1378–87.

157. Hyatt G, Melamed R, Park R, Seguritan R, Laplace C, Poirot L, et al. Gene expression microarrays: glimpses of the immunological genome. Nat. Immunol. 2006 Jul;7(7):686–91.

158. Alizadeh A, Eisen M, Botstein D, Brown PO, Staudt LM. Probing lymphocyte biology by genomic-scale gene expression analysis. J. Clin. Immunol. 1998 Nov;18(6):373–9.

159. Teague TK, Hildeman D, Kedl RM, Mitchell T, Rees W, Schaefer BC, et al. Activation changes the spectrum but not the diversity of genes expressed by T cells. Proceedings of the National Academy of Sciences. 1999 Oct 26;96(22):12691–6.

160. Kaech SM, Hemby S, Kersh E, Ahmed R. Molecular and functional profiling of memory CD8 T cell differentiation. Cell. 2002 Dec 13;111(6):837–51.

161. Holmes S, He M, Xu T, Lee PP. Memory T cells have gene expression patterns intermediate between naive and effector. Proc. Natl. Acad. Sci. U.S.A. 2005 Apr 12;102(15):5519–23.

162. Appay V, Bosio A, Lokan S, Wiencek Y, Biervert C, Küsters D, et al. Sensitive gene expression profiling of human T cell subsets reveals parallel post-thymic differentiation for CD4+ and CD8+ lineages. J. Immunol. 2007 Dec 1;179(11):7406–14.

163. Willinger T, Freeman T, Hasegawa H, McMichael AJ, Callan MFC. Molecular signatures distinguish human central memory from effector memory CD8 T cell subsets. J. Immunol. 2005 Nov 1;175(9):5895–903.

164. Walker LJ, Kang Y-H, Smith MO, Tharmalingham H, Ramamurthy N, Fleming VM, et al. Human MAIT and CD8αα cells develop from a pool of type-17 precommitted CD8+ T cells. Blood. 2012 Jan 12;119(2):422–33.

165. Wu JQ, Dwyer DE, Dyer WB, Yang YH, Wang B, Saksena NK. Genome-wide analysis of primary CD4+ and CD8+ T cell transcriptomes shows evidence

for a network of enriched pathways associated with HIV disease. Retrovirology. 2011;8:18.

166. Wherry EJ, Ha S-J, Kaech SM, Haining WN, Sarkar S, Kalia V, et al. Molecular Signature of CD8+ T Cell Exhaustion during Chronic Viral Infection. Immunity. 2007 Oct;27(4):670–84.

167. Quigley M, Pereyra F, Nilsson B, Porichis F, Fonseca C, Eichbaum Q, et al. Transcriptional analysis of HIV-specific CD8+ T cells shows that PD-1 inhibits T cell function by upregulating BATF. Nat. Med. 2010 Oct;16(10):1147–51.

168. Doering TA, Crawford A, Angelosanto JM, Paley MA, Ziegler CG, Wherry EJ. Network Analysis Reveals Centrally Connected Genes and Pathways Involved in CD8(+) T Cell Exhaustion versus Memory. Immunity. 2012 Nov 12.

169. van Stijn A, Rowshani AT, Yong SL, Baas F, Roosnek E, Berge ten IJM, et al. Human cytomegalovirus infection induces a rapid and sustained change in the expression of NK cell receptors on CD8+ T cells. J. Immunol. 2008 Apr 1;180(7):4550–60.

170. Sallusto F, Lenig D, Förster R, Lipp M, Lanzavecchia A. Two subsets of memory T lymphocytes with distinct homing potentials and effector functions. Nature. 1999 Oct 14;401(6754):708–12.

171. Casey KA, Fraser KA, Schenkel JM, Moran A, Abt MC, Beura LK, et al. Antigen-independent differentiation and maintenance of effector-like resident memory T cells in tissues. J. Immunol. 2012 May 15;188(10):4866–75.

172. Mackay LK, Stock AT, Ma JZ, Jones CM, Kent SJ, Mueller SN, et al. Long-lived epithelial immunity by tissue-resident memory T (TRM) cells in the absence of persisting local antigen presentation. Proc. Natl. Acad. Sci. U.S.A. 2012 May 1;109(18):7037–42.

173. Szabo SJ, Kim ST, Costa GL, Zhang X, Fathman CG, Glimcher LH. A novel transcription factor, T-bet, directs Th1 lineage commitment. Cell. 2000 Mar 17;100(6):655–69.

174. Xue L, Chiang L, He B, Zhao Y-Y, Winoto A. FoxM1, a forkhead transcription factor is a master cell cycle regulator for mouse mature T cells but not double positive thymocytes. PLoS ONE. 2010;5(2):e9229.

175. Harty JT, Badovinac VP. Shaping and reshaping CD8+ T-cell memory. Nat. Rev. Immunol. 2008 Feb;8(2):107–19.

176. Baubet V, Xiang C, Molczan A, Roccograndi L, Melamed S, Dahmane N. Rp58 is essential for the growth and patterning of the cerebellum and for glutamatergic and GABAergic neuron development. Development. 2012 Jun;139(11):1903–9.

177. Hirai S, Miwa A, Ohtaka-Maruyama C, Kasai M. RP58 controls neuron and astrocyte differentiation by downregulating the expression of Id1-4 genes in

the developing cortex : Abstract : The EMBO Journal. The EMBO …. 2012.

178. Mandal M, Borowski C, Palomero T, Ferrando AA, Oberdoerffer P, Meng F, et al. The BCL2A1 gene as a pre-T cell receptor-induced regulator of thymocyte survival. J. Exp. Med. 2005 Feb 21;201(4):603–14.

179. Virador VM, Davidson B, Czechowicz J, Mai A, Kassis J, Kohn EC. The anti-apoptotic activity of BAG3 is restricted by caspases and the proteasome. PLoS ONE. 2009;4(4):e5136.

180. Mittrucker HW. Requirement for the Transcription Factor LSIRF/IRF4 for Mature B and T Lymphocyte Function. Science. 1997 Jan 24;275(5299):540–3.

181. Grant GD, Gamsby J, Martyanov V, Brooks L, George LK, Mahoney JM, et al. Live-cell monitoring of periodic gene expression in synchronous human cells identifies Forkhead genes involved in cell cycle control. Mol. Biol. Cell. 2012 Aug;23(16):3079–93.

182. Boise LH, González-García M, Postema CE, Ding L, Lindsten T, Turka LA, et al. bcl-x, a bcl-2-related gene that functions as a dominant regulator of apoptotic cell death. Cell. 1993 Aug 27;74(4):597–608.

183. Kishimoto T. IL-6: from its discovery to clinical applications. Int. Immunol. 2010 May;22(5):347–52.

184. Sepulveda H, Cerwenka A, Morgan T, Dutton RW. CD28, IL-2-independent costimulatory pathways for CD8 T lymphocyte activation. J. Immunol. 1999 Aug 1;163(3):1133–42.

185. Teague TK, Marrack P, Kappler JW, Vella AT. IL-6 rescues resting mouse T cells from apoptosis. J. Immunol. 1997 Jun 15;158(12):5791–6.

186. Takeda K, Kaisho T, Yoshida N, Takeda J, Kishimoto T, Akira S. Stat3 activation is responsible for IL-6-dependent T cell proliferation through preventing apoptosis: generation and characterization of T cell-specific Stat3-deficient mice. J. Immunol. 1998 Nov 1;161(9):4652–60.

187. Gagnon J, Ramanathan S, Leblanc C, Cloutier A, McDonald PP, Ilangumaran S. IL-6, in Synergy with IL-7 or IL-15, Stimulates TCR-Independent Proliferation and Functional Differentiation of CD8+ T Lymphocytes. he Journal of Immunology. 2008.

188. Fujioka N, Akazawa R, Ohashi K, Fujii M, Ikeda M, Kurimoto M. Interleukin-18 protects mice against acute herpes simplex virus type 1 infection. J. Virol. 1999 Mar;73(3):2401–9.

189. Gherardi MM, Ramírez JC, Esteban M. IL-12 and IL-18 act in synergy to clear vaccinia virus infection: involvement of innate and adaptive components of the immune system. J Gen Virol. 2003 Aug;84(Pt 8):1961–72.

190. Groom JR, Luster AD. CXCR3 ligands: redundant, collaborative and

antagonistic functions. Immunol. Cell Biol. 2011 Feb;89(2):207–15.

191. Saether PC, Westgaard IH, Hoelsbrekken SE, Benjamin J, Lanier LL, Fossum S, et al. KLRE/I1 and KLRE/I2: a novel pair of heterodimeric receptors that inversely regulate NK cell cytotoxicity. J. Immunol. 2008 Sep 1;181(5):3177–82.

192. Nichols KE, Ma CS, Cannons JL. Molecular and cellular pathogenesis of X-linked lymphoproliferative disease - Nichols - 2005 - Immunological Reviews - Wiley Online Library. Immunological …. 2005.

193. Crotty S, Kersh EN, Cannons J, Schwartzberg PL, Ahmed R. SAP is required for generating long-term humoral immunity. Nature. 2003 Jan 16;421(6920):282–7.

194. Goldstein JS, Chen T, Gubina E, Pastor RW, Kozlowski S. ICAM-1 enhances MHC-peptide activation of CD8(+) T cells without an organized immunological synapse. Eur J Immunol. 2000 Nov;30(11):3266–70.

195. Beavis PA, Stagg J, Darcy PK, Smyth MJ. CD73: a potent suppressor of antitumor immune responses. Trends Immunol. 2012 May;33(5):231–7.

196. Mandapathil M, Hilldorfer B, Szczepanski MJ, Czystowska M, Szajnik M, Ren J, et al. Generation and accumulation of immunosuppressive adenosine by human CD4+CD25highFOXP3+ regulatory T cells. J. Biol. Chem. 2010 Mar 5;285(10):7176–86.

197. Morimoto C, Schlossman SF. The structure and function of CD26 in the T-cell immune response. Immunological Reviews. 1998 Feb;161:55–70.

198. Blackburn SD, Shin H, Haining WN, Zou T, Workman CJ, Polley A, et al. Coregulation of CD8+ T cell exhaustion by multiple inhibitory receptors during chronic viral infection. Nat. Immunol. Nature Publishing Group; 2008 Nov 30;10(1):29–37.

199. Krieg C, Boyman O, Fu Y-X, Kaye J. B and T lymphocyte attenuator regulates CD8+ T cell-intrinsic homeostasis and memory cell generation. Nat Immunol. 2007 Feb;8(2):162–71.

200. Deppong C, Degnan JM, Murphy TL, Murphy KM, Green JM. B and T Lymphocyte Attenuator Regulates T Cell Survival in the Lung. he Journal of Immunology. 2008.

201. Danial NN, Korsmeyer SJ. Cell death: critical control points. Cell. 2004 Jan 23;116(2):205–19.

202. Bakhshi A, Jensen JP, Goldman P, Wright JJ, McBride OW, Epstein AL, et al. Cloning the chromosomal breakpoint of t(14;18) human lymphomas: clustering around JH on chromosome 14 and near a transcriptional unit on 18. Cell. 1985 Jul;41(3):899–906.

203. Lee H-W, Park S-J, Choi BK, Kim HH, Nam K-O, Kwon BS. 4-1BB promotes

the survival of CD8+ T lymphocytes by increasing expression of Bcl-xL and Bfl-1. J. Immunol. 2002 Nov 1;169(9):4882–8.

204. Ambrosini G, Adida C, Altieri DC. A novel anti-apoptosis gene, survivin, expressed in cancer and lymphoma. Nat. Med. 1997 Aug;3(8):917–21.

205. Watts TH. TNF/TNFR family members in costimulation of T cell responses. Annu. Rev. Immunol. 2005;23:23–68.

206. Snell LM, McPherson AJ, Lin GHY, Sakaguchi S, Pandolfi PP, Riccardi C, et al. CD8 T cell-intrinsic GITR is required for T cell clonal expansion and mouse survival following severe influenza infection. J. Immunol. 2010 Dec 15;185(12):7223–34.

207. Ronchetti S. Role of GITR in activation response of T lymphocytes. Blood. 2002 Apr 30;100(1):350–2.

208. Pende D, Castriconi R, Romagnani P, Spaggiari GM, Marcenaro S, Dondero A, et al. Expression of the DNAM-1 ligands, Nectin-2 (CD112) and poliovirus receptor (CD155), on dendritic cells: relevance for natural killer-dendritic cell interaction. Blood. 2006 Mar 1;107(5):2030–6.

209. Dardalhon V, Schubart AS, Reddy J, Meyers JH, Monney L, Sabatos CA, et al. CD226 is specifically expressed on the surface of Th1 cells and regulates their expansion and effector functions. J. Immunol. 2005 Aug 1;175(3):1558–65.

210. Welch MJ, Teijaro JR, Lewicki HA, Colonna M, Oldstone MBA. CD8 T cell defect of TNF-α and IL-2 in DNAM-1 deficient mice delays clearance in vivo of a persistent virus infection. Virology. 2012 Aug 1;429(2):163–70.

211. Cella M, Presti R, Vermi W, Lavender K, Turnbull E, Ochsenbauer-Jambor C, et al. Loss of DNAM-1 contributes to CD8+ T-cell exhaustion in chronic HIV-1 infection. Eur J Immunol. 2010 Apr;40(4):949–54.

212. Gilfillan S, Chan CJ, Cella M, Haynes NM, Rapaport AS, Boles KS, et al. DNAM-1 promotes activation of cytotoxic lymphocytes by nonprofessional antigen-presenting cells and tumors. Journal of Experimental Medicine. 2008 Dec 22;205(13):2965–73.

213. Seth S, Qiu Q, Danisch S, Maier MK, Braun A, Ravens I, et al. Intranodal interaction with dendritic cells dynamically regulates surface expression of the co-stimulatory receptor CD226 protein on murine T cells. J. Biol. Chem. 2011 Nov 11;286(45):39153–63.

214. Castellino F, Huang AY, Altan-Bonnet G, Stoll S, Scheinecker C, Germain RN. Chemokines enhance immunity by guiding naive CD8+ T cells to sites of CD4+ T cell-dendritic cell interaction. Nature. 2006 Apr 13;440(7086):890–5.

215. Dorner BG, Dorner MB, Zhou X, Opitz C, Mora A, Güttler S, et al. Selective expression of the chemokine receptor XCR1 on cross-presenting dendritic cells determines cooperation with CD8+ T cells. Immunity. 2009 Nov

20;31(5):823–33.

216. Miaw SC, Choi A, Yu E, Kishikawa H, Ho IC. ROG, repressor of GATA, regulates the expression of cytokine genes. Immunity. 2000 Mar;12(3):323–33.

217. Piazza F, Costoya JA, Merghoub T, Hobbs RM, Pandolfi PP. Disruption of PLZP in mice leads to increased T-lymphocyte proliferation, cytokine production, and altered hematopoietic stem cell homeostasis. Mol. Cell. Biol. 2004 Dec;24(23):10456–69.

218. Yang XO, Pappu BP, Nurieva R, Akimzhanov A, Kang HS, Chung Y, et al. T helper 17 lineage differentiation is programmed by orphan nuclear receptors ROR alpha and ROR gamma. Immunity. 2008 Jan;28(1):29–39.

219. Qi S, Song Y, Peng Y, Wang H, Long H, Yu X, et al. ZEB2 mediates multiple pathways regulating cell proliferation, migration, invasion, and apoptosis in glioma. PLoS ONE. 2012;7(6):e38842.

220. Kohlmeier JE, Reiley WW, Perona-Wright G, Freeman ML, Yager EJ, Connor LM, et al. Inflammatory chemokine receptors regulate CD8(+) T cell contraction and memory generation following infection. Journal of Experimental Medicine. 2011 Aug 1;208(8):1621–34.

221. White G. Fractalkine: A Survivor's Guide. Arteriosclerosis. 2012.

222. Boehme SA, Lio FM, Maciejewski-Lenoir D, Bacon KB, Conlon PJ. The chemokine fractalkine inhibits Fas-mediated cell death of brain microglia. J. Immunol. 2000 Jul 1;165(1):397–403.

223. Wherry EJ. Antigen-independent memory CD8 T cells do not develop during chronic viral infection. Proceedings of the National Academy of Sciences. 2004 Nov 2;101(45):16004–9.

224. Khanna KM, Bonneau RH, Kinchington PR, Hendricks RL. Herpes simplex virus-specific memory CD8+ T cells are selectively activated and retained in latently infected sensory ganglia. Immunity. 2003 May;18(5):593–603.

225. Lang A, Nikolich-Zugich J. Functional CD8 T cell memory responding to persistent latent infection is maintained for life. J. Immunol. 2011 Oct 1;187(7):3759–68.

226. Gebhardt T, Wakim LM, Eidsmo L, Reading PC, Heath WR, Carbone FR. Memory T cells in nonlymphoid tissue that provide enhanced local immunity during infection with herpes simplex virus. Nat. Immunol. Nature Publishing Group; 2009 Mar 22;10(5):524–30.

227. Steven NM, Leese AM, Annels NE, Lee SP, Rickinson AB. Epitope focusing in the primary cytotoxic T cell response to Epstein-Barr virus and its relationship to T cell memory. J. Exp. Med. 1996 Nov 1;184(5):1801–13.

228. Catalina MD, Sullivan JL, Brody RM, Luzuriaga K. Phenotypic and functional

heterogeneity of EBV epitope-specific CD8+ T cells. J. Immunol. 2002 Apr 15;168(8):4184–91.

229. Hislop AD, Annels NE, Gudgeon NH, Leese AM, Rickinson AB. Epitope-specific evolution of human CD8(+) T cell responses from primary to persistent phases of Epstein-Barr virus infection. J. Exp. Med. 2002 Apr 1;195(7):893–905.

230. Colloca S, Barnes E, Folgori A. Vaccine Vectors Derived from a Large Collection of Simian Adenoviruses Induce Potent Cellular Immunity Across Multiple Species. Science. 2012.

231. Proffitt JL, Sharma E, Blair GE. Adenovirus 12-mediated down-regulation of the major histocompatibility complex (MHC) class I promoter: identification of a negative regulatory element responsive to Ad12 E1A. Nucleic Acids Res. 1994 Nov 11;22(22):4779–88.

232. Sester M, Koebernick K, Owen D, Ao M, Bromberg Y, May E, et al. Conserved amino acids within the adenovirus 2 E3/19K protein differentially affect downregulation of MHC class I and MICA/B proteins. J. Immunol. 2010 Jan 1;184(1):255–67.

233. Murdoch C, Finn A. Chemokine receptors and their role in inflammation and infectious diseases. 2000.

234. Xavier Blanchet MLCWRRKPVH. Touch of Chemokines. Front Immunol. Frontiers Media SA; 2012;3.

235. Tan JT. Interleukin (IL)-15 and IL-7 Jointly Regulate Homeostatic Proliferation of Memory Phenotype CD8+ Cells but Are Not Required for Memory Phenotype CD4+ Cells. Journal of Experimental Medicine. 2002 Jun 17;195(12):1523–32.

236. Bradley LM, Haynes L, Swain SL. IL-7: maintaining T-cell memory and achieving homeostasis. Trends Immunol. 2005 Mar;26(3):172–6.

237. Buentke E, Mathiot A, Tolaini M, Di Santo J, Zamoyska R, Seddon B. Do CD8 effector cells need IL-7R expression to become resting memory cells? Blood. 2006 Sep 15;108(6):1949–56.

238. Veillette A. Immune regulation by SLAM family receptors and SAP-related adaptors. Nat. Rev. Immunol. 2006 Jan;6(1):56–66.

239. Seckert CK, Schader SI, Ebert S, Thomas D, Freitag K, Renzaho A, et al. Antigen-presenting cells of haematopoietic origin prime cytomegalovirus-specific CD8 T-cells but are not sufficient for driving memory inflation during viral latency. Journal of General Virology. 2011 Aug 17;92(9):1994–2005.

240. Seckert CK, Grießl M, Büttner JK, Scheller S, Simon CO, Kropp KA, et al. Viral latency drives “memory inflation”: a unifying hypothesis linking two hallmarks of cytomegalovirus infection. Med. Microbiol. Immunol. 2012 Sep 19.

241. Orange JS, Biron CA. Characterization of early IL-12, IFN-alphabeta, and TNF effects on antiviral state and NK cell responses during murine cytomegalovirus infection. J. Immunol. 1996.

242. Arase H, Mocarski ES, Campbell AE, Hill AB, Lanier LL. Direct Recognition of Cytomegalovirus by Activating and Inhibitory NK Cell Receptors. Science Signaling. AAAS; 2002 May 17;296(5571):1323.

243. Lathbury LJ, Allan JE, Shellam GR, Scalzo AA. Effect of host genotype in determining the relative roles of natural killer cells and T cells in mediating protection against murine cytomegalovirus infection. Journal of General Virology. 1996 Oct 1;77(10):2605–13.

244. Podlech J, Holtappels R, Wirtz N, Steffens HP, Reddehase MJ. Reconstitution of CD8 T cells is essential for the prevention of multiple-organ cytomegalovirus histopathology after bone marrow transplantation. Journal of general …. 1998.

245. Steffens HP, Kurz S, Holtappels R, Reddehase MJ. Preemptive CD8 T-cell immunotherapy of acute cytomegalovirus infection prevents lethal disease, limits the burden of latent viral genomes, and reduces the risk of virus recurrence. J. Virol. 1998 Mar;72(3):1797–804.

246. Polić B, Hengel H, Krmpotić A, Trgovcich J, Pavić I, Lučin P, et al. Hierarchical and Redundant Lymphocyte Subset Control Precludes Cytomegalovirus Replication during Latent Infection. 1998.

247. Simon CO, Holtappels R, Tervo H-M, Böhm V, Däubner T, Oehrlein-Karpi SA, et al. CD8 T cells control cytomegalovirus latency by epitope-specific sensing of transcriptional reactivation. J. Virol. 2006 Nov;80(21):10436–56.

248. Barchet W, Oehen S, Klenerman P. Direct quantitation of rapid elimination of viral antigen-positive lymphocytes by antiviral CD8+ T cells in vivo. European journal …. 2000.

249. Loewendorf AI, Arens R, Purton JF, Surh CD, Benedict CA. Dissecting the Requirements for Maintenance of the CMV-Specific Memory T-Cell Pool. Viral Immunology. 2011 Aug;24(4):351–5.

250. Stirpe F, Gasperi-Campani A, Barbieri L, Falasca A, Abbondanza A, Stevens WA. Ribosome-inactivating proteins from the seeds of Saponaria officinalis L. (soapwort), of Agrostemma githago L. (corn cockle) and of Asparagus officinalis L. (asparagus), and from the latex of Hura crepitans L. (sandbox tree). Biochem. J. 1983 Dec 15;216(3):617–25.

251. Tazzari PL, Polito L, Bolognesi A, Pistillo MP, Capanni P, Palmisano GL, et al. Immunotoxins containing recombinant anti-CTLA-4 single-chain fragment variable antibodies and saporin: in vitro results and in vivo effects in an acute rejection model. J. Immunol. 2001 Oct 15;167(8):4222–9.

252. Hess PR, Barnes C, Woolard MD, Johnson MDL, Cullen JM, Collins EJ, et al.

Selective deletion of antigen-specific CD8+ T cells by MHC class I tetramers coupled to the type I ribosome-inactivating protein saporin. Blood. 2007 Apr 15;109(8):3300–7.

253. Coombs D, Kalergis AM, Nathenson SG, Wofsy C, Goldstein B. Activated TCRs remain marked for internalization after dissociation from pMHC. Nat. Immunol. 2002 Oct;3(10):926–31.

254. Vincent BG, Young EF, Buntzman AS, Stevens R, Kepler TB, Tisch RM, et al. Toxin-coupled MHC class I tetramers can specifically ablate autoreactive CD8+ T cells and delay diabetes in nonobese diabetic mice. J. Immunol. 2010 Apr 15;184(8):4196–204.

255. Jonjić S, Pavić I, Lucin P, Rukavina D, Koszinowski UH. Efficacious control of cytomegalovirus infection after long-term depletion of CD8+ T lymphocytes. J. Virol. 1990 Nov;64(11):5457–64.

256. Zimmermann H. 5'-Nucleotidase: molecular structure and functional aspects. Biochem. J. 1992 Jul 15;285 (Pt 2):345–65.

257. Colgan SP, Eltzschig HK, Eckle T, THOMPSON LF. Physiological roles for ecto-5'-nucleotidase (CD73). Purinergic Signalling. 2006 Jun 1;2(2):351–60.

258. Robson SC, Sévigny J, Zimmermann H. The E-NTPDase family of ectonucleotidases: Structure function relationships and pathophysiological significance. Purinergic Signalling. 2006 Jun;2(2):409–30.

259. Kameoka J, Tanaka T, Nojima Y, Schlossman SF, Morimoto C. Direct association of adenosine deaminase with a T cell activation antigen, CD26. Science. 1993 Jul 23;261(5120):466–9.

260. Mariathasan S, Weiss DS, Newton K, McBride J, O'Rourke K, Roose-Girma M, et al. Cryopyrin activates the inflammasome in response to toxins and ATP. Nature. 2006 Mar 9;440(7081):228–32.

261. Hoskin DW, Mader JS, Furlong SJ, Conrad DM, Blay J. Inhibition of T cell and natural killer cell function by adenosine and its contribution to immune evasion by tumor cells (Review). Int. J. Oncol. 2008 Mar;32(3):527–35.

262. Haskó G, Linden J, Cronstein B, Pacher P. Adenosine receptors: therapeutic aspects for inflammatory and immune diseases. Nat Rev Drug Discov. 2008 Sep;7(9):759–70.

263. Ohta A, Ohta A, Madasu M, Kini R, Subramanian M, Goel N, et al. A2A adenosine receptor may allow expansion of T cells lacking effector functions in extracellular adenosine-rich microenvironments. J. Immunol. 2009 Nov 1;183(9):5487–93.

264. Deaglio S, Dwyer KM, Gao W, Friedman D, Usheva A, Erat A, et al. Adenosine generation catalyzed by CD39 and CD73 expressed on regulatory T cells mediates immune suppression. J. Exp. Med. 2007 Jun 11;204(6):1257–65.

265. Wilson JM, Ross WG, Agbai ON, Frazier R, Figler RA, Rieger J, et al. The A2B adenosine receptor impairs the maturation and immunogenicity of dendritic cells. J. Immunol. 2009 Apr 15;182(8):4616–23.

266. Schnurr M, Toy T, Shin A, Hartmann G, Rothenfusser S, Soellner J, et al. Role of adenosine receptors in regulating chemotaxis and cytokine production of plasmacytoid dendritic cells. Blood. 2004 Feb 15;103(4):1391–7.

267. Marashi SM, Raeiszadeh M, Workman S, Rahbar A, Soderberg-Naucler C, Klenerman P, et al. Inflammation in common variable immunodeficiency is associated with a distinct CD8(+) response to cytomegalovirus. J. Allergy Clin. Immunol. 2011 Jun;127(6):1385–93.e4.

268. Kobie JJ, Shah PR, Yang L, Rebhahn JA, Fowell DJ, Mosmann TR. T regulatory and primed uncommitted CD4 T cells express CD73, which suppresses effector CD4 T cells by converting 5'-adenosine monophosphate to adenosine. J. Immunol. 2006 Nov 15;177(10):6780–6.

269. Kinsey GR, Huang L, Jaworska K, Khutsishvili K, Becker DA, Ye H, et al. Autocrine adenosine signaling promotes regulatory T cell-mediated renal protection. J. Am. Soc. Nephrol. 2012 Sep;23(9):1528–37.

270. Tew JG, Mandel TE. Prolonged antigen half-life in the lymphoid follicles of specifically immunized mice. Immunology. 1979 May;37(1):69–76.

271. Ciurea A, Klenerman P, Hunziker L, Horvath E, Odermatt B, Ochsenbein AF, et al. Persistence of lymphocytic choriomeningitis virus at very low levels in immune mice. Proc. Natl. Acad. Sci. U.S.A. 1999 Oct 12;96(21):11964–9.

272. Freitas AA, Rocha B. Population biology of lymphocytes: the flight for survival. Annu Rev Immunol. 2000;18:83–111.

273. GORONZY J, LEE W, WEYAND C. Aging and T-cell diversity☆. Experimental Gerontology. 2007 May;42(5):400–6.

274. Cicin-Sain L, Brien JD, Uhrlaub JL, Drabig A, Marandu TF, Nikolich-Zugich J. Cytomegalovirus Infection Impairs Immune Responses and Accentuates T-cell Pool Changes Observed in Mice with Aging. PLoS Pathog. Public Library of Science; 2012 Aug 16;8(8):e1002849.

275. Smithey MJ, Li G, Venturi V, Davenport MP, Nikolich-Zugich J. Lifelong Persistent Viral Infection Alters the Naive T Cell Pool, Impairing CD8 T Cell Immunity in Late Life. 2012.

276. Watanabe N, Gavrieli M, Sedý JR, Yang J, Fallarino F, Loftin SK, et al. BTLA is a lymphocyte inhibitory receptor with similarities to CTLA-4 and PD-1. Nat. Immunol. Nature Publishing Group; 2003 Jun 8;4(7):670–9.

277. Han P, Goularte OD, Rufner K, Wilkinson B, Kaye J. An Inhibitory Ig Superfamily Protein Expressed by Lymphocytes and APCs Is Also an Early Marker of Thymocyte Positive Selection. he Journal of Immunology. 2004.

278. Serriari N-E, Gondois-Rey F, Guillaume Y, Remmerswaal EBM, Pastor S, Messal N, et al. B and T Lymphocyte Attenuator Is Highly Expressed on CMV-Specific T Cells during Infection and Regulates Their Function. he Journal of Immunology. 2010.

279. Cheung TC, Humphreys IR, Potter KG, Norris PS, Shumway HM, Tran BR, et al. Evolutionarily divergent herpesviruses modulate T cell activation by targeting the herpesvirus entry mediator cosignaling pathway. Proceedings of the …. 2005.

280. Mjösberg J, Bernink J, Peters C. Transcriptional control of innate lymphoid cells - Mjösberg - 2012 - European Journal of Immunology - Wiley Online Library. European Journal of …. 2012.

281. Shi X, Wallis AM, Gerard RD, Voelker KA, Grange RW, Depinho RA, et al. Foxk1 promotes cell proliferation and represses myogenic differentiation by regulating Foxo4 and Mef2 factors. J. Cell. Sci. 2012 Sep 6.